



Monitoring Report M-1417 | 2019

---

# Monitoring ocean acidification in Norwegian seas in 2018

---

MADE BY:  
Institute of Marine Research, NORCE Norwegian Research  
Centre, University of Bergen, Norwegian  
Institute for Water Research



# COLOPHON

---

**-Executive institution (the institution is responsible for the content in this report)**

Institute of Marine Research, NORCE Norwegian Research Centre, University of Bergen,  
Norwegian Institute for Water Research

**Project manager for the contractor**

Melissa Chierici

**Contact person in the  
Norwegian Environment Agency**

Gunnar Skotte

**M-no**

1417

**Year**

2019

**Pages**

105

**Contract number**

17078007

**Publisher**

[Utgiver]

**The project is funded by**

Norwegian Environment Agency

**Author(s)**

Elizabeth Jones\*, Melissa Chierici\*, Ingunn Skjelvan\*\*, Marit Norli\*\*\*, Knut Yngve Børshheim\*,  
Helene Hodal Lødemel\*, Tina Kutting\*, Kai Sørensen\*\*\*, Andrew Luke King\*\*\*, Siv Lauvset\*\*,  
Kristin Jackson\*\*\*\*, Tor de Lange\*\*\*\*, Truls Johannessen\*\*\*\*, C. Mourguet\*.

**Title - tittel**

Monitoring ocean acidification in Norwegian seas in 2018 /  
Havforsuringsovervåking i norske farvann i 2018

---

\*Havforskningssinstituttet (IMR), \*\*NORCE Norwegian Research Centre (NORCE), \*\*\*Norsk institutt for vannforskning (NIVA), \*\*\*\*Universitetet i Bergen (UiB)

## **Summary - sammendrag**

This is the annual report from 2018 based on the program: ‘Monitoring ocean acidification in Norwegian waters’ funded by the Norwegian Environment Agency. The measurements are performed by the Institute of Marine Research (IMR), Norwegian Institute for Water Research (NIVA), NORCE Norwegian Research Centre (NORCE) and the University of Bergen (UiB). The measurements cover the area from North Sea/Skagerrak, the Norwegian Sea, and the seasonally ice covered Barents Sea. IMR conducted water column measurements along repeated transects, mainly in winter in the Skagerrak (Torungen-Hirtshals section), Norwegian Sea (Svinøy-NW, Gimsøy-NW sections), Barents Sea (Fugløya-Bjørnøya, NE Barents Sea section), and at Skrova and Arendal coastal stations. NORCE-UiB conducted water column measurements at Station M, continuous surface measurements at the same site, and water column measurements at three stations in the Hardanger region. NIVA performed surface water measurements on two sections; Oslo-Kiel (North Sea/Skagerrak) and Tromsø-Longyearbyen (Barents Sea opening) during all of 2018. This report presents and discusses some time series for the period 2011-2018.

Denne rapporten gjelder undersøkelser av havforsuring i 2018 utført av Havforskningsinstituttet (IMR), Norsk institutt for vannforskning (NIVA), NORCE Norwegian Research Centre (NORCE) og Universitetet i Bergen (UiB) på oppdrag fra Miljødirektoratet. Måleområdet i rapporten går fra Skagerrak/Nordsjøen, Norskehavet og til nordlige deler av Barentshavet. IMR har gjort vannsøylemålinger, i hovedsak vinterstid, langs faste snitt i Nordsjøen (Torungen-Hirtshals), Norskehavet (Svinøy-NV, Gimsøy-NV), i Barentshavet (Fugløya-Bjørnøya, stasjoner i det nordøstlige Barentshavet), og ved Arendal og Skrova kyststasjon. NORCE-UiB har gjort vannsøylemålinger gjennom store deler av året på Stasjon M i Norskehavet, kontinuerlige overflatemålinger på Stasjon M, og vannsøylemålinger på tre kyststasjoner i Hardanger. NIVA har gjort overflatemålinger store deler av året på strekningen Oslo-Kiel og Tromsø-Longyearbyen. I denne rapporten presenteres og diskuteres tidsserier fra perioden 2011-2018.

### **4 emneord**

Karbonmålinger, mellomårlig-og sesongsvariasjon, biogeokjemiske prosesser

### **4 subject words**

Carbonate system, interannual and seasonal variability, biogeochemical processes

### **Front page photo**

Ingunn Skjelvan (NORCE)

*Tromsø, mai 2019*

This report should be cited: Jones, E., M. Chierici, I. Skjelvan, M. Norli, K.Y. Børshheim, H.H. Lødemel, K. Sørensen, A.L. King, S. Lauvset, K. Jackson, T. de Lange, T. Johannessen og C. Mourgués. 2019. Monitoring ocean acidification in Norwegian seas in 2018, Rapport, Miljødirektoratet, M-1417|2019.

# Content

Content .....	3
Summary .....	4
Extended Norwegian Summary .....	7
1. Introduction .....	11
2. Methods and Data.....	13
2.1 Sampling and Variables.....	16
2.2 Measurements of Total Alkalinity and Total Inorganic Carbon .....	17
2.3 pH Measurements.....	18
2.4 pCO <sub>2</sub> Measurements.....	18
2.5 Calculation of pH and Saturation State of Calcite and Aragonite .....	19
3. Results .....	19
3.1 Skagerrak .....	19
3.1.1 Spatial variability along Torungen-Hirtshals section .....	19
3.1.2 Seasonal variability at Arendal station .....	22
3.1.3 Seasonal variability in surface water .....	25
3.1.4 Trend analysis at selected stations .....	28
3.2 Norwegian Sea .....	30
3.2.1 Spatial variability along the Svinøy-NW section .....	30
3.2.2 Spatial variability along the Gimsøy-NW section .....	33
3.2.3 Seasonal variability in open ocean .....	35
3.2.4 Seasonal variability in coastal water.....	40
3.2.5 Trend analysis at selected stations .....	52
3.3 Barents Sea .....	55
3.3.1 Spatial variability along the Fugløya-Bjørnøya section .....	55
3.3.2 Spatial variability along the northeastern Barents Sea section .....	58
3.3.3 Seasonal variability in surface water .....	59
3.3.4 Trend analysis at selected stations .....	62
3.4 Norwegian Coast.....	66
3.5 Cold Water Coral Reefs.....	68
4. Conclusion and Recommendations.....	72
5. References .....	74
6. Appendix .....	77
6.1 Plots .....	77
6.2 Data Tables.....	86
6.3 Definitions .....	108

## Summary

This is the annual report of the ‘Monitoring ocean acidification in Norwegian waters’ program for 2018, which began in 2013 and is funded by the Norwegian Environment Agency. The report is based on measurements of  $A_T$ ,  $C_T$ ,  $pCO_2$  and pH made by the Institute of Marine Research (IMR), Norwegian Institute for Water Research (NIVA) and NORCE Norwegian Research Centre (NORCE) and University of Bergen (UiB) with new data from 2018. IMR conducted water column measurements along repeat transects in the North Sea/Skagerrak (Torungen-Hirtshals in January), at two sections in the Norwegian Sea (Svinøy-NW, Gimsoy-NW in May-June), and at two sections in the Barents Sea (Fugløya-Bjørnøya in January, and in the northeastern Barents Sea in August-September). The water column of the Norwegian Sea was also investigated by NORCE-UiB, which performed seasonal studies and continuous surface  $pCO_2$  and surface and subsurface pH measurements at Station M. NIVA performed seasonal cruises (winter, spring, summer, autumn) for surface water measurements between Oslo-Kiel (North Sea/Skagerrak), Bergen-Kirkenes and Tromsø-Longyearbyen (Barents Sea opening) and present data on both seasonal and interannual basis. In addition, monthly measurements at coastal sites at Skrova, in Lofoten, and Arendal, in Skagerrak (IMR), and from several coastal sites in Hardanger (NORCE-UiB) were carried out. All sampling positions are shown in *Figure 1*.

This report includes carbonate chemistry data and ancillary variables such as salinity, temperature, and inorganic nutrient concentrations to provide baseline observations of variability attributed to oceanographic and anthropogenic processes, such as the influence of mixing of water masses, freshwater/meltwater inputs, oceanic  $CO_2$  uptake, and biological production and respiration. The data provide information that can be used in projections of future  $CO_2$  emission scenarios and estimates in changes in the depth of the calcium carbonate ( $CaCO_3$ ) saturation horizon. However, to determine the individual drivers of ocean acidification and their regional, seasonal and interannual variability, integrated monitoring including measurements or proxies for biological productivity, ocean physics, and land-ocean exchanges, in both surface water and in the water column is essential.

### North Sea/Skagerrak

Winter sampling from the water column along the Torungen-Hirtshals section (*Figure 2*) and monthly sampling at the coastal station Arendal was carried out in the Skagerrak region (*Figure 3*). Variability in the  $CO_2$  system is driven by salinity changes as a result of a balance of freshwater inputs from riverine and Baltic sources with salty waters from the southern North Sea and Atlantic Ocean. The oceanographic conditions were characterised by colder and fresh surface waters, in contrast to the core of Atlantic water ( $> 7.5^{\circ}C$ ) at 50-300 m depth (*Figure 1, Appendix 6.1*). Deepest parts of the water column (600 m) were occupied by cold, older water with elevated  $C_T$  due to remineralisation of organic matter. The Atlantic water had  $C_T$  in the range 2160-2175  $\mu mol\ kg^{-1}$ , consistent with data from earlier years. The upper ocean was characterised by low  $A_T$  and  $C_T$  as a result of the fresh coastal current and biological activity. Highest pH and aragonite saturation occurred in the upper 50 m (*Figure 4*). At the deepest (600 m) part of the region, temperatures increased by  $0.29^{\circ}C\ yr^{-1}$  since 2010, which indicates warming of the water masses at these depths in the Skagerrak region (*Figure 12*). This impacted pH and the state of aragonite saturation, which showed decreasing trends of 0.010 and 0.01 per year, respectively.

The oceanographic conditions at Arendal coastal station reveal strong seasonality with cold and fresh surface waters in the upper 40 m from January to May and warm, deep mixed layers from July to October (**Figure 2, Appendix 6.1**). Depletion in nitrate (**Figure 5**) from spring to summer was accompanied by strong drawdown in  $C_T$  (< 1800  $\mu\text{mol kg}^{-1}$ ) and elevated pH and aragonite saturation (**Figure 6**) in the upper 20 m as primary production dominated the seasonal changes in  $C_T$ .

The underway measurements made by NIVA in 2018 from MS *Color Fantasy* between Oslo and Kiel (**Figure 7**) showed the impacts of fresh water on the ocean across the Skagerrak region (**Figure 8**). Freshwater had a greater influence in spring and summer, with very low salinities of 12.28 in outer Oslofjord in May. Due to low biomass of primary producers (**Figure 10**), seawater pH showed small seasonal variations, with the exception of outer Oslofjord in May where the influence of freshwater reduced the pH to 7.83 (**Figure 9**). The average pH for the Skagerrak stations was 8.10 during late autumn (November), and 8.04 during spring. The aragonite saturation reached the lowest state during winter and had higher values during summer and autumn. The saturation state was 1.39 on average during winter and 2.59 during autumn. The inner Oslofjord was undersaturated ( $\Omega\text{Ar} < 1$ ) with respect to aragonite in winter, and likewise the outer Oslofjord during the period of very low salinity in May. On average, the whole Oslofjord had low aragonite saturation of around 1.05 during winter.

#### Norwegian Sea

Data from the Norwegian Sea (**Figure 1**) were collected from two oceanographic sections Svinøy-NW (**Figure 15**) and Gimsøy-NW (**Figure 16**) and from the fixed station Station M (**Figures 18-21**) and the coastal station Skrova (**Figures 35-39**). The distribution of  $A_T$  and  $C_T$  along the Svinøy-NW section shows lower values towards the coast typical of the Norwegian coastal current over the shelf (**Figure 3, Appendix 6.1**). Values of  $A_T$  of 2315-2320  $\mu\text{mol kg}^{-1}$  characterise the Atlantic water that extends from the shelf into the deeper parts of the Norwegian Sea. Seasonal biological activity reduced upper ocean  $C_T$  and lower concentrations often persist into the winter. pH showed similar values to previous years, ranging 8.04-8.05 in the upper 500 m for most of the section (**Figure 15**). Water of low pH ~8.01 occurred at the deepest point in the Norwegian Sea. The saturation state for aragonite varied from highest values ( $\Omega\text{Ar} > 1.8$ ) in the upper 400 m to reach the saturation horizon at around 2000 m depth offshore. Waters below 2000 m were undersaturated ( $\Omega\text{Ar} < 1.0$ ). **Figure 41** shows variation in aragonite saturation at different depths at 1°E from 2011 to 2018. The data show interannual variability related to the presence of cold and fresh Arctic water, with greatest variability at 1000 m, likely due to fluctuations in the presence of Arctic water and warmer Atlantic water mass.

Measurements from Station M (**Figures 18-21; Figure 4, Appendix 6.1**) show increases in pH and aragonite saturation in the surface water starting in April due to biological activity. The aragonite saturation horizon is at approximately 2000 m, which is deeper compared to earlier years, illustrating the variability of the system. Continuous winter surface data from 2011 to 2018 show an annual decrease for pH and  $\Omega\text{Ar}$  0.0039 and 0.017, respectively (**Figure 40**). These are similar to the trends based on the years 2011-2017, which showed a slightly stronger trend in pH and a slightly weaker trend in  $\Omega\text{Ar}$  and are comparable to the negative trends estimated for the Norwegian Basin by Skjelvan et al. (2014).

In 2018, seasonal measurements were collected from three sites in the Bergen-Hardanger area, and these measurements are combined with data from previous years from the same area (Vatlestraumen, Korsfjorden, Langenuen, Hardangerfjorden). This study (**Figures 24-33**)

showed well-defined seasonality in surface temperatures. Monthly variability was larger for the upper 50 m compared to the upper 10 m, which is due to stratification with river and rain influenced surface layer (< 10 m) compared to influences of Atlantic water reaching subsurface depths (*Figures 25-26*). pH exhibited a more defined cycle for the shallowest data with increases due to primary production (*Figures 27-28*). The upper 50 m was more variable with patchy blooms that depend on the depth of the photic zone. In late summer, the pH decreases due to increasing temperatures, and autumn is characterized by more vertical mixing that remixes remineralized organic matter to the surface and lowers pH.

Cold water coral reefs were sampled in Hardangerfjord and the full water column showed large gradients in the upper 50 m (*Figure 56*). Freshwater inputs reduced salinity and strong biological uptake reduced  $C_T$  in the surface layer. This was accompanied by high pH values 8.05-8.10 and aragonite saturation states > 1.9. At 50 m, increases in  $C_T$  due to reduced biological uptake and mixing with carbon-rich Atlantic water below, increased  $C_T$  and created pH and aragonite saturation minimum values compared to the rest of the water column.

Monthly measurements at coastal station Skrova in Vestfjorden (*Figures 35-39*) show strong seasonal signals in the upper 100 m, with warming up to 14 °C and freshening in summer. Biological processes in spring consume CO<sub>2</sub> and increase seawater pH and in autumn the degradation of organic material releases CO<sub>2</sub> and pH decreases to minimum values by winter. The seasonal variation is large compared to long-term trends (*Figure 43*).

The distribution of  $C_T$  along the Gimsøy-NW section shows lower values in the upper 100 m due to seasonal biological production (*Figure 5, Appendix 6.1*). Values of  $A_T$  of 2310-2320 µmol kg<sup>-1</sup> in the Atlantic water extend across the section. The saturation state for aragonite was highest ( $\Omega_{\text{Ar}} > 1.8$ ) in the upper 400 m and decreased to the saturation horizon around 2000 m depth offshore (*Figure 17*). The pH and aragonite saturation state at 1500 m at 12.3 °E from 2011 to 2018 shows variability related to fluctuations in the presence of Arctic water and warmer Atlantic water (*Figure 42*). This was a similar pattern to the variability seen along the Svinøy-NW section (*Figure 41*).

#### The Barents Sea

Sampling was carried out along the Fugløya-Bjørnøya and Vardø-N transects in the Barents Sea (*Figures 44*). The latter transect is sampled in conjunction with the IMR-PINRO Barents Sea ecosystem surveys ‘ØKOTOKT’. Waters near Fugløya are influenced by the fresh Norwegian coastal current and deepest levels are occupied by Atlantic water (*Figure 6, Appendix 6.1*). Near Bjørnøya the inflow of Arctic water creates strong horizontal gradients in the upper 200 m at the Polar Front at around 73.5°N. Between Fugløya and Bjørnøya, Atlantic water was characterised by  $A_T$  around 2320-2330 µmol kg<sup>-1</sup> where strong decreasing gradients to lowest values (2280-2290 µmol kg<sup>-1</sup>) indicate coastal waters to the south and Arctic water to the north. The distribution of  $C_T$  showed a slightly different pattern, with lowest concentrations (2115-2140 µmol kg<sup>-1</sup>) in the upper 100 m in the south, that increased to 2140-2160 µmol kg<sup>-1</sup> in the upper water column along the section. pH values were highest (~8.10) in the south with lowest values 8.02-8.04 in water overlying the seafloor at 72-73 °N (*Figure 46*). The saturation state for aragonite was lowest at 1.4-1.5 below 300 m depth at 73.5 °N and in the upper 100 m north of 74 °N.

In the northeastern Barents Sea, Atlantic water over the shelf in the south had  $A_T$  values of 2310-2320 µmol kg<sup>-1</sup> (*Figure 7, Appendix 6.1*).  $C_T$  was lowest (< 2100 µmol kg<sup>-1</sup>) in the upper

100 m, especially in the sea ice influenced areas north of 79 °N. Similar distributions in the southern and northern Barents Sea were found for pH and aragonite saturation state, with higher values in the upper 100 m in the productive sea ice zone in the north (*Figure 47*).

Temperature and  $C_T$  concentrations at 300-400 m depth at ~72.8°N along the Fugløya-Bjørnøya section showed interannual variability associated with the Polar Front from 2012 to 2018 (*Figure 53*). Cooler waters were associated with higher  $C_T$  concentrations and indicate a larger volume of cold, carbon-rich Arctic water in 2018. Salinity changes revealed the waters at 300-400 m tended to become fresher with time, which supports the presence of fresher polar water, and was accompanied by a reduction in the aragonite saturation state to lowest values of 1.4-1.6 in 2018. The distribution of seawater temperature and salinity at 250-300 m depth along the northeastern Barents Sea section show changes of  $-0.32 \text{ }^{\circ}\text{C yr}^{-1}$  and  $-0.021$ , respectively, from 2012 to 2018 (*Figure 54*). Alongside the general freshening and cooling trend, pH exhibits a general increase of  $0.006 \text{ yr}^{-1}$ . The saturation state for aragonite varied throughout the time series, with an average value of  $1.32 \pm 0.13$ . Similar to the trends at 300-400 m depth along the Fugløya-Bjørnøya section (~72.8°N), increased cold, fresh Arctic water induces a lot of variability in the region.

Carbonate chemistry from surface waters was measured throughout 2018 by NIVA in the Barents Sea opening between Tromsø and Longyearbyen (*Figure 48*). Freshwater inputs, biological production during summer, and circulation played important roles. The average pH for the Norwegian coast varied between 8.06 in the winter across the area and 8.14 in the summer (*Figure 50*) and the aragonite saturation was lowest at 1.78 in winter in the southern open ocean section. The trend of seawater salinity and temperature in surface waters of the Barents Sea opening at 74-76 °N showed a freshening of  $0.013 \text{ yr}^{-1}$  and a cooling of  $0.083 \text{ }^{\circ}\text{C yr}^{-1}$ , accompanied by an increase in both pH and  $\Omega$  aragonite of  $0.003 \text{ yr}^{-1}$  and  $0.026 \text{ yr}^{-1}$ , respectively (*Figure 52*).

## Extended Norwegian Summary

Denne rapporten omhandler overvåking av havforsuring av norske farvann i 2018 og arbeidet er gjort av Havforskningsinstituttet (IMR), Norsk institutt for vannforskning (NIVA) og NORCE Norwegian Research Centre (NORCE) og Universitetet i Bergen (UiB) på oppdrag fra Miljødirektoratet innenfor programmet ‘Havforsuringsovervåking i norske farvann’, som startet i 2013. Rapporten er basert på diskrete målinger av total alkalinitet ( $A_T$ ), totalt uorganisk karbon ( $C_T$ ) og pH, samt kontinuerlige målinger av  $\text{pCO}_2$  og pH. Både overflaten og vannsøylen er målt og målefrekvens, parameter og dyp er beskrevet i *Tabell 1*. IMR har samlet inn vannsøyleprøver fra faste snitt i Skagerrak (Torungen-Hirtshals), i Norskehavet (Svinøy-NV og Gimsøy-NV), i Barentshavet (Fugløya-Bjørnøya og stasjoner i det nordøstlige Barentshavet), og fra kyststasjonene Arendal og Skrova. Norskehavet er også undersøkt av NORCE-UiB, som har samlet prøver fra vannsøylen på Stasjon M og gjort kontinuerlige overflate- og blandingslagsmålinger fra samme posisjon. I tillegg har NORCE-UiB tatt vannsøyleprøver fra tre kyststasjoner i Hardanger. NIVA har gjort overflatemålinger i vestlige deler av Barentshavet (Tromsø-Longyearbyen), Bergen-Kirkenes og Skagerrak samt deler av Oslofjorden (Oslo-Kiel). Alle målepunkt er vist i *Figur 1*.

Rapporten inkluderer karbonatsystemdata ( $A_T$ ,  $C_T$ , pH,  $\text{pCO}_2$ ) og tilleggsdata som salt, temperatur og næringssalt. Karbonatsystemet påvirkes av ulike prosesser som blanding av vannmasser (f.eks. atlantisk vann, kystvann, smeltevann), biologisk produksjon, respirasjon

og opptak av atmosfærisk CO<sub>2</sub>. Det er viktig å få kunnskap om den naturlige variabiliteten i systemet for å detektere små menneskeskapte endringer, og målingene i programmet komplementerer hverandre i så henseende. Vannkolonnemålingene som tas årlig gir over tid informasjon om mellomårlige variasjoner og trender i karbonatsystemet.

Vannkolonnemålingene som tas hver/annenhver måned gir grunnleggende kunnskap om sesongvariasjonen til systemet, og kontinuerlige overflatemålinger gir oss en god prosessforståelse. Rapporten presenterer målinger gjort i 2018, men her diskuteres også målinger fra tidligere år og hvordan trender i de ulike havområdene utvikler seg.

De dominerende vannmassene i det norske havområdet er kyststrømmen, Atlanterhavsvann og polarvann, og en stor del av den observerte variasjonen mellom sesonger og fra år til år er drevet av endringer i det innstrømmende atlantiske vannet og av blanding med ferskt kystvann, polarvann eller smeltevann. For å få full oversikt over enkeltfaktorene bak havforsuring, regional variabilitet og sesong- og mellomårlige endringer trengs en bred overvåkning som inkluderer målinger/estimat for biologisk produksjon, havfysikk i overflate og dyp og utveksling mellom land og hav, og ikke minst trengs langsiktighet i overvåkningen.

#### Nordsjøen/ Skagerrak

Fra Skagerrak finnes i 2018 vinterdata fra hele vanndypet langs snittet Torungen-Hirtshals (*Figur 2*) og i Skagerrak (*Figur 3*) er det tatt månedlige prøver fra kyststasjonen ved Arendal (IMR) og overflateprøver mellom Oslo og Kiel (NIVA). I denne regionen er variabiliteten i CO<sub>2</sub>-systemet hovedsakelig drevet av endringer i saltinnholdet. Saltinnholdet er bestemt av innstrømmende ferskvann fra elver og fra Østersjøen og saltere vann fra sørlige nordsjøen og Atlanterhavet. Stasjonen ved Arendal hadde relativt kaldt og ferskt overflatevann som kontrast til den varme kjernen av atlanterhavsvann (> 7,5 °C) ved 50-300 m (*Figur 1, Vedlegg 6.1*). På dypet (600 m) var det kaldt og gammelt vann. Det atlantiske vannet hadde C<sub>T</sub>-konsentrasjoner på 2160-2175 µmol kg<sup>-1</sup> som også er observert tidligere fra dette området. Øvre vannlag hadde lavere A<sub>T</sub> og lavere C<sub>T</sub> som et resultat av innblanding av den ferske kyststrømmen og biologisk aktivitet. I de øvre 50 m var pH og aragonittmetningen høy, men verdiene avtok nedover i dypet når andelen av atlantisk vann ble høyere (*Figur 4*). Lavest pH og aragonittmetning ble observert på 600 m dyp ved den dypeste delen av snittet mot danskekysten. Her har temperaturen økt med 0,29°C år<sup>-1</sup> siden 2010 og saltinnholdet har også økt, som indikerer at mer varmt og salt vann har strømmet inn i Skagerak (*Figur 12*). Dette har påvirket pH og aragonittmetningen, og pH har avtatt med 0,010 per år de siste årene.

De oseanografiske forholdene ved Arendals kyststasjon viser sterkt sesongvariasjon med kaldt og friskt overflatevann i de øvre 40 m fra januar til mai, som oppvarmes for å danne sesongmessige dype blandede lag fra juli til oktober (*Figur 2, Vedlegg 6.1*). Reduksjon av nitrat (*Figur 5*) fra vår til sommer var ledsgaget av sterkt reduksjon i C<sub>T</sub> (< 1800 µmol kg<sup>-1</sup>) og forhøyet pH- og aragonittmetning (*Figur 6*) i de øvre 20 m av vannsøylen som primærproduksjon dominerer sesongmessige endringer i C<sub>T</sub>.

Underveismålinger av overflatevann mellom Oslo og Kiel (MS *Color Fantasy*; NIVA) viser sesongvariasjoner i området og innstrømming av ferskvann påvirker karboninnholdet i Skagerrak. Gjennomsnittstemperaturen for Skagerrak-stasjonene var 4,04 °C om vinteren og 19,78 °C om sommeren. Ferskvann hadde større innflytelse om vår og sommer, med spesielt lave saltholdigheter (12,28) i ytre Oslofjord i mai. Gjennomsnittlig salinitet for Skagerrak-stasjonene var 21,35 om våren og 30,97 sent på høsten. På grunn av lav biomasse av primærprodusenter i 2018 (*Figur 10*) viste pH-verdien i sjøvann små sesongvariasjoner, med unntak av ytre Oslofjord i mai, hvor ferskvannspåvirkning reduserte pH til 7,83 (*Figur 9*).

Gjennomsnittlig pH for Skagerrak-stasjonene var 8,10 senhøstes (november) og 8,04 i løpet av våren. Aragonittmetningen var lavest om vinteren og hadde høyere verdier om sommer og høst. Metningen var 1,39 i gjennomsnitt om vinteren og 2,59 i løpet av høsten. Den indre Oslofjorden var undermettet ( $\Omega_{\text{Ar}} < 1$ ) med hensyn til aragonitt om vinteren, og undermetning ble observert i den ytre Oslofjorden i perioden med svært lav saltholdighet i mai. I gjennomsnitt hadde hele Oslofjorden lav aragonittmetning på rundt 1,05 om vinteren.

#### Norskehavet

Data fra Norskehavet (**Figur 1**) ble samlet fra de oseanografiske seksjonene Svinøy-NV (IMR; **Figur 15**) og Gimsøy-NV (IMR; **Figur 16**) og månedlig fra Stasjon M (NORCE-UiB; **Figur 18-21**) og kyststasjon Skrova (IMR; **Figur 35-39**). Den norske kyststrømmen påvirket kyststasjonene med et relativt kaldere og ferskere overflatelag. I det øverste 400 m var det varmt og salt atlantisk vann, og dypere enn dette var det kaldt og relativt ferskt arktiske vann.

Fordelingen av  $A_T$  og  $C_T$  langs Svinøy-NV snittet viser lavere verdier mot kysten som er typisk for den norske kyststrømmen over kontinentsokkelen (**Figur 3, Vedlegg 6.1**).  $A_T$ -verdier på 2315-2320  $\mu\text{mol kg}^{-1}$  karakteriserer kjernen av atlantisk vann som strekker seg fra enden av kontinentsokkelen og ut mot de dypere delene av Norskehavet. Biologisk aktivitet reduserer  $C_T$  i de øvre vannmassene og lave konsentrasjoner fortsetter ofte til langt ut på høsten. pH-verdiene var sammenlignbare med tidligere år og varierte fra 8,04-8,05 i de øvre 500 m langs mesteparten av snittet (**Figur 15**). Vann med lav pH (8,01) ble observert på det dypeste punktet i Norskehavet. Metningsgraden for aragonitt varierte fra høyeste verdier ( $\Omega_{\text{Ar}} > 1,8$ ) i den øvre 400 m av vannkolonnen med en avtagende vertikal gradient ned mot metningshorisonten på rundt 2000 m dyp. Vann under 2000 m var undermettet ( $\Omega_{\text{Ar}} < 1,0$ ). **Figur 41** viser aragonittmetningen på forskjellige dyb langs Svinøy-NV ved 1 °E fra 2011 til 2018. Dataene viser mellomårlige variasjoner knyttet til hvor mye kaldt og fersk arktisk vann som var til stede. Den største variasjonen finnes på 1000 m, og dette kan skyldes svingninger i mengden arktisk vann i forhold til varmere atlantisk vann.

Målinger fra Stasjon M (**Figur 18-21; Figur 4, Vedlegg 6.1**) viste sesongvariabilitet i 2018 som tilsvarer det som er observert tidligere år, men med litt endret start for oppblomstringen.  $C_T$  avtok, og pH og aragonittmetningen økte i de øvre vannlag i april på grunn av biologisk aktivitet. Sesongvariasjonene var, som før, større i de øverste vannlag enn på større dyp. Metningshorisonten for aragonitt ble observert omkring 2000 m dyp som tilsvarer det som ble observert i 2017. Dette er noe dypere enn tidligere år og illustrerer variabiliteten i systemet. Trenden over årene 2011 til 2018 fra Stasjon M viser at pH i overflata avtar med 0,0039 enheter pr år mens aragonittmetningen avtar med 0,017 enheter pr år (**Figur 40**). Trendene er sammenlignbare med det som er observert tidligere, med bare små forskjeller Skjelvan *et al.* (2014).

I 2018 ble sesongmålinger fra tre kyststasjoner i Hardanger samlet inn og disse ble satt sammen med historiske data fra tilsvarende område (**Figur 24-33**). Studien viste veldefinert sesongvariasjon for både temperatur og pH i overflatelaget (< 10 m), og et noe mer broket bilde for de øverste 50 m. Dette er knyttet innblanding av elve- og regnvann i det øverste lagdelte vannet, og et mer atlantisk preget signal i dypere vann. pH øker med økende biologisk produksjon, og dybden på den fotiske sonen spiller også en rolle for den observerte variabiliteten i de øverste 50 m.

Kaldvannskoralrev i Hardangerfjorden har store graderenter i de øvre 50 m (figur 56). Ferskvann redusert saltholdig og biologisk opptak redusert  $C_T$  i overflatelaget (< 10 m) med

høy pH 8,05-8,10 og aragonittmetning 1,9. På 50 m, øker  $C_T$  på grunn av biologisk opptak og blanding med karbonrik atlantisk vann under, økt  $C_T$  og oppnådd minimumsverdier for pH og aragonittmetning sammenlignet med resten av vannsøylen.

Målinger fra Skrova kyststasjon i Vestfjorden (*Figur 35-39*) viste sterk sesongvariasjon i de øverste 100 m med oppvarming til 14 °C og ferskere vann om sommeren. pH økte i de øverste 50 m tidlig på sommeren og dette var trolig en kombinasjon av ferskvannsinnstrømming (som reduserer saltholdigheten) og CO<sub>2</sub>-opptak i våroppblomstringen. Aragonittmetningen varierte med vannmasse, primærproduksjon og tilførsel av smeltevann. Sesongvariasjonen er stor sammenlignet med den langsiktige trenden i data (*Figur 43*).

Fordelingen av  $C_T$  langs Gimsøy-NV snittet viser lavere verdier i de øvre 100 m og mot enden av kontinentalsokkelen på grunn av biologiske produksjon (*Figur 5, Vedlegg 6.1*). Verdier av  $A_T$  på 2310-2320 µmol kg<sup>-1</sup> karakteriserer atlantisk vann som strekker seg over snittet. Metningsgraden for aragonitt var høyest ( $\Omega_{Ar} > 1,8$ ) i de øvre 400 m og blir redusert nedover i dypet mot metningshorisonten som ligger på rundt 2000 m dyb i Norskehavet (*Figur 17*). pH og aragonittmetning ved 1500 m ved 12,3 °E fra 2011 til 2018 viser variasjon i forhold til mengden arktisk og varmere atlantisk vann i området (*Figur 42*). Dette tilsvarer det som ble observert langs Svinøy-NV snittet (*Figur 41*).

#### Barentshavet

Fra Barentshavet finnes det i 2018 målinger fra vannkolonna langs snittet Fugløya-Bjørnøya i sørvestlige Barentshavet og langs Vardø-N i nordøstlige Barentshavet (IMR; *Figur 44*). Sistnevnte snittet blir samlet inn i forbindelse med IMR-PINRO Barentshavet økosystem undersøkelser 'ØKOTOKT'. Kystvann nær Fugløya påvirkes av den ferske norske kyststrømmen og i dypet finner vi atlantisk vann (*Figur 6, Vedlegg 6.1*). I nærheten av Bjørnøya påvirkes vannet av polart vann som strømmer sørover fra nordøstre deler av Svalbard, og dette fører til sterke horisontale graderinger i den øvre 200 meter ved Polarfronten som ligger på rundt 73,5 °N. Langs Fugløya-Bjørnøya snittet har atlantisk vann  $A_T$  rundt 2320-2330 µmol kg<sup>-1</sup>, mens kystvann i sør og arktisk vann til nord har lave  $A_T$ -verdier (2280-2290 µmol kg<sup>-1</sup>). Fordelingen av  $C_T$  viste et litt annet mønster, fra laveste konsentrasjoner på 2115-2140 µmol kg<sup>-1</sup> i de øvre 100 m i sør til 2140-2160 µmol kg<sup>-1</sup> for de øvre vannmassene langs snittet. Høy pH (~8,10) ble observert ved den sørlige delen av seksjonen og laveste verdier (8,02-8,04) i bunnvann ved 72-73 °N (*Figur 46*). Aragonittmetningen var lavest (1,4-1,5) dypere enn 300 m ved 73,5 °N og i de øvre 100 m nord for 74 °N. I det nordøstlige Barentshavet ble det funnet atlantisk vann over kontinentalsokkelen i sør med  $A_T$ -verdier rundt 2310-2320 µmol kg<sup>-1</sup> (*Figur 7, Vedlegg 6.1*), noe lavere sammenlignet med det sørlige Barentshavet. Laveste  $C_T$ -konsentrasjoner (< 2100 µmol kg<sup>-1</sup>) ble funnet i de øvre 100 m i sjøis-påvirkede områder nord for 79 °N. Lignende fordelinger i det sørlige og nordlige Barentshavet ble funnet for pH og aragonittmetninger, med høyere verdier i de øvre 100 m i den produktive sjøis-sonen i nord (*Figur 47*).

Temperatur og  $C_T$  konsentrasjon ved 300-400 m dybde fra 2012 til 2018 ved ~72.8 °N langs Fugløya-Bjørnøya snittet viste mellomårlig variasjon knyttet til avstand til polarfronten, som igjen er knyttet til variasjoner i atlantisk vann i sør og arktisk vann i nord (*Figur 53*). Generelt var kaldere vann forbundet med høyere  $C_T$  konsentrasjoner og angir et større volum karbonrikt arktisk vann i 2018. Saltholdighet viste at vannet ved 300-400 m hadde en tendens til å bli ferskere med tiden, noe som støtter nærværet av ferskt polarvann. Dette ble ledsgaget av en reduksjon i aragonittmetningen til laveste verdier på 1,4-1,6 i 2018. Fordelingen av sjøvannstemperatur og saltholdighet ved 250-300 m dybde langs den

nordøstlige delen av Barentshavet viser endringer på  $-0,32\text{ }^{\circ}\text{C yr}^{-1}$  og  $-0,021$ , fra 2012 til 2018 (*Figur 54*). Ved siden av den generelle trenden mot ferskere og kaldere vann viser pH en generell økning på  $0,006\text{ }^{\circ}\text{C yr}^{-1}$ . Aragonittmetningen varierte over årene med en gjennomsnittsverdi på  $1,32 \pm 0,13$ . I likhet med trender på 300-400 m dybde langs Fugløya-Bjørnøya snittet ( $\sim 72,8\text{ }^{\circ}\text{N}$ ), fører tilstedevarerelsen av kaldt, fersk arktisk vann til større variasjon i regionen.

Karbonatkjemi fra overflatevann ble målt i 2018 i Barentshavetsåpningen mellom Tromsø og Longyearbyen, Svalbard (NIVA; *Figur 48*). Ferskvannsproduksjon, biologisk produksjon om sommeren, og sirkulasjon spilte viktige roller i den observerte variabiliteten. Saltholdigheten i det åpne hav var i gjennomsnitt lavest ( $34,56$ ) sør for Bjørnøya om sommeren og høyest ( $35,03$ ) nord for Bjørnøya om vinteren og våren (*Figur 49*). Temperaturen var lav ( $5,38\text{ }^{\circ}\text{C}$ ) om vinteren og økte til  $8,54\text{ }^{\circ}\text{C}$  i gjennomsnitt i det åpne havet nord for Bjørnøya, mens gjennomsnittet var  $5,31\text{ }^{\circ}\text{C}$  om vinteren og  $9,52\text{ }^{\circ}\text{C}$  på sommeren sør for Bjørnøya. Gjennomsnittlig pH for norsk kyst var lavest ( $8,06$ ) om vinteren og høyest ( $8,14$ ) om sommeren (*Figur 50*). Aragonittmetningen var  $1,81$  om vinteren og nådde  $2,32$  i gjennomsnitt i det nordlige åpne havområdet og  $1,78$  om vinteren og  $2,36$  om sommeren i sørlige havområder. Trenger i saltholdighet og temperatur i overflatevann i Barentshavetsåpningen ved  $74\text{--}76\text{ }^{\circ}\text{N}$  viste en saltreduksjon på  $0,013\text{ yr}^{-1}$  og en avkjøling på  $0,083\text{ }^{\circ}\text{C yr}^{-1}$ , ledset av en økning i både pH og  $\Omega$  aragonitt av henholdsvis  $0,003\text{ yr}^{-1}$  og  $0,026\text{ }\text{Å}^{-1}$  (*Figur 52*).

For stasjonene nær kysten av Norge var laveste gjennomsnittlig saltholdighet  $33,79$  sent på høsten og  $34,30$  om vinteren, og temperaturen var  $10,95\text{ }^{\circ}\text{C}$  om sommeren og  $5,32\text{ }^{\circ}\text{C}$  om vinteren, pH var  $8,10$  om sommeren og  $8,06$  om vinteren og aragonittmetning var  $2,30$  om sommeren og  $1,75$  om vinteren. For stasjonene nærmere Svalbard-kysten var gjennomsnittlig saltholdighet lavest på  $33,47$  om sommeren og så høyt som  $35,0$  om vinteren. Temperaturen var  $7,16\text{ }^{\circ}\text{C}$  om sommeren og  $3,80\text{ }^{\circ}\text{C}$  om våren, pH var høyest ( $8,20$ ) om våren og lavest ( $8,05$ ) om vinteren og aragonittmetning var  $2,33$  om sommeren og så lav som  $1,73$  om vinteren.

## 1. Introduction

In 2013 a marine acidification program was established by the Norwegian Environment Agency. The background for the initiative was based on the fact that the global oceans currently absorb about 25% of the anthropogenic carbon dioxide ( $\text{CO}_2$ ) emitted annually from combustion of fossil fuels and deforestation (e.g., Takahashi et al., 2009; Le Quéré et al., 2016; 2018). Oceanic uptake of  $\text{CO}_2$  affects the inorganic carbon system of the ocean, with a subsequent reduction in seawater pH and the saturation state of calcium carbonate minerals, e.g. aragonite and calcite. Ocean acidification is occurring at a higher rate compared to changes determined during the last 55 million years. It is expected that ocean acidification will affect the structure and function of numerous marine ecosystems, and thus also have significant consequences for harvestable marine resources. Therefore, it is important to monitor the degree of ocean acidification.

The northernmost Norwegian seas have a naturally high content of inorganic carbon, and in addition, the low temperatures enhance the  $\text{CO}_2$  solubility in seawater. Oceanic uptake of atmospheric  $\text{CO}_2$  leads to an increased concentration of hydrogen ions and lower availability of carbonate minerals in seawater. As a result, the content of carbonates in polar waters is low compared to more southern areas, and we expect the higher latitude seas will be the first

regions to experience lower levels of seawater carbonates as a result of ocean acidification. For example, the Arctic Ocean will become undersaturated with respect to calcium carbonate during this century if CO<sub>2</sub> emissions continue as they are today (AMAP 2013; Steinacher et al., 2009).

The ocean carbonate system is an important part of the global carbon cycle. About 90% of the inorganic carbon in the ocean is in the form of hydrogen carbonate (HCO<sub>3</sub><sup>-</sup>), 9% is in the form of carbonate (CO<sub>3</sub><sup>2-</sup>) and about 1% exists as dissolved CO<sub>2</sub>. When CO<sub>2</sub> from the air is absorbed by the sea, the gas becomes dissolved in the seawater and carbonic acid (H<sub>2</sub>CO<sub>3</sub>) is formed. This also causes hydrogen ions (H<sup>+</sup>) to be released. Carbonic acid is rapidly transformed into hydrogen carbonate and carbonate ions, which are naturally present in the seawater and form the so-called carbonate system (Eq.1).



Overall, uptake of CO<sub>2</sub> by the ocean leads to increases in the hydrogen ion concentration and decreases the availability of carbonate minerals in seawater. This results in a decrease in seawater pH, thus the process has been called ocean acidification. The pH of the global oceans is generally around 8, but the natural variations are large and are influenced by, for example, temperature, primary production, respiration and physical processes like mixing of different water masses. It is worth noting that the oceans will not become acidic (pH lower than 7) but rather it will become less basic. In the marine environment, it is the reduction of available carbonates that creates the most concern. Carbonate forms an important building block for many marine organisms, primarily those with calcium scales and shells, and calcium carbonate is formed only biologically (Eq. 2) while the dissolution is a chemical process (Eq. 3). When large quantities of CO<sub>2</sub> are absorbed, the concentration of carbonate ions (CO<sub>3</sub><sup>2-</sup>) in seawater is reduced, and then calcium carbonate (CaCO<sub>3</sub>) is likely to dissolve and the shells of some organisms becomes chemically unstable (Orr et al., 2005).



Organisms with calcium carbonate (chalk) shells and skeletons will have reduced ability to survive when carbonate concentration is reduced as a result of CO<sub>2</sub> uptake. According to Talmange and Gobler (2009), Andersen et al. (2013) and Agnalt et al. (2013), ocean acidification can weaken a number of economically important shellfish species, and Mortensen et al. (2001), Turley et al. (2007) and Järnegren and Kutti (2014) show that this could also be the case for the large deposits of cold water corals that are found along the Norwegian coast. It has also been found that non-calcareous organisms can be adversely affected by changes in CO<sub>2</sub> or low pH. Further, there are also organisms that respond positively to high CO<sub>2</sub> content and low pH (Dupont and Pörtner, 2013). It is therefore difficult to predict which organisms will be the most effected to changes in ocean chemistry and pH, and thus, it is very important to study the natural variations of the ocean carbonate system in

order to monitor the development of carbonate concentration and the saturation state of the two most common types of calcium carbonate in the ocean; aragonite and calcite.

## 2. Methods and Data

The aim of the Ocean Acidification (OA) monitoring program is to get an overview of the status and development of OA in Norwegian waters. The program will facilitate future monitoring of the effects of OA on marine ecosystems. Most of the data is available in international databases such as CDIAC (<http://cdiac.ornl.gov/oceans/CARINA/>) and SOCAT ([www.socat.info](http://www.socat.info)). The data are also published in the database “Vannmiljø” ([www.vannmiljo.miljodirektoratet.no](http://www.vannmiljo.miljodirektoratet.no)) of the Norwegian Environment Agency, as well as archived in the Norwegian Marine Data Centre (NMDC).

In 2017, the OA monitoring program and the Ecosystem Monitoring in Coastal Water (ØKOKYST) program coordinated the monitoring activities, based on the need to increase the climate relevance of the latter program. ØKOKYST aims to monitor the environmental status of selected areas along the Norwegian coast. This effort included monthly sample collection of macronutrients (ammonia, phosphate, nitrate, silicate, total nitrogen and total phosphorous), chlorophyll-a concentration, and dissolved organic carbon on 9 stations using FerryBox on MS *Trollfjord* and MS *Color Fantasy*. This monitoring also included continuous FerryBox data for temperature, salinity and chlorophyll-a fluorescence among others. The reporting, however, has been done separately in the ØKOKYST reports, and will not be repeated in this report, but some chlorophyll-a fluorescence data has been used to discuss the seasonal variation in carbonate chemistry. Similar coordination of sampling has been arranged for the seasonal monitoring at Arendal and Skrova coastal stations.

**Table 1**  
A summary of transects and cruises where sampling was performed in 2018.

Section/station (sample type)	Sampling month	Depth	Parameters	Institution	Financing
Torungen-Hirtshals (discrete)	January	Water column	A <sub>T</sub> , C <sub>T</sub>	IMR	Environment Agency
Svinøy-NW (discrete)	January	Water column	A <sub>T</sub> , C <sub>T</sub>	IMR	Environment Agency
Gimsøy-NW (discrete)	May, June	Water column	A <sub>T</sub> , C <sub>T</sub>	IMR	Environment Agency
Fugløya-Bjørnøya (discrete)	January	Water column	A <sub>T</sub> , C <sub>T</sub>	IMR	Environment Agency
NE Barentshav (discrete)	August, September	Water column	A <sub>T</sub> , C <sub>T</sub>	IMR	Environment Agency/ FRAM
Tromsø-Longyearbyen/ Ny-Ålesund (discrete)	March, June, August, November	Surface	A <sub>T</sub> , C <sub>T</sub> , pH (March, June)	NIVA	Environment Agency/ FRAM
Bergen-Kirkenes (continuous)	January-September	Surface	A <sub>T</sub> , C <sub>T</sub> , pH (February, May)	NIVA	Environment Agency
Oslo-Kiel (discrete)	February, May, August, November	Surface	A <sub>T</sub> , C <sub>T</sub> , pH (February, May)	NIVA	Environment Agency
Station M (discrete)	January, April, May x 2, August, November	Water column	A <sub>T</sub> , C <sub>T</sub>	NORCE/UiB	Environment Agency
Coastal station Skrova (discrete)	January - November	Water column	A <sub>T</sub> , C <sub>T</sub>	IMR	Environment Agency
Coastal station Arendal (discrete)	January - November	Water column	A <sub>T</sub> , C <sub>T</sub>	IMR	Environment Agency
Station M (continuous)	January-May, November-December	Surface, subsurface	pCO <sub>2</sub> , pH	NORCE/UiB	Environment Agency /RCN/EU
Coastal stations Hardanger (discrete)	January, April, August, November	Water column	A <sub>T</sub> , C <sub>T</sub>	NORCE/UiB	Environment Agency /RCN/EU
Cold water coral reefs (discrete)	May, July (April, October 2017)	Water column	A <sub>T</sub> , C <sub>T</sub>	IMR	Environment Agency

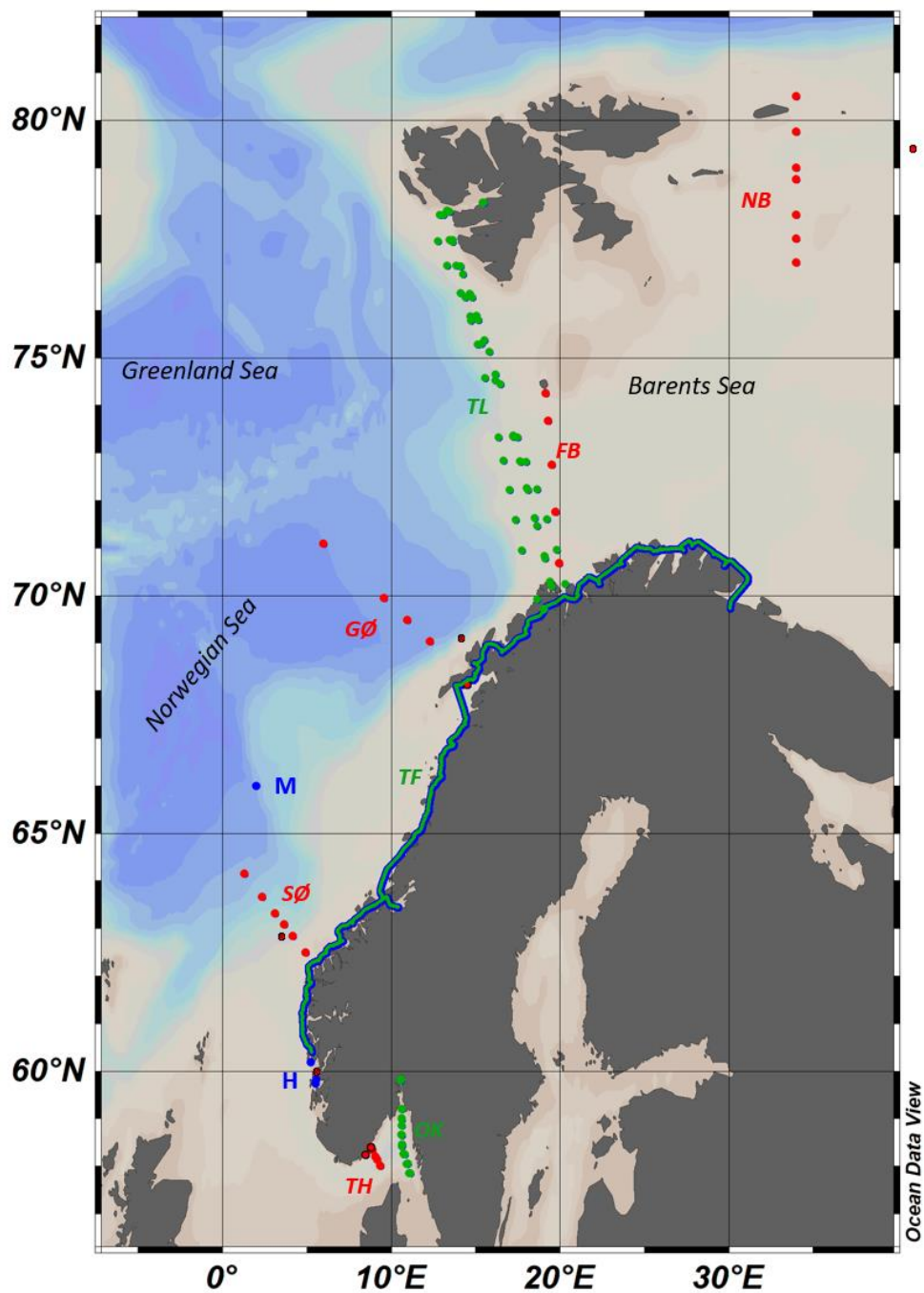


**Figure 1.** Map showing positions of data in the programs Ocean Acidification Monitoring 2018. Red dots show transects where IMR sampled the water column; TH=Torungen-Hirtshals, SØ=Svinøy-NW, GØ=Gimsøy-NW, FB=Fugløya-Bjørnøya, NB=stations in the northeast Barents Sea. Red dots with black outline show the coastal stations Arendal in the south and the Skrova in the north. Red dots with black cross show the cold water coral reefs in Hardangerfjord in the south, Aktivneset, and Hola in the north. Green dots are stations where NIVA has collected surface samples; OK=Oslo-Kiel, TL=Tromsø-Longyearbyen. Green-blue line along the coast indicate NIVA's Trollfjord transect for pCO<sub>2</sub> measurements. Blue dots indicate where NORCE and UiB have sampled the water column; M=Station M, H=Hardanger coastal stations.

**Figur 1.** Kart over stasjoner som har inngått i programmene Havforsuringsovervåkningen i 2018. Røde prikker viser snitt der IMR har tatt prøver fra hele vanndypet; TH=Torungen-Hirtshals, SØ=Svinøy-NV, GØ=Gimsøy-NV, FB=Fugløya-Bjørnøya, NB=stasjon i nordøstlige Barentshav. Røde prikker med svart kant viser kyststasjoner; Arendal i sør og Skrova i nord. Røde prikker med svart kors viser korallrevene i Hardangerfjord i sør, Aktivneset og Hola i nord. Grønne prikker viser NIVA sine overflatestasjoner; OK=Oslo-Kiel, TL=Tromsø-Longyearbyen. Grøn-blå linje langs kysten viser NIVAs Trollfjord-linje med preliminære pCO<sub>2</sub> data. Blå prikker viser hvor NORCE og UiB har tatt prøver fra hele vanndypet; M=Stasjon M, H=Hardanger kyststasjoner.

Positions for fixed sections, transects and fixed stations that are part of the measurement program in 2018 are shown in **Figure 1**. The Institute of Marine Research (IMR) has conducted regular sections in the Skagerrak region of the North Sea/Skagerrak (Torungen-Hirtshals), the Norwegian Sea (Svinøy-NW, Gimsøy-NW), and in the Barents Sea (Fugløya-Bjørnøya) and in the northeastern Barents Sea. In addition, monthly sampling was carried out at the coastal stations at Arendal and Skrova, which is a collaboration with the ØKOKYST program (Environment Agency). In 2018, the NORCE Norwegian Research Centre (NORCE) and University of Bergen (UiB) conducted continuous and discrete measurements at Station M and seasonally measurements at three stations in Hardanger. NIVA has measured transects in the Barents Sea opening (Longyearbyen-Tromsø), Norwegian coast (Bergen-Kirkenes) and in Skagerrak (Oslo-Kiel).

The Environment Agency has funded the sampling activities presented in this report but the participants in the program have also contributed data and expertise from other projects. The Fram Center Flag Ship for Ocean Acidification program funded parts of the Barents Sea opening cruises on MS *Norbjørn* and during previous years NIVA's activities related to ocean acidification (OA-SIS) have funded the technology development. For IMR, there are two projects in the Flag Ship for "Ocean acidification and ecosystem effects in Norwegian waters" at the Fram Center and IMR's ecosystem surveys program that provides expertise and infrastructure that is included in the 2018 report.

## 2.1 Sampling and Variables

This project uses internationally recognized methods and procedures for seawater sampling and instrumentation, as described in Dickson et al. (2007); Guide to Best Practices for Ocean CO<sub>2</sub> Measurements. Following the previous report (Jones et al., 2018), sampling of the water column at fixed sections was performed by IMR aboard the IMR vessel FF GM Dannevig in the North Sea/Skagerrak, FF Kristine Bonnevie in the Norwegian Sea and FF Johan Hjort and RV Kronprins Haakon in the Barents Sea.

NORCE-UiB collected samples from the full water column at Station M in the Norwegian Sea using IMR research vessels FF *Johan Hjort*, FF *Kristine Bonnevie*, FF G.O. Sars and FF Lance and the three western coastal stations in Hardanger were operated by RV *H. Brattstrøm*. From these stations, hydrography, C<sub>T</sub>, A<sub>T</sub>, and nutrients were measured. In addition, NORCE-UiB was responsible for continuous surface and sub-surface measurements at Station M, and the surface measurements covered pCO<sub>2</sub> in sea and atmosphere, as well as pH, dissolved oxygen, and hydrography. In sub-surface water, pH and hydrography was continuously determined.

NIVA collected surface water samples manually on Ships of Opportunity equipped with FerryBoxes between Tromsø and Longyearbyen on the cargo ship MS *Norbjørn* and between

Oslo and Kiel on the cruise ship *MS Color Fantasy*. Continuous measurements of pCO<sub>2</sub> were obtained for shorter periods on *MS Norbjørn* and *MS Color Fantasy*, in addition to the coastal ferry *MS Trollfjord* that operates between Bergen and Kirkenes. The chlorophyll-a fluorescence sensor data was corrected for biofouling and calibrated using the chlorophyll-a measured from water samples.

The carbonate system in seawater can be described using four measurable parameters: total alkalinity ( $A_T$ ), total inorganic carbon ( $C_T$ ), pH, and the partial pressure of CO<sub>2</sub> (pCO<sub>2</sub>).  $A_T$  is a measure of the capacity of seawater to neutralize acid (buffer capacity) and consists of the sum of the bases of the solution formed by weak acids (Eq. 4, Appendix 6.3). In seawater, carbonates and hydrogen carbonate form the largest part of these bases.  $C_T$  is defined as the sum of carbonic acid and dissolved CO<sub>2</sub> in water (CO<sub>2</sub>\*), carbonates and hydrogen carbonates (Eq. 5, Appendix 6.3). The acidity or pH of seawater indicates the concentration of hydrogen ions (H<sup>+</sup>) (Eq. 6, Appendix 6.3). The pCO<sub>2</sub> is defined as the ratio of dissolved CO<sub>2</sub>\* concentration in water and solubility of CO<sub>2</sub> gas,  $K_0$  (Eq. 7, Appendix 6.3).

Throughout the report we have used pCO<sub>2</sub> for the partial pressure of CO<sub>2</sub>. In fact, fCO<sub>2</sub>, which is the fugacity of CO<sub>2</sub>, is measured, which takes into account that fact that CO<sub>2</sub> does not behave as an ideal gas. The difference between pCO<sub>2</sub> and fCO<sub>2</sub> is around 0.3%. In order to avoid the effects of continued biological activity in the water sample after it is collected, which will shift the balance of organic and inorganic carbon, water samples for  $C_T$  and  $A_T$  are fixed with saturated mercury chloride solution. In addition, the samples are stored in the dark at approx. 4 °C before being analysed. Discrete pH analyses were made immediately after sampling (NIVA).

## 2.2 Measurements of Total Alkalinity and Total Inorganic Carbon

Measurements of  $C_T$  and  $A_T$  were performed on water column samples from the sections Torungen-Hirtshals, Svinøy-NW, Gimsoy-NW, Fugløya-Bjørnøya, northeastern Barents Sea, Arendal coastal station, Skrova coastal station, from station M, from stations in Hardanger and from surface water during the crossing Tromsø-Longyearbyen and Oslo-Kiel. The samples were analyzed by IMR, NORCE-Uib and NIVA with VINDTA 3C (Marianda, Germany) and CM5011 coulometer (UIC instruments, USA). The measured values were calibrated against certified reference material (CRM) for quality assurance and as an accuracy check for all data (Certified Reference Material, CRM, A. Dickson, SIO, USA).

Sodium chloride salt is added to the hydrochloric acid for the  $A_T$  titration to be comparable to the ionic strength of natural seawater, about 0.7M. The pH electrodes used by all groups are adapted to seawater samples with high ionic strength (Metrohm 6.0259.100). The VINDTA instruments at IMR and NORCE-Uib use 20 ml and 100 ml sample volume for  $C_T$  and  $A_T$ , respectively. NIVA uses approximately 250 ml in total for  $A_T$ ,  $C_T$ , salinity and cleaning between samples. In the  $A_T$  titrations, semi-open titration cells are used at all three institutions. Equivalence points were calculated using a curve fit method recommended by Dickson et al. (2007). The analysis method for determining  $C_T$  concentrations is described in Johannessen et al. (2011).

## 2.3 pH Measurements

NIVA used the spectrophotometric pH method onboard for determining in situ pH on the total scale ( $\text{pH}_T$ ). In situ pH was calculated using CO2SYS from  $\text{pH}_T$  at in situ temperature, salinity and pressure (Pierrot et al., 2006). The measurements were performed on a HACH DR-2800 field spectrophotometer (5 cm cuvette) using m-cresol purple as the indicator dye in two concentrations and measurement from 434, 578 and 730 nm were used in calculations (SOP 6B; Dickson et al., 2007). Two replicates were measured for each sample. A potentiometric pH (Metrohm 680 pH-meter) was also measured on the NBS scale ( $\text{pH}_{\text{NBS}}$ ). The manual spectrophotometric pH measurements will be replaced with automatic spectrophotometric pH in the following years of the monitoring program.

NORCE-UiB measured *in situ* pH on the total scale using a spectrophotometric pH sensor from Sunburst Technologies, USA; the Submersible Autonomous Moored Instrument (SAMI2-pH). An indicator (*meta*-cresol-purple; *mCP*) is mixed with seawater flowing through a cuvette, the pH of the seawater induces a colour change of the mixture and this is detected by a spectrophotometer. pH is calculated based on the detected colour change. This sensor was used at Station M.

## 2.4 pCO<sub>2</sub> Measurements

NORCE-UiB measured surface pCO<sub>2</sub> using infra-red (IR) technology. Measurements of pCO<sub>2</sub> are made every 3<sup>rd</sup> hour using an instrument from Battelle Memorial Institute, USA; the MAPCO<sub>2</sub> system, which utilizes an air-water bubble equilibrator to extract CO<sub>2</sub> from the surface water. The gas is determined by a LI-820 IR detector, which is frequently calibrated by running a span reference gas (NOAA/ESRL) in addition to a zero-reference gas through the system, the pCO<sub>2</sub> in atmosphere is also measured by the IR detector.

The membrane based Franatech/NIVA pCO<sub>2</sub> sensors were deployed on three FerryBox lines MS *Trollfjord*, MS *Norbjørn* and MS *Color Fantasy*. The sensors were updated by the manufacturer in 2017 with new infra-red CO<sub>2</sub> detectors (Gassmitter, Sensors Europe GmbH, Germany) with a lower volume equilibrium chamber, and new check valves and pressure regulators. This new sensor has been used on MS *Norbjørn* and MS *Fantasy* while MS *Trollfjord* still uses the old solid-state detector from 2018. Improvements have been made to the flow, so it is now possible to have a higher water volume throughput that improves the measurements. In 2018, the sensors were brought back for further testing and calibration in the laboratory and were therefore not operational for the whole year. This work included design of a new gas calibration system that can be used regularly onboard the ships. A set of 3 AGA CO<sub>2</sub> gases (with nominal CO<sub>2</sub> concentrations approx. 200, 400, 800 ppm) and nitrogen (0 ppm CO<sub>2</sub>) are calibrated with NOAA references gas (297.31, 547.41, 735.97). Again, this resulted in periods without operation of the sensors on the ships. Some of this work was carried out at the NIVA Research Station at Solbergstrand on a stationary FerryBox setup where a new calibration laboratory is built.

## 2.5 Calculation of pH and Saturation State of Calcite and Aragonite

If two out of the four measurable parameters ( $C_T$ ,  $A_T$ , pH and  $pCO_2$ ) are known then others can be calculated, which includes the saturation states ( $\Omega$ ) of calcium carbonate biominerals: calcite ( $\Omega$  calcite) and aragonite ( $\Omega$  aragonite). The degree of saturation is an indicator of the concentration of carbonates in the water, where  $\Omega > 1$  means the water is over-saturated with respect to carbonate. If  $\Omega < 1$  then the seawater is undersaturated with carbonate and the chemical environment is therefore unfavorable to organisms with carbonate shells, such as winged snails or coral reefs.

To calculate all of the carbon parameters, the chemical model CO2SYS is used (Pierrot et al., 2006). The primary couple of parameters used are  $A_T$  and  $C_T$  alongside temperature, depth (pressure), salinity, phosphate and silica as input values for CO2SYS and the output includes in situ pH,  $pCO_2$ , and saturation for calcite and aragonite. In these calculations, carbonic acid constants from Mehrbach et al. (1973), modified by Dickson and Millero (1987), were used. The pH is given in total scale ( $pH_T$ ) and the constant for  $HSO_4^-$  from Dickson (1990) and in situ temperature is used in the pH calculations. Calcium ion concentration ( $[Ca_2^+]$ ) was assumed to be proportional to the salinity (Mucci, 1983), and corrected for pressure according to Ingle (1975). NIVA measures pH directly in addition to using calculated pH derived from  $A_T$  and  $C_T$  in the CO2SYS program.

## 3. Results

### 3.1 Skagerrak

#### 3.1.1 Spatial variability along Torungen-Hirtshals section

In the Skagerrak region, measurements have been made at six hydrographic stations along the Torungen-Hirtshals section in January 2018 (*Figure 2*). This region is strongly affected by the warm and salty Atlantic water (red) and fresh coastal waters (green, *Figure 3*) that characterize the oceanic conditions. Position, depth and sampling data are displayed in *Table 1, Appendix 6.2*.

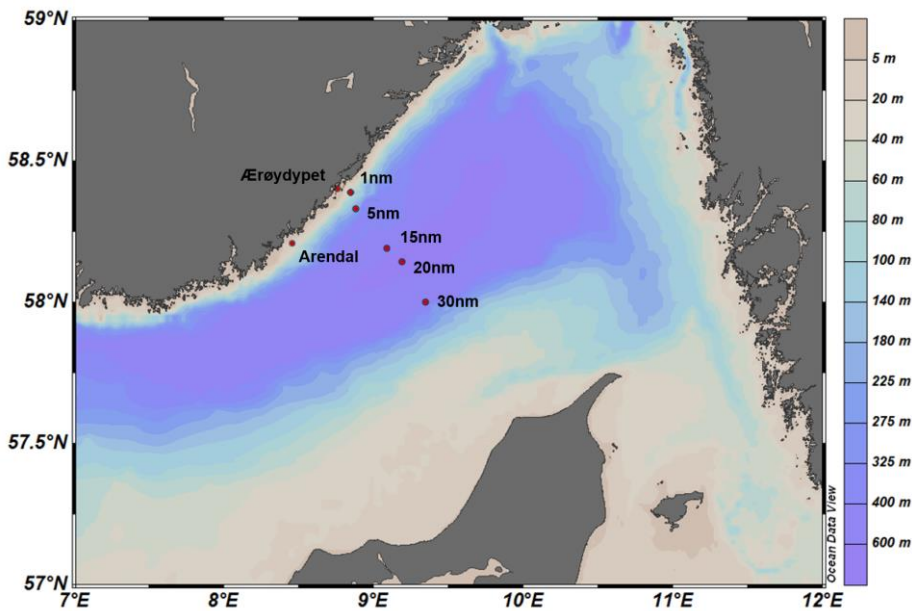


**Figure 2.** Stations from the Torungen-Hirtshals section in January 2018 and Arendal coastal station.

**Figur 2.** Stasjoner fra Torungen-Hirtshals snittet i januar 2018 og Arendal kyststasjon.

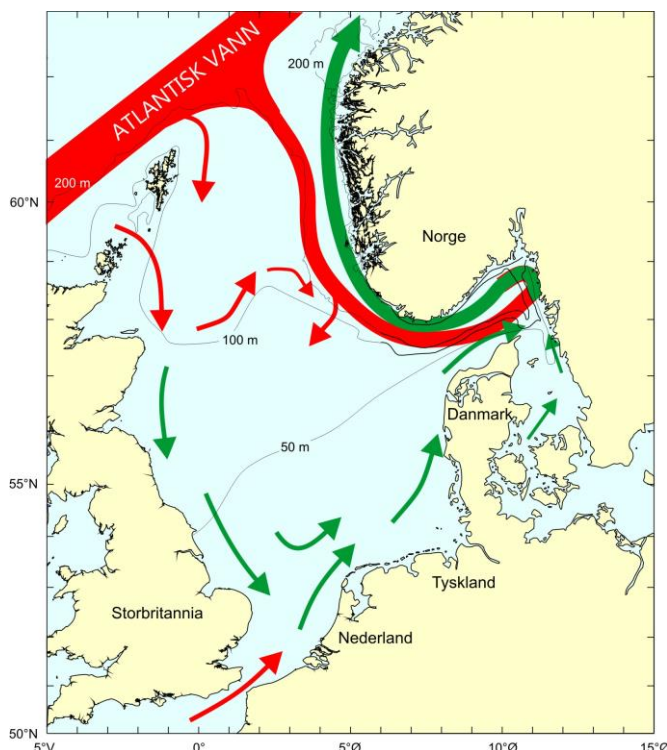


**Figure 3.** Schematic map of the main currents in the North Sea and Skagerrak regions. The red arrows indicate the influx of Atlantic water, mostly at 100-200 m, while the green arrows indicate the main circulation patterns of coastal waters, typically in the top 20m ([www.imr.no](http://www.imr.no)). The Norwegian coastal current receives inputs from the southern North Sea and the Baltic Sea.

**Figur 3.** Skjematiske kart over de viktigste transportveiene i Nordsjøen og Skagerrak. De røde pilene indikerer innstrømning av atlantisk vann, for det meste i 100-200 m dyp, mens de grønne pilene angir hovedretningene til sirkulasjon av kystvann, typisk beliggende i de øverste 20m ([www.imr.no](http://www.imr.no)). Kyststrømmen får tilførsler fra Nordsjøen og Østersjøen.

Winter data from January 2018 show high pH values in the upper 50 m of the water column that reached maxima (8.10-8.11) towards the Norwegian and Danish coasts (**Figure 4**). This high pH is due to the low  $C_T$  and  $A_T$  values in the surface waters, particularly close to the Norwegian coast, due to the influence of freshwater (**Figure 1, Appendix 6.1**). The pH decreases with depth with stronger vertical gradients between 50-200 m due to the presence of warm Atlantic water. Low pH (7.88) occurred at 100-200 m depth over the Norwegian shelf and at 600 m depth (pH 7.96) in the central part of the section. This corresponded to highest values of  $C_T$ , which is likely due to remineralization of exported organic matter out of productive coastal waters and the presence of an older water mass enriched with  $CO_2$  from respiration, respectively.

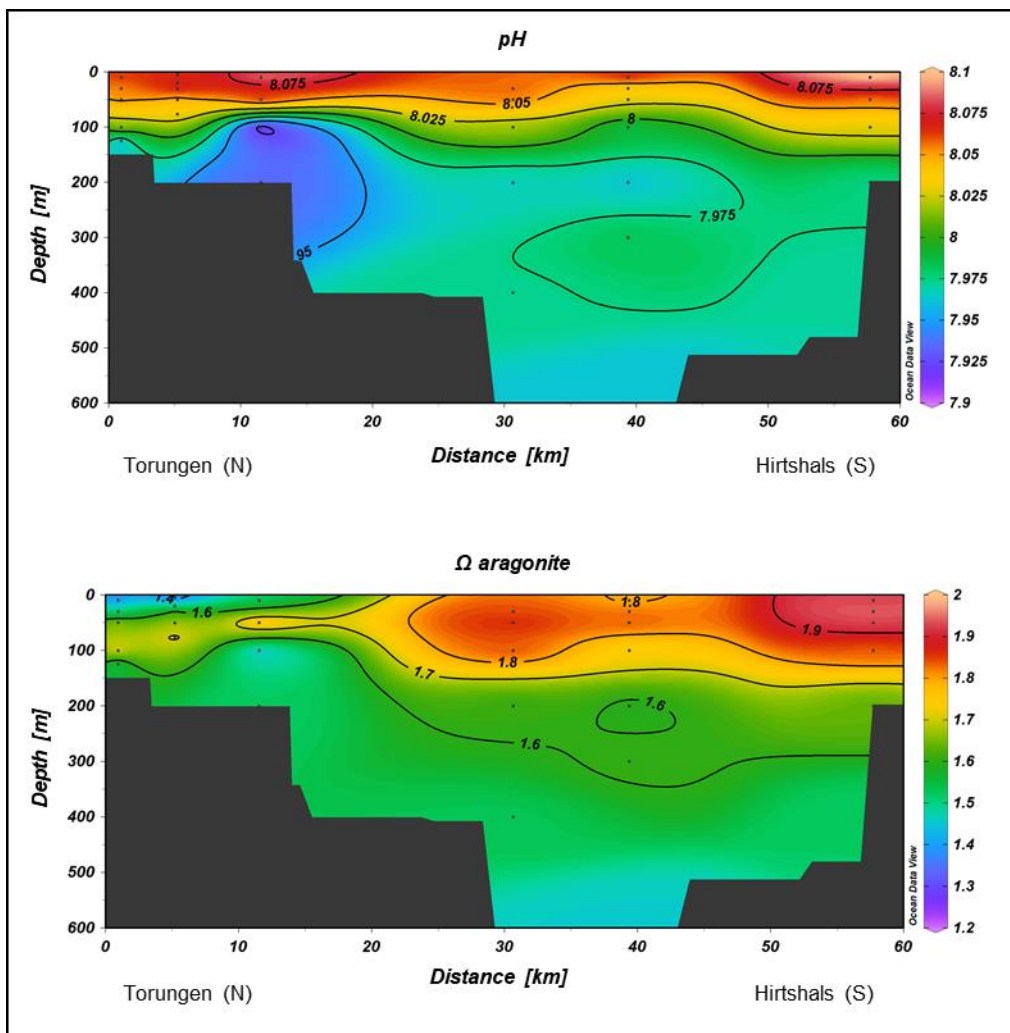


**Figure 4.** pH and aragonite saturation state along the Torungen-Hirtshals section in January 2018.

**Figur 4.** pH og aragonittmetningsgrad langs snittet Torungen-Hirtshals i januar 2018.

The distribution of the saturation state for aragonite (and calcite, not shown) in 2018 had maximum values ( $\Omega$  aragonite up to 1.96) in surface layer at the Danish coast. In contrast, low saturation states ( $\Omega$  aragonite of 1.26) occurred in the freshest surface waters close to the Norwegian coast. Within the Atlantic water,  $\Omega$  aragonite was around 1.7 and saturation states decreased with depth to low values close to 1.5 at 600 m depth.

### 3.1.2 Seasonal variability at Arendal station

Measurements were made at Arendal coastal station by IMR from January to November 2018 (*Figure 1*). Position, depth and sampling data are displayed in *Table 2, Appendix 6.2*. This region of the Skagerrak is strongly influenced by the fresh coastal waters in the upper 20 m and the warm and salty Atlantic water at 100-200 m depth offshore (*Figure 2, Appendix 6.1*).

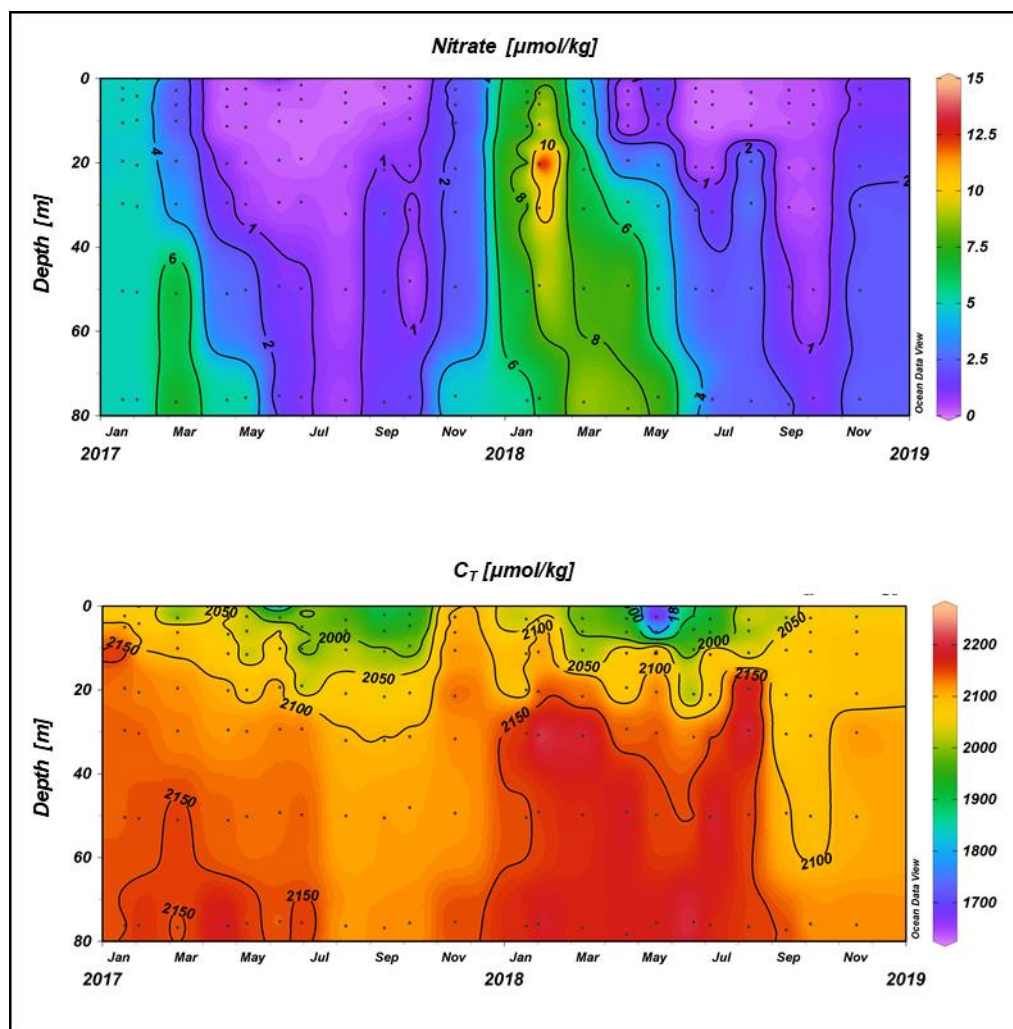


**Figure 5.** Monthly nitrate and  $C_T$  in the upper 80 m at Arendal coastal station in 2017-2018. Black dots indicate sample depths.

**Figur 5.** Månedlig nitrat og totalt uorganisk karbon i de øverste 80 m ved Arendal kyststasjon i 2017-2018. Svarte prikker viser prøvedyp.

The distribution of temperature in 2018 shows that during the winter, the whole water column is relatively well mixed and cold at 2-6°C. The seasonal variability of salinity showed increases in the upper part of the water column due to mixing of surface waters with the underlying salty Atlantic water. Reduced salinity in the upper 20 m in March and May is likely due to enhanced freshwater input from rivers and rainfall and higher inputs from the cold and fresh coastal current. Seasonal warming from early May stratifies the surface layers with increased temperatures from June until October, reaching 19 °C in July. The extent of the warming reaches the full water column as 10-14 °C occurred at 70-80 m depth.

Further insights into seasonal variability can be obtained by looking at the full time series data at Arendal station, for the years 2017 and 2018. Colder winter temperatures in the upper 30 m in 2018 compared to 2017 reflect the natural variability in freshwater inputs and the coastal current at this location. This was also reflected in salinity, as lower salinity was recorded in the upper 20 m from March to May 2018. The water column was less stratified in summer 2017 compared to summer 2018, with temperatures greater than 14°C extending to 80 m depth. In summer 2018, higher temperatures were recorded in the surface layer.

Higher concentrations of  $C_T$  (2160-2230  $\mu\text{mol kg}^{-1}$ ) and nitrate (5-15  $\mu\text{mol kg}^{-1}$ ) were found below 40 m depth from incursions of Atlantic water from below (*Figure 5*). This was particularly notable from January to May, as nitrate concentrations were enriched in the whole water column from deep winter mixing with the Atlantic water. Biological production in spring and summer reduced  $C_T$  to less than 2100  $\mu\text{mol kg}^{-1}$ , alongside depletion of nitrate, in the upper 20 m. Minimum values of  $C_T$  of ~1650  $\mu\text{mol kg}^{-1}$  occurred in the surface layer due to a combination of biological uptake and effects of fresh coastal water.

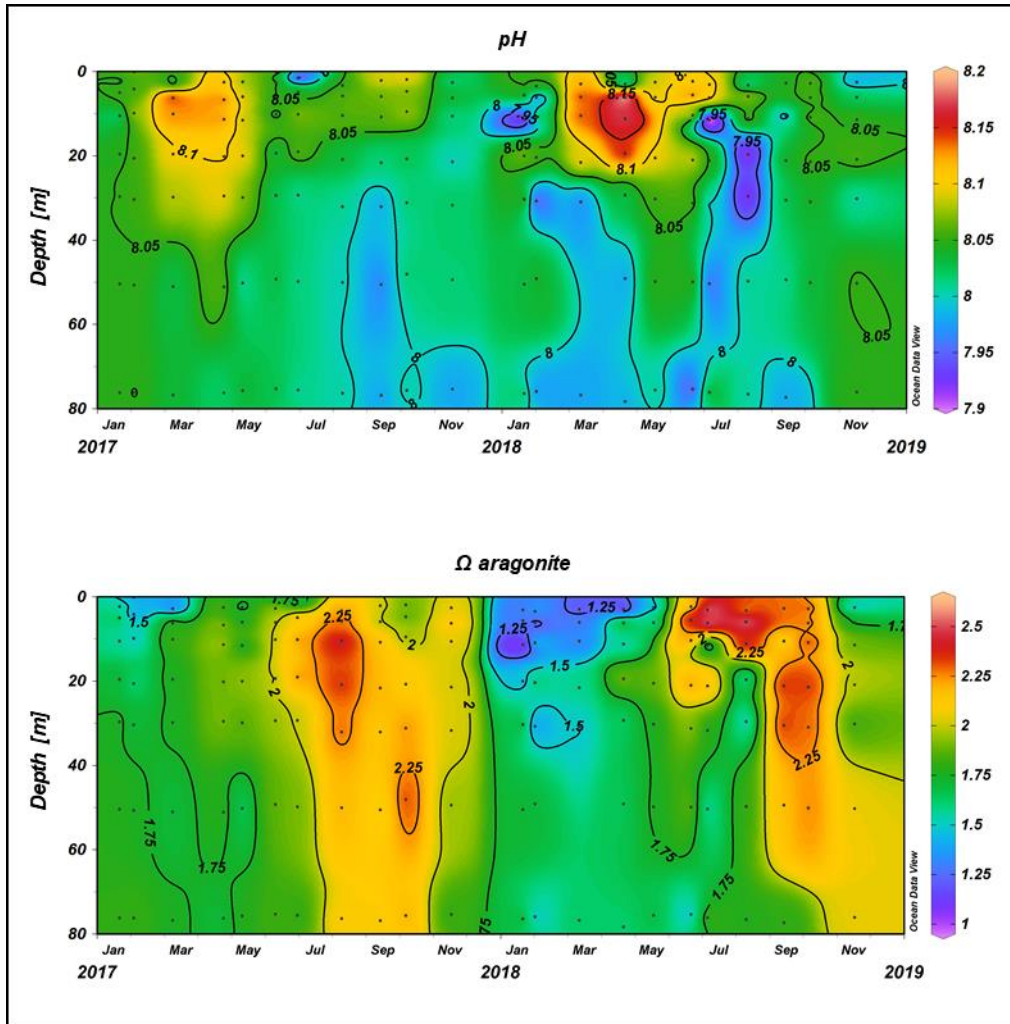


**Figure 6.** Monthly pH and aragonite saturation state in the upper 80 m at Arendal coastal station in 2017-2018. Black dots indicate sample depths.

**Figur 6.** Månedlig pH og metningsgrad av aragonitt i de øverste 80 m ved Arendal kyststasjon i 2017-2018. Svarte prikker viser prøvedyp.

High pH ( $> 8.1$ ) was found in the upper 20 m with maximum values in spring and summer (Figure 6). The influence of Atlantic water could be distinguished by lower pH ( $< 7.9$ ) water being projected upwards in the water column. The saturation state for aragonite (and calcite, not shown) was highest ( $\Omega$  aragonite up to 2.6) in summer surface water. The saturation state was reduced at the sea surface to minimum values ( $\Omega$  aragonite  $< 1.5$ ) during the winter, with undersaturation ( $\Omega$  aragonite of 0.86) at 10 m during January. Reductions in pH and  $\Omega$  aragonite at the sea surface in 2017 and 2018 occurred within periods of lower salinity from freshwater inputs and natural variability in the coastal current at this location. The less stratified water column in summer 2017 had higher saturation levels compared to summer 2018.

### 3.1.3 Seasonal variability in surface water

The stations covered using *MS Color Fantasy* going between Oslo-Kiel are shown in **Figure 7**. Position, depth and sampling data are displayed in **Table 13, Appendix 6.2**. The Skagerrak is influenced by freshwater runoff and riverine inputs, Atlantic water and Baltic water. The three northernmost stations cover the Oslofjord, where Oslo is situated at about 60 °N.

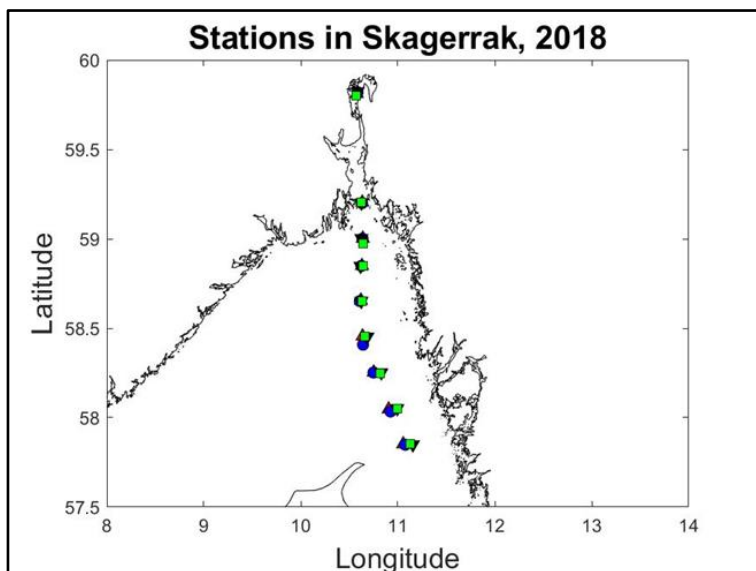


**Figure 7.** Stations from Oslo-Kiel in 2018. 18.2 (red ▲); 23.5 (blue ●); 5.8 (black ▼) ; 1.11 (green ■).

**Figur 7.** Stasjonskart for snittet mellom Oslo-Kiel, 18.2 (rød ▲), 23.5 (blå ●), 5.8 (sort ▼) og 1.11 (grønn ■).

The seasonal variation of temperature and salinity since 2012 is shown in **Figure 8**. The average temperature for the Skagerrak area reached 4.04 °C in the winter and increased to 19.78 °C in summer. Freshwater had a strong influence during spring and summer, with especially low salinities in outer Oslofjord in May, as low as 12.28. The average salinity for the Skagerrak region was 21.35 in spring and 30.97 in late autumn (November).

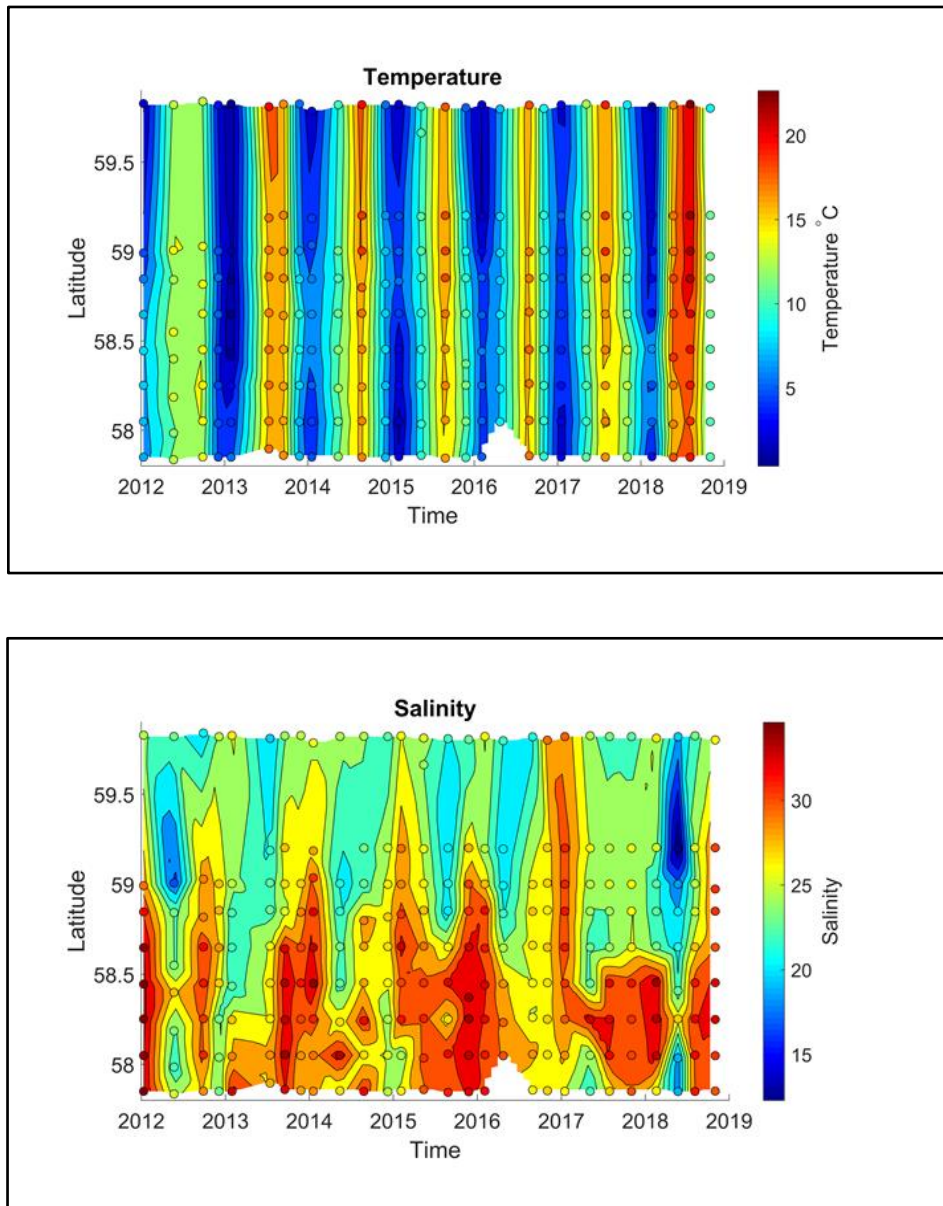


**Figure 8.** Salinity and sea surface temperature in the Oslofjord and Skagerrak. The circles show the measured values, while the interpolated values are shown in the background.

**Figur 8.** Saltholdighet og temperatur i overflatelaget i Oslofjorden og Skagerrak. Ringene viser målte verdier, mens interpolerte verdier vises i bakgrunnen.

The seasonal variation of pH and aragonite saturation state (calculated from  $A_T$  and  $C_T$ ) since 2012 is shown in **Figure 9**. The pH showed small seasonal variations in 2018, with the exception of outer Oslofjord in May where the influence of freshwater lowered pH to 7.83. The average pH for the Skagerrak region was highest (8.10) during late autumn (November), and was at its lowest during spring (8.04). The aragonite saturation reached the lowest state during winter and had higher values during summer and autumn. The saturation was as low as 1.39 on average in the Skagerrak during winter and as high as 2.59 during autumn. The inner Oslofjord was undersaturated ( $\Omega_{\text{Ar}} < 1$ ) with respect to aragonite in winter, and likewise the outer Oslofjord during the event with very low salinity in May. On average, the whole Oslofjord was very low (1.05) in aragonite saturation during winter.

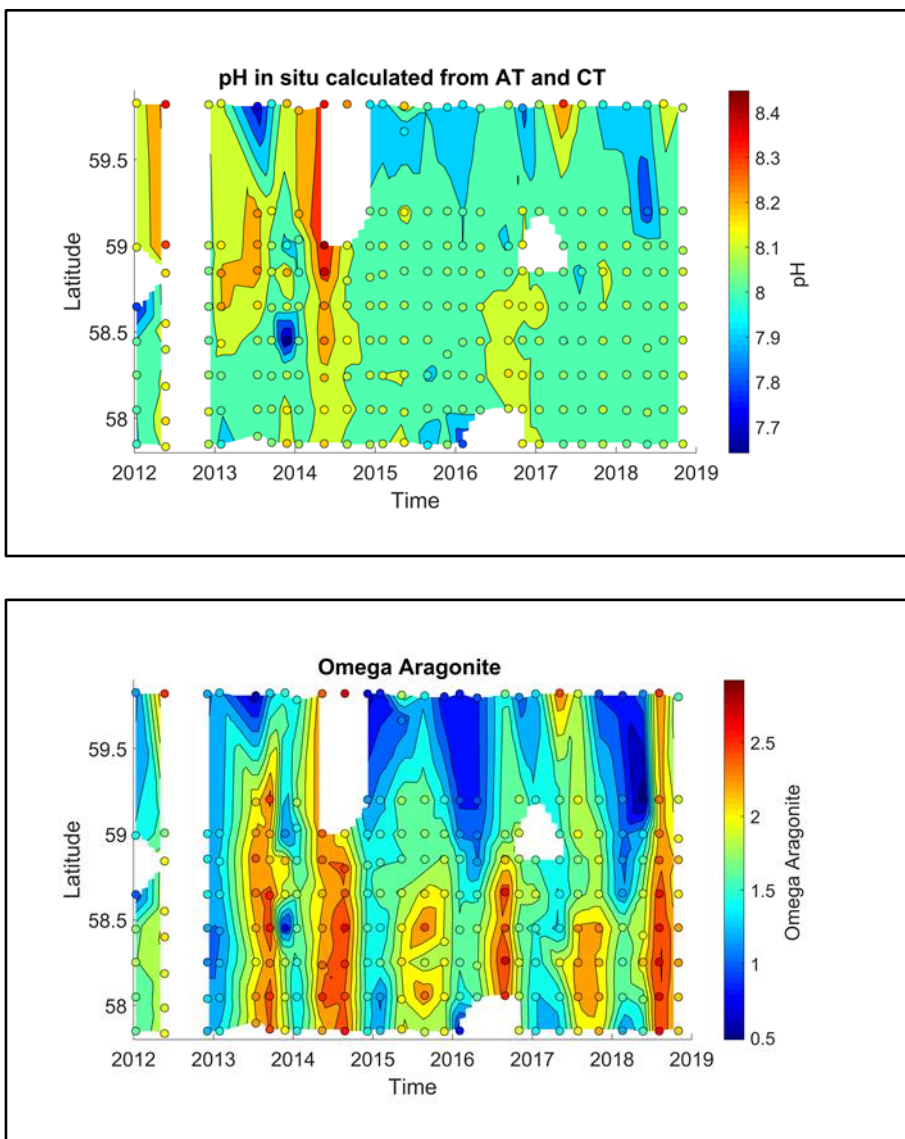


**Figure 9.**  $pH_T$  and Omega Aragonite, calculated from  $C_T$  and  $A_T$ , in the Oslofjord and Skagerrak. The circles show the measured values, while the interpolated values are shown in the background.

**Figur 9.**  $pH_T$  og Omega Aragonitt, beregnet fra  $C_T$  og  $A_T$ ) i Oslofjorden og Skagerrak. Ringene viser målte verdier, mens interpolerte verdier vises i bakgrunnen.

The seasonal and interannual variation of seawater temperature, salinity, pH and aragonite saturation state shown in **Figures 8-9** is based upon observations from cruises over 7 years. This time series is starting to reveal the extent of natural variation and it makes it possible to identify unusual variation, such as the relatively low pH and aragonite saturation states that were observed during spring 2018 in Oslofjord. By using some data from the 'ØKOKYST' program, we looked at how representative our data was for showing the influence of biological production on pH. We see that the sampling did not overlap with any blooms.

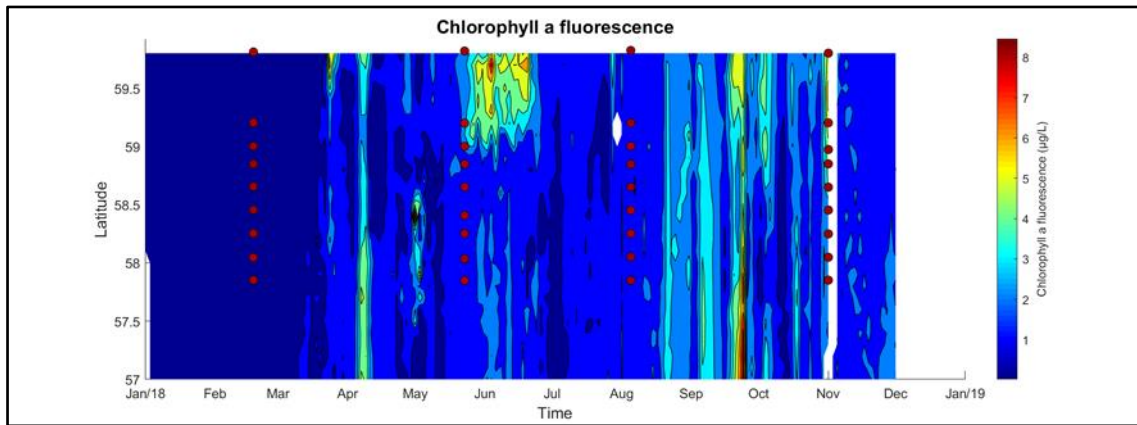


**Figure 10.** Stations in the OA monitoring (circles) and chlorophyll-a fluorescence during the year.

**Figur 10.** Stasjoner fra havforsningsprogrammet (punkt) og klorofyll a fluorescens over året.

In **Figure 10** the sampling stations were plotted against the continuous data of calibrated and quality-controlled chlorophyll-a fluorescence. It shows how the cruise in May was timed just before a phytoplankton bloom (seen as higher chlorophyll-a fluorescence) in Oslofjord. Higher chlorophyll-a fluorescence implies higher phytoplankton biomass and primary production and, therefore, an enhanced drawdown in  $\text{CO}_2$  and increase in pH. However, the balance of impacts of very low salinity during the sampling period resulted in a net reduction in pH and aragonite saturation state, explaining the unusual low pH and aragonite saturation we see in Oslofjord in spring 2018.

### 3.1.4 Trend analysis at selected stations

#### 3.1.4.1 Trend analysis by linear regression

**Figure 11** shows the trend analyses using linear regression on annual average surface winter data from Oslo-Kiel data in the Skagerrak region. The temporal changes showed a general decrease in sea surface temperature at a rate of  $0.27 \text{ }^{\circ}\text{C yr}^{-1}$  and slight freshening signal of  $0.26 \text{ yr}^{-1}$ . This is likely the result of increased fresh coastal waters at this location. However, pH and aragonite saturation state did not show any temporal change in the time series data so far.

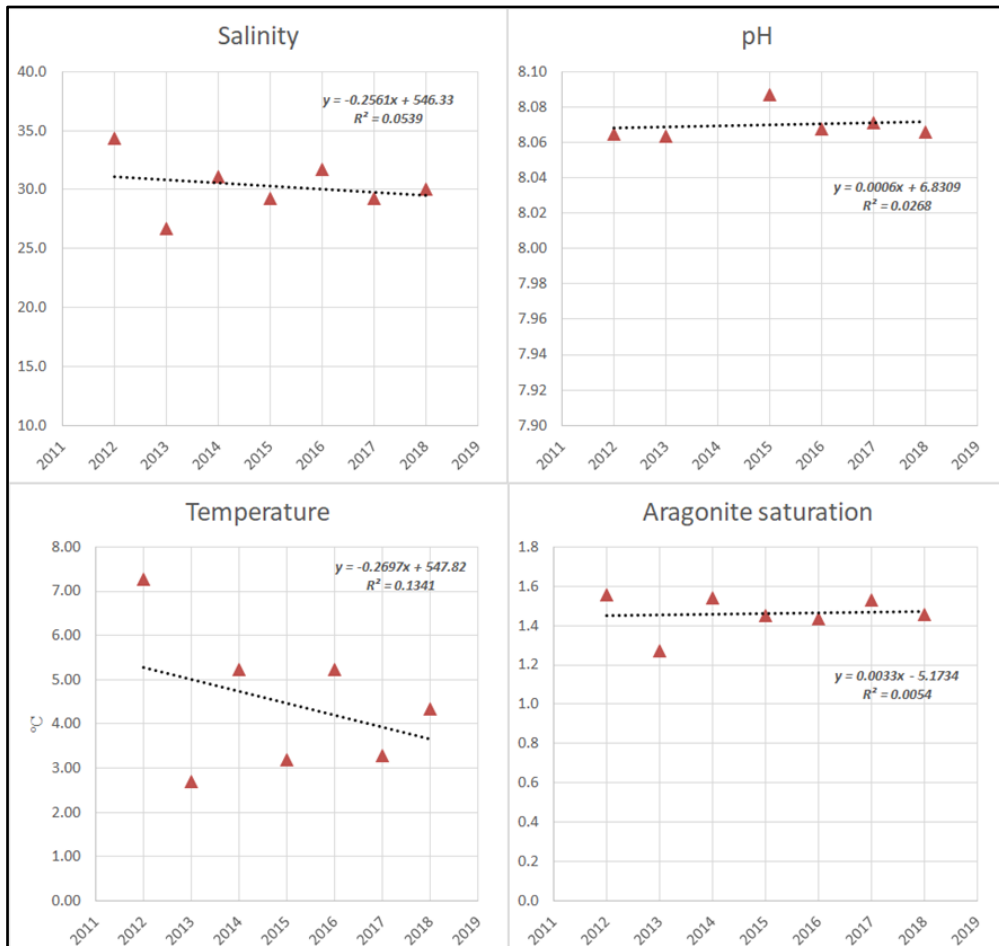


**Figure 11.** Linear regression trends in temperature, salinity, pH, aragonite saturation state in surface (4 m) waters from 2011 to 2018 in the Skagerrak.

**Figur 11.** Lineær regresjon i temperatur, saltholdighet, pH og metningsgrad av aragonitt av midlede overflatedata (4 m) fra vinter 2011 til 2018 i Skagerak.

The temporal changes in pH and aragonite saturation state and the time-trend analyses in the deepest water mass station (600 m depth) from the Torungen-Hirtshals section in the Skagerrak are affected by increased temperature by almost 3 °C in 8 years, a rate of 0.29 °C yr<sup>-1</sup> (**Figure 12**). This was accompanied by a general increase in salinity to 2017, however measurements in 2018 show a reduction in salinity and fresher water compared to that measured for the previous 6 years. The variation in pH and the saturation state for aragonite at 600 m from 2010 to 2018 show variability from lower and higher values, relative to measurements in 2010, alternating from year to year. Overall, there is a decreasing time trend of pH and aragonite saturation over the 8-year time series, giving an average reduction in pH and saturation state of 0.010 and 0.01 per year, respectively. These trends indicate increasing amounts of warm, saline Atlantic water entering the deeper parts of the Skagerrak region.

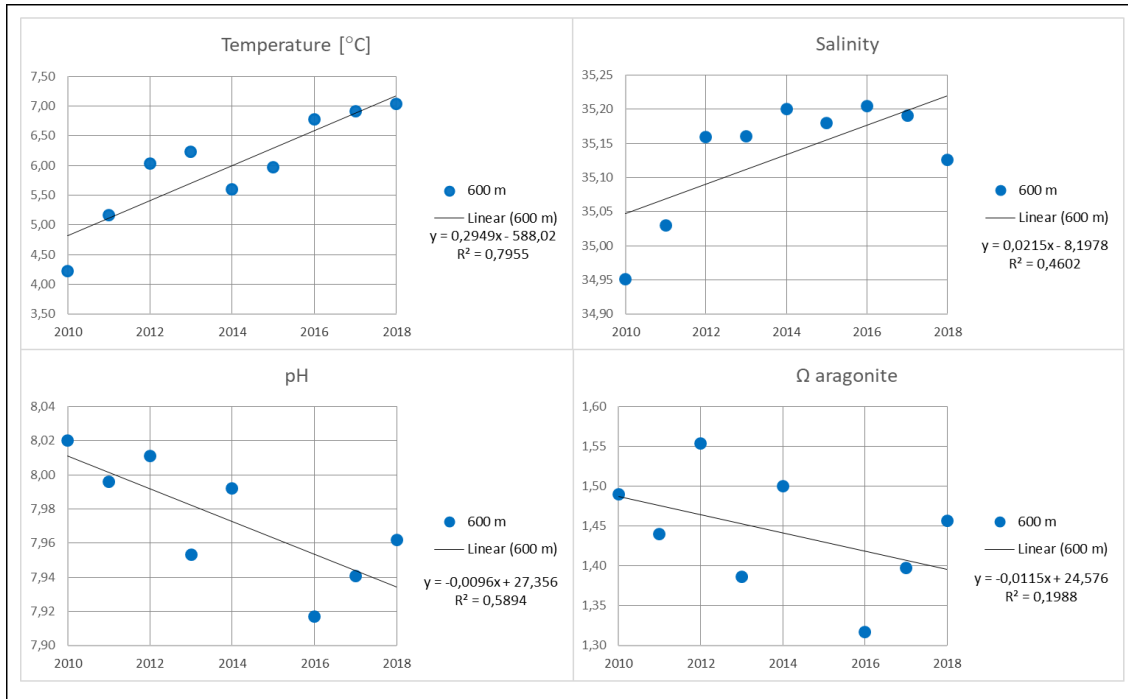


**Figure 12.** Trend analyses over 8 years of temperature, salinity, pH and aragonite saturation state at 600 m depth from the station in central Skagerrak (20 nm) along the Torungen-Hirtshals section.

**Figur 12.** 8 års trendanalyse av temperatur, saltinnhold, pH og aragonittmetning ved 600 m dyp på stasjonen i sentrale Skagerrak (20 nm) langs Torungen-Hirtshals snittet.

## 3.2 Norwegian Sea

### 3.2.1 Spatial variability along the Svinøy-NW section

In January 2018, carbon chemistry measurements were carried out by IMR on water samples from the whole water column at six stations along the hydrographic section between Svinøy and 64.15 °N, 1.29 °E; Svinøy-NW (Figure 13). Position, depth and sampling data are displayed in **Table 6, Appendix 6.2**.

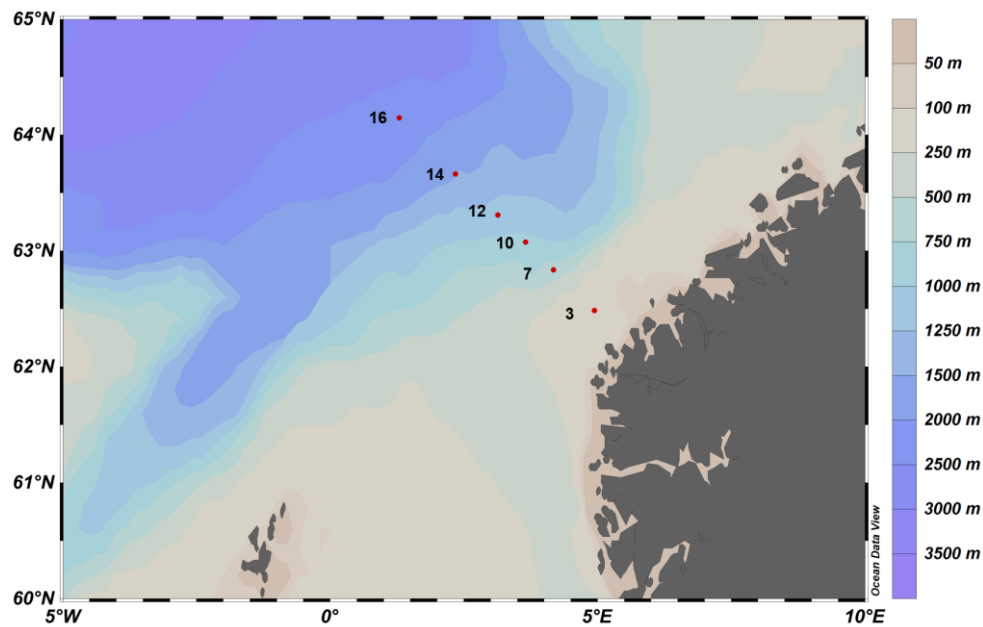


**Figure 13.** Map and numbers of the stations from Svinøy-NW in the Norwegian Sea in January 2018.

**Figur 13.** Kart og nummer over stasjoner langs Svinøy-NV i Norskehavet i januar 2018.

The Svinøy-NW section extends from the Norwegian coast with warm and fresh surface water offshore into Atlantic and Arctic water masses in the Norwegian Sea (**Figure 14**). The Svinøy section has completed hydrographic sampling since 1935.

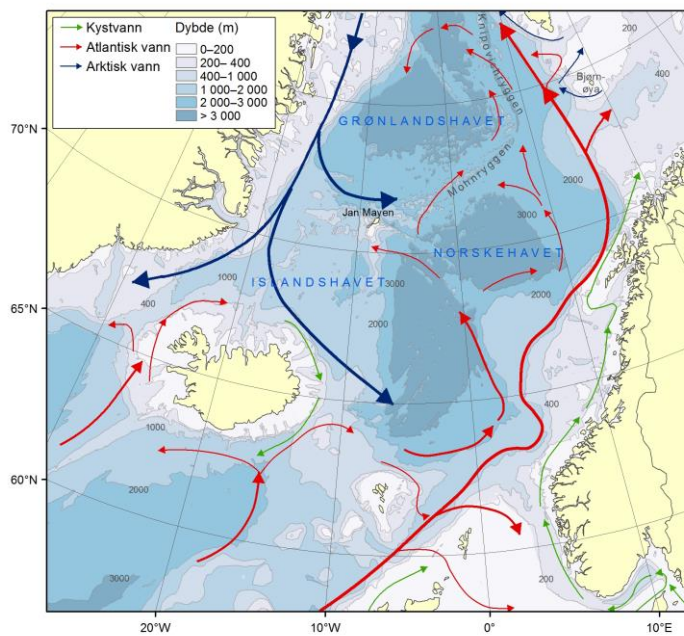


**Figure 14.** Major currents and water masses in Norwegian Sea: Atlantic water (red), polar water (blue) and coastal water (green). [www.imr.no](http://www.imr.no).

**Figur 14.** Strømmer og hovedsakelige tre vannmasser i både Norskehavet og Barentshavet: atlantisk havsvann (rød), arktisk vann (blå) og kystvann (grønn).

Warm and salty Atlantic waters enter the Norwegian Sea between Shetland, the Faroe Islands and Iceland and flow northwards following the topography. The Atlantic water becomes cooler during the passage north and is able to absorb a lot of atmospheric CO<sub>2</sub>. The distribution of pH along the Svinøy section in 2018 varies from lower pH (8.04-8.05) in the Atlantic water down to 400 m (**Figure 15**). Relatively cold and fresh surface waters of the Norwegian coastal current had low A<sub>T</sub> and C<sub>T</sub> and moderate pH ~8.06 (**Figure 3, Appendix 6.1**). Strong vertical gradients in temperature from 500 m are due to Arctic Intermediate Water that naturally has lower A<sub>T</sub>, due to lower salinity compared to Atlantic water, and highest C<sub>T</sub> concentrations (2169-2183 μmol kg<sup>-1</sup>) between 500 and 1000 m depth. Arctic water is characterized by higher pH of 8.05-8.06. Lowest pH (8.01) was found below 2000 m in the Norwegian Sea.

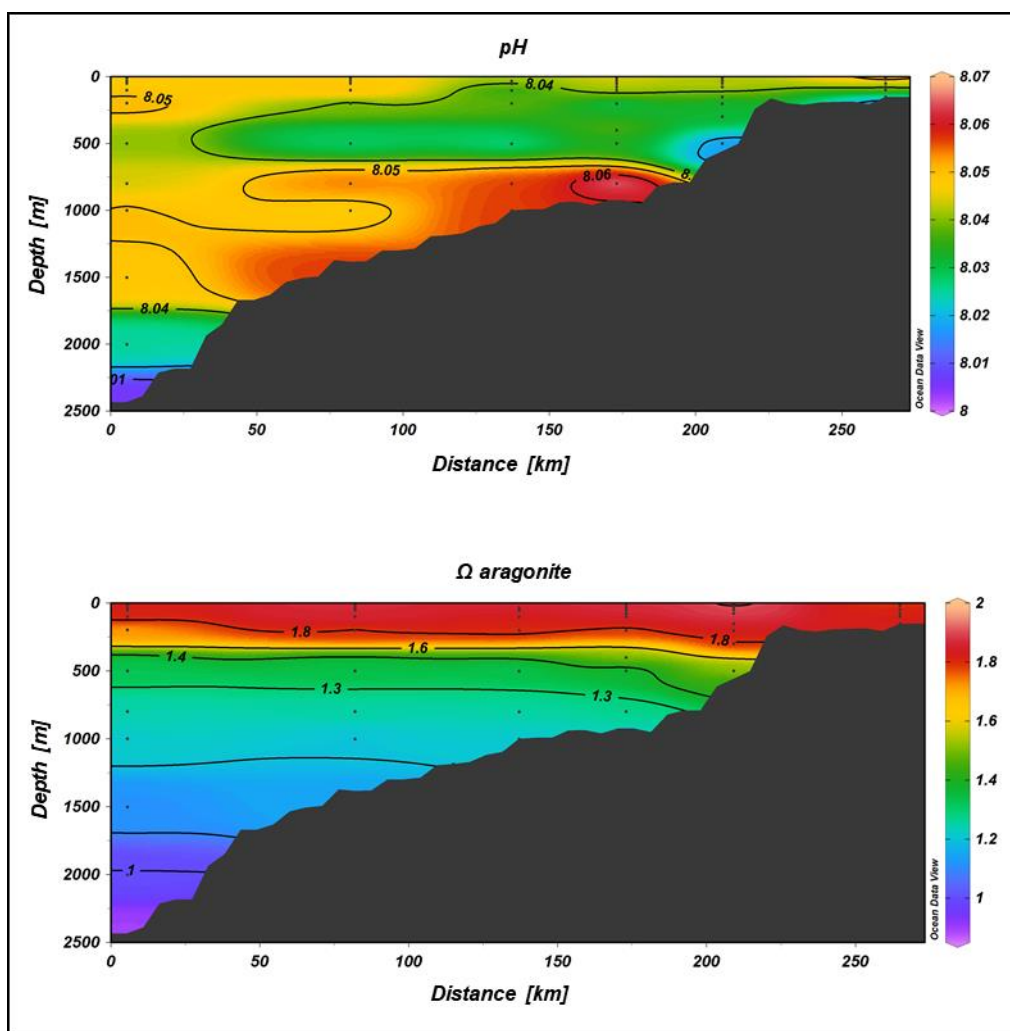


**Figure 15.** pH and aragonite saturation state along the Svinøy-NW section in January 2018.

**Figur 15.** pH og aragonittmetningsgrad langs Svinøy-NV snittet i januar 2018.

The saturation state for aragonite (and calcite, not shown) varied from highest values (1.93) as a result of seasonal biological C<sub>T</sub> uptake in the surface layers to lowest (0.90) in the deepest parts of the Norwegian Sea. Surface water saturation states varied between 1.78 and 1.93 as a result of competing processes such as freshwater inputs, biological production and mixing with sub-surface Atlantic water. Beneath the Atlantic water is the fresher Arctic water, which is distinguished by lower saturation states ( $\Omega$  aragonite 1.3-1.5) and the saturation horizon for aragonite was located at 2000 m depth.

### 3.2.2 Spatial variability along the Gimsøy-NW section

Measurements of carbon chemistry in the full water column along Gimsøy-NW in the northern part of the Norwegian Sea were carried out by IMR in May-June 2018 (*Figure 16*). Normally, sampling is carried out during the winter months to reduce the impact of biological production (carbon uptake) on the vertical distribution of carbonate chemistry in the water column. Due to logistical constraints, sampling along the Gimsøy section in 2018 was carried out during summer and therefore data in the upper 100 m will reflect the signal of carbon removal during the productive seasons. A total of 4 hydrographic stations were occupied along a transect extending from the edge of the Lofoten basin to the Norwegian Sea. Position, depth and sampling data are displayed in *Table 8, Appendix 6.2*.

The Gimsøy-NW section encompasses the surface Norwegian coastal current, Arctic water at intermediate depths and Atlantic water that flow northwards into the Barents Sea. This region supports numerous cold-water coral reefs that are potentially particularly sensitive to low pH water and low calcium carbonate mineral saturation. Together with the Norwegian basin, this area has experienced faster rates of pH decrease in comparison to other parts of the Norwegian Sea (Skjelvan et al., 2014) and the global ocean average (Takahashi et al. 2014).

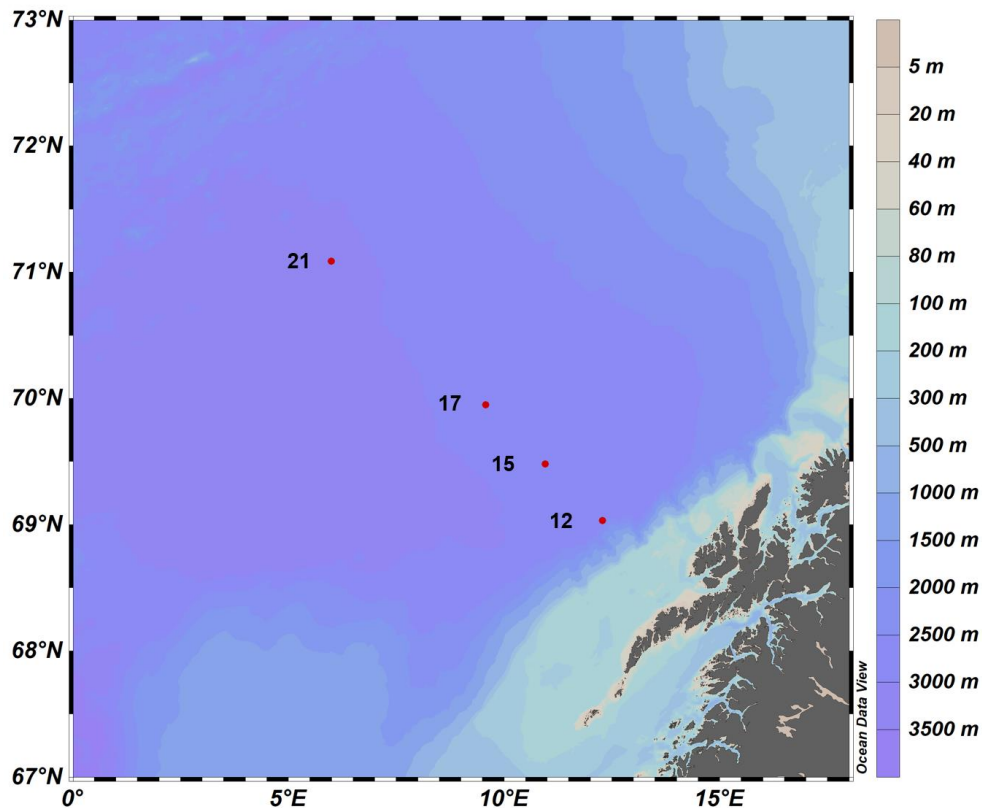


**Figure 16.** Map and numbers of the stations along the Gimsøy-NW section in the northern Norwegian Sea in May and June 2018.

**Figur 16.** Kart og nummer over stasjoner langs Gimsøy-NV snittet i nordlige Norskehavet i mai og juni 2018.

The section is dominated by warm and salty Atlantic water in the upper 500 m with relatively high  $C_T$  of 2150-2170  $\mu\text{mol kg}^{-1}$  (**Figure 5, Appendix 6.1**). Colder Arctic water occupies intermediate depths below 500 m. Lowest pH (7.90) was found around 500 m depth in the Atlantic water close to the continental slope. In the deeper parts of the Norwegian Sea, the Arctic water is characterized by higher  $C_T$  and lower  $A_T$  values (approx. 2170-2190 and 2310  $\mu\text{mol kg}^{-1}$ , respectively) compared to the Atlantic water. High pH values (8.04) were found extending northwest from the continental slope at 1500 m depth (**Figure 17**). Aragonite (and calcite, not shown) saturation showed a general decreasing gradient from highest values ( $\Omega_{\text{aragonite}} > 1.8$ ) in the productive surface waters to lowest saturation levels (0.74) at 3125 m in the Norwegian Sea. The saturation horizon for aragonite was generally located between 1500-2000 m depth, becoming deeper to 2000-2500 m in the central part of the section. This was similar to saturation horizon depth at Station M further offshore and shallower compared to the Svinøy section to the south.

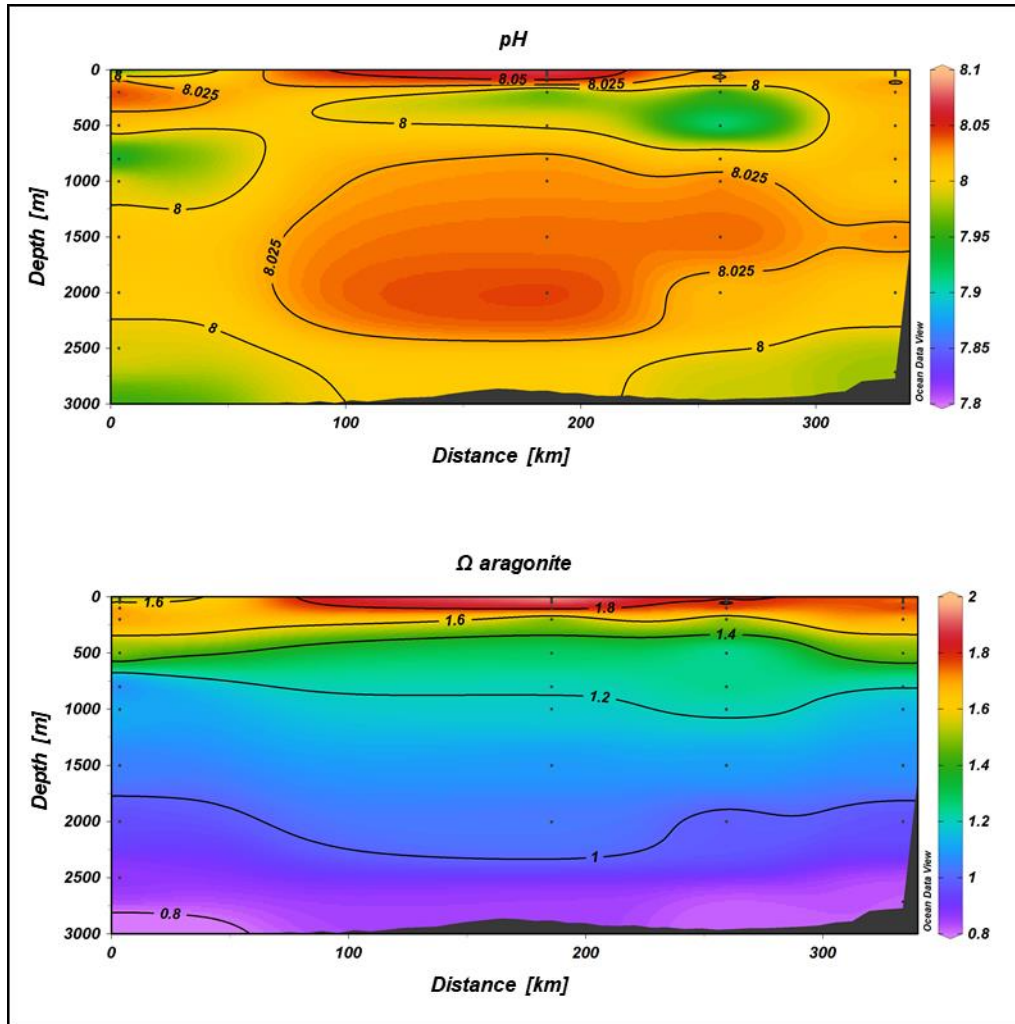


Figure 17. pH and aragonite saturation state along the Gimsøy-NW section in May and June 2018.

Figur 17. pH og aragonittmetningsgrad langs Gimsøy-NV snittet i mai og juni 2018.

### 3.2.3 Seasonal variability in open ocean

In the Norwegian Sea, seasonal variability has been determined from the Ocean Weather Station M (Station M), which is an open ocean fixed station positioned at 66°N 2°E, between the Svinøy and Gimsøy sections (*Figure 1*). The station was initiated in 1948 starting with meteorological and oceanographic (salinity and temperature) measurements, and since then other measurements have been added, and some retracted. Regular carbon measurements were started by NORCE and UiB in 2001, and in 2018, discrete water samples were collected from the whole water column in January, April, May (twice), August, and November. The samples (12 from each cruise) have been analyzed for  $C_T$  and  $A_T$  (*Table 7, Appendix 6.2*).

In addition to the discrete water column measurements, the station also delivers continuous measurements. Station M is equipped with a surface buoy and a deep-water mooring, both with a number of sensors attached. The buoy and mooring deliver, amongst other variables, continuous  $pCO_2$ , pH, and hydrography. The buoy and mooring are usually deployed during early

summer and retrieved during spring the following year. In 2018, the equipment was retrieved in end of May, and due to lack of ship time and personnel, the equipment was deployed in November. This report presents data that are available from the mooring and buoy at the time of reporting.

Discrete (*Figures 18-21*) and continuous (*Figures 22-23*) measurements from the same station provide supplementary information. The discrete measurements illustrate how the carbonate system varies between seasons at all depths of the water column, while the continuous measurements provide information about small scale variations over a day or a week in addition to the annual cycle, however, only from selected depths. At Station M, the continuous monitoring is performed in the surface water, and, currently, at 500 m depth.

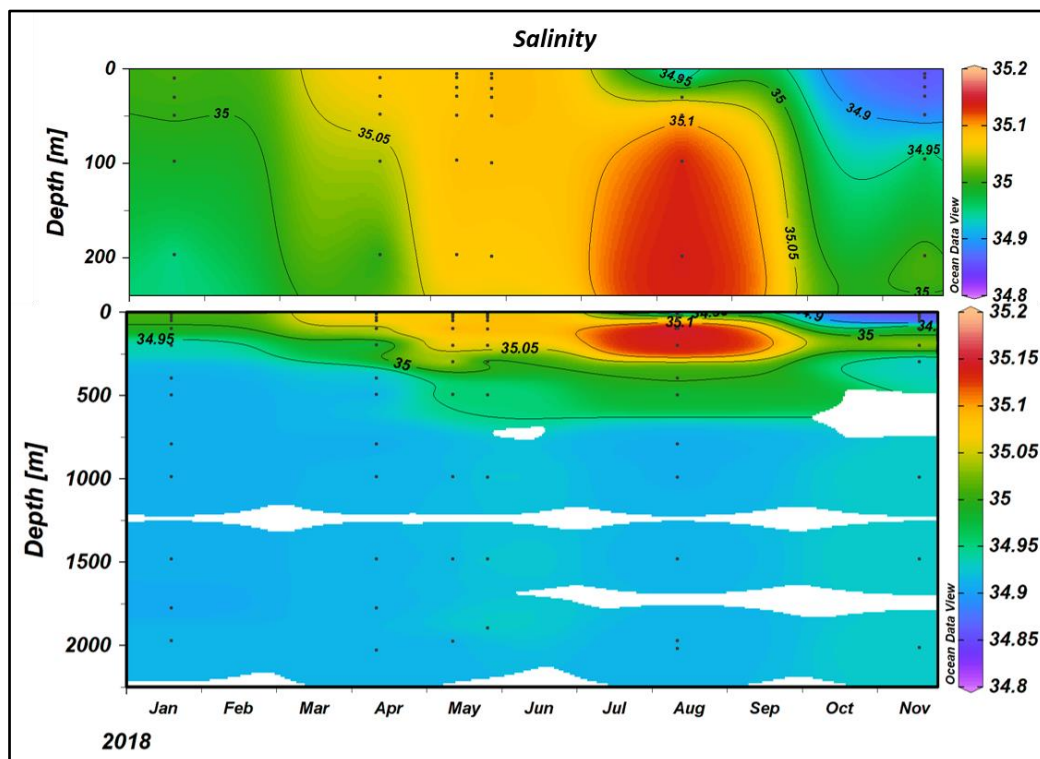


**Figure 18.** Salinity at Station M in 2018. Black dots indicate the depths of the samples.

**Figur 18.** Saltinnhold på Stasjon M i 2018. Svarte prikker viser prøvedyp.

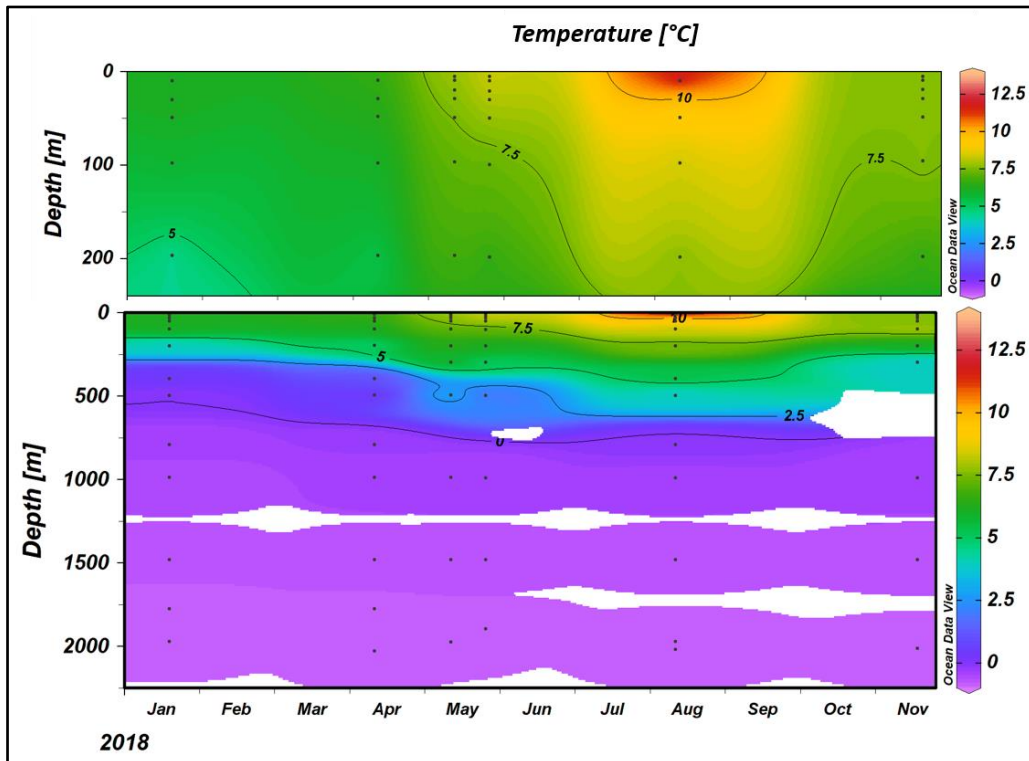


**Figure 19.** Temperature ( $^{\circ}\text{C}$ ) at Station M in 2018. Black dots indicate the depths of the samples.

**Figur 19.** Temperatur ( $^{\circ}\text{C}$ ) på Stasjon M i 2018. Svarte prikker viser prøvedyp.

Like the Svinøy and Gimsøy sections in the Norwegian Sea, Station M also encompasses the Norwegian Atlantic Current (NAC) flowing northwards off the Norwegian coast, carrying warm and saline Atlantic water. The thickness of the Atlantic water varies northwards, and at Station M, the upper 300-500 m is occupied with water with Atlantic characteristics, whilst at Gimsøy section, this layer is shallower. In 2018, surface temperature at Station M varied from 6.2  $^{\circ}\text{C}$  during winter to 13.9  $^{\circ}\text{C}$  during summer (**Figure 19**). The winter temperature was lower than that of 2017 (7.5  $^{\circ}\text{C}$ ) but similar to that of 2016, and the winter surface temperature of 2018 was confirmed by the continuous buoy measurements from February ( $6.4 \pm 0.7 ^{\circ}\text{C}$ ). A surface salinity minimum is frequently seen during August-September at Station M, and this is a signal of the coastal current meandering in the vicinity of the station (**Figure 18**). In 2018, however, the lowest surface salinity occurred in November.

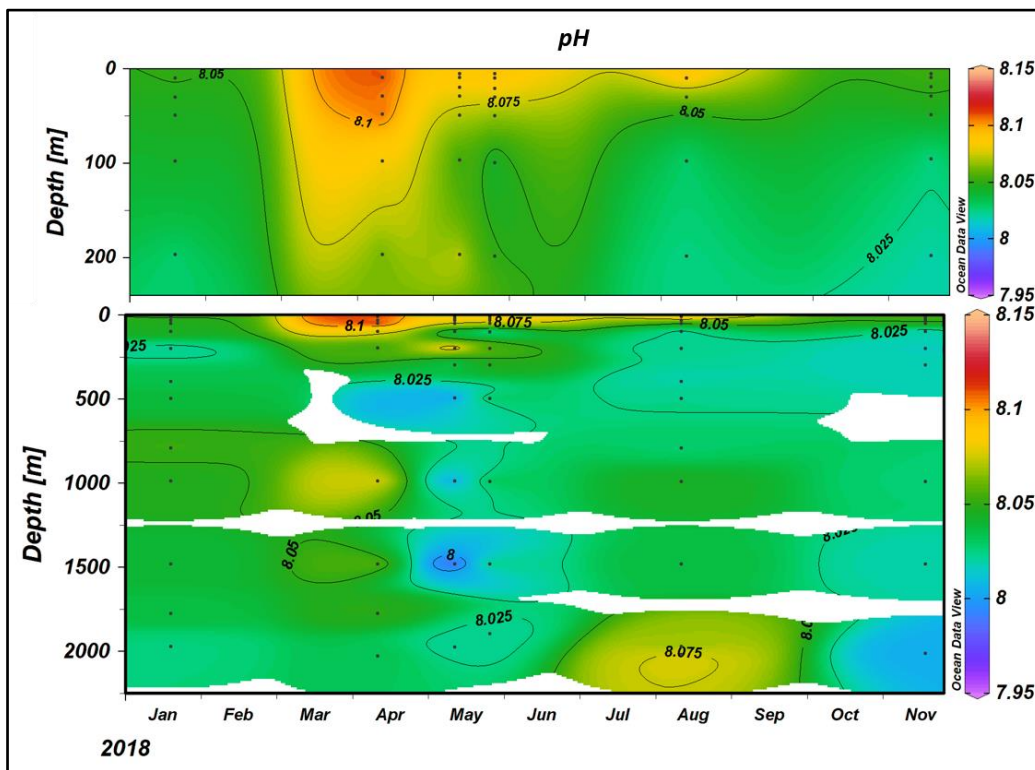


**Figure 20.** pH in situ at Station M in 2018. Black dots indicate the depths of the samples.

**Figur 20.** pH in situ på Stasjon M i 2018. Svarte prikker viser prøvedyp.

In April 2018, a decrease in  $C_T$  (**Figure 4**, **Appendix 6.1**) and an increase in pH (**Figure 20**) and  $\Omega_{Ar}$  (**Figure 21**) was observed, and this was the response of the phytoplankton spring bloom. When the temperature starts to increase at the onset of summer, the pH decreases again, and the  $\Omega_{Ar}$  increases towards late summer as a function of both increased primary production and increasing temperature. In August, the  $C_T$  is at its minimum (**Figure 4**, **Appendix 6.1**) while the  $\Omega_{Ar}$  is at its maximum. Towards the autumn, the water cools again. Seasonal changes were seen in the upper 200 m or so. Below this depth no seasonal changes were seen and the observed variability at these intermediate depths were rather connected to mixing of water masses, which occurs with variable frequency and strength.

Deeper than approximately 1000-1200 m, the Norwegian Basin is filled with relative fresh and cold water. At these depths the characteristics of the water are relatively stable; however, changes are seen over years (Østerhus and Gammelsrød, 1999; Skjelvan et. al., 2008; Skjelvan et. al., 2014). In 2018, the following averaged deep-water characteristics at Station M were found; temperature of  $-0.77^\circ\text{C}$ , salinity of 34.92,  $A_T$  of  $2306 \mu\text{mol kg}^{-1}$ ,  $C_T$  of  $2167 \mu\text{mol kg}^{-1}$ , pH of 8.035, and  $\Omega_{Ar}$  of 1.02, and these are relatively similar to those observed in 2017. As for 2017, the saturation horizon, where  $\Omega_{Ar}$  equals 1, in 2018 was found around 2000 m depth (**Figure 21**). Winter surface water characteristics in 2018 were for  $C_T$ , pH and  $\Omega_{Ar}$   $2147 \mu\text{mol kg}^{-1}$ , 8.055 and 1.82, respectively, and the corresponding summer characteristics were  $2057 \mu\text{mol kg}^{-1}$ , 8.12 and 2.68.

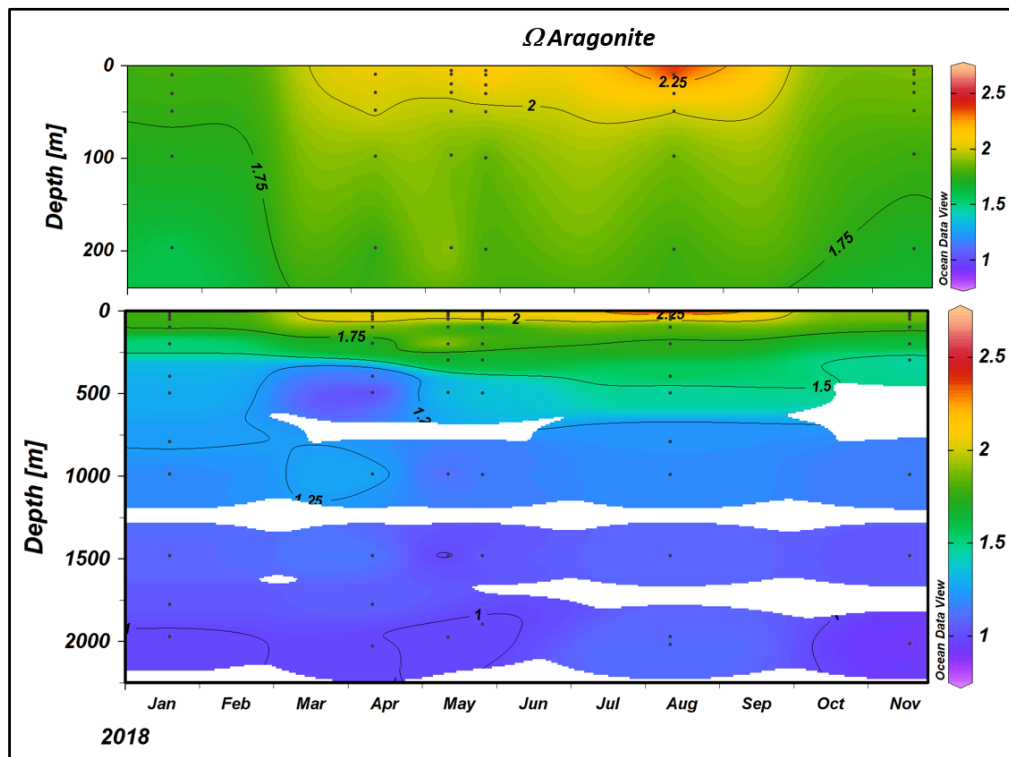


**Figure 21.**  $\Omega_{\text{Ar}}$  in situ at Station M in 2018. Black dots indicate the depths of the samples.

**Figur 21.**  $\Omega_{\text{Ar}}$  in situ på Stasjon M i 2018. Svarte prikker viser prøvedyp.

Continuous surface water pH and  $\Omega_{\text{Ar}}$  between 2011 and 2018 are shown in **Figure 22 and 23** (surface  $f\text{CO}_2$  (μatm) from 2011 to 2018 is shown in **Figure 8, Appendix 6.1**). The observed seasonality is driven by primary production/remineralisation and temperature changes. By comparing the winter values from the whole period, it is clear that both pH and  $\Omega_{\text{Ar}}$  have decreased over the years. This is as expected, and connected to, the increasing  $\text{CO}_2$  concentration in the atmosphere and sea surface.

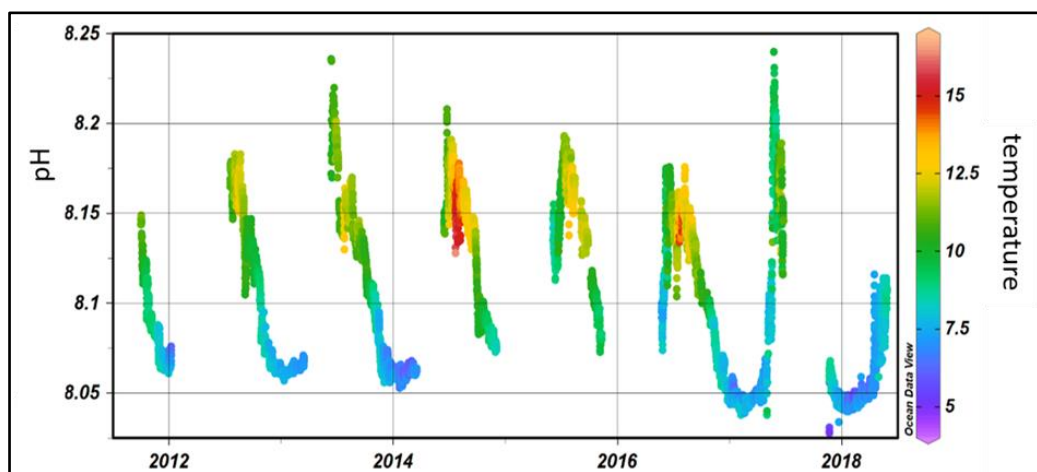


**Figure 22.** pH in surface water at Station M between 2011 and 2018 The colour scale indicates temperature.

**Figur 22.** pH i overflatevann på Stasjon M i perioden 2011 til 2018. Fargeskala viser temperatur.

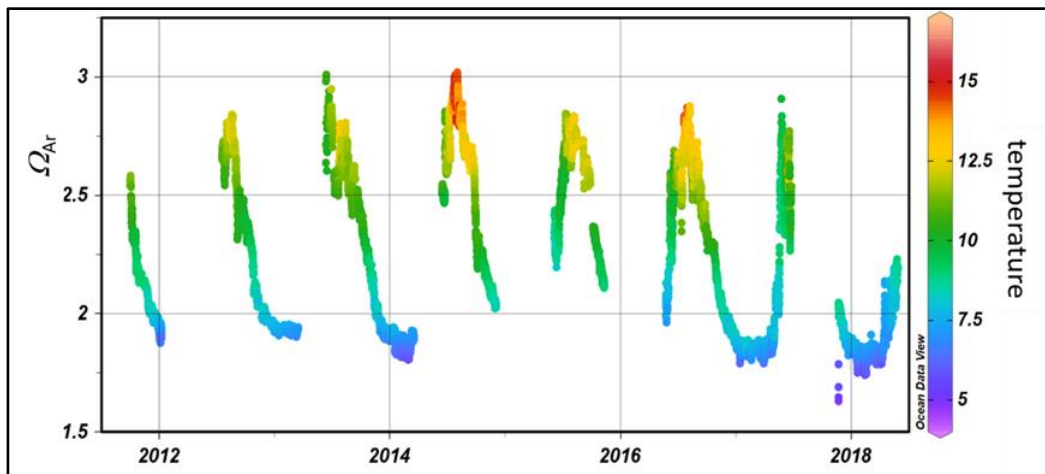


**Figure 23.**  $\Omega_{\text{Ar}}$  in surface water at Station M between 2011 and 2018 The colour scale indicates temperature.

**Figur 23.**  $\Omega_{\text{Ar}}$  i overflatevann på Stasjon M i perioden 2011 til 2018. Fargeskala viser temperatur.

### 3.2.4 Seasonal variability in coastal water

#### 3.2.4.1 Hardanger - west coast

In 2018, NORCE-Uib continued the costal studies in the Hardanger area, where seawater carbonate measurements from the full water depth have been performed irregularly since 2007. During the years 2007 to 2010, samples were collected between Bergen and Hardanger as part of the EU project CarboSchools, and since 2015, the Norwegian Environment Agency has funded the carbonate system sampling. In 2018, a thorough compilation of the Bergen - Hardanger coastal data series was performed and the results are included in this report. The sampled areas are shown in **Figure 24**, and the locations differ in terms of, e.g. depth, frequency of sampling, and length of time series. Here, we have focused on the encircled areas in **Figure 24**, and **Figures 25-28** show variations over time. Position, depth and sampling data are displayed in **Tables 3-5**, **Appendix 6.2**.

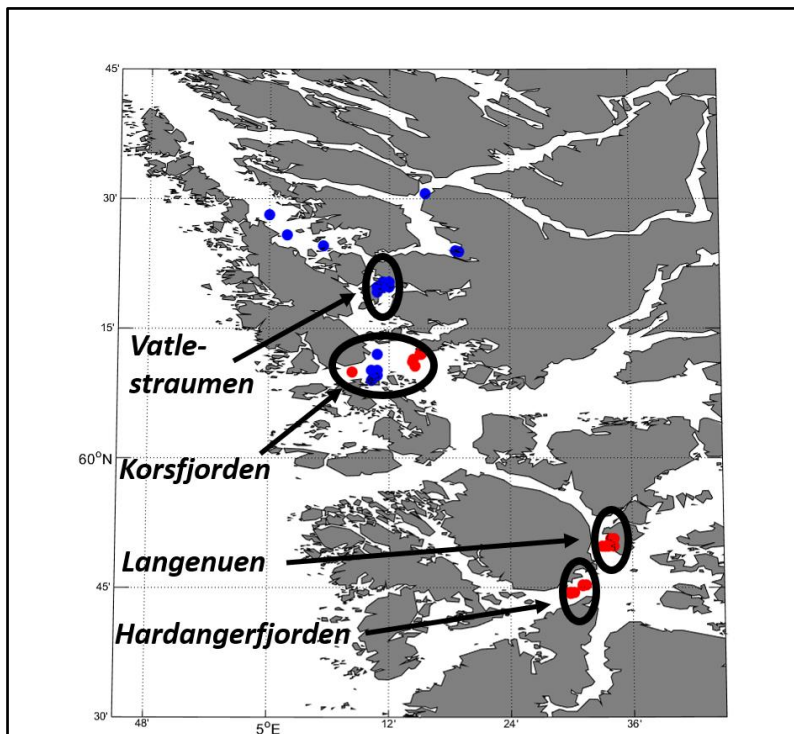


**Figure 24.** A map over the Bergen - Hardanger area. Blue dots show the sample locations in the period 2007 to 2010, and red dots are the locations from 2015 to 2018. The black circles show the focus areas.

**Figur 24.** Kart over området Bergen - Hardanger. Blå prikker viser hvor data ble samlet inn i perioden 2007 til 2010, røde prikker viser innsamling i årene 2015-2018, og svarte ringer er områdene denne analysen har fokusert på

The seasonal cycle has been studied by calculating monthly averages based on data from all years. The surface temperature showed a well-defined seasonality, with data from the upper 10 m and the upper 50 m (**Figure 25-26**). However, the monthly variability (size of blue boxes) is larger for the upper 50 m compared to the upper 10 m. This is connected to a relatively stratified water column, with river and rain influenced surface layer (< 10 m), Atlantic influenced water at larger depths, and a mixture of water masses in between.

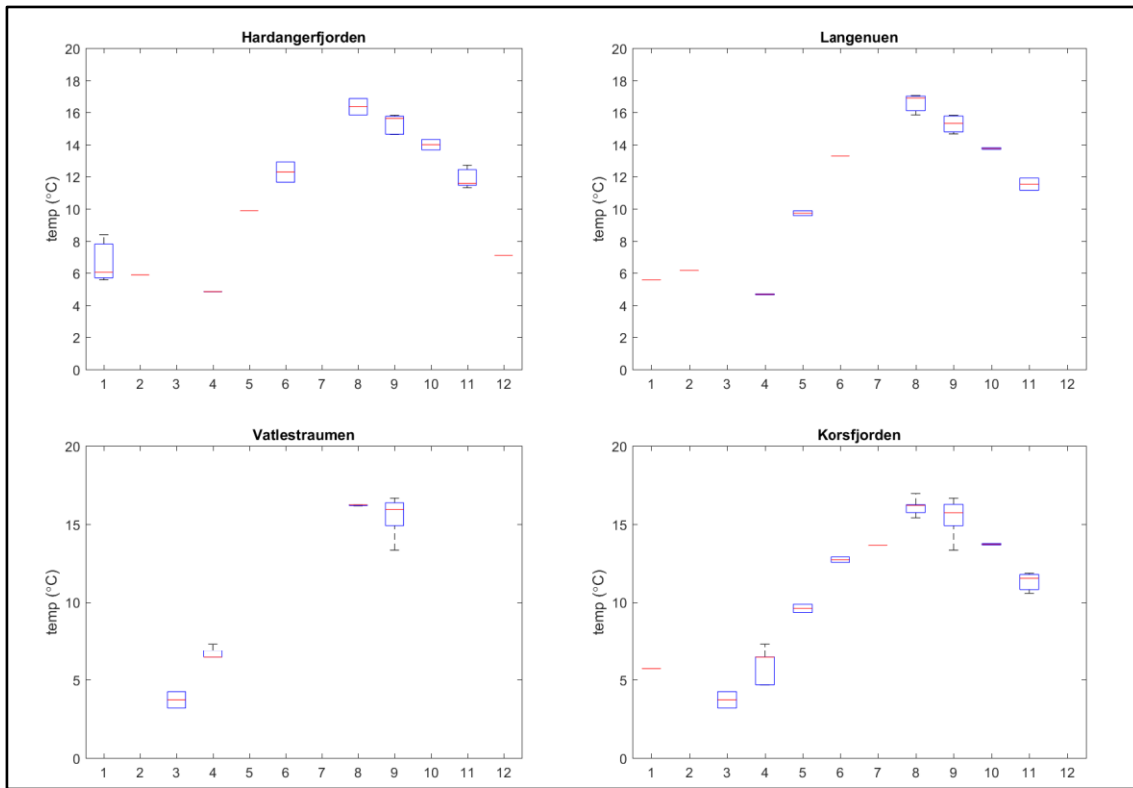


**Figure 25.** Seasonal cycle of surface temperature (<10 m). Data from the black circles in **Figure 24**. Red lines are the monthly averages, the blue boxes represent 75% of the data, the error bars (black lines) enclose 99.3% of the data, and the red crosses are the remaining data.

**Figur 25.** Sesongvariasjon av temperatur i overflatevann (<10 m). Data er fra de svarte sirklene i **Figur 24**. Røde linjer representerer månedsmiddel, blå bokser inneholder 75% av dataene den aktuelle måneden, 99.3% av måneden data ligger innenfor de svarte strekene og de rød kryssene er resten av dataene.

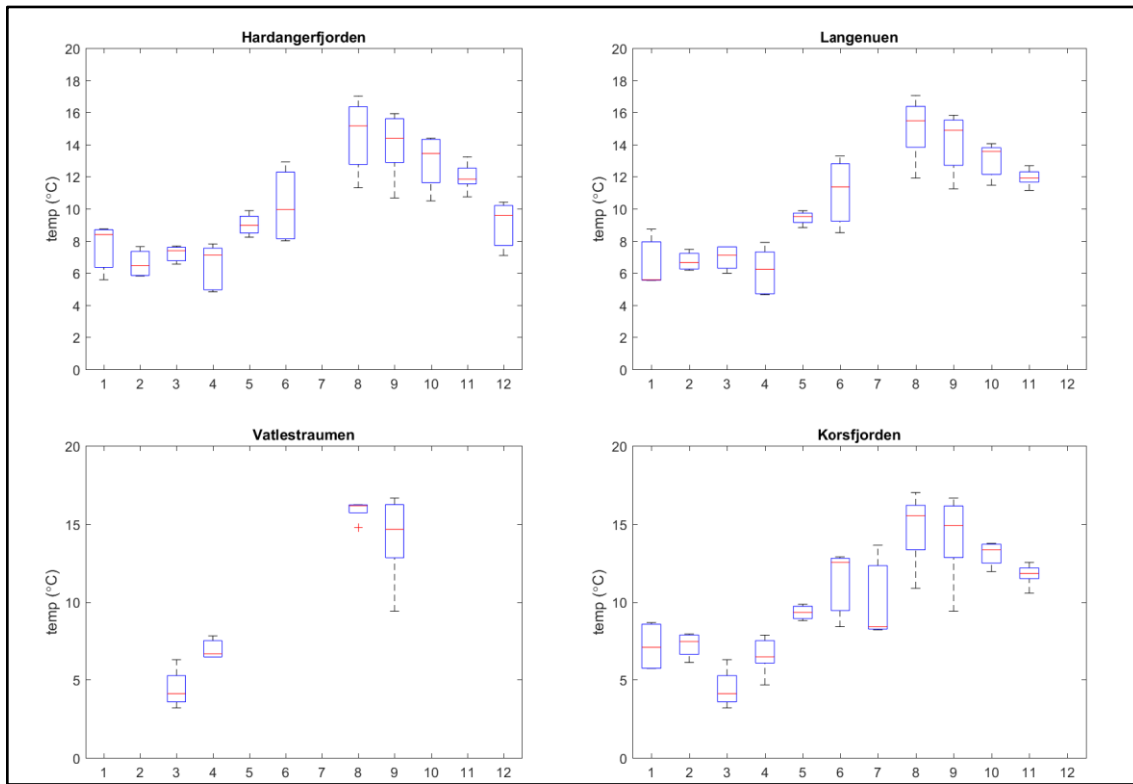


**Figure 26.** Seasonal cycle of surface temperature (< 50 m). Data from the black circles in **Figure 24**.

**Figur 26.** Sesongvariasjon av temperatur i overflatevann (< 50 m). Data er fra de svarte sirklene i **Figur 24**.

The seasonality is also reasonably clear for the monthly averaged pH (**Figure 27-28**), with a more defined cycle for the shallowest (< 10 m) data, which, similar to the temperature, have smaller intra-monthly variability (**Figure 27**) compared to the data from the upper 50 m (**Figure 28**). pH increases as a result of primary production. The most intense primary production takes place in the upper layer (<10 m). Deeper than this the blooming is patchy and strongly depends on the depth of the photic zone, which is why the variability within a month is larger in the upper 50 m. In late summer, the pH decreases due to increasing temperatures, and when autumn comes with more intense vertical mixing, remineralized matter is brought to the surface and pH decreases again. During 2017, monthly carbonate samples were collected, and thus, this is the year with highest sample density. However, the picture is similar to that shown in **Figures 25-28**, and thus, we find no evidence of significant inter-annual variations in seasonality.

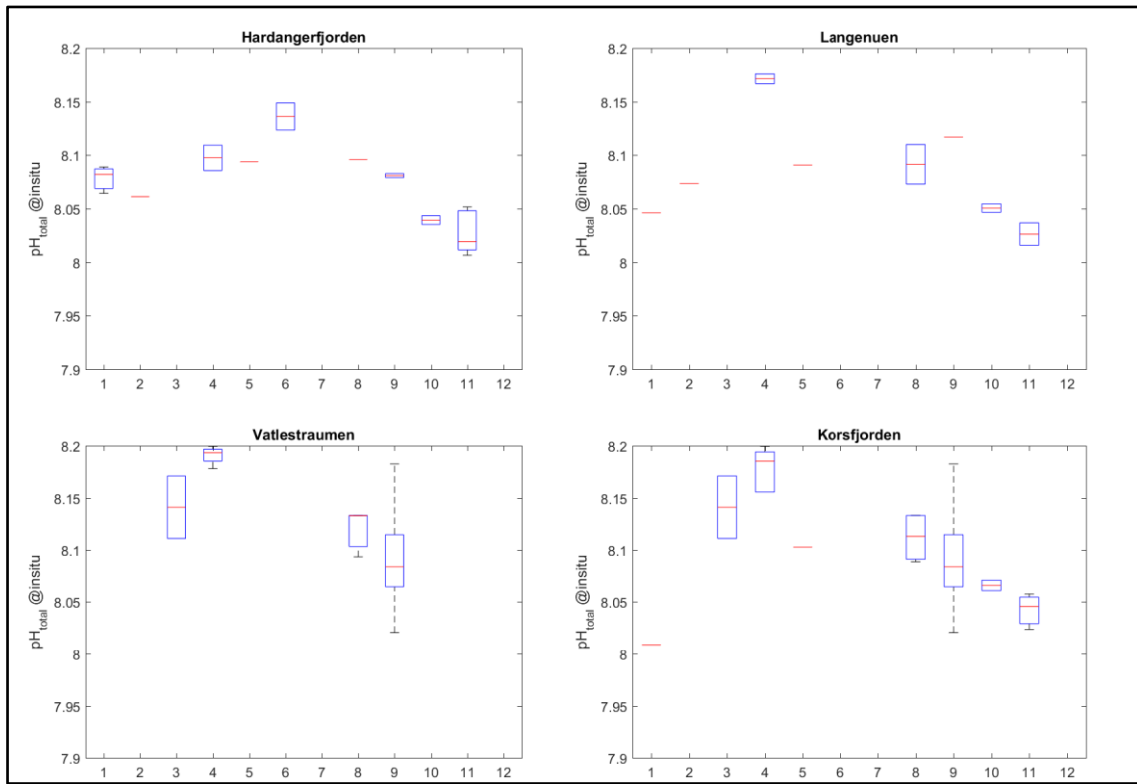


**Figure 27.** Seasonal cycle of surface pH ( $<10$  m). Data from the black circles in **Figure 24**.

**Figur 27.** Sesongvariasjon av pH i overflatevann ( $<10$  m). Data er fra de svarte sirklene i **Figur 24**.

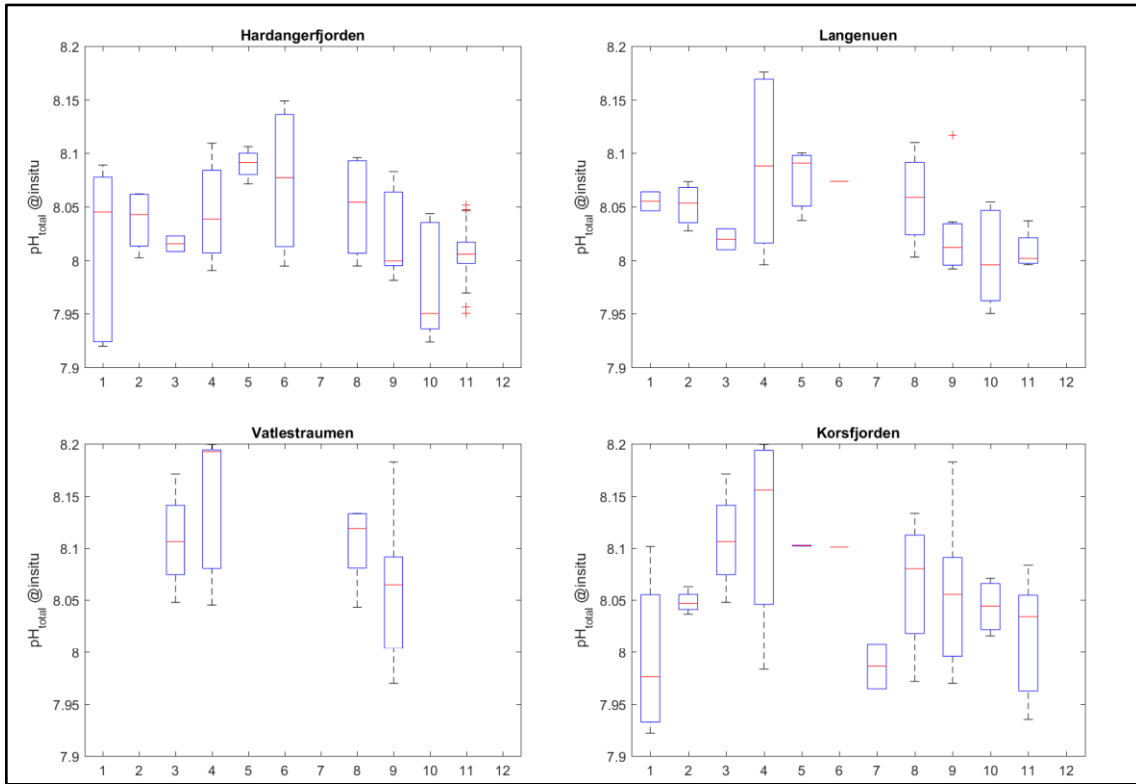


**Figure 28.** Seasonal cycle of surface pH (< 50 m). Data from the black circles in **Figure 24**.

**Figur 28.** Sesongvariasjon av pH i overflatevann (< 50 m). Data er fra de svarte sirklene i **Figur 24**.

Further, it was checked if there were any latitudinal variability in the seasonal data, and temperature, salinity, and pH was plotted as a function of latitude and month (**Figure 29 to 31**). During winter, the area between 60.3 and 60.4 °N experienced a higher pH and colder and fresher water compared to further south. This might be connected to the fact that the northernmost area is more open to the ocean than the southern part, and thus more exposed to the current flowing northwards along the coast. The strongest seasonality in salinity is seen in the southernmost area while in the north there is much weaker seasonal signal. It must be remarked that the picture is patchy and complicated to analyze. Additional information about runoff from land (e.g. from the Norwegian Water Resources and Energy Directorate-NVE) will possibly contribute to our understanding of the seasonality.

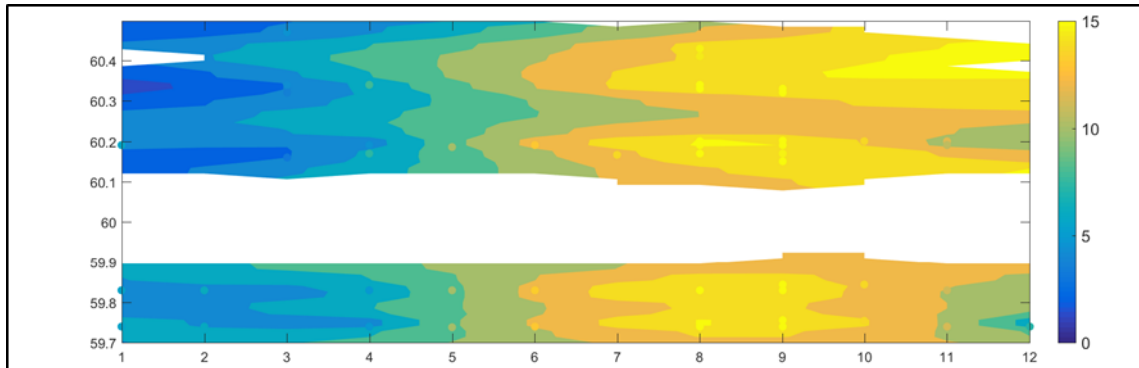


**Figure 29.** Sea surface temperature (< 10 m) as a function of latitude (y axis) and month (x axis). Circles indicate actual data, which are from the black circles in Figure 24.

**Figur 29.** Temperatur i overflatevann (< 10 m) som funksjon av breddegrad (y-akse) og måned (x-akse. Sirkler viser hvor det finnes data, og data er fra de svarte sirklene i Figur 24.

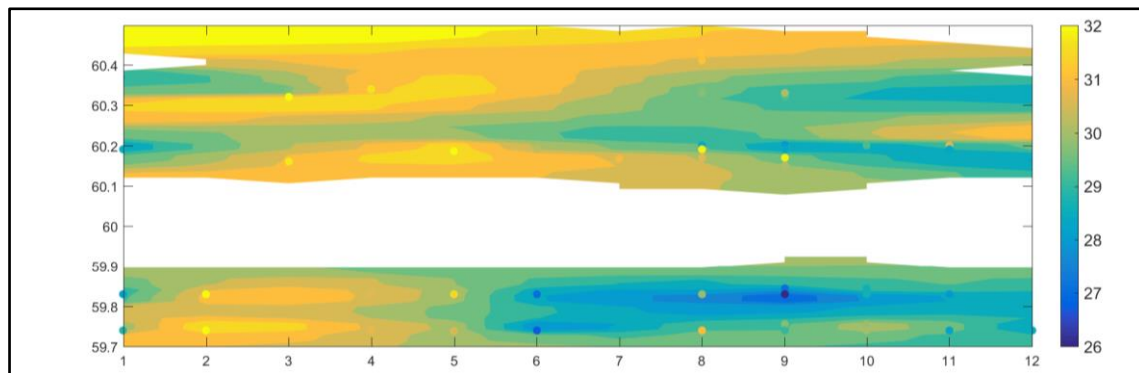


**Figure 30.** Sea surface salinity (< 10 m) as a function of latitude (y axis) and month (x axis). Circles indicate actual data, which are from the black circles in Figure 24.

**Figur 30.** Saltinnhold i overflatevann (< 10 m) som funksjon av breddegrad (y-akse) og måned (x-akse. Sirkler viser hvor det finnes data, og data er fra de svarte sirklene i Figur 24.

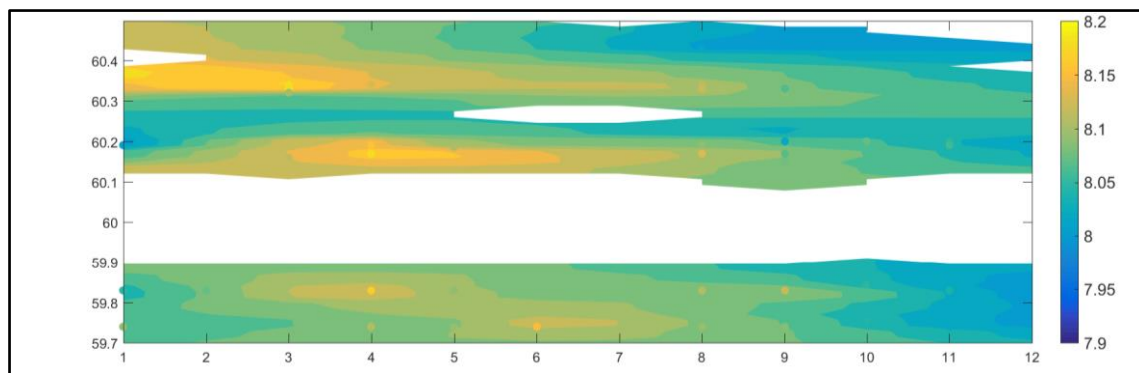


**Figure 31.** Sea surface pH (< 10 m) as a function of latitude (y axis) and month (x axis). Circles indicate actual data, which are from the black circles in Figure 24.

**Figur 31.** pH i overflatevann (< 10 m) som funksjon av breddegrad (y-akse) og måned (x-akse. Sirkler viser hvor det finnes data, og data er fra de svarte sirklene i Figur 24.

Interannual trends were examined by plotting temporal winter and summer pH from the upper 10 m (**Figure 32**), March and September pH from the upper 50 m (**Figure 33**), and winter and summer pH from the deepest water (**Figure 34**). Note that the deepest water is from Korsfjorden area only (**Figure 24**). The surface variability within a season (size of blue boxes, **Figure 32**) varies from year to year, and the surface variability within one month (size of blue boxes, **Figure 33**) also varies greatly from one year to another. There might be indications of a decreasing trend over time in the winter data from the surface, however, this might also be accounted for by the fact that the samples were collected from different locations. **Figure 31** already showed that pH varies slightly with the latitude.

Also, for the deep water from Korsfjorden (**Figure 34**), there seem to be a decreasing pH trend, but the results have to be handled with care since also here, the samples are collected with some spatial spread (see Korsfjorden encircle in **Figure 24**). However, the deep water in general show less variability than the surface water and it is more likely that the trend in the deep water is real than that of the surface waters.

In the Ocean Acidification 2017 report (Jones et al., 2018), we present a trend in the deep-water pH from Korsfjorden of -0.007 over the years 2007 to 2017. Adding the 2018 data does not change the trend value significantly, however, as pointed out above, the number must be used with care and one needs to add information about the differences in sampling location.

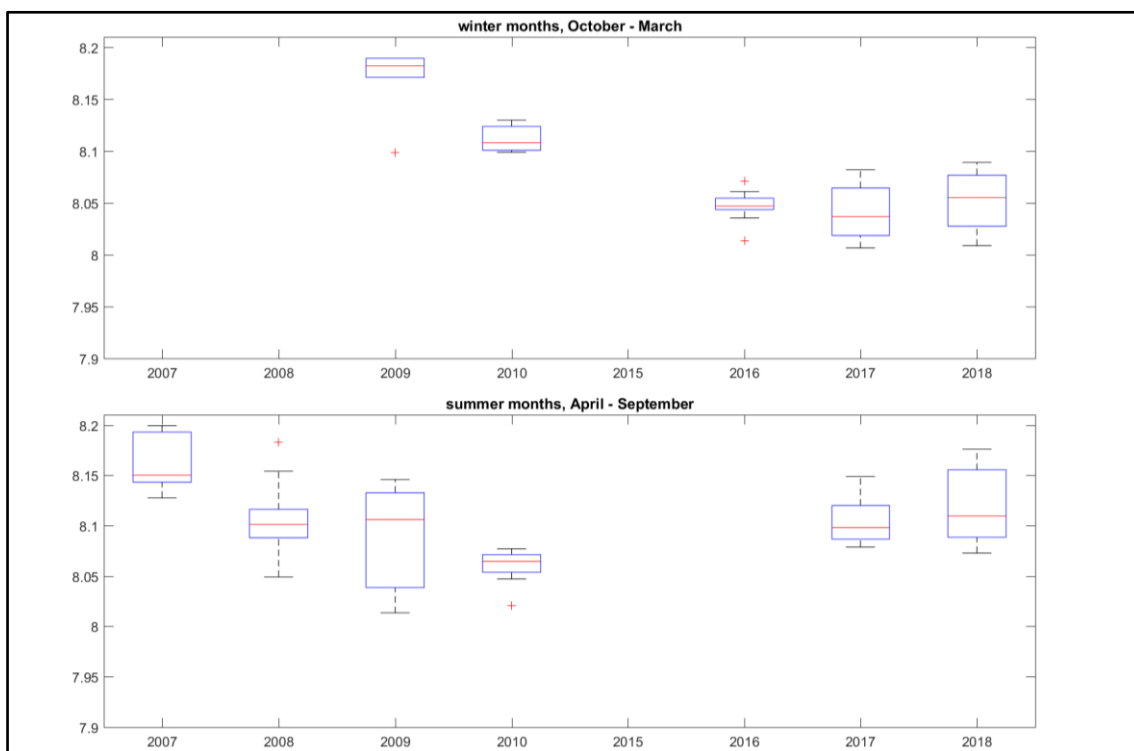


**Figure 32.** Temporal trend of surface ocean pH (< 10 m) in winter (top) and summer (bottom) (data from the black circles in **Figure 24**). Red lines are the annual medians, the blue boxes represent 75 % of the data, the error bars (black lines) enclose 99.3% of the data, and the red crosses are the remaining data.

**Figur 32.** pH-endring over tid i overflata (< 10 m) om vinter (øverst) og sommer (nederst). Data er fra de svarte sirklene i Figur 24. Røde linjer representerer årsmedian, blå bokser inneholder 75 % av dataene det aktuelle året, 99.3% av at års data ligger innenfor de svarte strekene og de rød kryssene er resten av dataene.

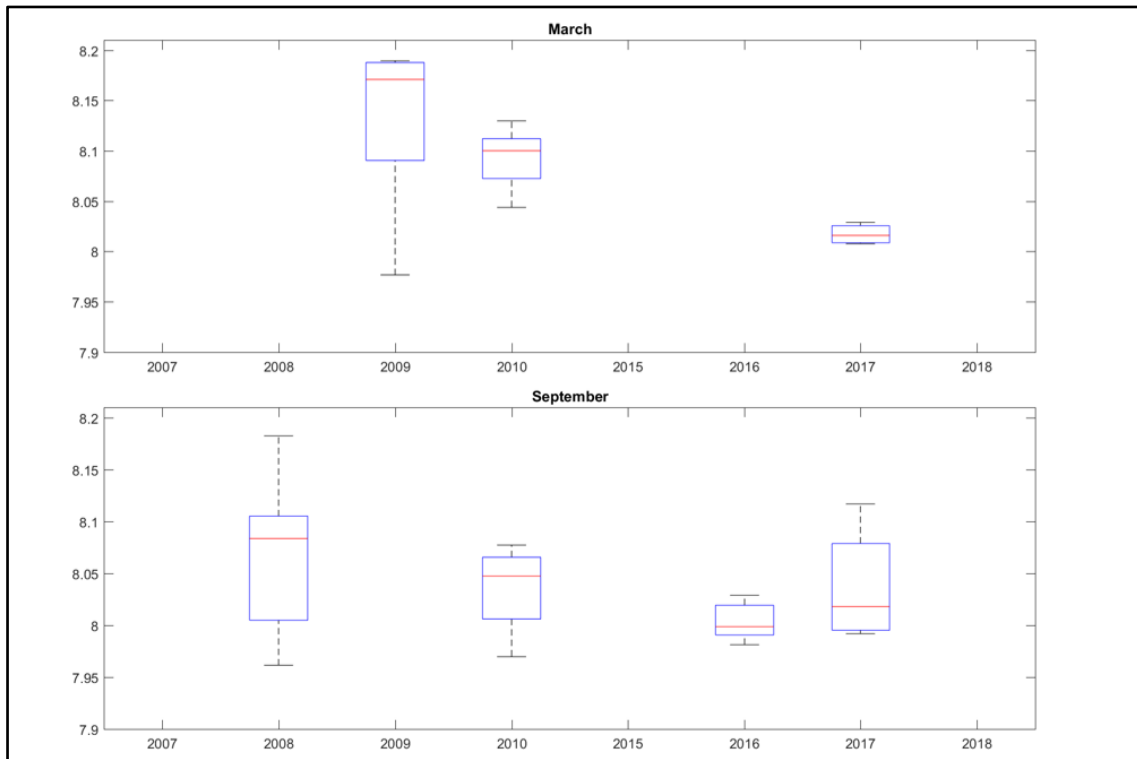


**Figure 33.** Temporal trend of surface ocean pH (< 50 m) in March (top) and September (bottom) (data from the black circles in **Figure 24**).

**Figur 33.** pH-endring over tid i overflata (< 50 m) i mars (øverst) og september (nederst). Data er fra de svarte sirklene i **Figur 24**.

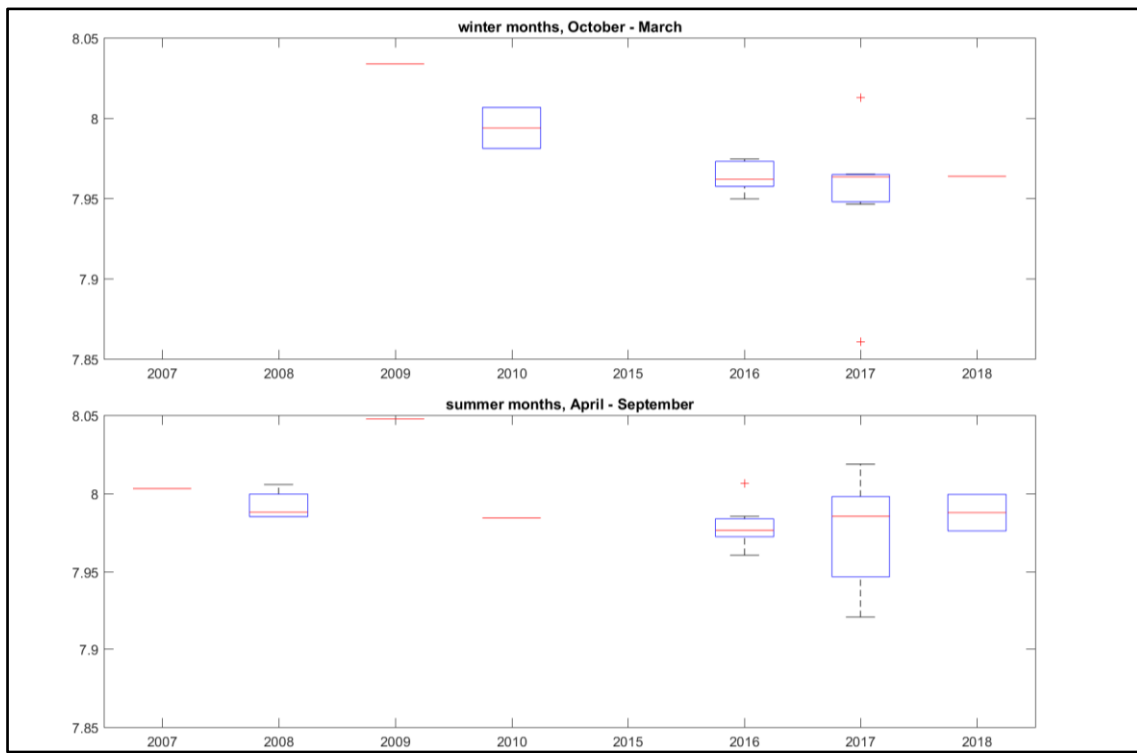


**Figure 34.** Temporal trend of deep ocean pH (> 300 m) in winter (top) and summer (bottom) (data from Korsfjorden, the biggest black circles in Figure 24).

**Figur 34.** pH-endring over tid i dypvann (> 300 m) om vinter (øverst) og sommer (nederst). Data er fra Korsfjorden, den største svarte sirkelen i Figur 24.

### 3.2.4.2 Skrova

Skrova is a coastal station in Vestfjorden at 68.1°N, 14.5E and has been sampled each month for carbonate chemistry by IMR since 2015. Position, depth and sampling data are displayed in **Table 9, Appendix 6.2**. This time series provides valuable data on seasonal variation of inorganic carbon in the Norwegian Coastal Current, to 300 m depth (**Figure 35**).

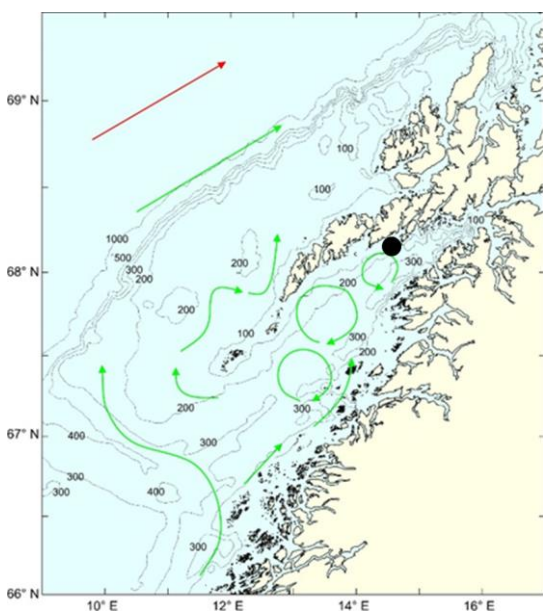


**Figure 35.** The location and current patterns in the Lofoten region. Green arrows indicate Coastal Current flow patterns, Red arrow indicate the Norwegian Atlantic Current. Skrova station is marked by a black circle.

**Figur 35.** Kart over Lofoten som viser de viktigste strømmene. Grønne piler viser kyststrømmen og rød pil viser den norske Atlanterhavssstrømmen. Svart prikk viser Skrova kyststasjon.

Observations and modelling show that the exchange of coastal current water in Vestfjorden is high and efficient, and the residence time of the upper 100 m of fjord water in summer is less than a month. Therefore, the variation at the Skrova coastal station reflects the natural variability in the Norwegian current, which fluctuates between the exchanges with Atlantic water. This is reflected in salinity and temperature temporal variations. However, the pattern in the upper mixed layer is repeated every year as a function of the spring bloom of phytoplankton and the productive season of photosynthesis and biological carbon uptake, leading to increases in pH and elevated levels of aragonite saturation. The 2015 and 2018 data showed similarly high values in pH in the upper layers due to spring and summer photosynthetic consumption of CO<sub>2</sub>.

The variation in salinity (**Figure 36**) shows that in January the upper 100 m was well mixed, and that the depth of the mixed layer shallowed rapidly to about 60 m and continued shallowing until around the middle of May. From June to August the mixed layer was about 30 m deep and from the end of August it deepened to approx. 100 m depth by the end of the year. The distribution of salinity mainly governs the variation in total alkalinity (**Figure 37**).

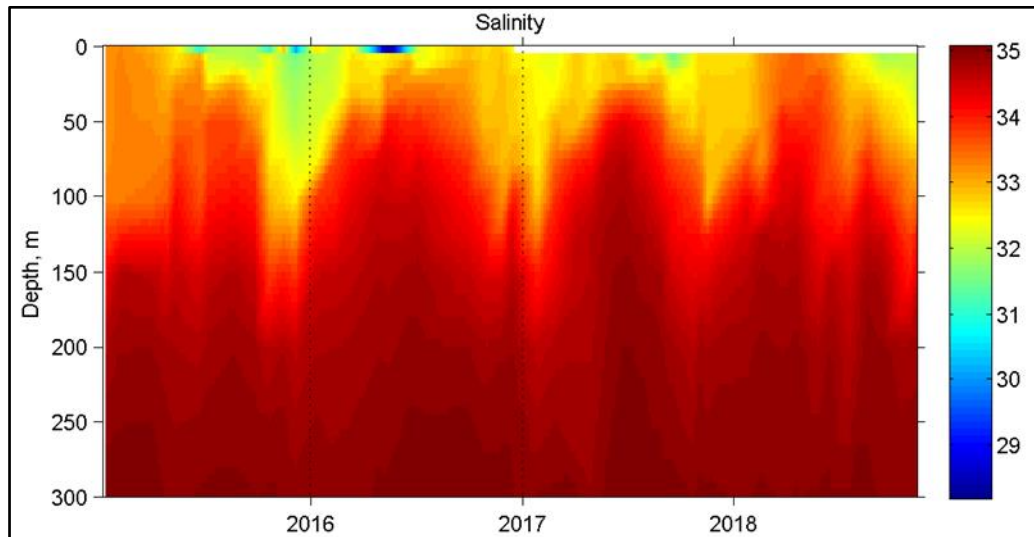


**Figure 36.** Seasonal and annual variation in salinity in the water column at the coastal station Skrova 2015-2018.

**Figur 36.** Års- og mellomårlig variasjon i saltholdighet i hele vannsøylen ved kyststasjon Skrova i 2015-2018.

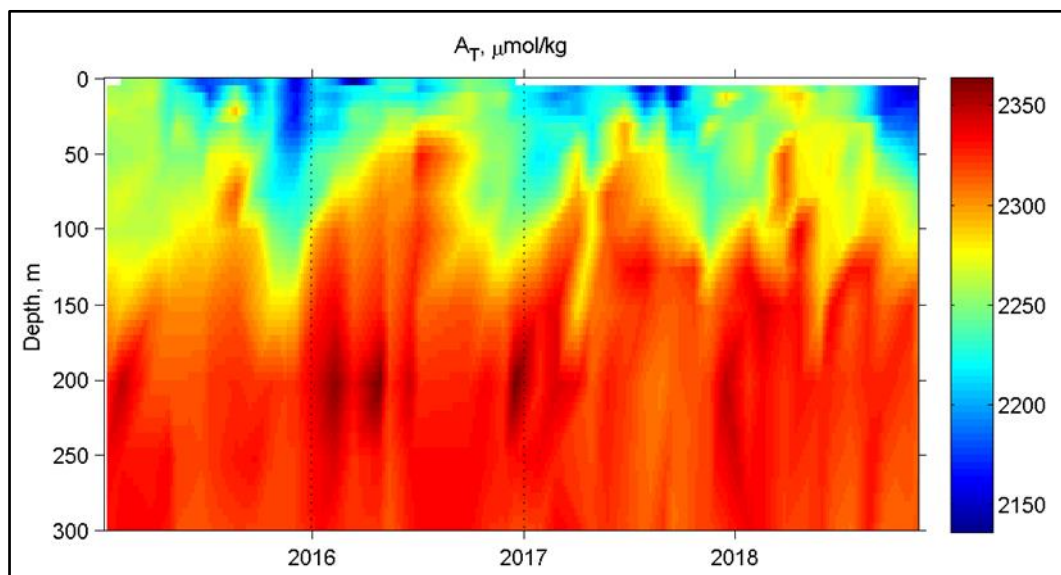


**Figure 37.** Seasonal and annual variation in  $A_T$  in the water column at the coastal station Skrova 2015-2018.

**Figur 37.** Års- og mellomårlig variasjon i  $A_T$  i hele vannsøylen ved kyststasjon Skrova i 2015-2018.

The variation in pH through the water column (**Figure 38**) shows considerable interannual variation, partly driven by varying degrees of freshwater dilution in the upper 100 m. Each

year, there is an increase in pH in the spring in the upper 150-200 m and a subsequent decrease throughout the water column by late autumn. The saturation state of aragonite is above 2.5 in the upper 100 m almost every year, then in late autumn the value decreases sharply to similar values as the bottom waters (*Figure 39*).

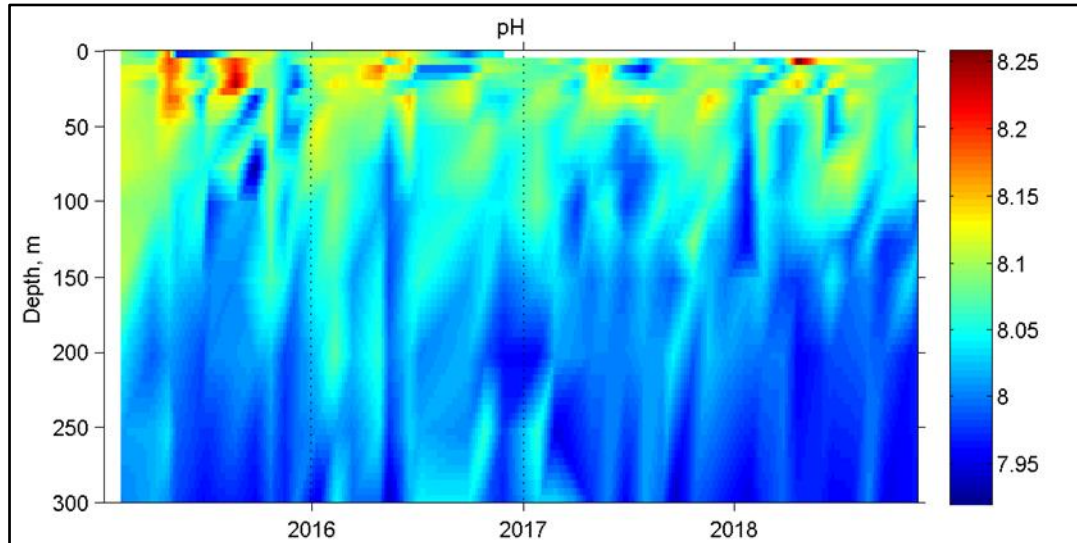


*Figure 38. Seasonal and annual variation in pH in the water column at the coastal station Skrova 2015-2018.*

*Figur 38. Års- og mellomårlig variasjon i pH i hele vannsøylen ved kyststasjon Skrova i 2015-2018.*

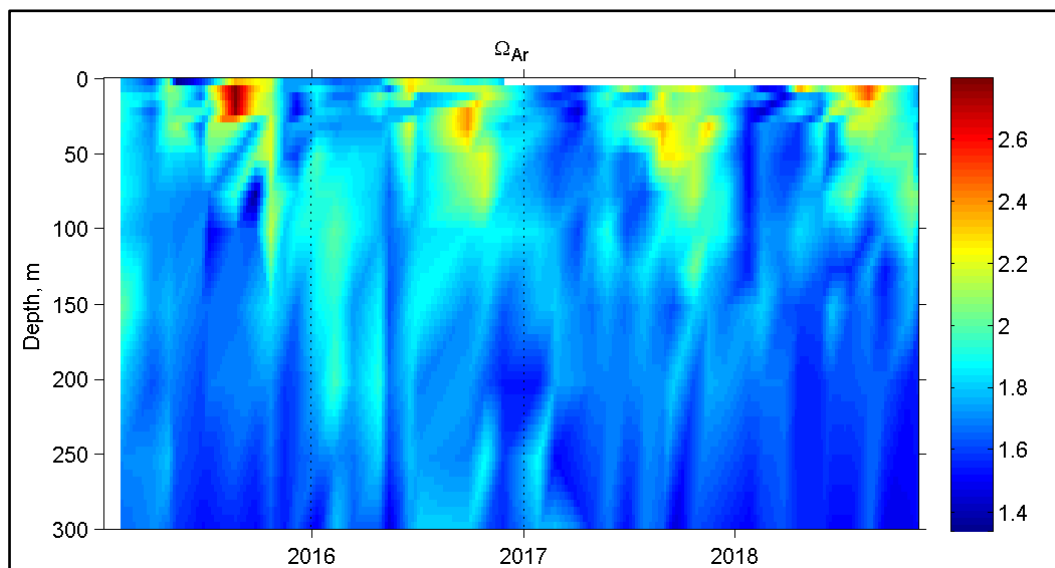


*Figure 39. Seasonal and annual variation in <math>\Omega</math> aragonite in the water column at the coastal station Skrova 2015-2018.*

*Figur 39. Års- og mellomårlig variasjon av aragonittmetningsgrad i hele vannsøylen ved kyststasjon Skrova i 2015-2018.*

### 3.2.5 Trend analysis at selected stations

Continuous winter data (January to March) from Station M over the years 2011 to 2018 have been examined, and **Figure 40** shows the interannual decrease in pH and  $\Omega_{\text{Ar}}$ . By including only winter data, biological influence of the data is avoided. The annual decrease is for pH and  $\Omega_{\text{Ar}}$  0.0039 and 0.017, respectively, and the correlations are strong. These trends are slightly weaker for pH and slightly stronger for  $\Omega_{\text{Ar}}$  compared to the years 2011-2017. The trends are comparable to the negative trends estimated for the Norwegian Basin by Skjelvan et al. (2014) of -0.0041 and -0.012 for pH and  $\Omega_{\text{Ar}}$ , respectively. The pH trends are stronger than those in Bates et al. (2014), who presented surface trends from 7 time series around the globe. Small variations in the trends from year to year are expected due to natural variability in the oceanographic conditions.

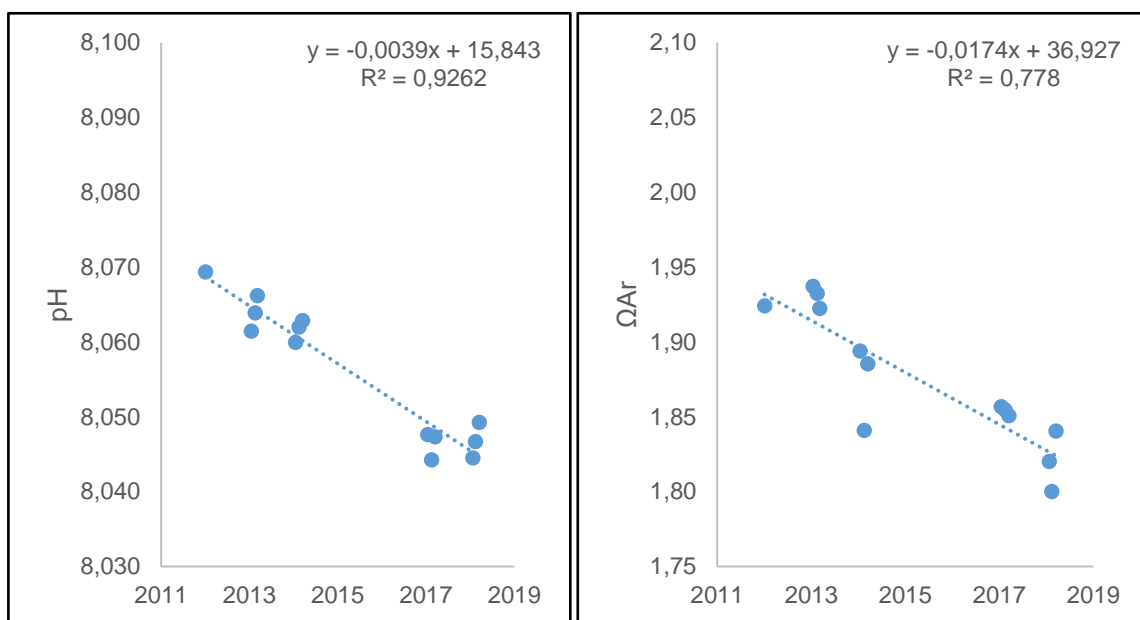


**Figure 40.** Winter surface water trends of pH (left) and  $\Omega_{\text{Ar}}$  (right) at Station M during the years 2011-2018. The values are calculated from continuous measurements and further averaged over month. Winter is defined as January to March.

**Figur 40.** Vinter trend i overflate pH (til venstre) og  $\Omega_{\text{Ar}}$  (til høyre) fra Stasjon M i årene 2011 til 2018. Dataene er beregnet fra kontinuerlige målinger og videre midlet over måned. Vinter er definert som januar til mars.

Further analysis of temporal changes in the Norwegian Sea can be identified from the hydrographic station located at ~1°E along the Svinøy-NW section. The temperature,  $C_T$ ,  $A_T$  and aragonite saturation state at 1000, 1500, 2000 and 2400 m for the 1°E station along the Svinøy section shows temporal trends and interannual variability related to the variations in Arctic water at this locations (**Figure 41**).

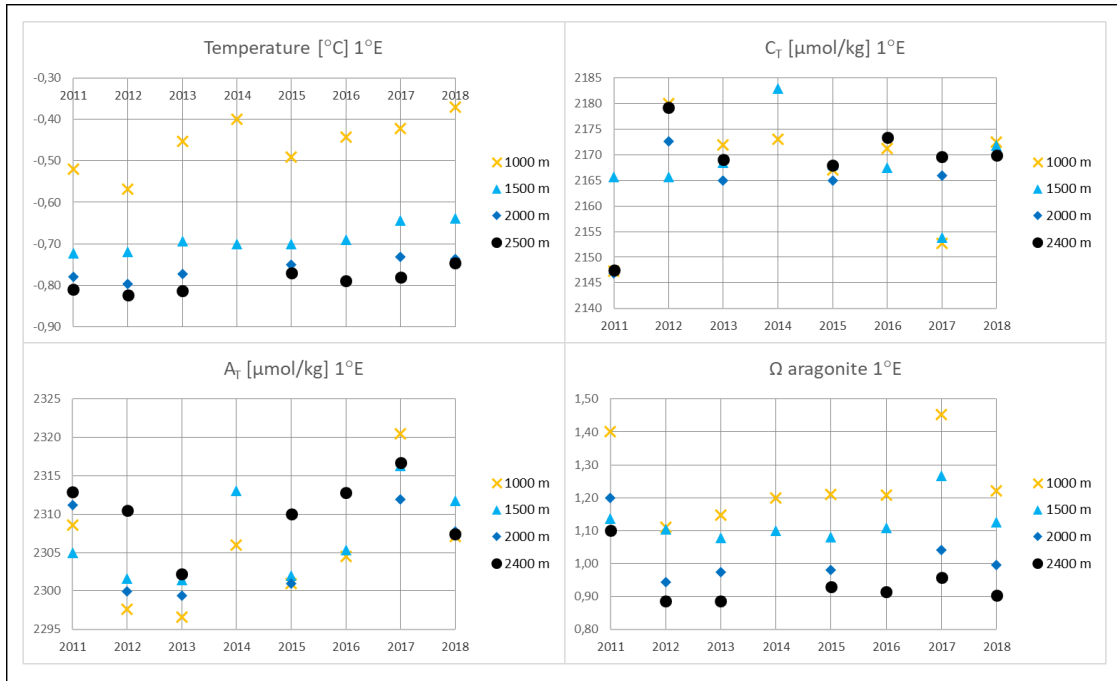


**Figure 41.** Trend analysis based on the years 2011 to 2018 in temperature and aragonite saturation state at 1000, 1500, 2000, 2500 m depth from the 1°E station along the Svinøy-NW section.

**Figur 41.** Trendanalyse basert på årene 2011 til 2018 av temperatur og aragonittmetning ved 1000, 1500, 2000 2500 m dyp på stasjonen 1 °E langs Svinøy-NV snittet.

The temperature at 1000 m is higher and more variable compared to those from deeper waters, likely due to mixing between the cold Arctic water with the overlying warm and salty Atlantic water. The concentration of C<sub>T</sub> had relatively little variation at  $2167 \pm 9 \mu\text{mol kg}^{-1}$  across the 1000-2400 m depth range at all years. However, A<sub>T</sub> followed the warming with a slightly increasing trend from  $\sim 2300 \mu\text{mol kg}^{-1}$  in 2013 to  $\sim 2310 \mu\text{mol kg}^{-1}$  in 2018. This was accompanied by increased aragonite saturation from 2012, especially at 1000 and 1500 m. The depth of the saturation horizon varied from just above and below 2000 m depth during the time series, as is also seen at Station M further north.

Analysis of temporal changes in northern the Norwegian Sea can be identified from the hydrographic station located at  $\sim 12.3^\circ\text{E}$  (**Figure 42**) along the Gimsøy-NW section. The temperature and salinity at 1500 m showed increasing trends between 2011 and 2018, likely due to variability in mixing between the cold Arctic water with the overlying warm and salty Atlantic water. Analogous to the Svinøy data, C<sub>T</sub> had relatively little variation over the time series with concentrations of  $2167 \pm 5 \mu\text{mol kg}^{-1}$ . The 2018 data showed slight cooling and increased salinity, relative to the 2017 data, which was accompanied by reductions in A<sub>T</sub> and C<sub>T</sub> and subsequently lower pH and aragonite saturation with comparable values to those in 2011.

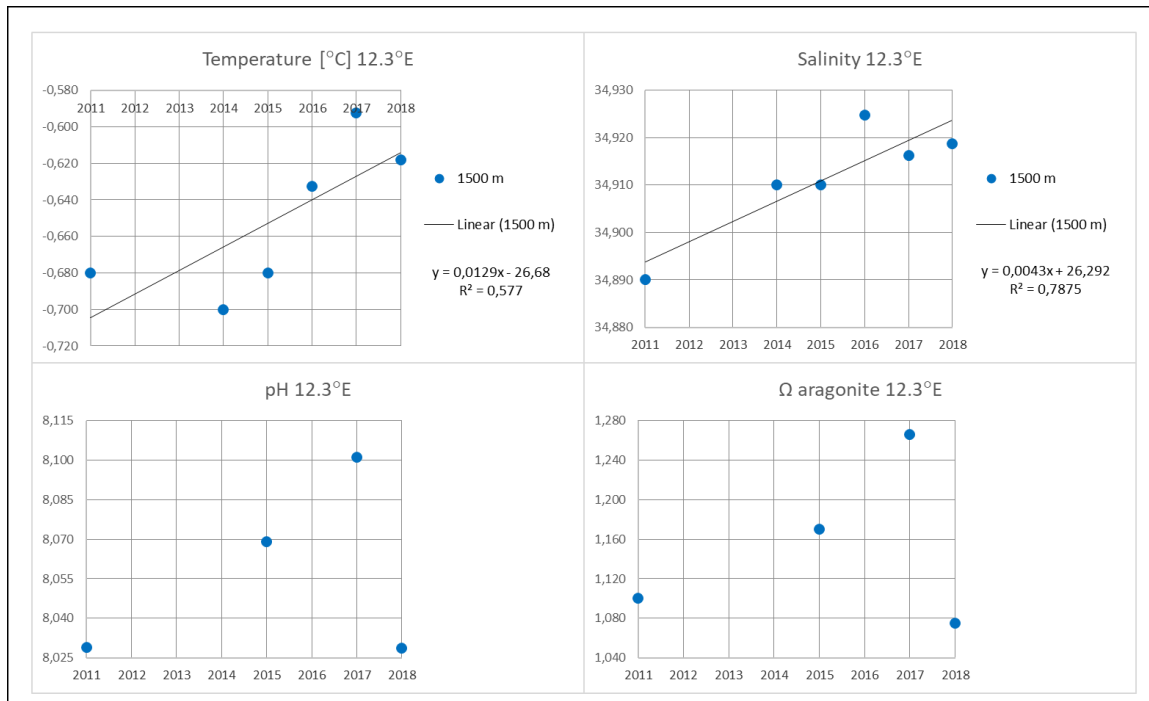


**Figure 42.** Yearly trend analysis in temperature, salinity, pH and aragonite saturation state at 1500 m depth at station 12.3 °E along the Gimsøy-NW section

**Figur 42.** Årlig trendanalyse av temperatur, saltholdighet, pH og aragonittmetning ved 1500 m dyp på stasjonen 12.3 °E langs Gimsøy-NV snittet.

At the coastal station Skrova, the large seasonal variation throughout the time series shows the dominating biological process in spring is phytoplankton production, which consumes CO<sub>2</sub> and consequently increases seawater pH (**Figure 43**). In the autumn, degradation of organic material releases CO<sub>2</sub> and pH decreases to reach minimum values in the winter.

As the seasonal variation is much greater compared to the long-term trend, any emerging yearly time trends are relatively very small and not significant at this stage. In order to estimate reliable time trends of ocean acidification, a ten-year period of observation is generally recommended (Henson et al. 2016), so it is early in the Skrova time series to determine such a trend. However, the data demonstrate that the seasonal variation has a considerable amplitude (winter-summer) compared to any slight long-term trend so far, which for global surface waters is estimated at 0.002 pH units year<sup>-1</sup> (Takahashi et al. 2014).

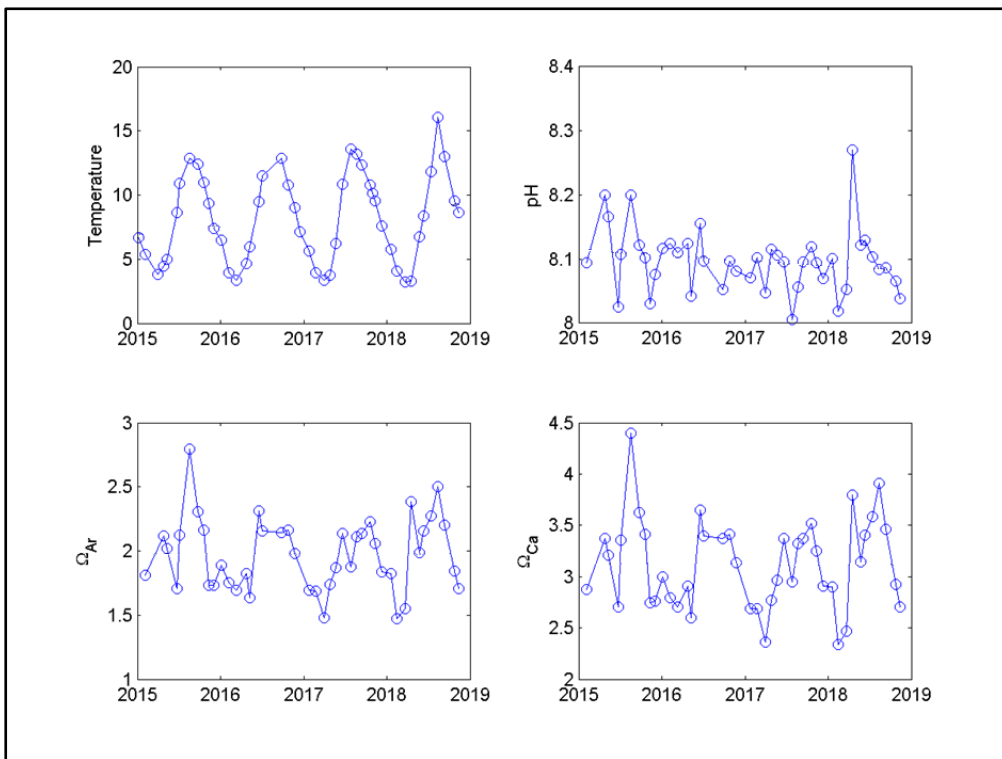


**Figure 43.** Seasonal variation in temperature, pH and aragonite- and calcite saturation state at Skrova.

**Figur 43.** Årsvariasjon i temperatur, pH og aragonitt- og kalsittmetning ved Skrova.

### 3.3 Barents Sea

#### 3.3.1 Spatial variability along the Fugløya-Bjørnøya section

In January 2018, carbon chemistry measurements were carried out by IMR in the whole water column at five fixed stations along the hydrographic section between Fugløya and Bjørnøya, southeastern Barents Sea (**Figure 44**). Position, depth and sampling data are displayed in **Table 10, Appendix 6.2**.

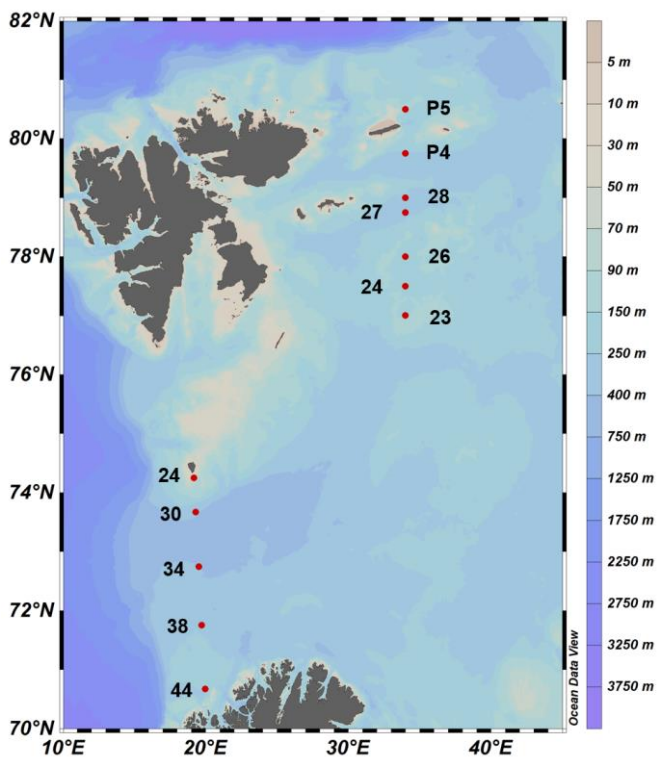


**Figure 44.** Map and station numbers from stations along the Fugløya-Bjørnøya section in January 2018 and in the northeastern Barents Sea in August and September 2018.

**Figur 44.** Kart og nummer over stasjoner langs Fugløya-Bjørnøya snittet i januar 2018 og i nordøstlige Barentshav i august og september 2018.

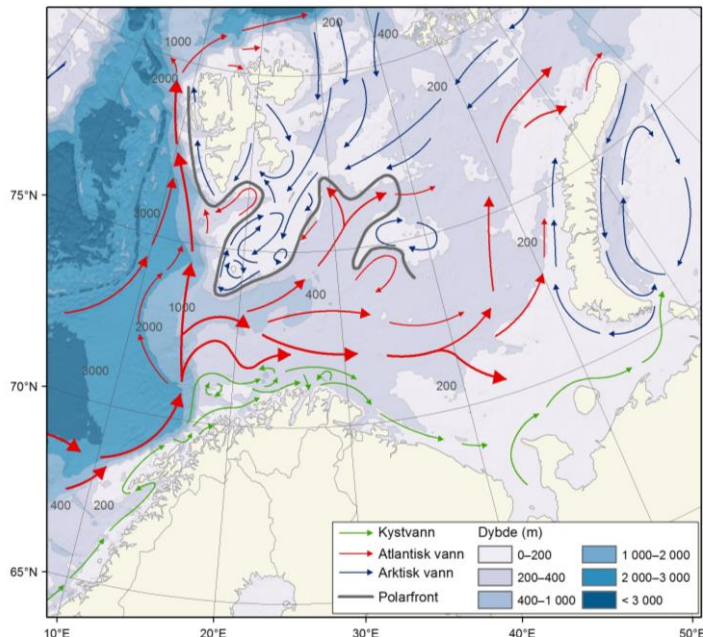


**Figure 45.** Map showing major currents in the Barents Sea. Red arrows show Atlantic water, green coastal current and blue arrows show the Arctic water. Grey line shows the position of the polar front. Map from [www.imr.no](http://www.imr.no).

**Figur 45.** Kart som viser hovedstrømmene i Barentshavet. Røde piler viser atlantisk vann, grønne piler er kyststrømmen og blå piler viser arktisk vann. Grå linje viser omtrentlig posisjon til polarfronten. Kart fra [www.imr.no](http://www.imr.no).

The Barents Sea is a relatively shallow basin with maximum depths around 400 m. The Fugløya-Bjørnøya section extends from the Norwegian coastal current in the south and passes through the region of Atlantic water inflow into the Barents Sea (**Figure 44**). The entire water column northwards to approximately 72 °N is influenced by the Norwegian coastal water of relatively low salinity and temperatures of 5-7 °C (**Figure 6, Appendix 6.1**). The central part of the section was deepest at 500 m depth at 73.5 °N in the Barents Sea. Atlantic

water with salinity > 35.1 and temperature ~6 °C occupied the upper layers of the water column between 71.5 and 73.5 °N. Further north, the water becomes less salty towards Bjørnøya with strong horizontal gradients in salinity and temperatures in the upper 200 m as the Atlantic waters meet the relatively fresh and cold Arctic waters.

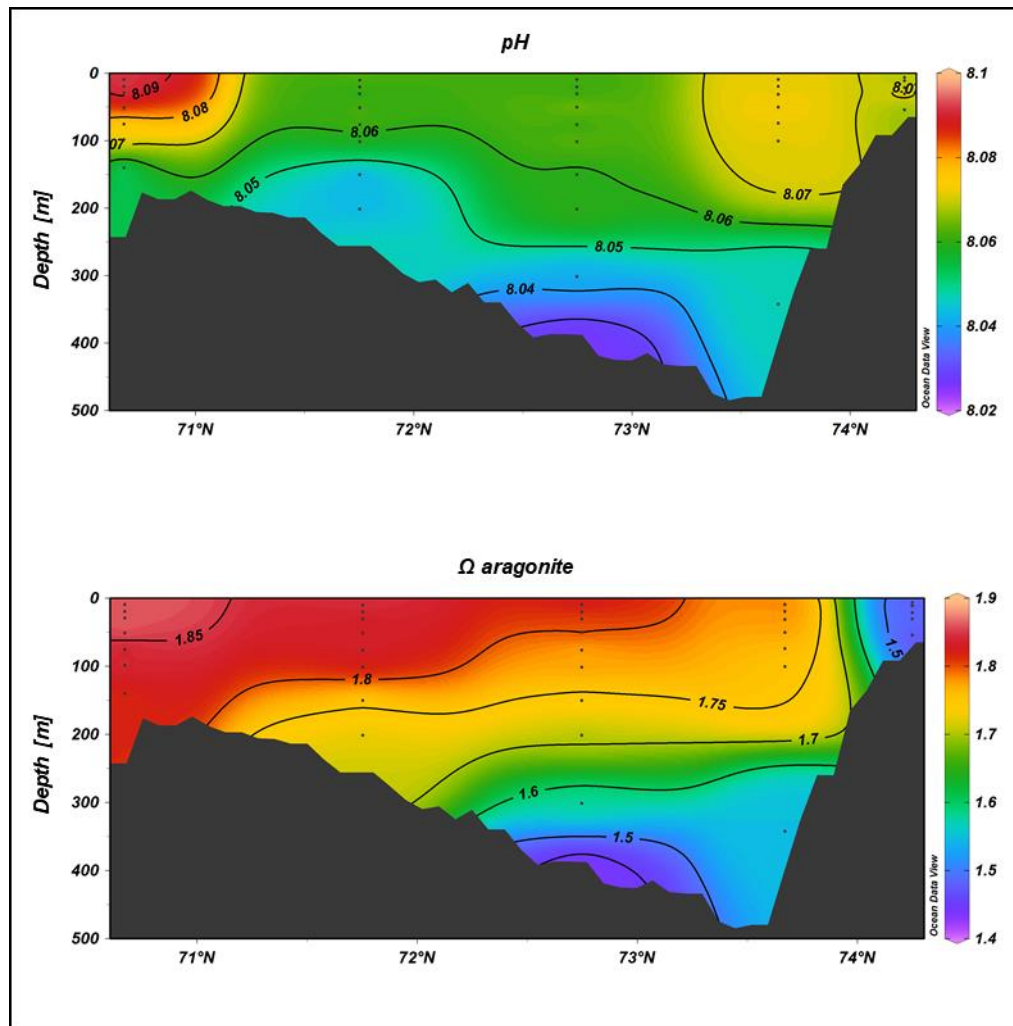


**Figure 46.** pH and aragonite saturation state along the Fugløya-Bjørnøya section in January 2018.

**Figur 46.** pH og aragonittmetningsgrad langs Fugløya-Bjørnøya snittet i januar 2018.

Close to Bjørnøya, the inflow of Arctic water travelling southwards from north east Svalbard creates strong horizontal gradients at the polar front around 73.5 °N. The upper water column at the northern extent of the section has lower salinity (< 34.7) and lower temperatures (< 1 °C). The distribution of  $A_T$  reflects the presence of the coastal water, Atlantic water and Arctic water. The Atlantic water has higher  $A_T$  of 2320-2330  $\mu\text{mol kg}^{-1}$ , which decreases rapidly to lowest values around 2290-2300  $\mu\text{mol kg}^{-1}$  in the Arctic water (**Figure 6, Appendix 6.1**). The concentration of  $C_T$  was lowest (~2110  $\mu\text{mol kg}^{-1}$ ) in the south and increased to more homogenous distribution 2150-2160  $\mu\text{mol kg}^{-1}$  in the Atlantic water in the central part of the section. This was accompanied by high pH (> 8.09) in the upper 100 m of the water column at the southern part of the section. Lowest pH values around 8.04 were found in the

deepest water at 73.5-73.8 °N (**Figure 46**). The saturation state for aragonite decreased with depth from 1.8-1.9 in the upper 200 m south of 73 °N. The lowest aragonite saturation of ~1.5 occurred at 300-400 m depth at 73 °N, which was likely a result of increased CO<sub>2</sub> from respiration.

### 3.3.2 Spatial variability along the northeastern Barents Sea section

In August and September 2018, carbon chemistry measurements were carried out by IMR on water samples collected throughout the water column at seven fixed stations in the northern Barents Sea (**Figure 44**). This region is influenced by recirculated Atlantic water from Fram Strait to the south and Arctic water from the north, as well impacted by seasonal sea ice processes. Position, depth and sampling data are displayed in **Table 11, Appendix 6.2**.

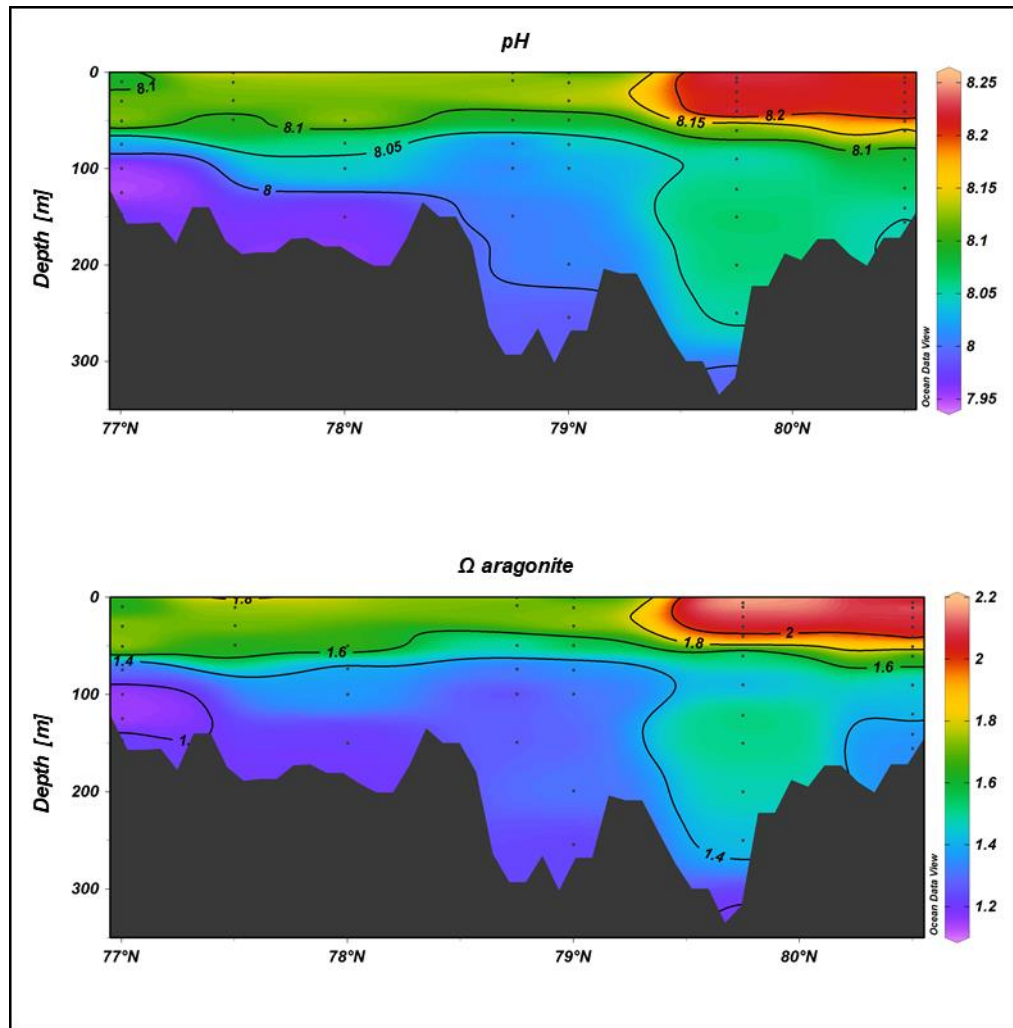


**Figure 47.** pH and aragonite saturation state along the Barents Sea section in August and September 2018.

**Figur 47.** pH og aragonittmetningsgrad fra nordøstlige Barentshav i august og september 2018.

Salinity in the upper 50 m decreased northwards along the section to lower values in the fresher Arctic water north of 79.5 °N. Lowest salinity is around 80 °N in water affected by seasonal ice cover and recent ice melt (**Figure 7, Appendix 6.1**). In the upper 50 m, the

temperature was 2-3 °C, with warmest surface waters at the northern and southern parts of the section. Between 50 and 100 m, the cold (< 0 °C) Arctic water spread across the length of the section. Below 100 m, recirculated Atlantic water from Fram Strait can be seen as a relative warm and saline water mass in the southern part of the section.

In the surface, both  $C_T$  and  $A_T$  decrease northwards to lowest values north of 80°N. Lowest  $A_T$  (~2270  $\mu\text{mol kg}^{-1}$ ) and  $C_T$  (~2068  $\mu\text{mol kg}^{-1}$ ) distinguished the fresh polar water in the upper 50 m with influence of meltwater from sea ice and biological carbon uptake. Surface layer pH was highest in the upper 50 m with maximum values of 8.23 in the north (**Figure 47**). The highest  $A_T$  values around 2310  $\mu\text{mol kg}^{-1}$  and high  $C_T$  of 2211  $\mu\text{mol kg}^{-1}$  were found at 100-200 m depth within the Atlantic water in the southern part of the section.

Lowest pH of around 7.95 was found in the deepest water along the length of the section, especially in the south. Part of the pH variation is driven by temperature changes, since low temperatures are accompanied by higher pH. The saturation state for aragonite (and calcite, not shown) largely followed the distribution of pH with saturated levels throughout the water column. Maximum values ( $\Omega$  aragonite > 2.1) occurred in the upper layer at the northern end of the section. Lowest saturation states of 1.1 were found in the deepest part of the section, especially in the south. This is probably due to increased  $\text{CO}_2$  resulting from microbial degradation of organic matter and not from anthropogenic ocean acidification.

### 3.3.3 Seasonal variability in surface water

The stations covered using MS *Norbjørn* between Tromsø-Longyearbyen are shown in **Figure 48**. Position, depth and sampling data are displayed in **Table 12, Appendix 6.2**. Surface water from 4 m depth was sampled on four cruises in March, June, August and November 2018. The ship's route varies depending on weather and ice conditions as well as different port calls for cargo deliveries (e.g., Bjørnøya (~74 °N) in March) between cruises.

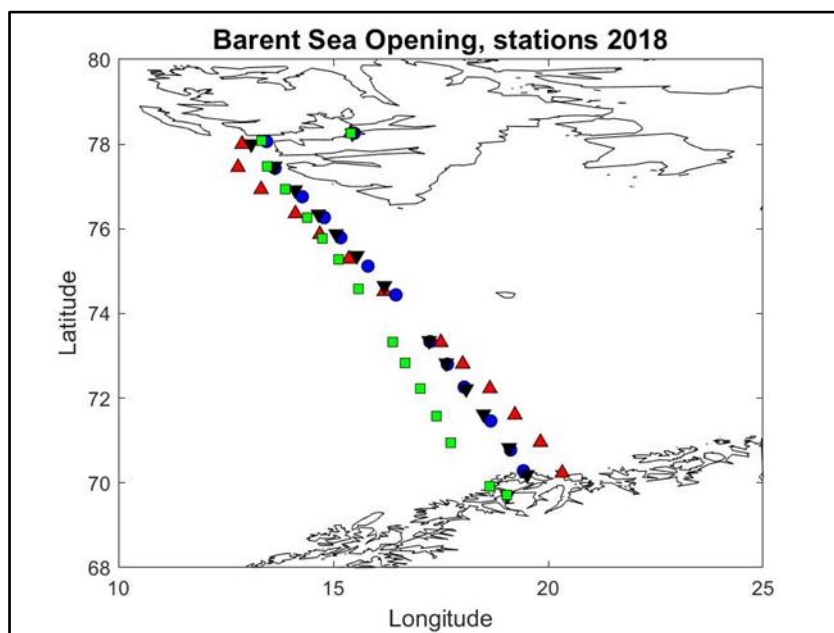


**Figure 48.** Station map for the Barents Sea opening. Samples were taken during 3-5.3 (red ▲), 13-15.6 (blue ●) 22-24.8 (black ▼) and 13-15.11 (green ■). The stations locations varied because of weather or ice conditions.

**Figur 48.** Stasjoner langs Barentshavssåpningen i året 2018. Toktene ble gjort 3-5.3 (rød ▲), 13-15.6 (blå ●) 22-24.8 (sort ▼) og 13-15.11 (grønn ■). Stasjonene er noe værværhengig som man kan se av spredningen i lengdegrader.

The Barents Sea opening is influenced by Atlantic water, Norwegian coastal water and Arctic water (**Figure 45**). Atlantic Water is the dominant water mass in the open sea between Tromsø and Svalbard, but it is heavily mixed with meltwater from sea ice during the summer. Along the coast of Svalbard, the Atlantic water mixes with Arctic water and meltwater during summer. The Norwegian Coastal Current flows along the coast of Norway, and this is mixed with Atlantic water towards the north into the Barents Sea. For calculating the seasonal averages of the different parameters, the transect between the coast of Norway to Isfjord in Svalbard was divided into sections of 69-72 °N (Norwegian coast), 72-74 °N (open sea south of Bjørnøya), 74-76 °N (open sea north of Bjørnøya) and 76-78 °N (Svalbard Coast).

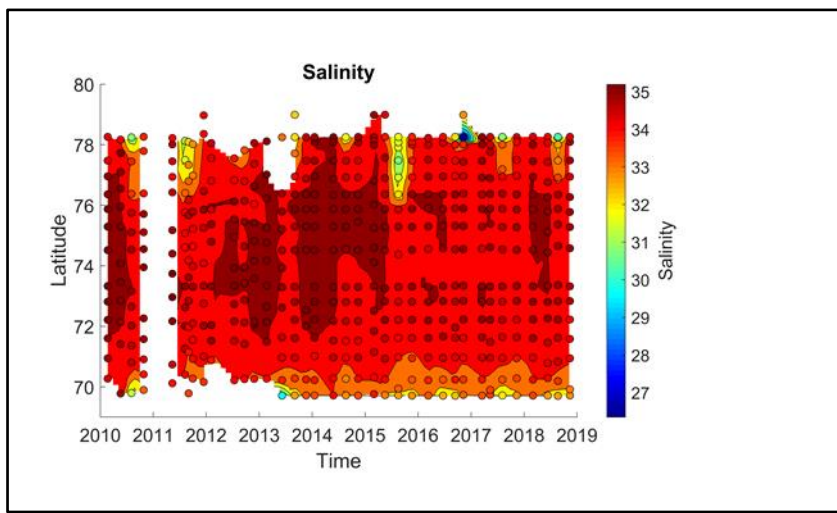
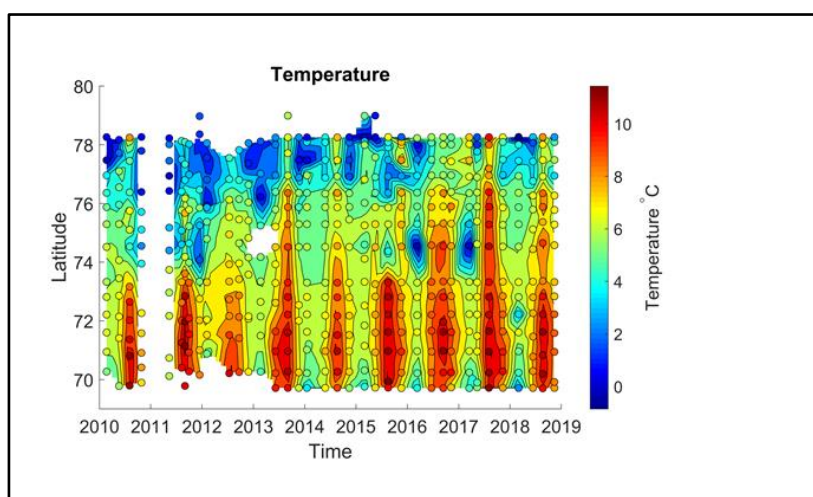


**Figure 49.** Nine years of temperature and salinity measurements from the Barents Sea entrance as part of the Tilførselprogrammet and the Ocean Acidification monitoring program. The circles show the measured values, while the interpolated values are shown in the background.

**Figur 49.** Ni års målinger i Barentshavssåpningen av temperatur og saltholdighet målt under Tilførselsprogrammet og Havforsuringsovervåkningen. Ringene viser målte verdier, mens interpolerte verdier vises i bakgrunnen.

Temperature and salinity since 2010 are shown in **Figure 49**. The average temperature for the Norwegian coast reached 5.32 °C in the winter and increased to 10.91 °C in the summer. The average temperature for the Svalbard coastal stations reached 3.80 °C in the spring and 7.16 °C in summer. The average winter temperature for the open water stations south and north of Bjørnøya reached as low as 5.31 and 5.38 °C, respectively, and in the summer as high as 9.52 and 8.54 °C, respectively. The temperature ranges were very similar to those reported for the 2017 data, but with less northward extension of warmer waters during summer. The average salinity for the Norwegian coast reached as low as 33.79 in late autumn (November) and as high as 34.30 in the winter.

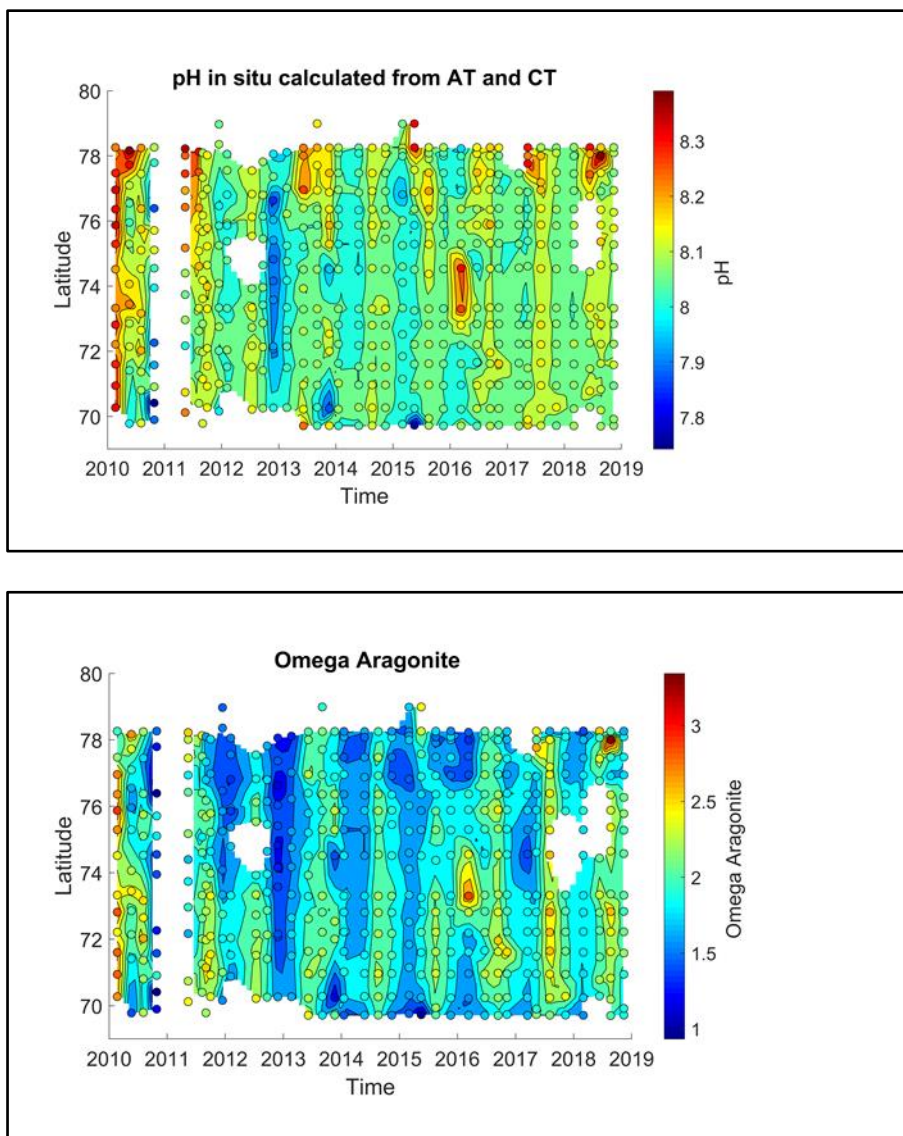


**Figure 50.** In situ  $\text{pH}_\text{r}$  and  $\Omega_\text{Ar}$  from the Barents Sea opening. The circles show the measured and calculated values, while the interpolated values are shown in the background.

**Figur 50.** In situ  $\text{pH}_\text{r}$  og  $\Omega_\text{Ar}$  fra Barentshavsvåpningen. Ringene viser målte og beregnede verdier, mens interpolerte verdier vises i bakgrunnen.

The average salinity for the Svalbard coastal stations reached as low as 33.47 in the summer and as high as 35.0 in winter. The average salinity for the open water stations south and north of Bjørnøya reached as low as 34.56 and 34.85, respectively, in the summer, and as high as 35.0 in spring south of Bjørnøya and 35.03 in winter and spring north of Bjørnøya. The seasonal ranges in salinity were also similar to those reported for the 2017 data, however average summer salinities for the different areas tended to be slightly lower compared to 2017 and indicate freshening, alongside cooling, at the sea surface of the Barents Sea opening from increased sea ice melt in the Arctic source waters from NW Svalbard.

The pH and aragonite saturation since 2010 are shown in **Figure 50**. The average pH for the Norwegian coast reached as low as 8.06 in the winter and as high as 8.10 in the summer. The average pH for the open water stations South of Bjørnøya and North of Bjørnøya reached as low as 8.06 in the winter and as high as 8.13 and 8.14, respectively, in the summer. The average pH for the Svalbard coastal stations reached as low as 8.05 in the winter and highest for the whole Barents Sea opening with average pH of 8.20 in spring. This is likely to reflect the drawdown of C<sub>T</sub> in the spring blooms in the Svalbard coastal stations, before large scale freshening from sea ice melt has occurred in the polar waters travelling southwards. The average pH values for winter were very similar to those in 2017, but summer average pH for all areas was slightly lower in 2018.

The average aragonite saturation state for the Norwegian coastal waters reached as low as 1.75 in the winter and as high as 2.30 in the summer. The average aragonite saturation for the Svalbard coastal stations reached as low as 1.73 in the winter and as high as 2.33 in the summer. The average aragonite saturation for the open water stations South of Bjørnøya reached as low as 1.78 in the winter and as high as 2.36 in the summer. The average aragonite saturation for the open water stations North of Bjørnøya reached as low as 1.81 in the winter and as high as 2.32 in the summer. Winter and summer averages for aragonite saturation were slightly lower in all regions, compared to 2017 data.

### 3.3.4 Trend analysis at selected stations

#### 3.3.4.1 Trend by linear regression

Shown in **Figures 51-52** below are the trend analyses using linear regression on average yearly surface winter data from the sections 72-74 °N and 74-76 °N from the Tromsø-Longyearbyen crossing, with Atlantic water ( $S > 35$  and  $T > 4$  °C). There was not enough data to do trend analyses on polar water ( $T < 0$  °C).

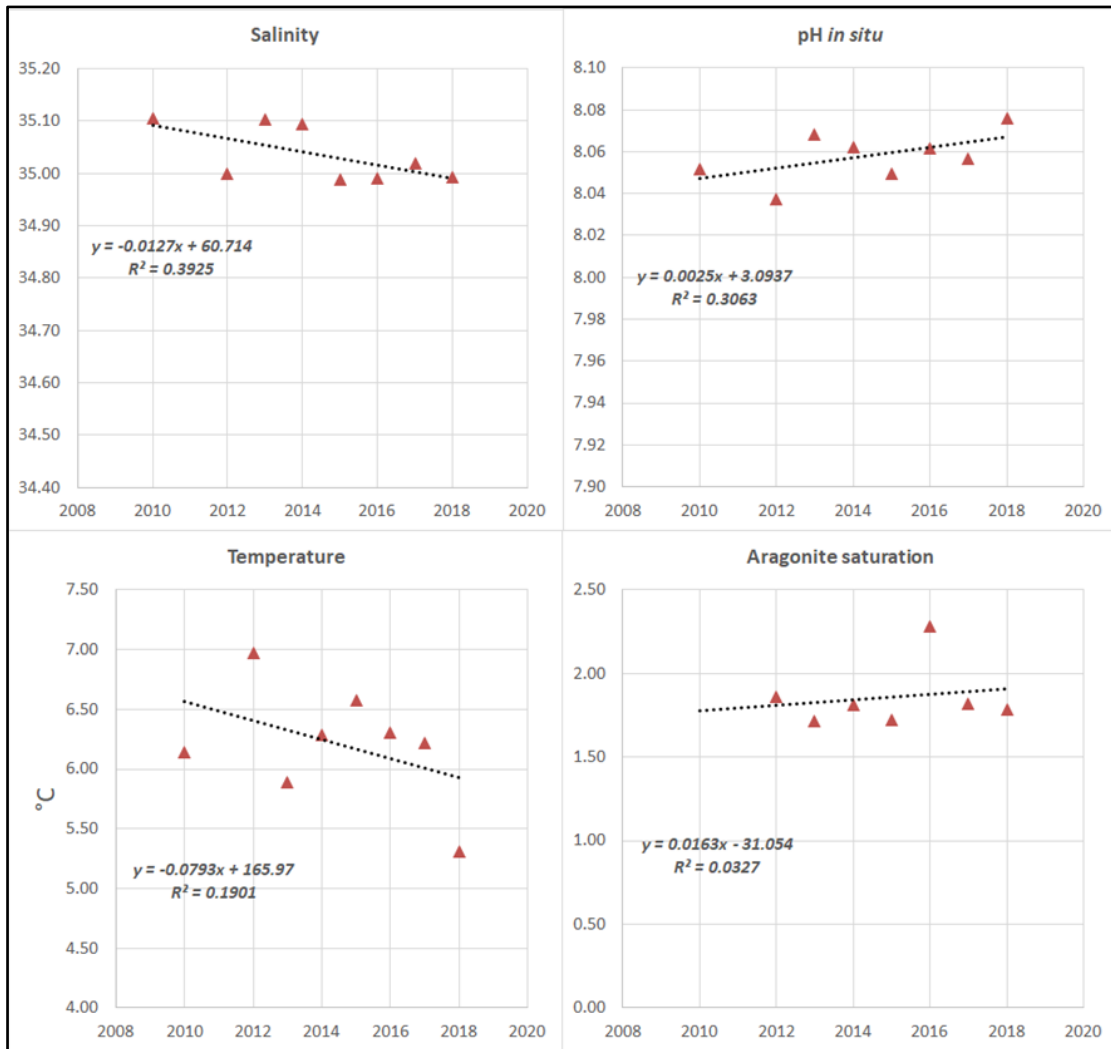


**Figure 51.** Linear regression trends in temperature, salinity, pH and aragonite saturation state of winter data in the surface (4 m) at 72-74 °N in the Barents Sea Opening.

**Figur 51.** Lineær regresjon av temperatur, saltholdighet, pH og metningsgrad av aragonitt av midlede vinterdata fra overflata (4 m) fra 72-74°N i Barentshavsvåpningen.

The seawater salinity and temperature in surface waters at 72-74 °N showed a freshening of  $0.013 \text{ yr}^{-1}$  and cooling of  $0.079 \text{ °C yr}^{-1}$ , accompanied by an increase in both pH and  $\Omega$  aragonite of  $0.003 \text{ yr}^{-1}$  and  $0.016 \text{ yr}^{-1}$ , respectively (**Figure 51**). The 2010 aragonite was regarded an outlier and removed because of an old method for determining  $A_T$  and  $C_T$ .

The trend of seawater salinity and temperature in surface waters of the Barents Sea opening at 74-76 °N showed a freshening of  $0.013 \text{ yr}^{-1}$  and a cooling of  $0.083 \text{ °C yr}^{-1}$ , accompanied by an increase in both pH and  $\Omega$  aragonite of  $0.003 \text{ yr}^{-1}$  and  $0.026 \text{ yr}^{-1}$ , respectively (**Figure 52**).

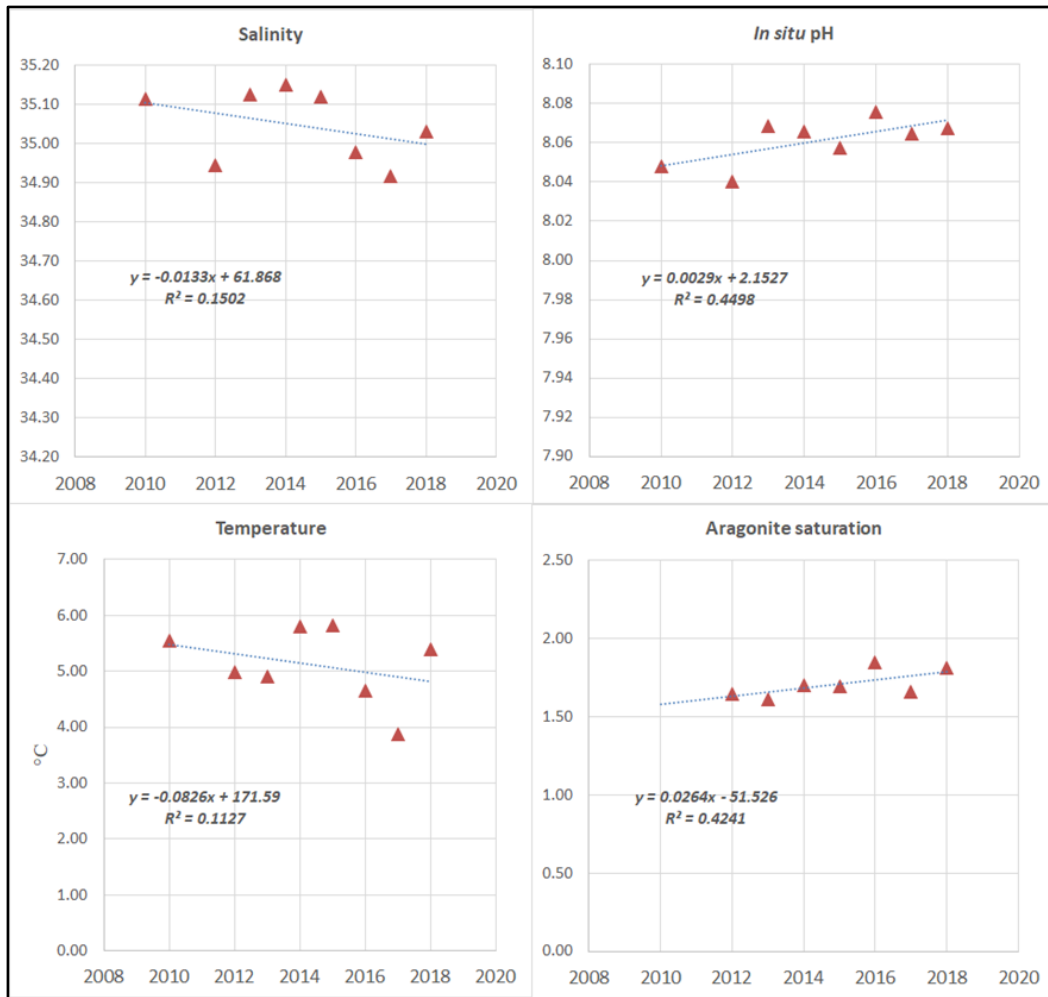


**Figure 52.** Linear regression trends in temperature, salinity, pH and aragonite saturation state of winter data in the surface (4 m) at 74-76°N in the Barents Sea Opening (Tromsø-Longyearbyen). The aragonite saturation in 2010 was considered such an outlier that it was removed.

**Figur 52.** Lineær regresjon av temperatur, saltholdighet, pH og metningsgrad av aragonitt av midlede vinterdata fra overflata (4 m) fra 74-76°N i Barentshavsvåpeningen (Tromsø-Longyearbyen).

The 2010 aragonite was regarded an outlier and removed because of an old method for determining  $A_T$  and  $C_T$ . Competing physical and biological processes drive the changes over time. Colder and fresher waters, likely from polar and coastal origins, are typically more productive, compared to more Atlantic-influenced water, and therefore have lower  $C_T$  and thus higher pH and aragonite saturation states. An increase in Arctic water at the Barents Sea Opening would lead to the changes described above.

The distribution of seawater temperature and  $C_T$  concentrations at 300-400 m depth (deepest stations) from 2012 to 2018 at ~72.8°N along the Fugløya-Bjørnøya section showed interannual variability associated with proximity to the Polar Front due to the variations in Atlantic water to the south and Arctic water to the north (**Figure 53**). In general, cooler waters were associated with higher  $C_T$  concentrations and indicate a larger volume of cold, carbon-rich Arctic water in 2018. Salinity changes revealed the waters at 300-400 m tended to become fresher with time, which supports the presence of fresher polar water, and was

accompanied by a reduction in the aragonite saturation state to lowest values of 1.4-1.6 in 2018.

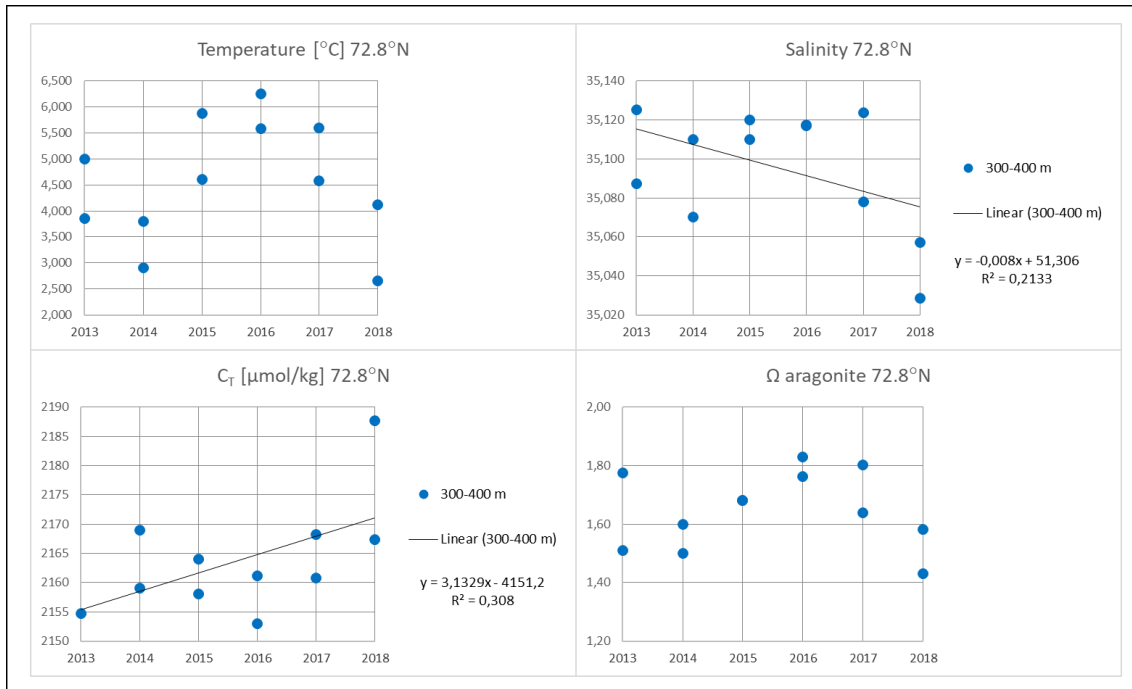


**Figure 53.** Trend analysis of temperature, salinity,  $C_T$  and aragonite saturation state at 300-400 m depth station 72.8°N along the Fugløya-Blørnøya section.

**Figur 53.** Trendanalyse av temperatur, saltholdighet,  $C_T$  og aragonittmetning ved 300-400 m dyp på stasjonen 72.8°N langs Fugløya-Bjørnøya snittet.

The distribution of seawater temperature and salinity at 250-300 m depth along the northeastern Barents Sea section show changes of  $-0.32 \text{ }^{\circ}\text{C yr}^{-1}$  and  $-0.021$ , respectively, from 2012 to 2018 (**Figure 54**). Alongside the general freshening and cooling trend, pH exhibits a general increase of  $0.006 \text{ yr}^{-1}$ . The saturation state for aragonite varied throughout the time series, with an average value of  $1.32 \pm 0.13$ . Similar to the trends at 300-400 m depth along the Fugløya-Bjørnøya section (~72.8°N), increased cold, fresh Arctic water induces a lot of variability in the region.

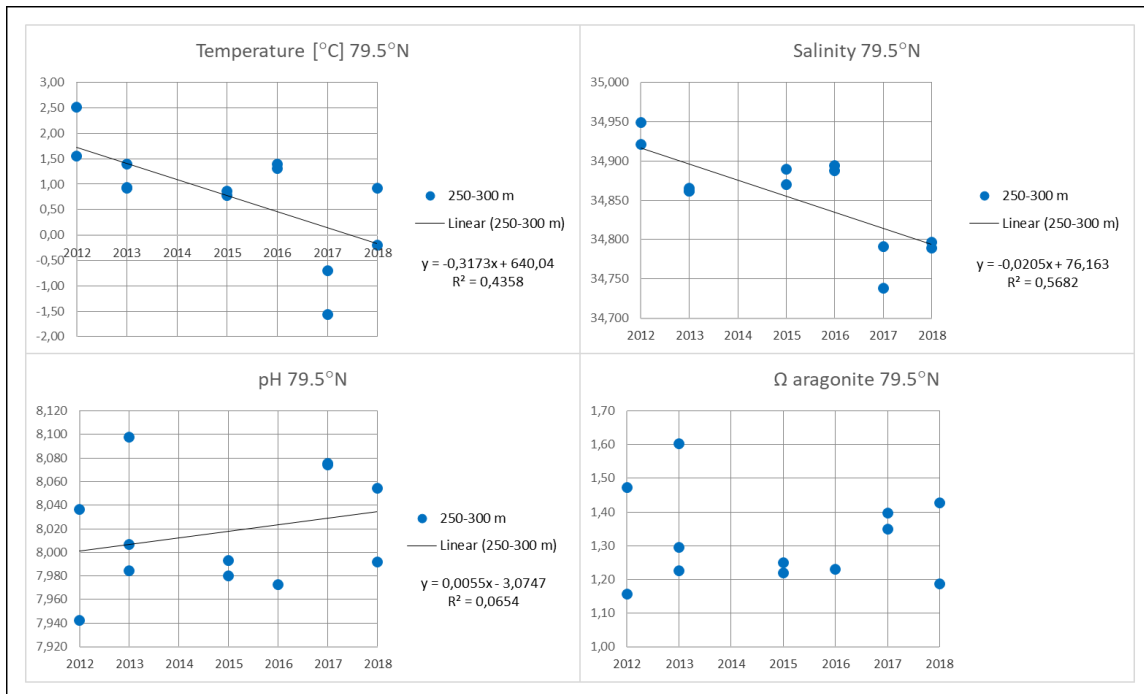


**Figure 54.** Trend analysis of temperature, salinity, pH and aragonite saturation state at 250-300 m depth from the station 79.5 °N along the section in the northwestern Barents Sea.

**Figur 54.** Trendanalyse av temperatur, saltholdighet, pH og aragonittmetning på 250-300 m dyp på stasjonen 79.5 °N langs snittet i nordøstlige Barentshav.

### 3.4 Norwegian Coast

The FerryBox line between Bergen and Kirkenes (MS *Hurtigruten Trollfjord*) was equipped with salinity, temperature, chlorophyll a fluorescence, and membrane equilibrator-based pCO<sub>2</sub> sensors (**Figure 55**). fCO<sub>2</sub> observations between February and May were flagged for quality control due to a high temperature difference (>3 °C) between the pCO<sub>2</sub> sensor and the FerryBox inlet, and data after September are not available due to a sensor malfunction. The elevated temperature difference was likely due to poor flow rate either due to tubing/fitting obstruction or pump failure. Based on estimates of uncertainties from the pCO<sub>2</sub> detector uncertainty (~2 µatm), detector drift (~20 µatm), and an estimated ~0.5 °C uncertainty of seawater temperature at the equilibrator (~10 µatm), the combined uncertainty of the measurements was ~22.5 µatm using a root sum of the squares approach. Low fCO<sub>2</sub> was associated with high phytoplankton biomass as indicated by high chlorophyll a fluorescence during spring and summer. Elevated photosynthetic activity by phytoplankton was likely a primary contributor to the observed ~100-200 µatm decrease in fCO<sub>2</sub>. In late summer, fCO<sub>2</sub> increased to near or slightly above atmospheric levels. This may have been due to the thermodynamic warming effect as sea surface temperature increased by roughly 4-8 °C between July, when the phytoplankton bloom had mostly subsided, to August. Further work is currently underway to improve continuous seawater supply at adequate flow rates (changing fittings used to connect to the pCO<sub>2</sub> sensor and also a new pump model) to reduce downtime of the sensor, and an on-board calibration gas system has been built for regular detector calibrations to reduce uncertainty due to detector drift.

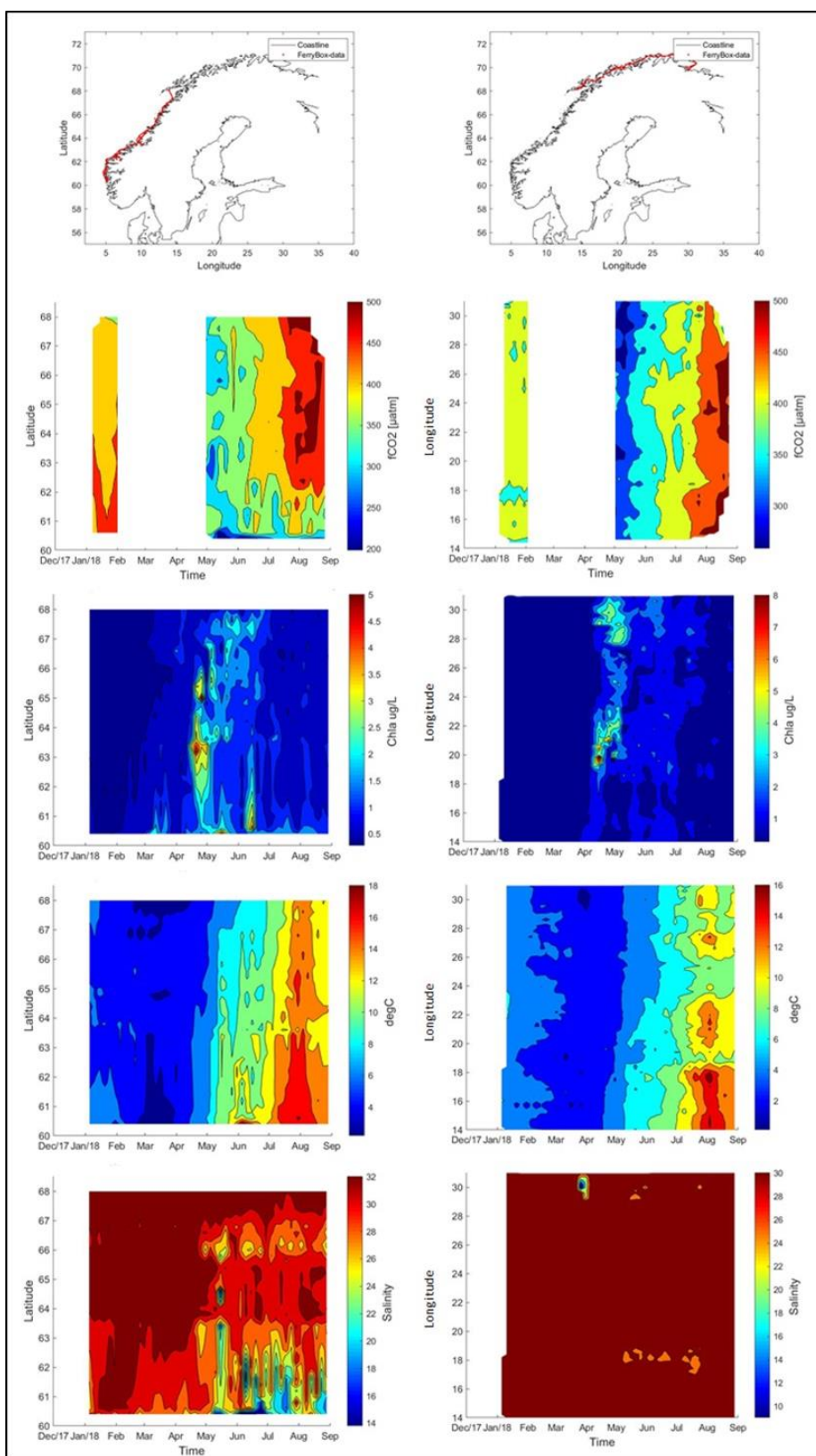


**Figure 55.** Variation in  $f\text{CO}_2$  ( $\mu\text{atm}$ ) measured with FerryBox on MS Trollfjord, with Chl a fluorescence, temperature and salinity. Left: Data between Bergen and Vestfjorden; Right: Data between Vestfjorden and Kirkenes.

**Figur 55.** Variasjon i  $\text{fCO}_2$  ( $\mu\text{atm}$ ) målt fra FerryBox på MS Trollfjord, med klorofyll *a* fluorescens, temperatur og saltholdighet. Venstre: Data mellom Bergen og Vestfjorden, Høyre: Data mellom Vestfjorden og Kirkenes.

### 3.5 Cold Water Coral Reefs

In 2018, IMR conducted a series of studies of the carbonate chemistry around selected cold-water coral reefs. The aim was to study natural variation in physical and chemical processes to better understand how these ecosystems respond and adapt to ocean acidification and warmer seas. Samples were taken at sites with coral gardens and wall reefs on 17 and 21 May in Hardangerfjord (Huglhammaren, Straumsneset, Bekkjarvik, Hornaneset, Nakken, Terskel) and on 15 May at coastal sites in Møre og Romsdal (Aktivneset) and Vesterålen (Hola). Depth and sampling data are displayed in **Table 14, Appendix 6.2**. Data will be used to get an idea of how the carbon chemistry at the sites varies over time and in space and to study to what extent the carbon chemistry affects where different deep-water coral species can grow.

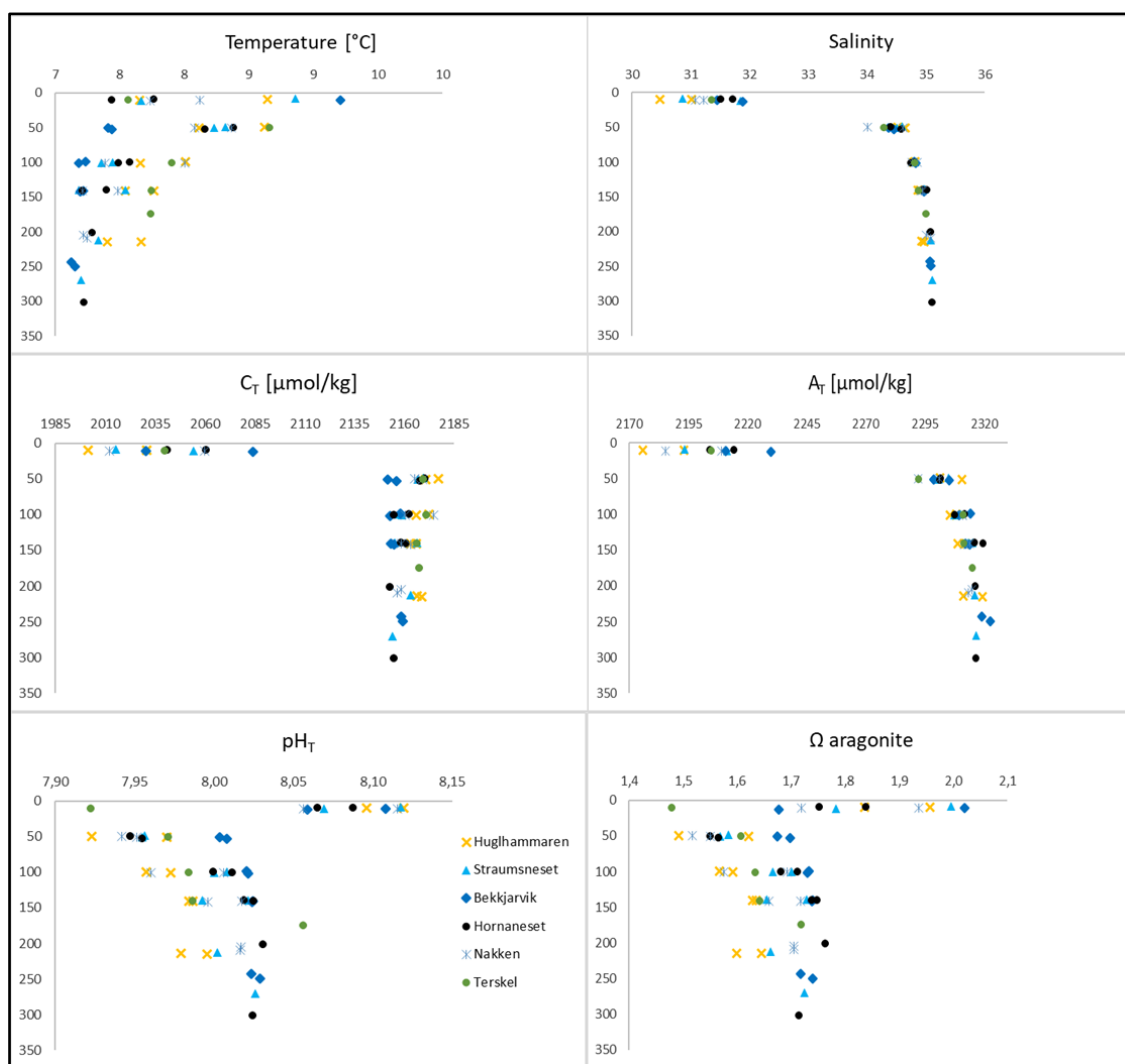


**Figure 56.** Variasjoner i temperatur, saltholdighet,  $\text{C}_T$ ,  $\text{A}_T$ , pH og aragonitt metning i vannkolonnen ved kaldtvannskorallrev i Hardanger, Hordaland.

**Figur 56.** Variasjoner i temperatur, saltholdighet,  $\text{C}_T$ ,  $\text{A}_T$ , pH og aragonitt metning i vannkolonnen ved kaldtvannskorallrev i Hardanger, Hordaland.

The full water column data showed the largest gradients in the upper 50 m, which was a consistent feature at the different reef sites (*Figure 56*). Freshwater inputs (rain and rivers) reduced salinity (30-32), and  $A_T$ , in the upper 50 m and biological production further reduced  $C_T$  (< 2085  $\mu\text{mol kg}^{-1}$ ) in the surface layer at all locations. This was accompanied by high pH values 8.05-8.10 and aragonite saturation states > 1.9.

Below 100 m depth, salinity increased to 35 in the Atlantic water layer and  $C_T$  and  $A_T$  had little variation around 2155-2170  $\mu\text{mol kg}^{-1}$  and 2310-2320  $\mu\text{mol kg}^{-1}$ , respectively. These values are consistent with concentrations measured in the Atlantic water at some of the sites in 2017. Distributions of pH and saturation states are more variable and have different profiles through the water column at the different reef sites. At 50 m, elevated  $C_T$  (up to 2177  $\mu\text{mol kg}^{-1}$ ) was accompanied by lower  $A_T$ , relative to values below, likely due to lesser effects of biological  $C_T$  uptake at this depth and mixing with Atlantic water below that increases  $C_T$ . Low values of pH and aragonite saturation were typically found at 50-100 m depth, with regional minima of 7.92 and 1.5, respectively, at 50 m depth at Huglhammaren.

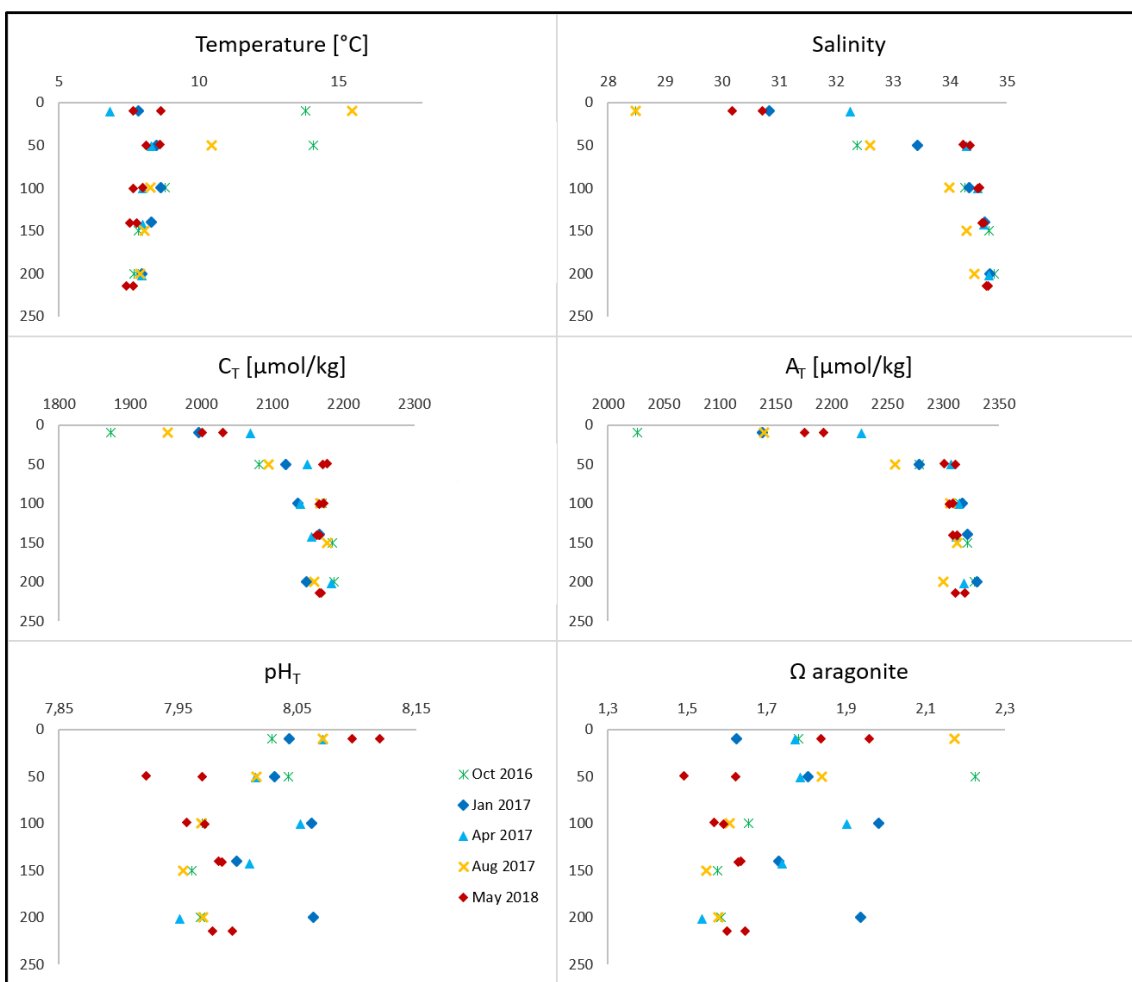


**Figure 57.** Variasjoner i temperatur, saltholdighet,  $C_T$ ,  $A_T$ , pH og aragonitt metning fra 2016-2018 i vannkolonnen ved kaldtvannskorallrev Huglhammaren i Hardanger, Hordaland.

**Figur 57.** Variasjoner i temperatur, saltholdighet,  $C_T$ ,  $A_T$ , pH og aragonitt metning fra 2016-2018 i vannkolonnen ved kaldtvannskorallrev Huglhammaren i Hardanger, Hordaland.

The full water column data at Huglhammaren wall reef from 2016 to 2018 showed largest gradients in hydrography and carbonate chemistry in the upper 50 m and the impacts of seasonal processes (*Figure 57*). Seasonal warming increased temperatures to 13.8-15.5 °C in the surface layer in October 2016 and August 2017 compared to coldest (6.8 °C) and well-mixed upper ocean in April 2017. Freshwater inputs in late spring and summer reduced salinity and lowered  $A_T$  in the upper 50 m and biological production further reduced  $C_T$  (< 2000  $\mu\text{mol kg}^{-1}$ ) by late summer, e.g. August-October. This was accompanied by high pH values 8.07-8.12 and aragonite saturation states > 2.

Below 100 m depth, salinity increased to around 34.9 within the Atlantic water and  $C_T$  and  $A_T$  were more consistent around 2155-2185  $\mu\text{mol kg}^{-1}$  and 2310-2330  $\mu\text{mol kg}^{-1}$ , respectively. The deep water (~214 m) values can be used to assess inter-annual consistency and show that  $C_T$  and  $A_T$  are within similar concentration ranges in all years and variability is attributed to fluctuations in the water masses, e.g. variations in salinity, and natural processes at these depths. Distributions of pH and saturation states are more variable and show different distribution in the depth profile. At 50 m, elevated  $C_T$  (up to 2177  $\mu\text{mol kg}^{-1}$ ) in winter and spring was accompanied by lower pH and aragonite saturation, likely due to remineralization and mixing with carbon-rich Atlantic water. Variability in pH and aragonite saturation in the deepest water shows highest values in January 2017 as  $C_T$  and  $A_T$  were at the lower and higher ends of the concentration ranges, respectively, from all years. Oppositely, lowest values in April 2017 occur as a result of slightly increased  $C_T$  and reduced  $A_T$  perhaps due to additional remineralization following spring blooms and increased amounts of Atlantic water at the time of sampling.

The data from Hola reef from 2015 to 2018 also typically showed largest gradients in hydrography and carbonate chemistry in the upper 50-100 m of the water column, however there are strong seasonal variations compared to the wall reefs, e.g., Huglhammaren (*Figure 58*). Seasonal warming was strongest in July 2016 and October 2017, where the extent of warming in 2017 extended throughout the water column to about 250 m. Saltiest surface layer with salinity up to 33.9 was found in July 2016, in contrast to lowest salinity of 33.4 in October 2017 due to continued fresh water input throughout spring and summer.

Biological production reduced  $C_T$  (< 2050  $\mu\text{mol kg}^{-1}$ ) during spring and summer in the upper layers in all years. This was accompanied by high pH values 8.07-8.12 and aragonite saturation states > 2.1. Large ranges of  $C_T$  concentrations, and to a lesser extent  $A_T$ , occurred in July 2016, compared to 2015 and 2017, with lower pH and aragonite saturation in the warmer and saltier surface layers compared to the rest of the time series data. This is likely due to incursions of Atlantic water towards the surface, showing elevated salinity in the whole of the water column. The characteristics of the deep water (~260 m) show variability in temperature and particularly salinity with less salty water (34.7) at 240 m depth.  $A_T$  had a larger range of 2303-2327  $\mu\text{mol kg}^{-1}$  at this depth, compared to  $C_T$  (2147-2152  $\mu\text{mol kg}^{-1}$ ). pH was more variable but both pH and aragonite saturation were at lowest values at 250 m depth in October 2017.

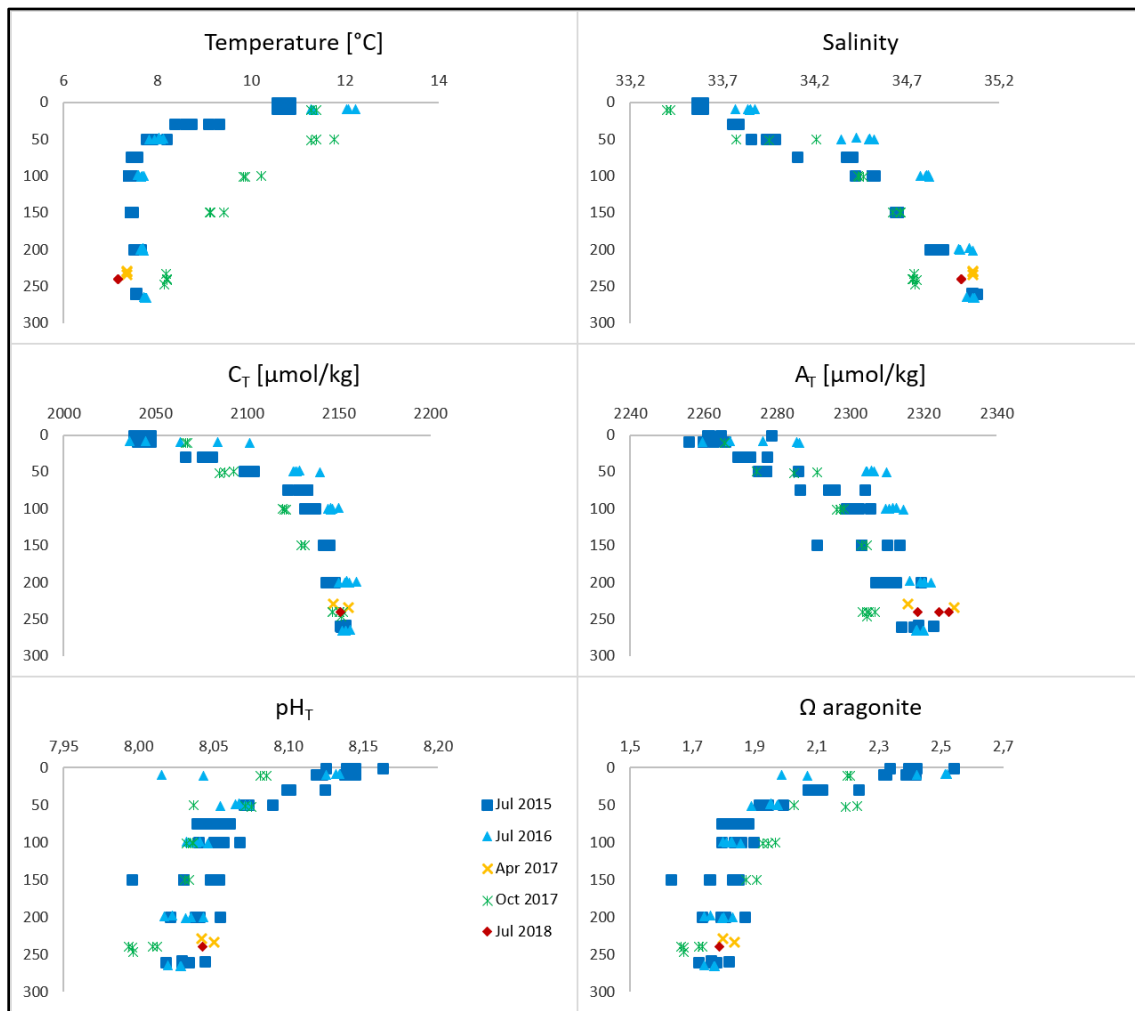


**Figure 58.** Variations in temperature, salinity,  $C_T$ ,  $A_T$ , pH and aragonite saturation state from 2015-2018 in the water column of cold-water coral reefs at Hola, Vesterålen.

**Figur 58.** Variasjoner i temperatur, saltholdighet,  $C_T$ ,  $A_T$ , pH og aragonitt metning fra 2015-2018 i vannkolonnen ved kaldtvannskorallrev i Hola, Vesterålen.

## 4. Conclusion and Recommendations

The Ocean Acidification monitoring program aims to get an overview of the state of ocean acidification in Norwegian waters and to better understand the variations from season to season and between years. The program started in 2013, and 2018 is the sixth consecutive year of measurements, and the report also includes previous acidification data, e.g. from the Tiltførselsprogrammet.

In the Skagerrak, the deepest parts of the water column (600 m) showed increased temperatures by  $0.29 \text{ }^{\circ}\text{C yr}^{-1}$  since 2010, which was accompanied by a reduction in pH and aragonite saturation state of  $0.010 \text{ yr}^{-1}$  and  $0.01 \text{ yr}^{-1}$  at this depth. This was attributed to increased volumes of Atlantic water entering the Skagerrak. In general, as ocean temperatures are increasing, it will be interesting to monitor this region and see if the trend persists or whether other circulation and mixing processes become important.

In the open oceanic surface waters of the Norwegian Sea, the time series data from 2011 to 2018 show decreasing trends in pH and  $\Omega\text{Ar}$  of approximately  $0.004$  and  $0.017 \text{ yr}^{-1}$ , respectively, which only differs slightly from what has been estimated previously. The location of the saturation horizon varied around 2000 m depth in the deepest parts of the Norwegian Sea, as found previously.

The seawater temperature and aragonite saturation state in the Arctic water at 1000 and 1500 m depth at  $1^{\circ}\text{E}$  along the Svinøy-NW section shows interannual variability related to the variations in the mixing with Atlantic water. A slight increasing trend in seawater temperature since 2011 and increased aragonite saturation from 2012 could be identified at these depths. The gradual warming trend from 2012 is likely to reflect the general increase in ocean temperatures in the Arctic Intermediate Water, which is formed from mixing with the overlying warmer Atlantic water. The seawater temperature and salinity at 1500 m depth for the  $12.3^{\circ}\text{E}$  station along the Gimsøy-NW section shows interannual variability due to the interaction of water masses at this depth. Since 2011, a warming of  $0.013 \text{ }^{\circ}\text{C yr}^{-1}$  and increase in salinity of  $0.004$  could be identified in the Arctic Intermediate Water and similarly to the Svinøy data, likely reflects mixing with warmer Atlantic water in the upper layers. The pH and the saturation state of aragonite have tended to increase, however exhibit a large degree of variability from 2011 to 2018, which is likely to continue into the future.

For the Barents Sea, trends at 300 m depth at the  $79.5 \text{ }^{\circ}\text{N}$  in the northeastern region showed a cooling of  $\sim 0.32 \text{ }^{\circ}\text{C yr}^{-1}$  and freshening of  $0.02$  salinity units per year. This is likely due to increased sea ice melt, from human-induced warming, in the Arctic domain that would result in cooler and fresher water being transported southwards. Trends in pH and aragonite saturation were found to slightly increase, although with large fluctuations between each year.

Data from the water column provides information that can be used to develop scenarios for future  $\text{CO}_2$  emission concentrations, the ocean's absorption of anthropogenic  $\text{CO}_2$ , and how the depth of the calcium carbonate saturation horizon changes. Even though we begin to get more of an overview of geographic and temporal variation in the ocean acidification

parameters (Jones et al., 2018), and some of the seasonal drivers, it is too early to fully determine the individual dominant processes of ocean acidification and their regional, seasonal and intermediate variability. This requires further monitoring in a comprehensive manner, i.e. integrated measurements and studies of primary production, ocean physics, and land-sea interactions and exchanges. This may be conducted by dedicated process research cruises as well as using autonomous sensors on moorings measuring a set of biogeochemical parameters in addition to  $\text{pCO}_2$  and pH, such as dissolved oxygen, dissolved organic matter, chlorophyll a and particulate organic matter.

The surface water pH of the Norwegian Sea in winter decreases at a rate of  $0.0039 \text{ yr}^{-1}$  (since 2011), which is comparable to previous estimates of  $0.0041$  at this site (Skjelvan et al., 2014). These time trends show that variations from year to year result from the addition of more data that capture greater longer-term variability and natural fluctuations in the oceanographic conditions. This rate of change in pH is faster than that reported for surface pH in the Iceland Sea during winter, which decreases at a rate of  $0.0024 \text{ yr}^{-1}$  (Olafsson et al., 2009) for the period 1985-2008. However, extending the time series in the Norwegian Sea is required, corresponding to the 20 years of monitoring that has been carried out in the Icelandic Sea (Olafsson et al., 2009), to enable the determination of the relationship between anthropogenic influence and natural variation. However, the Norwegian monitoring program provides insight into how the trend may project to certain marine areas. For example, measurements show that the pH in the Norwegian and Lofoten basins decreases rapidly (Skjelvan et al., 2014), and in view of the abundant amounts of cold-water corals and spawning grounds for commercially important fish species in the area, it is very important to continue monitoring the ocean acidification trends.

The monthly time series data at several coastal sites in this program have provided more insight into the seasonal changes along the coast, which has been very useful when trying to understand the highly variability of Norwegian inshore waters. The carbon measurements made in the Norwegian Sea and the Barents Sea in this program provide unique data from an area where there is a great deal of change related to climate, transport of Atlantic waters and decreasing sea ice cover. The program also contributes data and knowledge to the International Surface Surveillance Network (Global Network for the Ocean Acidification Observation GOA-ON and ICES Study Group of Ocean Acidification-SGOA).

## 5. References

- Agnalt, A-L, E.S. Grefsrud, E. Farestveit, M. Larsen & F. Keulder. Deformities in larvae and juvenile European lobster (*Homarus gammarus*) exposed to lower pH at two different temperatures, Biogeosciences 10 (12): 7883-7895, 2013.
- AMAP, Arctic Monitoring and Assessment programme. Arctic Ocean Acidification Assessment: Summary for Policymakers, 2013.
- Andersen, S., E.S. Grefsrud & T. Harboe. Effect of increased pCO<sub>2</sub> level on early shell development in great scallop (*Pecten maximus* Lamarck) larvae. Biogeosciences, 10: 6161-6184, 2013.
- Chierici, M., A. Fransson, Nojiri, Y. 2006, Biogeochemical processes as drivers of surface fCO<sub>2</sub> in contrasting provinces in the subarctic North Pacific, GBC, 20, doi:10.1029/2004GB002356.
- Chierici, M., I. Skjelvan, M. Norli, K.Y. Børshheim, S. K. Lauvset, H.H. Lødemel, K. Sørensen, A.L. King, T. Johannessen. 2017. Overvåking av havforsuring i norske farvann i 2016, Report (in Norwegian), Miljødirektoratet, M-776|2017.
- Chierici, M., I. Skjelvan, M. Norli, E. Jones, K.Y. Børshheim, S. K. Lauvset, H.H. Lødemel, K. Sørensen, A.L. King, T. Kutti, A. Renner, A. Omar, T. Johannessen. 2016. Overvåking av havforsuring i norske farvann i 2015, Report (in Norwegian), Miljødirektoratet, M-573|2016.
- Dickson, A. G. & F. J. Millero. A comparison of the equilibrium constants for the dissociation of carbonic acid in seawater media. Deep-Sea Res. 34, 1733-1743, 1987.
- Dickson, A.G., Standard potential of the reaction: AgCl(s) + ½H<sub>2</sub>(g) = Ag(s) + HCl(aq), and the standard acidity constant of the ion HSO<sub>4</sub><sup>-</sup> in synthetic sea water from 273.15 to 318.15 K. *J. Chem. Thermodyn.* 22: 113-127, 1990.
- Dickson, A.G., C.L. Sabine & J.R. Christian (eds.). Guide to Best Practices for Ocean CO<sub>2</sub> Measurements. PICES Special Publication 3, IOCCTP Report 8, 191 pp, 2007.
- Dupont, S & H. Pörtner. A snapshot of ocean acidification research. *Marine Biology*, 160:1765-1771. DOI 10.1007/s00227-013-2282-9, 2013.
- Ingle, S.E., Solubility of calcite in the ocean. *Mar. Chem.*, 3, 1975.
- Järnegren, J. & T. Kutti. Lophelia pertusa in Norwegian waters. What have we learned since 2008? - NINA Report 1028. 40 pp. ISSN: 1504-3312, ISBN: 978-82-426-2640-0, 2014.
- Johannessen, T., K. Sørensen, K.Y. Børshheim, A. Olsen, E. Yakushev, A. Omar & T.A. Blakseth. Tilførselsprogrammet 2010. Overvåking av forsuring av norske farvann med spesiell fokus på Nordsjøen. Report (in Norwegian), KLIF, TA 2809-2011, 2011.
- Le Quéré, C. et al.. Global carbon budget 2016, *Earth Syst. Sci. Data* 8, 405-448, 2016.

Le Quéré, C. et al.. Global carbon budget 2017, *Earth Syst. Sci. Data* 10, 605-649, 2018.

Mehrbach, C., C.H. Culberson, E.J. Hawley, & R M. Pytkowicz. Measurements of the apparent dissociation constants of carbonic acid in seawater at atmospheric pressure. *Limnol. Oceanogr.* 18, 897-907, 1973.

Mortensen, P.B., M.T. Hovland, J.H. Fosså, & D.M. Furevik. Distribution, abundance and size of Lophelia pertusa coral reefs in mid-Norway in relation to seabed characteristics. *J. Mar. Biol. Asso. U.K* 81, 581-597, 2001.

Mucci, A., The solubility of calcite and aragonite in seawater at various salinities, temperatures and at one atmosphere pressure, *Am. J. Sci.*, 283, 780-799, doi:10.2475/ajs.283.7.780, 1983.

Olafsson, J., S.R. Olafsdottir, A. Benoit-Cattin, M. Danielsen, T.S. Arnarson & T. Takahashi. Rate of Iceland Sea acidification from time series measurements, *Biogeosciences*, 6, 2661-2668, doi:10.5194/bg-6-2661-2009, 2009.

Orr, J. C., V. J. Fabry, O. Aumont et al., Anthropogenic ocean acidification over the twenty-first century and its impact on calcifying organisms. *Nature* 437, 681-686, 2005.

Pierrot, D., E. Lewis & D.W.R. Wallace. MS Excel Program Developed for CO<sub>2</sub> System Calculations. ORNL/CDIAC-105a. Carbon Dioxide Information Analysis Center, Oak Ridge National Laboratory, U.S. Department of Energy, Oak Ridge, Tennessee. doi: 10.3334/CDIAC/otg.CO2SYS\_XLS\_CDIAC105a, 2006.

Skjelvan, I., E. Falck, F. Rey & S.B. Kringstad. Inorganic carbon time series at Ocean Weather Station M in the Norwegian Sea, *Biogeosci.*, 5, 549-560, 2008.

Skjelvan, I., E. Jeansson, M. Chierici, A. Omar, A. Olsen, S. Lauvset & T. Johannessen. Ocean acidification and uptake of anthropogenic carbon in the Nordic Seas, 1981-2013, Report (in Norwegian), Norwegian Environment Agency, M244-2014, 2014.

Skjelvan, I. & A. M. Omar. Status of knowledge about ocean acidification in fjords at the west coast of Norway, Report (in Norwegian), Norwegian Environment Agency, M426-2015, 2015.

Skjelvan, I., M. Chierici, K. Sørensen, K. Jackson, T. Kutt, H. L. Lødemel, A. King, E. Reggiani, M. Norli, R. Bellerby, E. Yakushev, A. M. Omar. Ocean acidification in western Norwegian fjords and CO<sub>2</sub> variability in Lofoten, Report (in Norwegian), Norwegian Environment Agency, M642-2016, 2016.

Steinacher, M., F. Joos, T.L. Frölicher, G.-K. Plattner & S.C. Doney. Imminent ocean acidification in the Arctic projected with the NCAR global coupled carbon cycle-climate model. *Biogeosciences* 6, 515-533, 2009.

Takahashi, T, S.C. Sutherland, R. Wanninkhof et al., Climatological mean and decadal change in the surface ocean pCO<sub>2</sub> and net sea-air CO<sub>2</sub> flux over the global oceans. *Deep-Sea Res. II* 56, 554-577, 2009.

Takahashi, T, S.C. Sutherland, D.W. Chapman, J.G. Goddard, C. Ho, T. Newberger, C. Sweeney, D.R. Munro, Climatological distributions of pH, pCO<sub>2</sub>, total CO<sub>2</sub>, alkalinity, and CaCO<sub>3</sub> saturation in the global surface ocean, and temporal changes at selected locations. *Marine Chemistry* 164, 95-125, 2014.

Talmage, S. C., & C. J. Gobler. The effects of elevated carbon dioxide concentrations on the metamorphosis, size, and survival of larval hard clams (*Mercenariamercenaria*), bay scallops (*Argopectenirradians*) and Eastern oysters (*Crassostreavirginia*). *Limnol. Oceanogr.* 54, 2072-2080, 2009.

Turley, C.M., J.M. Roberts & J.M. Guinotte. Corals in deep-water: will the unseen hand of ocean acidification destroy cold-water ecosystems? *Coral Reefs* 26, 445-448, 2007.

Østerhus, S. & T. Gammelsrød. The abyss of the Nordic Seas is warming, *Jour. of Climate*, 2 (11), 3297-3304, 1999.

## 6. Appendix

### 6.1 Plots

Water column data from Torungen-Hirtshals section.

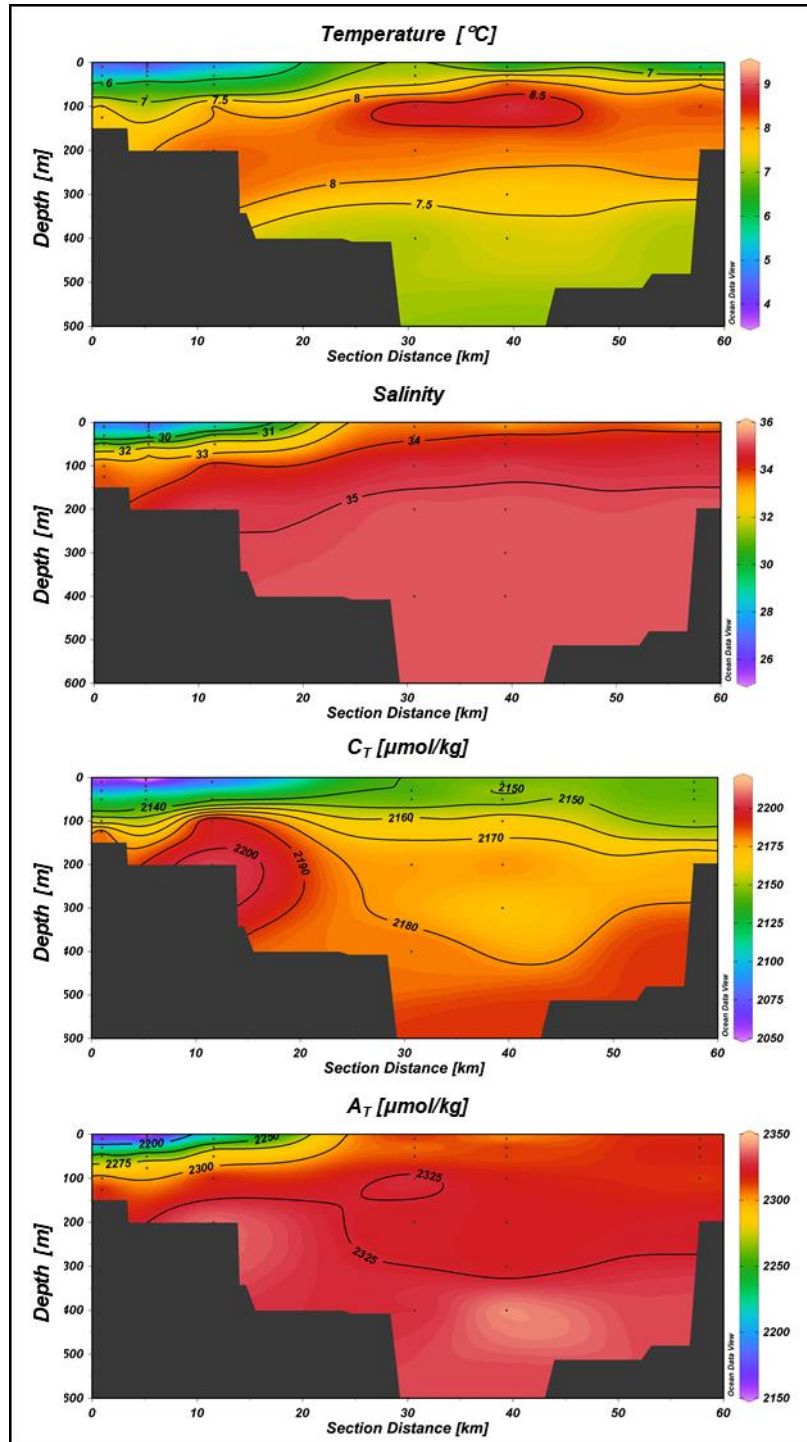


**Figure 1.** Temperature, salinity,  $C_T$  and  $A_T$  from Torungen-Hirtshals in January 2018. Black dots indicate sample depths.

**Figur 1.** Temperatur, saltholdighet,  $C_T$  og  $A_T$  langs Torungen-Hirtshals snittet i januari 2018. Svarte prikker viser prøvedyp.

Water column data from Arendal coastal station.

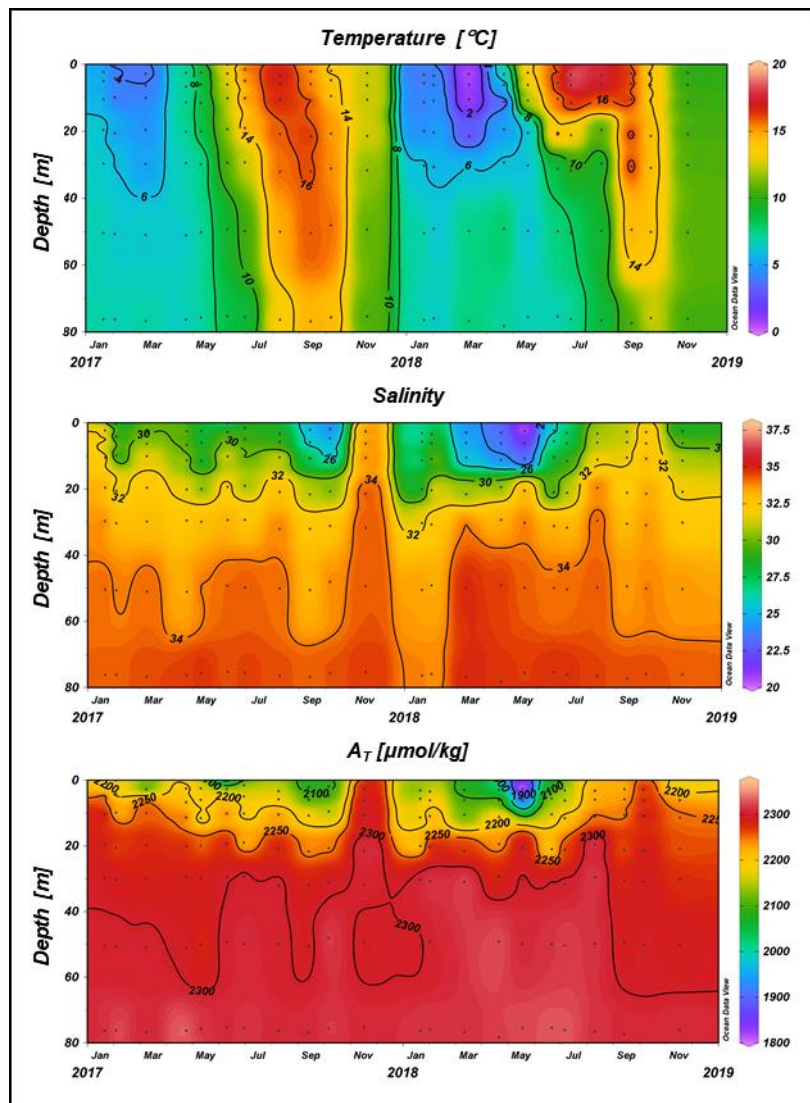


**Figure 2.** Monthly temperature, salinity and  $A_T$  in the upper 80 m at Arendal coastal station in 2017-2018. Black dots indicate sample depths.

**Figur 2.** Månedlig temperatur, saltholdighet og  $A_T$  i de gyerste 80 m ved Arendal kyststasjon i 2017-2018. Svarte prikker viser prøvedyp.

Water column data from Svinøy-NW section.

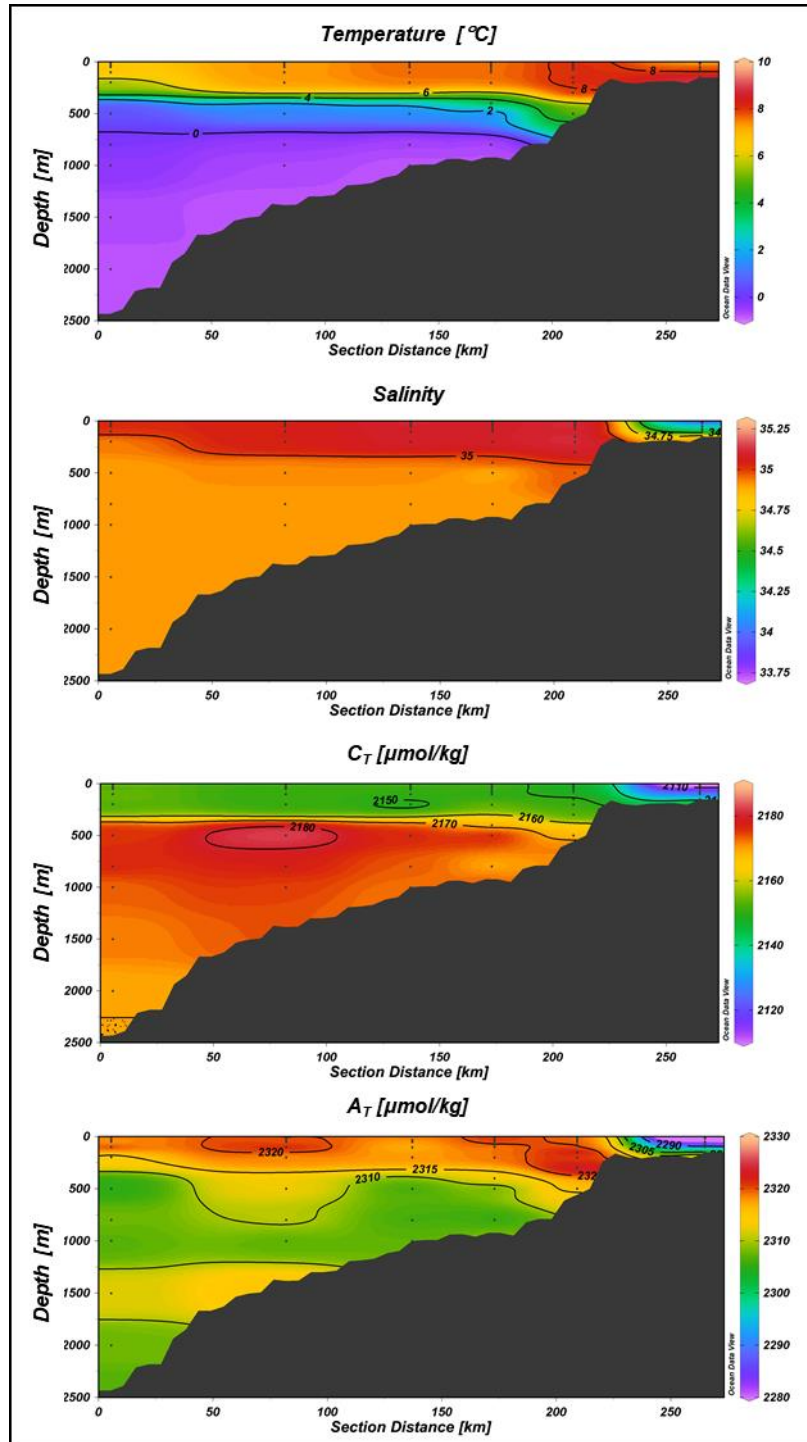
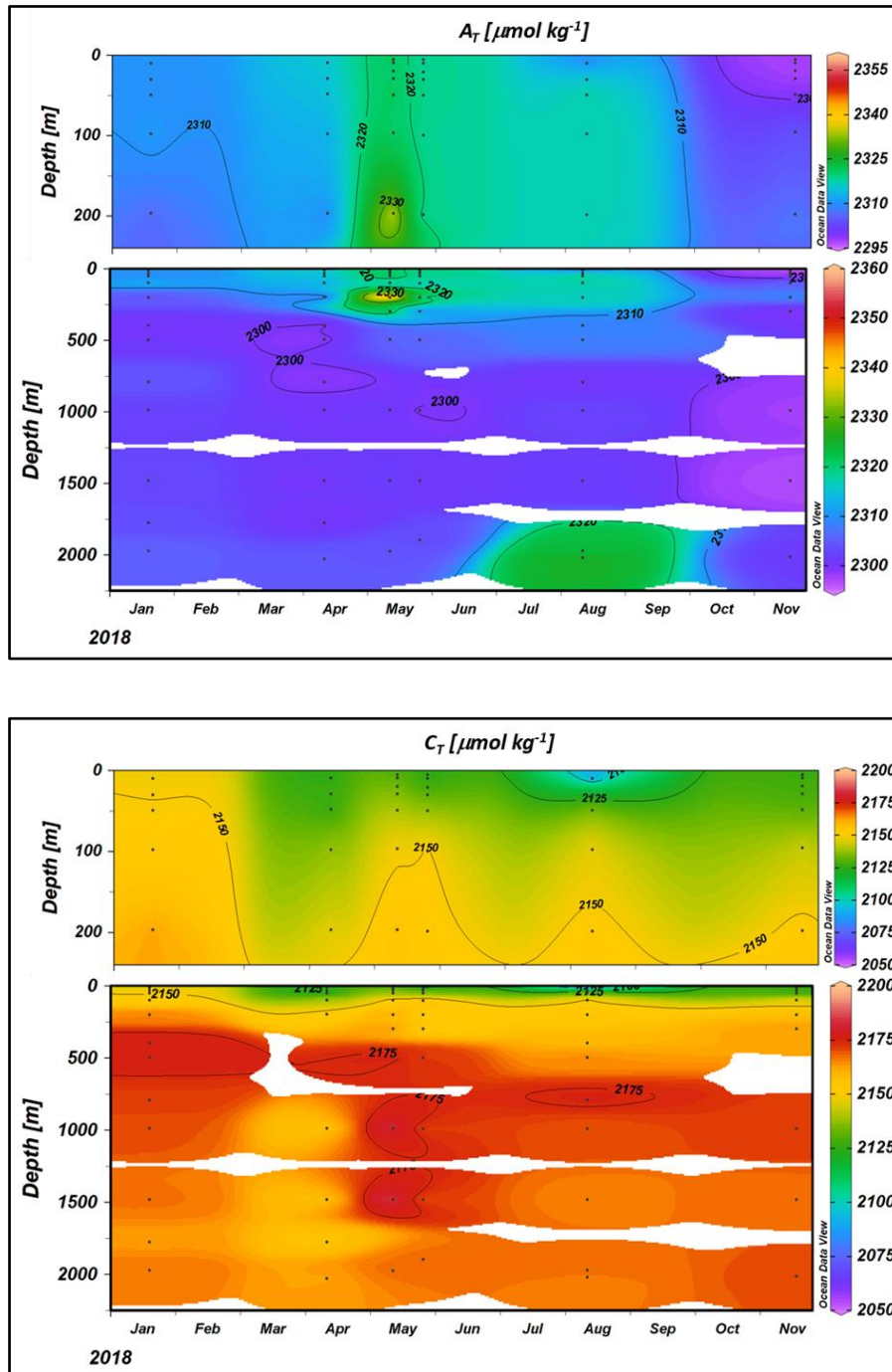


Figure 3. Temperature, salinity,  $C_T$  and  $A_T$  from Svinøy-NW in January 2018. Black dots indicate sample depths.

Figur 3. Temperatur, saltholdighet,  $C_T$  og  $A_T$  langs Svinøy-NV snittet i januari 2018. Svarte prikker viser prøvedyp.

Water column data from Station M.



**Figure 4.**  $A_T$  (total alkalinity;  $\mu\text{mol kg}^{-1}$ ) and  $C_T$  (total dissolved inorganic carbon;  $\mu\text{mol kg}^{-1}$ ) at Station M in 2018. Black dots indicate the depths of the samples.

**Figur 4.**  $A_T$  (total alkalinitet;  $\mu\text{mol kg}^{-1}$ ) og  $C_T$  (totalt løst uorganisk karbon;  $\mu\text{mol kg}^{-1}$ ) på Stasjon M i 2018. Svarte prikker viser prøvedyp.

Water column data from Gimsøy-NW section.

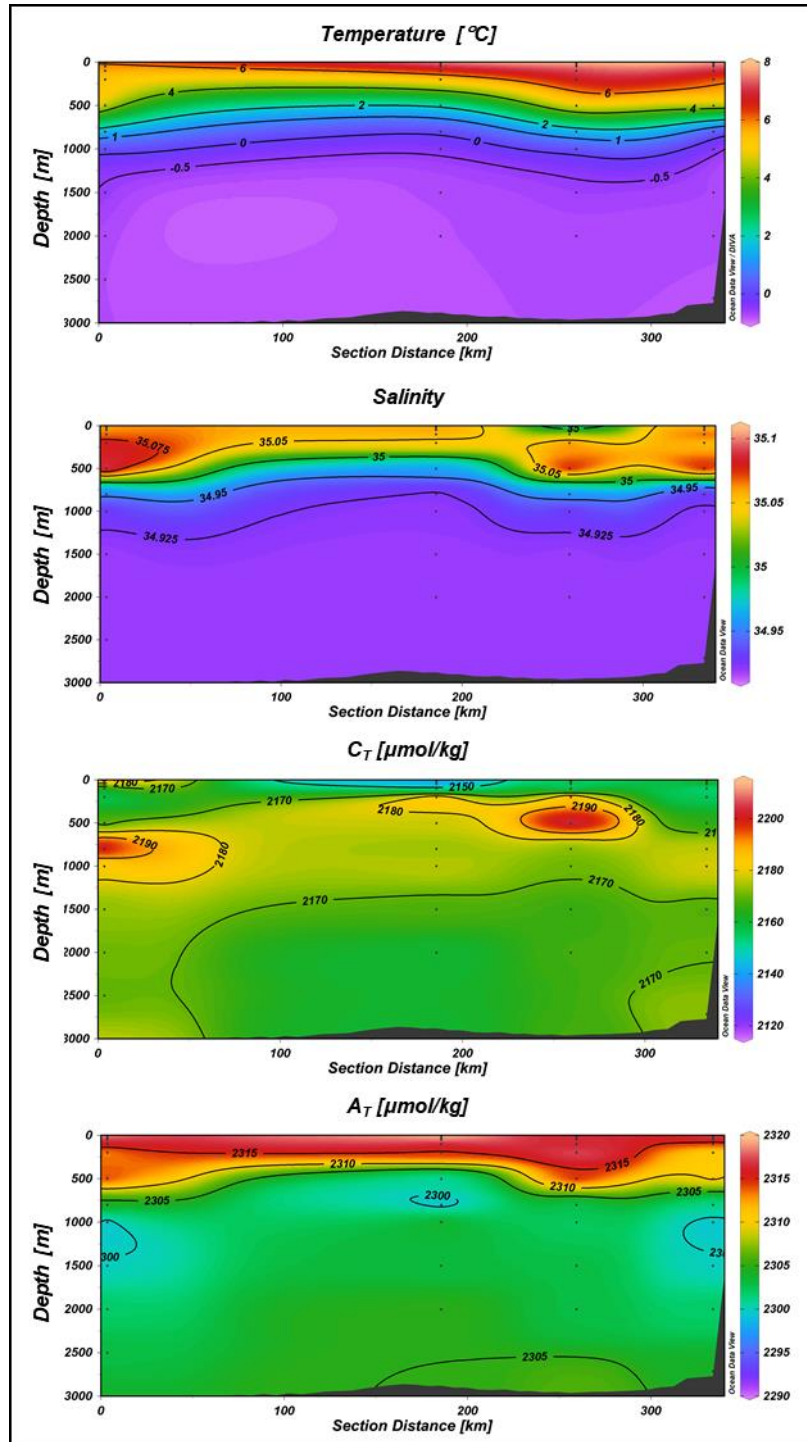


**Figure 5.** Temperature, salinity,  $C_T$  and  $A_T$  from Gimsøy-NW in January 2018. Black dots indicate sample depths.

**Figur 5.** Temperatur, saltholdighet,  $C_T$  og  $A_T$  langs Gimsøy-NV snittet i januari 2018. Svarte prikker viser prøvedyp.

Water column data from Fugløya-Bjørnøya section.

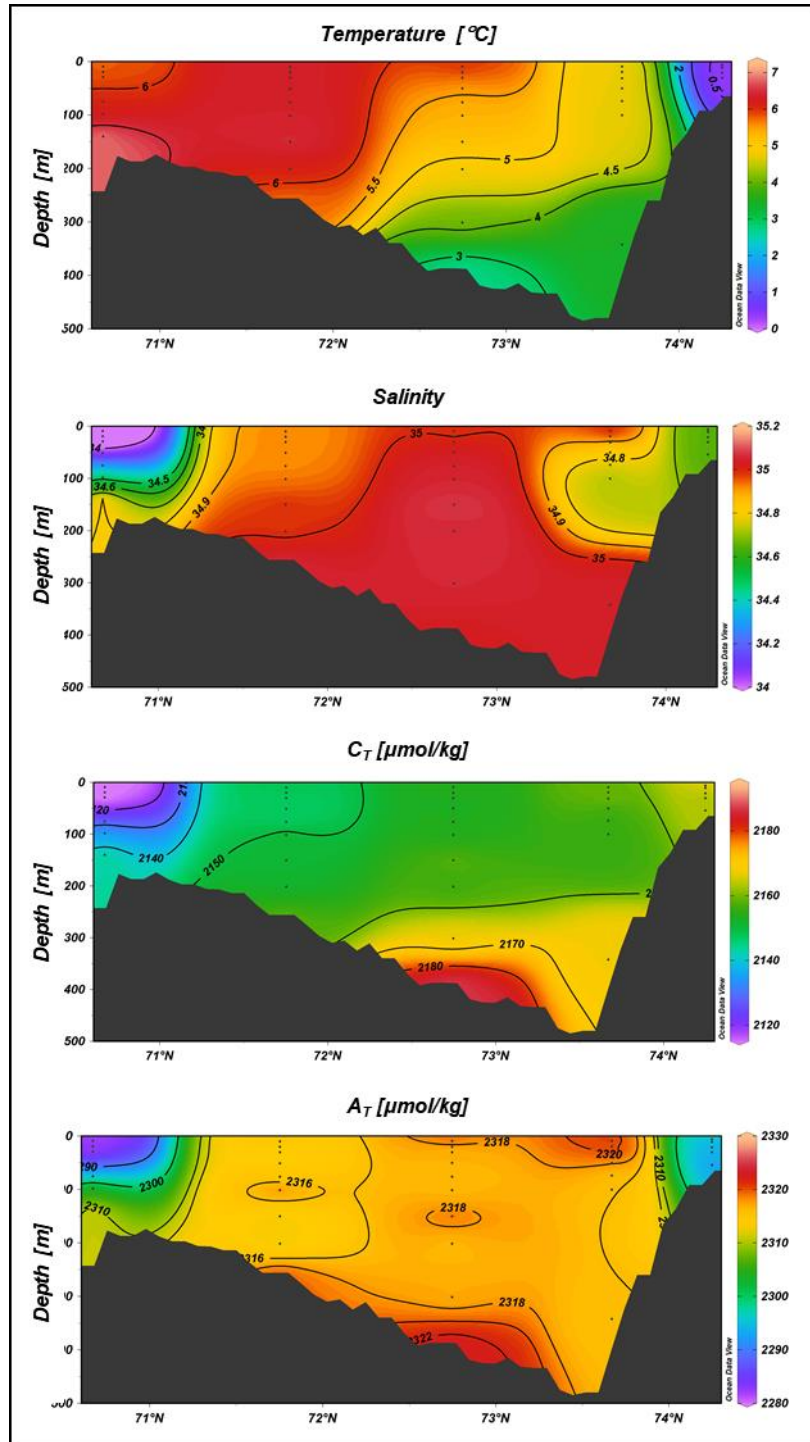


**Figure 6.** Temperature, salinity,  $C_T$  and  $A_T$  from Fugløya-Bjørnøya in January 2018. Black dots indicate sample depths.

**Figur 6.** Temperatur, saltholdighet,  $C_T$  og  $A_T$  langs Fugløya-Bjørnøya snittet i januar 2018. Svarte prikker viser prøvedyp.

Water column data from Barents Sea section.

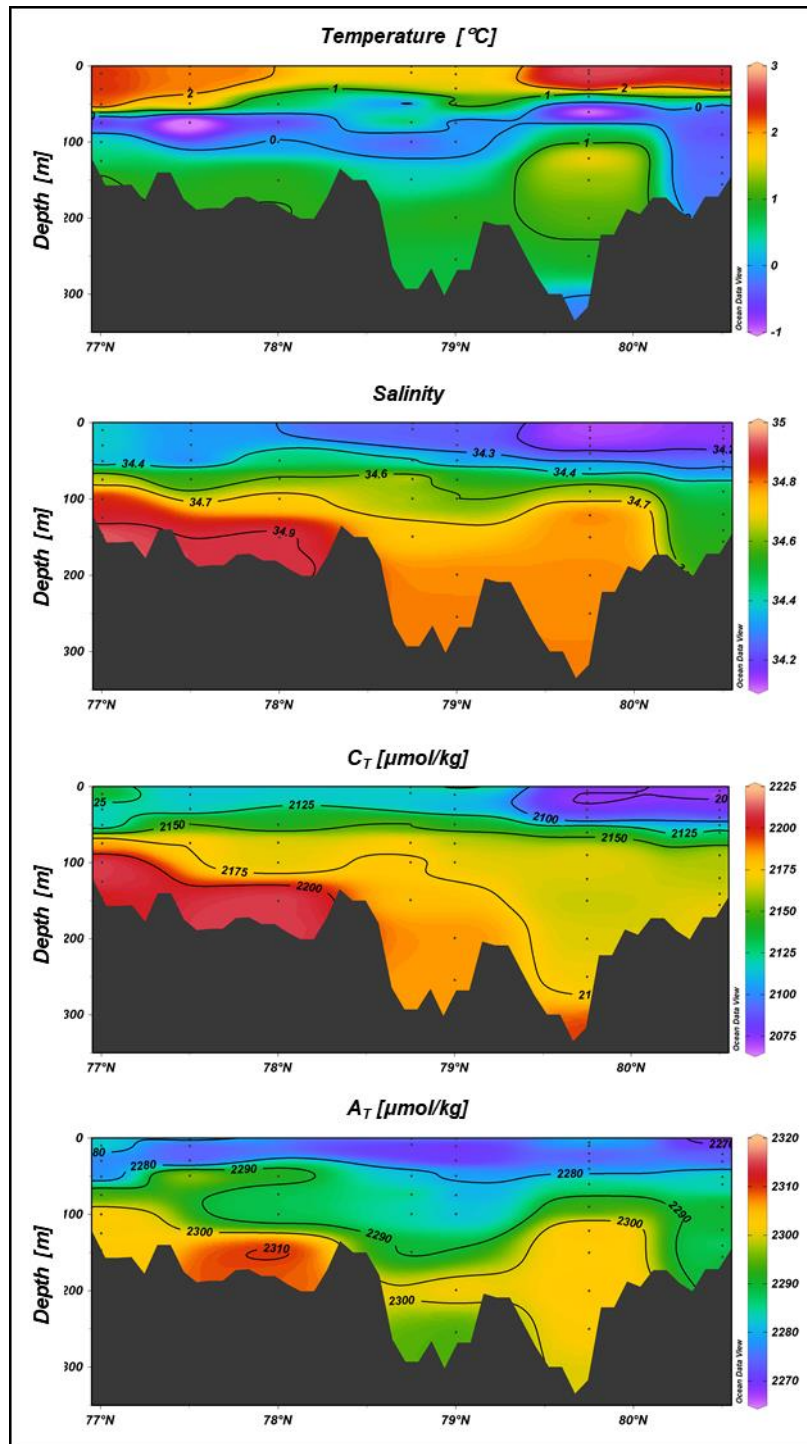


**Figure 7.** Temperature, salinity,  $C_T$  and  $A_T$  along the section in the northeast Barents Sea in August and September 2018. Black dots indicate sample depths.

**Figur 7.** Temperatur, saltholdighet,  $C_T$  og  $A_T$  langs snittet i nordøstlige Barentshav i august og september 2018. Svarte prikker viser prøvedyp.

Continuous measurements from Station M.

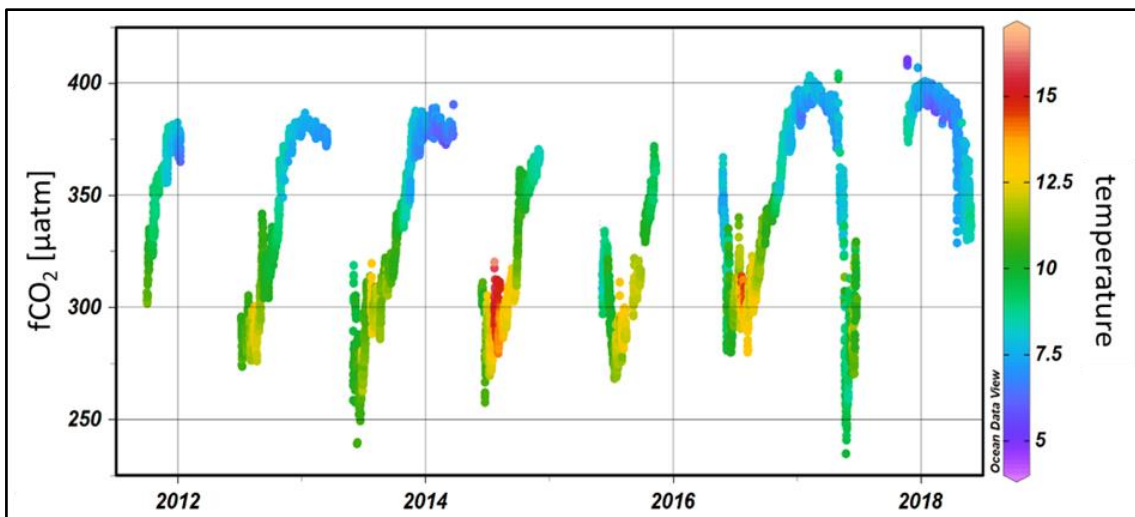


**Figure 8.**  $f\text{CO}_2$  ( $\mu\text{atm}$ ) in surface water at Station M between 2011 and 2018. The colour scale indicates temperature.

**Figur 8.**  $f\text{CO}_2$  ( $\mu\text{atm}$ ) i overflatevann på Stasjon M i perioden 2011 til 2018. Fargeskala viser temperatur.

## 6.2 Data Tables

**Table 1.** Torungen-Hirtshals; January 2018.

Stn	Date	Lat °N	Lon °E	Depth m	S	T C°	A <sub>T</sub> μmol/kg	C <sub>T</sub> μmol/kg	pH <sub>T</sub>	Ω <sub>Ca</sub>	Ω <sub>Ar</sub>	NO <sub>3</sub> μmol/kg	PO <sub>4</sub> μmol/kg	SiOH <sub>4</sub> μmol/kg
Ærøydypet	21.01	58.396	8.763	10.0	25.99	3.97	2133	2029	8.066	2.13	1.31	5.54	0.526	9.26
Ærøydypet	21.01	58.396	8.763	30.0	28.54	4.93	2203	2084	8.051	2.32	1.44	6.43	0.518	8.31
Ærøydypet	21.01	58.396	8.763	50.0	32.81	6.80	2299	2144	8.055	2.80	1.77	5.83	0.483	5.26
Ærøydypet	21.01	58.396	8.763	100.0	34.03	7.84	2305	2141	8.040	2.86	1.81	5.02	0.472	4.27
Ærøydypet	21.01	58.396	8.763	125.0	34.06	7.81	2329	2210	7.922	2.27	1.44	4.94	0.481	4.24
1nm	21.01	58.383	8.833	3.1	25.76	3.89	2114	2015	8.056	2.05	1.26	5.40	0.553	9.30
1nm	21.01	58.383	8.833	5.6	25.81	3.93	2125	2020	8.073	2.14	1.31	5.35	0.529	9.31
1nm	21.01	58.383	8.833	11.3	25.99	4.02	2138	*	*	*	*	5.50	0.557	9.26
1nm	21.01	58.383	8.833	20.0	26.86	4.34	2174	2059	8.074	2.27	1.40	5.45	0.556	8.98
1nm	21.01	58.383	8.833	30.3	31.46	6.26	2303	2144	8.088	2.89	1.82	6.23	0.500	6.67
1nm	21.01	58.383	8.833	50.4	33.67	7.34	2293	2140	8.029	2.74	1.73	5.24	0.453	4.34
1nm	21.01	58.383	8.833	76.4	34.03	7.16	2312	2155	8.034	2.78	1.76	4.73	0.447	3.63
5nm	21.01	58.332	8.882	10.0	27.40	4.61	2207	2080	8.096	2.47	1.52	5.93	0.528	8.24
5nm	21.01	58.332	8.882	30.0	32.59	6.22	2306	*	*	*	*	5.38	0.468	5.03
5nm	21.01	58.332	8.882	50.0	33.55	6.35	2315	2147	8.081	2.96	1.87	4.51	0.443	3.49
5nm	21.01	58.332	8.882	100.0	34.80	8.58	2327	2217	7.877	2.15	1.37	5.71	0.526	3.36
5nm	21.01	58.332	8.882	200.0	35.05	8.29	2338	2205	7.935	2.39	1.52	8.47	0.680	4.66
15nm	21.01	58.197	9.088	10.0	33.47	7.08	2319	*	*	*	*	5.37	0.437	4.51
15nm	21.01	58.197	9.088	30.0	33.81	6.89	2301	2137	8.062	2.91	1.84	4.88	0.447	3.92
15nm	21.01	58.197	9.088	50.0	34.16	7.48	2312	2141	8.063	2.99	1.89	4.67	0.466	3.42
15nm	21.01	58.197	9.088	100.0	34.98	9.01	2333	2165	8.018	2.93	1.86	6.59	0.544	3.36
15nm	21.01	58.197	9.088	200.0	35.14	8.19	2323	2179	7.965	2.52	1.60	10.48	0.766	5.05
15nm	21.01	58.197	9.088	400.0	35.12	7.10	2327	2183	7.974	2.40	1.53	10.51	0.858	7.87
20nm	21.01	58.135	9.181	10.0	32.84	5.36	2297	2140	8.080	2.82	1.77	4.87	0.439	3.94
20nm	21.01	58.135	9.181	30.0	34.19	7.81	2322	2160	8.035	2.89	1.83	4.69	0.455	3.34
20nm	21.01	58.135	9.181	50.0	34.76	8.95	2308	2141	8.022	2.92	1.85	5.35	0.484	2.99
20nm	21.01	58.135	9.181	100.0	35.06	9.04	2321	2169	7.976	2.68	1.71	8.51	0.645	3.98
20nm	21.01	58.135	9.181	200.0	35.15	8.13	2322	2181	7.960	2.49	1.58	10.96	0.783	5.08
20nm	21.01	58.135	9.181	300.0	35.14	7.67	2320	2170	7.984	2.53	1.61	10.26	0.751	4.75
20nm	21.01	58.135	9.181	400.0	35.13	7.29	2344	*	*	*	*	10.25	0.822	6.86
20nm	21.01	58.135	9.181	600.0	35.13	7.03	2332	2190	7.962	2.28	1.46	10.91	0.910	8.95
30nm	21.01	57.999	9.351	10.0	33.03	5.37	2316	2144	8.113	3.04	1.92	5.04	0.484	5.00
30nm	21.01	57.999	9.351	30.0	34.43	7.08	2319	2141	8.081	3.09	1.96	4.77	0.497	4.67
30nm	21.01	57.999	9.351	50.0	34.84	8.58	2319	2144	8.045	3.04	1.93	5.74	0.499	3.16
30nm	21.01	57.999	9.351	100.0	34.90	8.39	2314	2148	8.026	2.88	1.83	5.60	0.495	3.04
30nm	21.01	57.999	9.351	200.0	35.14	8.12	2324	2177	7.974	2.56	1.63	11.01	0.784	5.34
30nm	21.01	57.999	9.351	400.0	35.12	7.12	2332	2190	7.971	2.40	1.52	10.30	0.817	6.51

**Table 2.** Arendal coastal station; January-November 2018.

Date	Lat °N	Lon °E	Depth m	S	T C°	A <sub>T</sub> μmol/kg	C <sub>T</sub> μmol/kg	pH <sub>T</sub>	Ω <sub>Ca</sub>	Ω <sub>Ar</sub>	NO <sub>3</sub> μmol/kg	PO <sub>4</sub> μmol/kg	SiOH <sub>4</sub> μmol/kg
21.1	58.3832	8.8328	3.1	25.76	3.89	2114	2015	8.056	2.05	1.26	5.40	0.553	9.30
21.1	58.3832	8.8328	5.6	25.81	3.93	2125	2020	8.073	2.14	1.31	5.35	0.529	9.31
21.1	58.3832	8.8328	11.3	25.99	4.02	2138	2090	7.866	1.40	0.86	5.50	0.557	9.26
21.1	58.3832	8.8328	20.0	26.86	4.34	2174	2059	8.074	2.27	1.40	5.45	0.556	8.98
21.1	58.3832	8.8328	30.3	31.46	6.26	2303	2144	8.088	2.89	1.82	6.23	0.500	6.67
21.1	58.3832	8.8328	50.4	33.67	7.34	2293	2140	8.029	2.74	1.73	5.24	0.453	4.34
21.1	58.3832	8.8328	76.4	34.03	7.16	2312	2155	8.034	2.78	1.76	4.73	0.447	3.63
1.2	58.3848	8.8323	3.4	28.52	4.33	2172	2055	8.058	2.27	1.41	9.95	0.587	11.62
1.2	58.3848	8.8323	6.1	29.93	4.68	2240	2154	7.930	1.87	1.17	10.71	0.596	11.71
1.2	58.3848	8.8323	10.9	30.86	4.94	2256	2121	8.062	2.54	1.59	11.05	0.577	11.80
1.2	58.3848	8.8323	20.3	32.59	5.25	2312	2168	8.054	2.66	1.67	15.34	0.627	12.97
1.2	58.3848	8.8323	30.7	32.98	5.63	2326	2232	7.899	1.98	1.25	12.20	0.584	10.55
1.2	58.3848	8.8323	49.1	33.31	5.98	2310	2160	8.045	2.70	1.70	10.48	0.558	9.06
1.2	58.3848	8.8323	75.9	33.72	6.29	2318	2197	7.957	2.30	1.45	7.22	0.520	8.04
13.3	58.3837	8.8340	2.9	24.31	0.58	2076	1980	8.123	1.98	1.20	4.31	0.407	8.90
13.3	58.3837	8.8340	6.0	24.75	0.70	2101	1995	8.147	2.13	1.30	4.46	0.442	8.62
13.3	58.3837	8.8340	10.5	25.40	0.90	2119	2010	8.141	2.17	1.32	4.79	0.420	8.40
13.3	58.3837	8.8340	21.5	30.58	2.71	2269	2133	8.101	2.53	1.58	5.98	0.455	7.05
13.3	58.3837	8.8340	30.9	34.18	6.18	2326	2201	7.964	2.36	1.49	6.55	0.569	4.40
13.3	58.3837	8.8340	49.8	34.99	7.52	*	2166	*	*	*	7.87	0.631	4.18
13.3	58.3837	8.8340	76.7	35.04	7.63	2312	2169	7.979	2.56	1.63	8.86	0.691	4.54
22.4	58.3833	8.8335	2.9	23.40	6.23	2046	1969	7.985	1.78	1.08	0.17	0.051	0.60
22.4	58.3833	8.8335	6.2	23.62	5.06	2139	1990	8.220	2.90	1.76	0.17	0.058	0.39
22.4	58.3833	8.8335	11.2	24.29	3.00	2203	2076	8.170	2.53	1.54	0.23	0.083	0.34
22.4	58.3833	8.8335	19.4	30.47	4.92	2233	2063	8.160	3.04	1.90	2.58	0.362	1.55
22.4	58.3833	8.8335	29.3	33.30	6.06	2282	2141	8.025	2.57	1.62	5.48	0.534	3.39
22.4	58.3833	8.8335	49.1	34.69	7.96	2328	2185	7.978	2.61	1.65	8.21	0.674	5.27
22.4	58.3833	8.8335	78.3	34.82	7.23	2321	2179	7.985	2.56	1.62	8.52	0.700	5.51
19.5	58.3843	8.8332	2.5	20.16	14.20	1754	1637	8.091	2.38	1.44	2.18	0.091	8.76
19.5	58.3843	8.8332	6.1	21.62	13.73	1892	1763	8.090	2.60	1.59	1.62	0.092	7.16
19.5	58.3843	8.8332	10.8	22.96	12.51	*	2126	*	*	*	1.17	0.083	4.53
19.5	58.3843	8.8332	20.5	33.42	5.92	2303	2134	8.095	2.99	1.88	3.61	0.352	2.87
19.5	58.3843	8.8332	30.2	34.04	6.06	2304	2147	8.054	2.79	1.76	4.77	0.439	3.53
19.5	58.3843	8.8332	49.8	34.33	6.16	2309	2151	8.051	2.79	1.76	5.15	0.468	3.67
19.5	58.3843	8.8332	75.5	34.70	6.76	2326	2177	8.010	2.65	1.68	7.89	0.648	5.61
22.6	58.3830	8.8322	2.3	25.40	15.53	2065	1893	8.098	3.30	2.06	0.03	0.049	0.38
22.6	58.3830	8.8322	5.5	26.31	15.67	2147	1943	8.143	3.83	2.40	0.01	0.044	0.40
22.6	58.3830	8.8322	10.3	27.68	15.43	2150	1951	8.115	3.68	2.32	0.02	0.025	0.47
22.6	58.3830	8.8322	21.0	28.81	14.56	2183	1989	8.096	3.56	2.25	0.21	0.050	0.71
22.6	58.3830	8.8322	31.2	33.50	8.13	2304	2129	8.072	3.09	1.95	2.39	0.289	2.86
22.6	58.3830	8.8322	49.9	34.09	7.39	2314	2141	8.070	3.03	1.92	2.81	0.325	3.11
22.6	58.3830	8.8322	75.3	34.86	6.70	2330	2211	7.932	2.26	1.43	5.32	0.530	3.67
7.7	58.3835	8.8333	3.1	27.63	19.11	2159	1938	8.107	4.11	2.61	0.10	0.039	0.17
7.7	58.3835	8.8333	6.2	27.83	18.77	2157	1936	8.109	4.09	2.60	0.05	0.041	0.18
7.7	58.3835	8.8333	11.5	29.67	16.56	2229	2120	7.831	2.33	1.48	0.07	0.038	0.15

7.7	58.3835	8.8333	21.1	31.24	13.64	2282	2094	8.048	3.41	2.17	0.31	0.074	1.00
7.7	58.3835	8.8333	31.7	33.21	9.99	2306	2157	7.982	2.74	1.74	1.02	0.198	2.24
7.7	58.3835	8.8333	50.3	34.23	8.02	2326	2202	7.934	2.37	1.50	2.01	0.328	3.54
7.7	58.3835	8.8333	76.1	34.79	7.42	2331	2160	8.052	2.96	1.88	1.90	0.349	2.80
11.8	58.3832	8.8328	3.2	30.80	17.76	2231	2040	8.005	3.51	2.25	0.15	0.050	0.43
11.8	58.3832	8.8328	5.9	31.16	17.34	2230	2006	8.080	4.01	2.57	0.08	0.052	0.43
11.8	58.3832	8.8328	11.1	32.01	15.93	2255	2041	8.063	3.79	2.42	0.08	0.055	0.43
11.8	58.3832	8.8328	19.6	34.05	10.57	2321	2194	7.906	2.44	1.55	2.96	0.405	5.65
11.8	58.3832	8.8328	29.6	34.28	8.99	2322	2202	7.910	2.34	1.48	3.14	0.434	6.01
11.8	58.3832	8.8328	49.7	34.43	8.93	2315	2154	8.012	2.86	1.81	2.48	0.385	5.29
11.8	58.3832	8.8328	76.5	34.58	8.78	2315	2156	8.007	2.81	1.78	2.40	0.388	4.65
14.9	58.3830	8.8332	2.7	30.72	16.60	2211	2013	8.042	3.58	2.29	0.27	0.105	1.94
14.9	58.3830	8.8332	5.8	30.88	16.61	2224	*	*	*	*	0.35	0.120	1.96
14.9	58.3830	8.8332	10.5	31.59	16.60	2239	2062	7.980	3.25	2.08	0.23	0.097	2.00
14.9	58.3830	8.8332	21.1	32.01	16.57	2256	2048	8.042	3.72	2.38	0.23	0.087	1.93
14.9	58.3830	8.8332	30.5	32.94	16.72	2277	2068	8.026	3.69	2.37	0.25	0.104	2.26
14.9	58.3830	8.8332	49.4	33.55	14.70	2293	2101	8.008	3.38	2.17	1.11	0.166	2.32
14.9	58.3830	8.8332	77.3	34.44	10.45	2310	2152	7.981	2.82	1.80	2.32	0.272	3.04
6.10	58.3833	8.8330	2.8	33.14	13.58	2287	2082	8.063	3.62	2.31	0.34	0.111	1.77
6.10	58.3833	8.8330	6.2	33.14	13.57	2290	2087	8.059	3.59	2.29	0.26	0.117	1.77
6.10	58.3833	8.8330	10.8	33.24	13.73	2295	2086	8.065	3.67	2.34	0.36	0.116	1.79
6.10	58.3833	8.8330	21.4	33.61	14.15	2296	2086	8.057	3.67	2.35	0.37	0.119	1.88
6.10	58.3833	8.8330	30.9	33.75	14.22	2301	2095	8.043	3.59	2.30	0.28	0.233	2.04
6.10	58.3833	8.8330	50.1	33.98	14.19	2298	2093	8.037	3.55	2.27	0.41	0.102	1.73
6.10	58.3833	8.8330	75.8	34.48	12.72	*	2119	*	*	*	0.81	0.170	2.07
17.11	58.3830	8.8322	2.5	28.42	9.95	2166	2047	7.980	2.37	1.48	1.20	0.261	3.25
17.11	58.3830	8.8322	6.1	29.66	10.05	2238	2094	8.024	2.75	1.73	1.11	0.286	3.42
17.11	58.3830	8.8322	11.4	30.90	10.24	2251	2089	8.050	2.99	1.89	1.51	0.268	3.62
17.11	58.3830	8.8322	20.8	31.79	10.41	2259	2086	8.059	3.11	1.97	1.85	0.263	3.49
17.11	58.3830	8.8322	30.1	32.46	10.62	2276	2120	8.003	2.85	1.81	2.34	0.257	3.29
17.11	58.3830	8.8322	50.2	33.63	10.77	2294	2109	8.053	3.24	2.06	2.39	0.255	2.75
17.11	58.3830	8.8322	76.0	34.37	10.45	2311	2125	8.049	3.22	2.05	2.47	0.259	1.99

**Table 3.** Korsfjord; January, April, August, November 2018.

Stn	Date	Lat	Lon	Depth	S	T	A <sub>T</sub>	C <sub>T</sub>	pH <sub>T</sub>	Ω <sub>Ca</sub>	Ω <sub>Ar</sub>	NO <sub>3</sub>	PO <sub>4</sub>	SiOH <sub>4</sub>
		°N	°E	m	°C	μmol/kg	μmol/kg			μmol/kg	μmol/kg	μmol/kg	μmol/kg	μmol/kg
3	1/19	60.19	5.24	660	35.12	7.83	2322.9	2176.3	7.957	2.30	1.47	0.35	0.00	6.64
3	1/19	60.19	5.24	151	34.30	8.50	2323.0	2178.3	7.970	2.55	1.62	0.35	0.62	6.64
3	1/19	60.19	5.24	103	34.03	8.61	2298.8	2132.0	8.030	2.87	1.82	5.14	0.48	3.50
3	1/19	60.19	5.24	53	33.39	7.38	2291.0	2126.6	8.055	2.87	1.81	4.61	0.45	3.49
3	1/19	60.19	5.24	12	31.26	5.74	2268.0	2110.4	8.096	2.83	1.77	4.81	0.45	3.70
3	1/19	60.19	5.24	6	31.19	5.72	2117.0	1999.8	8.003	2.18	1.37	5.25	0.39	3.61
3	4/10	60.19	5.24	521	35.15	7.37	2305.2	2158.5	7.969	2.34	1.49	10.10	0.70	4.29
3	4/10	60.19	5.24	110	34.88	8.13	2310.5	2168.1	7.965	2.52	1.60	9.71	0.80	5.71
3	4/10	60.19	5.24	50	33.88	7.89	2286.5	2147.4	7.977	2.51	1.59	7.39	0.67	5.11
3	4/10	60.19	5.24	30	32.75	5.94	2254.6	2117.4	8.022	2.49	1.57	3.19	0.27	2.41
3	4/10	60.19	5.24	10	30.94	4.68	2177.2	2011.5	8.150	2.90	1.81	0.00	0.00	0.27
3	4/10	60.19	5.24	6	30.83	4.67	2175.6	2010.8	8.150	2.89	1.81	0.05	0.00	0.24
3	8/10	60.19	5.24	667	35.08	6.78	2319.8	2164.9	7.993	2.37	1.51	9.84	0.74	5.41
3	8/10	60.19	5.24	104	34.90	7.59	2312.8	2170.7	7.972	2.51	1.59	10.10	0.81	5.72
3	8/10	60.19	5.24	52	34.55	8.11	2329.1	2171.7	8.007	2.77	1.76	6.47	0.75	2.78
3	8/10	60.19	5.24	32	33.36	13.71	2265.2	2059.0	8.056	3.54	2.26	0.26	0.14	0.42
3	8/10	60.19	5.24	11	32.07	17.01	2239.6	2011.4	8.073	3.97	2.55	0.11	0.01	0.32
3	8/10	60.19	5.24	7	31.93	16.95	2241.8	2010.8	8.082	4.03	2.58	0.12	0.01	0.31
3	11/13	60.19	5.24	655	35.08	6.80	2318.5	2190.0	7.919	2.08	1.33	11.56	0.84	5.88
3	11/13	60.19	5.24	99	34.30	9.83	2305.3	2153.7	7.965	2.69	1.71	6.57	0.51	3.47
3	11/13	60.19	5.24	47	33.36	11.57	2279.5	2105.7	8.008	3.06	1.95	3.30	0.19	2.18
3	11/13	60.19	5.24	32	33.01	11.77	2249.4	2079.8	8.004	3.01	1.91	3.31	0.15	0.93
3	11/13	60.19	5.24	11	29.48	10.64	2061.2	1921.1	8.015	2.56	1.61	3.46	0.19	2.15
3	11/13	60.19	5.24	5	29.43	7.83	2031.7	1891.2	8.022	2.56	1.61	3.25	0.13	0.75

**Table 4.** Langenuen; January, April, August, November 2018.

Stn	Date	Lat	Lon	Depth	S	T	A <sub>T</sub>	C <sub>T</sub>	pH <sub>T</sub>	Ω <sub>Ca</sub>	Ω <sub>Ar</sub>	NO <sub>3</sub>	PO <sub>4</sub>	SiOH <sub>4</sub>
		°N	°E	m	°C	μmol/kg	μmol/kg			μmol/kg	μmol/kg	μmol/kg	μmol/kg	μmol/kg
2	1/19	59.83	5.56	193	34.83	8.47	2313.8	2176.5	7.946	2.43	1.54	0.34	0	6.46
2	1/19	59.83	5.56	152	34.59	9.00	2307.3	2164.8	7.954	2.51	1.60	0.34	0.6	6.47
2	1/19	59.83	5.56	105	34.13	8.94	2293.3	2134.2	8.006	2.76	1.75	5.01	0.47	3.41
2	1/19	59.83	5.56	53	33.24	7.14	2261.9	2104.7	8.046	2.75	1.74	4.49	0.44	3.4
2	1/19	59.83	5.56	11	30.84	5.54	2129.1	1994.9	8.058	2.42	1.52	4.69	0.44	3.61
2	1/19	59.83	5.56	6	30.80	5.58	2079.1	1953.1	8.040	2.28	1.43	5.12	0.38	3.52
2	4/10	59.83	5.56	194	35.09	7.74	2311.7	2157.1	7.996	2.62	1.67	10.9	0.75	5.17
2	4/10	59.83	5.56	100	34.77	8.29	2275.8	2181.9	7.833	1.90	1.20	9.73	0.78	5.87
2	4/10	59.83	5.56	48	33.71	7.31	2286.7	2147.1	7.990	2.52	1.59	8.35	0.7	5.15
2	4/10	59.83	5.56	29	32.36	5.17	2258.7	2104.7	8.082	2.73	1.71	3.54	0.39	2.13
2	4/10	59.83	5.56	9	30.47	4.65	2132.2	1963.3	8.170	2.93	1.83	0.6	0.12	0.22
2	4/10	59.83	5.56	6	30.45	4.70	2125.8	1960.8	8.161	2.87	1.79	0.25	0.03	0
2	8/10	59.83	5.56	205	35.06	7.01	2318.2	2160.4	8.015	2.66	1.69	9.8	0.73	5.2
2	8/10	59.83	5.56	102	34.95	7.73	2315.1	2181.7	7.946	2.40	1.52	10.8	0.87	7.2
2	8/10	59.83	5.56	51	34.56	8.88	2302.4	2155.9	7.971	2.61	1.66	7.7	0.69	4.6
2	8/10	59.83	5.56	31	33.29	13.95	2262.3	2063.7	8.037	3.44	2.20	0.8	0.18	0.4
2	8/10	59.83	5.56	10	31.18	17.05	2179.9	1964.7	8.066	3.77	2.41	0.2	0.05	0.3
2	8/10	59.83	5.56	6	30.02	16.90	2062.9	1847.4	8.103	3.74	2.39	0.1	0.04	0.3
2	11/13	59.83	5.56	206	35.01	7.31	2315.0	2181.9	7.942	2.35	1.49	10.9	0.85	6.4
2	11/13	59.83	5.56	104	34.30	9.54	2299.6	2150.2	7.964	2.65	1.68	7.7	0.58	4.7
2	11/13	59.83	5.56	52	33.31	10.95	2271.5	2099.0	8.016	3.03	1.93	4.2	0.28	2.8
2	11/13	59.83	5.56	32	32.96	11.02	2251.8	2076.9	8.028	3.08	1.95	3.6	0.23	2.5
2	11/13	59.83	5.56	12	31.94	11.26	2198.4	2059.2	7.955	2.58	1.64	3.7	0.21	2.0
2	11/13	59.83	5.56	6	28.32	10.46	1987.5	1861.1	8.005	2.36	1.47	3.5	0.14	0.9

**Table 5.** Hardangerfjord; January, April, August, November 2018.

Stn	Date	Lat	Lon	Depth	S	T	A <sub>T</sub>	C <sub>T</sub>	pH <sub>T</sub>	Ω <sub>Ca</sub>	Ω <sub>Ar</sub>	NO <sub>3</sub>	PO <sub>4</sub>	SiOH <sub>4</sub>
		°N	°E	m	°C	μmol/kg	μmol/kg			μmol/kg	μmol/kg	μmol/kg	μmol/kg	μmol/kg
1	1/19	59.74	5.5	334	35.01	8.08	2320.8	2181.7	7.946	2.36	1.50	0.04	0.92	7.53
1	1/19	59.74	5.5	150	34.59	8.92	2305.8	2160.8	7.962	2.55	1.62	0.11	0.43	4.33
1	1/19	59.74	5.5	100	34.17	8.74	2288.8	2134.2	7.999	2.71	1.72	0.04	0.00	4.14
1	1/19	59.74	5.5	49	33.20	7.25	2260.4	2105.8	8.039	2.72	1.72	0.05	0.46	4.24
1	1/19	59.74	5.5	10	32.21	6.05	2207.5	2060.2	8.058	2.62	1.65	0.04	0.59	4.69
1	1/19	59.74	5.5	5	31.49	5.58	2165.5	2017.0	8.083	2.63	1.65	0.05	0.74	5.56
1	4/10	59.74	5.5	336	35.11	7.73	2316.0	2175.8	7.955	2.38	1.51	0.04	0.04	5.12
1	4/10	59.74	5.5	98	34.81	8.04	2311.1	2179.6	7.939	2.38	1.51	0.08	0.82	6.29
1	4/10	59.74	5.5	48	33.83	7.13	2285.5	2148.5	7.984	2.48	1.57	0.18	0.69	5.13
1	4/10	59.74	5.5	29	32.44	5.24	2263.4	2111.7	8.074	2.70	1.70	0.14	0.41	2.31
1	4/10	59.74	5.5	10	30.87	4.83	2163.5	2024.2	8.080	2.51	1.57	0.08	0.26	0.96
1	4/10	59.74	5.5	5	30.62	4.85	2142.5	1996.8	8.104	2.60	1.63	0.04	0.00	0.51
1	8/10	59.74	5.5	339	35.039	7.05	2322.3	2165.3	8.007	2.57	1.64	0.06	0.76	5.40
1	8/10	59.74	5.5	103	34.916	7.59	2313.7	2168.9	7.979	2.55	1.61	0.09	0.80	5.80
1	8/10	59.74	5.5	52	34.738	8.10	2307.8	2165.3	7.970	2.55	1.62	0.12	0.74	5.18
1	8/10	59.74	5.5	31	33.370	13.05	2279.0	2096.7	8.011	3.20	2.04	0.11	0.35	1.69
1	8/10	59.74	5.5	11	31.977	17.01	2245.8	2012.8	8.083	4.05	2.60	0.03	0.03	0.46
1	8/10	59.74	5.5	6	31.144	16.86	2155.6	1933.0	8.089	3.87	2.47	0.05	0.03	0.43
1	11/13	59.74	5.5	347	35.04	7.21	2316.7	2175.8	7.958	2.38	1.51	0.07	0.88	6.90
1	11/13	59.74	5.5	102	34.48	9.04	2300.8	2149.4	7.974	2.67	1.69	0.09	0.66	5.31
1	11/13	59.74	5.5	51	33.41	10.86	2283.0	2102.1	8.035	3.15	2.01	0.16	0.28	2.86
1	11/13	59.74	5.5	31	33.25	10.80	2268.9	2093.1	8.028	3.09	1.96	0.33	0.22	2.53
1	11/13	59.74	5.5	11	31.52	10.76	2091.9	1943.1	8.006	2.65	1.68	0.27	0.15	0.89
1	11/13	59.74	5.5	6	28.85	10.42	2034.5	1893.6	8.034	2.58	1.62	0.32	0.15	0.85

**Table 6.** Svinøy-NW; January 2018.

Stn	Date	Lat °N	Lon °E	Depth m	S	T C°	A <sub>T</sub> μmol/kg	C <sub>T</sub> μmol/kg	pH <sub>T</sub>	Ω <sub>Ca</sub>	Ω <sub>Ar</sub>	NO <sub>3</sub> μmol/kg	PO <sub>4</sub> μmol/kg	SiOH <sub>4</sub> μmol/kg
2	17.01	62.484	4.944	9.0	33.61	7.01	2250	2090	8.057	2.82	1.78	4.56	0.362	2.63
2	17.01	62.484	4.944	19.0	34.04	7.03	2254	2092	8.056	2.84	1.80	4.47	0.361	2.59
2	17.01	62.484	4.944	49.0	34.34	7.97	2286	2120	8.042	2.89	1.83	5.11	0.420	2.57
2	17.01	62.484	4.944	76.0	34.24	7.93	2290	2127	8.037	2.85	1.81	5.53	0.439	2.58
2	17.01	62.484	4.944	98.0	34.32	7.94	2291	2125	8.043	2.89	1.83	5.64	0.430	2.55
2	17.01	62.484	4.944	151.0	35.06	8.96	2311	2142	8.019	2.88	1.83	7.49	0.527	2.92
2	17.01	62.484	4.944	193.0	35.05	9.05	2322	2155	8.010	2.84	1.81	10.55	0.673	3.85
6	17.01	62.836	4.175	591.0	34.98	3.65	2313	2173	8.016	2.23	1.41	13.25	0.869	7.29
6	17.01	62.836	4.175	499.0	34.97	5.45	2317	2167	8.017	2.42	1.54	11.66	0.820	6.05
6	17.01	62.836	4.175	298.0	35.10	8.17	2325	2153	8.032	2.84	1.81	11.23	0.683	4.10
6	17.01	62.836	4.175	201.0	35.13	8.16	2320	2151	8.029	2.85	1.82	11.41	0.683	3.77
6	17.01	62.836	4.175	150.0	35.13	8.16	2325	2152	8.038	2.94	1.87	11.30	0.683	3.85
6	17.01	62.836	4.175	75.0	35.13	8.15	2321	2148	8.043	2.99	1.90	10.68	0.683	3.65
6	17.01	62.836	4.175	50.0	35.13	8.14	2320	2147	8.045	3.01	1.91	10.60	0.673	3.96
6	17.01	62.836	4.175	30.0	35.13	8.14	2319	2150	8.036	2.96	1.88	10.45	0.683	3.90
6	17.01	62.836	4.175	10.0	35.13	8.13	2321	2147	8.047	3.04	1.93	10.70	0.683	3.93
9	18.01	63.075	3.655	970.0	34.91	-0.78	2309	2174	8.059	1.93	1.23	14.62	0.976	12.37
9	18.01	63.075	3.655	799.0	34.91	-0.70	2305	2169	8.067	2.02	1.28	14.22	0.927	10.54
9	18.01	63.075	3.655	499.0	34.86	0.90	2307	2179	8.034	2.10	1.33	13.04	0.888	7.21
9	18.01	63.075	3.655	399.0	34.99	3.86	2314	2167	8.038	2.41	1.53	13.03	0.859	6.55
9	18.01	63.075	3.655	201.0	35.09	7.55	2319	2155	8.028	2.79	1.77	11.56	0.722	4.46
9	18.01	63.075	3.655	100.0	35.09	7.62	2317	2149	8.040	2.90	1.84	11.51	0.722	4.21
9	18.01	63.075	3.655	75.0	35.10	7.67	2321	2150	8.045	2.95	1.87	11.08	0.712	4.19
9	18.01	63.075	3.655	51.0	35.08	7.62	2320	2152	8.041	2.93	1.86	10.84	0.703	3.99
9	18.01	63.075	3.655	30.0	35.08	7.61	2323	2153	8.046	2.97	1.88	10.68	0.693	4.06
9	18.01	63.075	3.655	10.0	35.08	7.60	2320	2151	8.045	2.97	1.88	9.80	0.703	4.14
11	18.01	63.310	3.134	1080.0	34.91	-0.77	2308	2172	8.057	1.89	1.20	*	*	*
11	18.01	63.310	3.134	1000.0	34.91	-0.76	2307	2173	8.057	1.91	1.22	*	*	*
11	18.01	63.310	3.134	800.0	34.91	-0.59	2306	2174	8.057	1.98	1.26	13.67	0.927	9.76
11	18.01	63.310	3.134	500.0	34.93	1.43	2306	2177	8.026	2.11	1.33	13.10	0.898	6.78
11	18.01	63.310	3.134	200.0	35.09	7.62	2318	2148	8.038	2.85	1.81	10.44	0.713	4.35
11	18.01	63.310	3.134	102.0	35.09	7.66	2316	2151	8.032	2.86	1.81	10.89	0.703	4.43
11	18.01	63.310	3.134	51.0	35.10	7.67	2316	2149	8.039	2.92	1.85	10.57	0.712	4.46
11	18.01	63.310	3.134	31.0	35.10	7.67	2320	2151	8.043	2.95	1.87	10.26	0.703	4.41
11	18.01	63.310	3.134	10.0	35.10	7.68	*	2154	*	*	*	*	*	*
13	18.01	63.662	2.345	1439.0	34.91	-0.79	2315	2174	8.057	1.80	1.15	14.79	0.957	12.49
13	18.01	63.662	2.345	1000.0	34.91	-0.62	2307	2175	8.047	1.88	1.20	13.91	0.918	10.20
13	18.01	63.662	2.345	798.0	34.91	-0.45	2311	2178	8.055	1.99	1.26	13.75	0.898	8.73
13	18.01	63.662	2.345	498.0	34.93	1.35	2313	2183	8.028	2.11	1.34	13.46	0.888	6.75
13	18.01	63.662	2.345	200.0	35.05	7.31	2318	2151	8.038	2.81	1.79	10.92	0.722	4.10
13	18.01	63.662	2.345	100.0	35.05	7.31	2323	2151	8.052	2.94	1.87	10.53	0.713	4.15
13	18.01	63.662	2.345	50.0	35.05	7.30	2319	2150	8.049	2.94	1.86	10.04	0.713	4.21
13	18.01	63.662	2.345	29.0	35.05	7.30	2322	2153	8.049	2.95	1.87	10.43	0.713	4.41
13	18.01	63.662	2.345	10.0	35.05	7.29	2319	2151	8.048	2.95	1.87	11.27	0.742	4.53
15	19.01	64.147	1.291	2442.0	34.91	-0.75	2307	2170	8.006	1.40	0.90	13.60	0.957	12.37

15	19.01	64.147	1.291	2000.0	34.92	-0.74	2308	2170	8.025	1.55	1.00	13.72	0.947	11.40
15	19.01	64.147	1.291	1500.0	34.91	-0.64	2312	2172	8.049	1.76	1.12	13.14	0.918	10.01
15	19.01	64.147	1.291	998.0	34.91	-0.37	2307	2173	8.051	1.92	1.22	11.93	0.888	7.85
15	19.01	64.147	1.291	799.0	34.91	-0.18	2308	2177	8.044	1.97	1.25	12.71	0.879	7.16
15	19.01	64.147	1.291	498.0	34.91	0.55	2305	2176	8.041	2.10	1.33	12.43	0.869	6.11
15	19.01	64.147	1.291	198.0	34.93	5.43	2313	2153	8.051	2.69	1.71	10.95	0.742	5.17
15	19.01	64.147	1.291	100.0	35.02	6.64	2322	2155	8.051	2.87	1.82	10.50	0.752	4.94
15	19.01	64.147	1.291	50.0	35.03	6.76	2317	2153	8.044	2.85	1.81	11.09	0.742	4.82
15	19.01	64.147	1.291	31.0	35.03	6.75	2317	2152	8.049	2.88	1.83	10.78	0.742	4.82
15	19.01	64.147	1.291	9.0	35.03	6.76	2321	2156	8.050	2.91	1.84	10.46	0.742	4.68

Table 7. Station M; January, April, May, August, November 2018.

Stn	Date	Lat °N	Lon °E	Depth m	S	T C°	A <sub>T</sub> μmol/kg	C <sub>T</sub> μmol/kg	pH <sub>T</sub>	Ω <sub>Ca</sub>	Ω <sub>Ar</sub>	NO <sub>3</sub> μmol/kg	PO <sub>4</sub> μmol/kg	SiOH <sub>4</sub> μmol/kg
19	1/19	65.835	2.174	1971	34.92	-0.76	2305.3	2167.1	8.026	1.55	1.00	14.28	0.94	11.69
19	1/19	65.835	2.174	1773	34.91	-0.74	2303.4	2164.1	8.037	1.63	1.05	14.18	0.93	11.14
19	1/19	65.835	2.174	1479	34.91	-0.71	2303.1	2167.3	8.040	1.71	1.10	13.13	0.92	10.52
19	1/19	65.835	2.174	986	34.91	-0.53	2302.3	2170.1	8.047	1.89	1.20	12.75	0.90	8.83
19	1/19	65.835	2.174	789	34.91	-0.39	2304.5	2172.6	8.052	1.98	1.26	13.77	0.89	7.90
19	1/19	65.835	2.174	494	34.91	-0.04	2301.0	2176.4	8.039	2.04	1.29	12.95	0.87	6.32
19	1/19	65.835	2.174	394	34.91	0.41	2300.6	2176.7	8.034	2.08	1.32	12.96	0.88	5.97
19	1/19	65.835	2.174	197	34.93	3.95	2304.5	2166.4	8.022	2.40	1.52	12.72	0.87	6.10
19	1/19	65.835	2.174	98	34.99	6.08	2313.0	2152.9	8.046	2.77	1.75	11.03	0.74	4.54
19	1/19	65.835	2.174	49	35.01	6.21	2309.4	2149.6	8.045	2.79	1.77	11.26	0.74	4.52
19	1/19	65.835	2.174	30	35.01	6.24	2309.8	2149.5	8.047	2.81	1.78	10.82	0.73	4.47
19	1/19	65.835	2.174	10	35.01	6.25	2310.8	2147.4	8.055	2.87	1.82	9.99	0.74	4.63
31	4/12	66.00	2.00	2026	34.92	-0.79	2304.6	2162.8	8.034	1.56	1.00	14.67	0.97	12.69
31	4/12	66.00	2.00	1774	34.92	-0.74	2300.6	2157.0	8.049	1.67	1.07	14.26	0.96	11.80
31	4/12	66.00	2.00	1479	34.91	-0.67	2300.8	2157.0	8.060	1.79	1.15	13.77	0.94	10.68
31	4/12	66.00	2.00	986	34.91	-0.45	2300.9	2156.1	8.080	2.02	1.29	13.54	0.91	8.68
31	4/12	66.00	2.00	789	34.91	-0.29	2299.4	2268.6	7.732	1.01	0.64	13.62	0.91	7.95
31	4/12	66.00	2.00	493	34.91	0.25	2299.1	2215.0	7.915	1.59	1.00	14.04	0.90	6.77
31	4/12	66.00	2.00	395	34.92	0.97	2299.0	2199.0	7.956	1.81	1.14	13.70	0.90	6.03
31	4/12	66.00	2.00	196	34.97	4.84	2306.1	2150.7	8.052	2.63	1.67	11.01	0.74	4.92
31	4/12	66.00	2.00	98	35.03	5.82	2311.6	2142.8	8.071	2.88	1.83	10.68	0.75	5.10
31	4/12	66.00	2.00	48	35.07	6.27	2314.1	2115.8	8.133	3.34	2.11	10.55	0.72	4.83
31	4/12	66.00	2.00	29	35.07	6.32	2313.9	2128.7	8.103	3.16	2.00	10.22	0.72	4.74
31	4/12	66.00	2.00	9	35.08	6.49	2315.2	2120.2	8.123	3.32	2.10	10.43	0.71	4.51
242	5/13	66.00	2.00	1973	34.91	-0.77	2304.5	2168.0	8.022	1.53	0.99	15.12	0.95	12.23
242	5/13	66.00	2.00	1478	34.91	-0.67	2302.3	2189.7	7.974	1.50	0.96	14.62	0.93	10.58
242	5/13	66.00	2.00	985	34.91	-0.32	2301.7	2187.1	7.995	1.71	1.09	14.04	0.91	7.98
242	5/13	66.00	2.00	493	34.96	3.21	2305.9	2177.0	7.997	2.13	1.35	13.56	0.86	6.19
242	5/13	66.00	2.00	295	35.06	6.33	2326.0	2167.0	8.029	2.65	1.68	11.85	0.74	5.01
242	5/13	66.00	2.00	197	35.08	6.70	2355.7	2165.0	8.098	3.16	2.00	11.82	0.75	4.85
242	5/13	66.00	2.00	96	35.11	7.15	2316.9	2158.3	8.024	2.76	1.75	11.31	0.71	4.71
242	5/13	66.00	2.00	49	35.08	7.27	2325.8	2148.0	8.069	3.06	1.94	8.18	0.58	4.34
242	5/13	66.00	2.00	29	35.08	7.38	2321.6	2142.9	8.071	3.09	1.96	8.13	0.57	4.25
242	5/13	66.00	2.00	19	35.07	7.55	2322.6	2136.4	8.085	3.21	2.03	7.72	0.53	4.16
242	5/13	66.00	2.00	9	35.07	7.79	2319.7	2126.1	8.099	3.32	2.10	6.43	0.49	4.12
242	5/13	66.00	2.00	5	35.07	7.94	2325.7	2129.2	8.103	3.37	2.14	6.25	0.46	4.16
574	5/27	65.869	2.181	1895	34.93	-0.77	2303.4	2167.7	8.023	1.55	1.00	*	*	*
574	5/27	65.869	2.181	1480	34.93	-0.69	2300.9	2166.6	8.035	1.70	1.09	*	*	*
574	5/27	65.869	2.181	989	34.93	-0.39	2299.3	2168.8	8.04	1.87	1.19	*	*	*
574	5/27	65.869	2.181	495	34.95	1.71	2306.3	2171.6	8.037	2.18	1.38	*	*	*
574	5/27	65.869	2.181	297	34.97	4.78	2306.3	2150.0	8.05	2.58	1.64	*	*	*
574	5/27	65.869	2.181	198	35.06	6.03	2311.4	2149.5	8.047	2.73	1.73	*	*	*
574	5/27	65.869	2.181	99	35.09	6.92	2313.9	2168.5	7.995	2.58	1.63	*	*	*
574	5/27	65.869	2.181	50	35.09	7.96	2317.8	2142.3	8.054	3.04	1.93	*	*	*
574	5/27	65.869	2.181	30	35.09	8.39	2320.1	2132.0	8.076	3.23	2.05	*	*	*

574	5/27	65.869	2.181	20	35.10	8.51	2316.4	2117.8	8.098	3.39	2.15	*	*	*
574	5/27	65.869	2.181	9	35.10	8.75	2318.3	2115.6	8.104	3.46	2.20	*	*	*
574	5/27	65.869	2.181	5	35.09	8.83	2316.2	2115.9	8.098	3.43	2.18	*	*	*
760	8/12	65.841	2.162	2016	34.91	-0.77	2326.8	2166.0	8.081	1.73	1.12	14.33	0.97	12.26
760	8/12	65.841	2.162	1970	34.91	-0.76	2322.3	2168.9	8.064	1.69	1.09	14.36	0.97	12.23
760	8/12	65.841	2.162	1479	34.91	-0.67	2301.7	2166.8	8.037	1.71	1.09	13.67	0.94	10.45
760	8/12	65.841	2.162	988	34.91	-0.39	2302.6	2170.4	8.045	1.89	1.20	13.82	0.92	8.26
760	8/12	65.841	2.162	790	34.91	-0.10	2300.6	2175.6	8.029	1.90	1.21	13.73	0.91	7.32
760	8/12	65.841	2.162	494	34.98	3.81	2308.5	2165.4	8.025	2.30	1.46	12.90	0.84	5.75
760	8/12	65.841	2.162	395	35.00	5.49	2309.1	2158.7	8.02	2.47	1.57	12.18	0.81	5.59
760	8/12	65.841	2.162	198	35.14	7.35	2316.8	2155.4	8.023	2.74	1.74	11.77	0.76	4.90
760	8/12	65.841	2.162	97	35.17	8.13	2317.5	2155.6	8.015	2.81	1.79	11.89	0.77	4.89
760	8/12	65.841	2.162	49	35.16	8.59	2321.2	2151.4	8.029	2.96	1.88	11.03	0.71	3.91
760	8/12	65.841	2.162	30	35.05	9.43	2317.2	2122.5	8.075	3.34	2.12	6.01	0.50	2.14
760	8/12	65.841	2.162	9	34.81	13.92	2303.9	2057.2	8.119	4.18	2.68	0.00	0.06	0.13
1004	11/18	65.839	2.170	2012	34.91	-0.76	2301.6	2170.6	8.005	1.47	0.95	*	*	*
1004	11/18	65.839	2.170	1480	34.91	-0.66	2297.3	2168.3	8.02	1.65	1.05	*	*	*
1004	11/18	65.839	2.170	989	34.91	-0.40	2298.0	2172.1	8.028	1.82	1.16	*	*	*
1004	11/18	65.839	2.170	295	34.91	3.78	2299.8	2163.0	8.018	2.32	1.47	*	*	*
1004	11/18	65.839	2.170	198	35.02	6.22	2309.2	2158.4	8.017	2.58	1.64	*	*	*
1004	11/18	65.839	2.170	95	35.01	7.92	2308.2	2152.4	8.007	2.73	1.73	*	*	*
1004	11/18	65.839	2.170	49	34.84	7.59	2298.7	2129.2	8.051	2.95	1.87	*	*	*
1004	11/18	65.839	2.170	29	34.84	7.60	2296.5	2126.9	8.052	2.96	1.87	*	*	*
1004	11/18	65.839	2.170	19	34.84	7.63	2296.4	2127.1	8.051	2.96	1.87	*	*	*
1004	11/18	65.839	2.170	9	34.84	7.64	2298.1	2126.7	8.056	3.00	1.90	*	*	*
1004	11/18	65.839	2.170	5	34.84	7.64	2296.9	2125.7	8.056	2.99	1.90	*	*	*
1004	11/18	65.869	2.181	1895	34.93	-0.77	2303.4	2167.7	8.023	1.55	1.00	*	*	*

**Table 8.** Gimsoy-NW; May and June 2018.

Stn	Date	Lat °N	Lon °E	Depth m	S	T C°	A <sub>T</sub> μmol/kg	C <sub>T</sub> μmol/kg	pH <sub>T</sub>	Ω <sub>Ca</sub>	Ω <sub>Ar</sub>	NO <sub>3</sub> μmol/kg	PO <sub>4</sub> μmol/kg	SiOH <sub>4</sub> μmol/kg
21	31.5	71.086	5.997	3125.4	34.92	-0.74	2304	2176	7.952	1.13	0.74	14.80	1.005	13.35
21	31.5	71.086	5.997	2499.5	34.92	-0.75	2303	2170	7.993	1.35	0.87	14.30	0.976	11.63
21	31.5	71.086	5.997	2000.1	34.92	-0.70	2302	2171	8.006	1.49	0.96	14.49	0.976	11.07
21	31.5	71.086	5.997	1499.2	34.92	-0.49	2300	2173	8.013	1.64	1.05	13.87	0.927	8.81
21	31.5	71.086	5.997	1000.4	34.92	0.09	2298	2176	8.009	1.79	1.14	13.27	0.898	6.64
21	31.5	71.086	5.997	799.1	34.95	1.56	2305	2209	7.920	1.63	1.03	13.19	0.888	6.05
21	31.5	71.086	5.997	498.9	35.10	4.86	2315	2166	8.022	2.40	1.52	11.84	0.781	4.95
21	31.5	71.086	5.997	200.0	35.09	5.33	2312	2154	8.049	2.68	1.70	11.46	0.761	5.22
21	31.5	71.086	5.997	99.3	35.07	5.71	2314	2143	8.077	2.91	1.84	8.32	0.634	4.13
21	31.5	71.086	5.997	49.6	35.06	5.94	2317	2147	8.074	2.94	1.86	7.94	0.586	4.12
21	31.5	71.086	5.997	28.8	35.06	5.98	2317	2218	7.888	2.02	1.28	7.93	0.576	3.93
21	31.5	71.086	5.997	9.6	35.06	5.99	2322	2207	7.930	2.22	1.40	7.89	0.576	3.64
17	1.6	69.950	9.580	2920.4	34.92	-0.77	2305	2161	8.004	1.30	0.85	15.22	1.005	13.47
17	1.6	69.950	9.580	2000.9	34.92	-0.75	2305	2160	8.044	1.61	1.03	14.53	0.986	11.77
17	1.6	69.950	9.580	1499.2	34.92	-0.65	2303	2168	8.036	1.71	1.09	14.13	0.957	10.14
17	1.6	69.950	9.580	999.0	34.92	-0.32	2305	2177	8.032	1.85	1.18	13.88	0.937	7.93
17	1.6	69.950	9.580	799.2	34.92	-0.06	2298	2173	8.029	1.91	1.21	13.44	0.918	6.97
17	1.6	69.950	9.580	499.8	34.96	1.99	2300	2177	7.999	2.03	1.28	13.48	0.908	5.93
17	1.6	69.950	9.580	199.3	35.04	5.50	2314	2205	7.916	2.05	1.30	11.76	0.791	5.26
17	1.6	69.950	9.580	99.7	35.06	6.38	2314	2152	8.045	2.80	1.77	10.02	0.722	4.57
17	1.6	69.950	9.580	50.0	35.06	7.25	2320	2141	8.074	3.08	1.95	6.72	0.517	3.10
17	1.6	69.950	9.580	30.0	35.06	7.32	2317	2130	8.093	3.21	2.04	6.33	0.508	3.27
17	1.6	69.950	9.580	9.6	35.06	7.40	2323	2146	8.066	3.07	1.95	6.42	0.488	3.08
15	1.6	69.481	10.952	2998.2	34.92	-0.75	2306	2167	7.987	1.24	0.81	15.77	1.015	13.64
15	1.6	69.481	10.952	1999.7	34.92	-0.70	2303	2167	8.018	1.53	0.98	14.71	0.976	11.14
15	1.6	69.481	10.952	1499.5	34.92	-0.52	2303	2166	8.038	1.72	1.10	13.88	0.947	9.16
15	1.6	69.481	10.952	999.7	34.92	0.06	2302	2170	8.037	1.89	1.20	14.00	0.918	6.96
15	1.6	69.481	10.952	799.6	34.96	1.60	2302	2171	8.017	1.99	1.26	13.68	0.879	6.10
15	1.6	69.481	10.952	499.6	35.09	5.39	2316	2208	7.903	1.92	1.22	12.05	0.839	5.00
15	1.6	69.481	10.952	198.7	35.08	6.76	2318	2206	7.903	2.10	1.33	11.27	0.761	4.77
15	1.6	69.481	10.952	99.8	35.05	7.18	2316	2147	8.050	2.91	1.84	7.71	0.595	3.20
15	1.6	69.481	10.952	49.3	35.05	7.44	2315	2130	8.086	3.17	2.01	6.79	0.517	2.97
15	1.6	69.481	10.952	29.4	34.99	7.71	2322	2211	7.894	2.18	1.38	5.70	0.478	3.07
15	1.6	69.481	10.952	10.1	34.91	7.81	2312	2120	8.099	3.30	2.09	4.81	0.439	3.25
12	1.6	69.033	12.284	2714.3	34.92	-0.77	2304	2173	7.978	1.27	0.82	15.29	1.005	13.09
12	1.6	69.033	12.284	2000.7	34.92	-0.73	2302	2170	8.009	1.49	0.96	14.67	0.986	11.44
12	1.6	69.033	12.284	1499.7	34.92	-0.62	2300	2168	8.029	1.68	1.08	14.57	0.957	9.73
12	1.6	69.033	12.284	1000.1	34.92	-0.25	2299	2179	8.010	1.77	1.12	14.04	0.937	7.72
12	1.6	69.033	12.284	799.1	34.92	0.06	2301	2177	8.021	1.89	1.20	13.95	0.918	6.75
12	1.6	69.033	12.284	499.7	35.09	4.86	2311	2164	8.016	2.36	1.50	12.24	0.800	4.90
12	1.6	69.033	12.284	199.8	35.05	6.06	2308	2157	8.019	2.58	1.64	11.75	0.781	5.05
12	1.6	69.033	12.284	100.1	35.08	7.16	2313	2144	8.049	2.90	1.84	8.70	0.644	3.42
12	1.6	69.033	12.284	49.3	35.06	7.37	2315	2142	8.057	2.99	1.89	6.93	0.527	2.89
12	1.6	69.033	12.284	30.6	35.06	7.51	2319	2218	7.868	2.05	1.30	6.52	0.498	2.93
12	1.6	69.033	12.284	10.0	35.05	7.70	2318	2123	8.103	3.33	2.11	5.62	0.449	2.94

**Table 8.** Skrova coastal station; January-December 2018.

Date	Lat °N	Lon °E	Depth m	T C°	S	A <sub>T</sub> µmol/kg	C <sub>T</sub> µmol/kg	pH <sub>T</sub>	Ω <sub>Ca</sub>	Ω <sub>Ar</sub>	NO <sub>3</sub> µmol/kg	PO <sub>4</sub> µmol/kg	SiOH <sub>4</sub> µmol/kg
19.01.	68.1170	14.5320	300.0	34.96	7.60	2336	2203	7.945	2.34	1.49	12.22	0.815	6.11
19.01.	68.1170	14.5320	200.0	34.83	7.61	2322	2170	8.000	2.64	1.67	11.16	0.742	5.24
19.01.	68.1170	14.5320	150.0	34.63	7.64	2331	2172	8.019	2.76	1.75	10.38	0.647	4.49
19.01.	68.1170	14.5320	125.0	34.48	7.72	2336	2204	7.952	2.43	1.54	7.30	0.562	2.88
19.01.	68.1170	14.5320	100.0	34.25	8.25	2302	2168	7.957	2.46	1.56	7.27	0.518	2.88
19.01.	68.1170	14.5320	75.0	33.59	7.86	2249	2120	7.963	2.38	1.51	3.69	0.285	1.54
19.01.	68.1170	14.5320	50.0	32.80	5.80	2267	2140	7.999	2.38	1.50	3.68	0.286	1.55
19.01.	68.1170	14.5320	30.0	32.78	5.80	2264	2134	8.010	2.43	1.53	3.69	0.280	1.53
19.01.	68.1170	14.5320	20.0	32.73	5.80	2239	2106	8.021	2.46	1.55	3.69	0.278	1.81
19.01.	68.1170	14.5320	10.0	32.69	5.80	2236	2085	8.070	2.72	1.71	3.65	0.289	1.80
19.01.	68.1170	14.5320	5.0	32.67	5.79	2241	2078	8.101	2.90	1.82	3.68	0.280	1.51
19.01.	68.1170	14.5320	1.0	32.67	5.78	2242	2079	8.099	2.89	1.82	3.87	0.288	1.55
12.02.	68.1170	14.5320	300.0	34.98	7.69	2334	2189	7.972	2.48	1.58	12.02	0.801	6.18
12.02.	68.1170	14.5320	200.0	34.89	7.73	2333	2180	7.998	2.65	1.68	11.73	0.766	5.63
12.02.	68.1170	14.5320	150.0	34.78	7.76	2344	2178	8.032	2.87	1.82	11.36	0.731	5.33
12.02.	68.1170	14.5320	125.0	34.66	7.78	*	*	*	*	*	11.19	0.756	5.04
12.02.	68.1170	14.5320	100.0	33.93	6.32	2275	2119	8.051	2.73	1.73	4.59	0.309	2.80
12.02.	68.1170	14.5320	75.0	33.18	4.26	2253	2100	8.088	2.69	1.69	4.75	0.332	2.09
12.02.	68.1170	14.5320	50.0	33.12	4.02	2247	2093	8.098	2.71	1.71	4.29	0.290	1.94
12.02.	68.1170	14.5320	30.0	33.12	4.04	2246	2091	8.101	2.74	1.72	3.30	0.225	1.92
12.02.	68.1170	14.5320	20.0	33.10	4.05	2254	2135	8.004	2.26	1.42	2.95	0.241	1.99
12.02.	68.1170	14.5320	10.0	33.09	4.03	2246	2086	8.114	2.82	1.77	3.10	0.213	1.91
12.02.	68.1170	14.5320	5.0	33.09	4.04	2258	2134	8.019	2.34	1.47	3.00	0.216	1.93
12.02.	68.1170	14.5320	1.0	33.05	4.08	2255	2150	7.964	2.09	1.31	4.43	0.251	1.94
21.03.	68.1170	14.5320	300.0	34.96	7.67	2320	2169	7.990	2.56	1.63	12.27	0.792	5.81
21.03.	68.1170	14.5320	200.0	34.85	7.70	2322	2169	8.001	2.65	1.68	11.58	0.744	5.08
21.03.	68.1170	14.5320	150.0	34.73	7.69	2330	2186	7.981	2.56	1.63	10.20	0.641	4.68
21.03.	68.1170	14.5320	125.0	34.61	7.50	2302	2151	8.008	2.66	1.69	9.59	0.635	4.23
21.03.	68.1170	14.5320	100.0	34.38	7.13	2286	2130	8.029	2.72	1.72	5.41	0.362	3.01
21.03.	68.1170	14.5320	75.0	34.24	6.56	2313	2170	8.006	2.58	1.63	7.55	0.502	3.38
21.03.	68.1170	14.5320	50.0	34.00	5.65	2317	2180	8.008	2.51	1.59	7.99	0.525	3.96
21.03.	68.1170	14.5320	30.0	33.56	3.67	2254	2104	8.086	2.65	1.67	5.12	0.387	2.62
21.03.	68.1170	14.5320	20.0	33.50	3.34	2264	2105	8.115	2.79	1.75	4.33	0.349	2.20
21.03.	68.1170	14.5320	10.0	33.43	3.24	2278	2155	8.023	2.32	1.46	3.95	0.321	2.01
21.03.	68.1170	14.5320	5.0	33.39	3.23	2280	2146	8.053	2.47	1.55	3.94	0.325	2.00
21.03.	68.1170	14.5320	1.0	33.31	3.22	2254	2105	8.098	2.67	1.68	3.94	0.343	2.00
17.04.	68.1170	14.5320	300.0	34.97	7.68	2317	2175	7.968	2.44	1.55	11.78	0.788	6.22
17.04.	68.1170	14.5320	200.0	34.90	7.70	2332	2195	7.956	2.43	1.54	11.11	0.745	5.42
17.04.	68.1170	14.5320	150.0	34.75	7.60	2333	2191	7.975	2.53	1.61	11.18	0.718	5.41
17.04.	68.1170	14.5320	125.0	34.65	7.49	2327	2169	8.020	2.76	1.75	10.36	0.675	4.95
17.04.	68.1170	14.5320	100.0	34.48	7.05	2341	2175	8.049	2.90	1.83	10.57	0.601	4.85
17.04.	68.1170	14.5320	75.0	34.27	6.38	2282	2126	8.044	2.73	1.73	7.35	0.545	2.85
17.04.	68.1170	14.5320	50.0	33.93	5.07	2279	2140	8.029	2.52	1.59	2.78	0.306	0.76
17.04.	68.1170	14.5320	30.0	33.55	3.22	2271	2132	8.065	2.52	1.58	0.07	0.113	0.19

17.04.	68.1170	14.5320	20.0	33.51	3.25	2280	2107	8.150	3.00	1.89	0.10	0.088	0.18
17.04.	68.1170	14.5320	10.0	33.52	3.26	2289	2130	8.116	2.82	1.77	0.39	0.101	0.22
17.04.	68.1170	14.5320	5.0	33.55	3.26	2270	2044	8.270	3.79	2.38	0.06	0.078	0.27
17.04.	68.1170	14.5320	1.0	33.46	3.27	2261	2046	8.250	3.63	2.28	0.03	0.069	0.17
24.05.	68.1170	14.5320	300.0	34.98	7.65	2325	2182	7.968	2.45	1.56	12.05	0.800	6.37
24.05.	68.1170	14.5320	200.0	34.77	7.46	2326	2187	7.969	2.46	1.56	11.60	0.732	5.39
24.05.	68.1170	14.5320	150.0	34.40	6.49	2292	2147	8.010	2.55	1.62	10.29	0.645	4.01
24.05.	68.1170	14.5320	125.0	34.22	5.90	2282	2134	8.031	2.60	1.64	7.61	0.531	3.09
24.05.	68.1170	14.5320	100.0	33.94	5.29	2282	2122	8.075	2.77	1.75	3.34	0.244	1.84
24.05.	68.1170	14.5320	75.0	33.87	5.33	2277	2119	8.073	2.77	1.75	3.38	0.313	1.77
24.05.	68.1170	14.5320	50.0	33.82	5.47	2272	2104	8.097	2.92	1.84	0.80	0.125	1.40
24.05.	68.1170	14.5320	30.0	33.71	6.32	2272	2092	8.114	3.11	1.96	0.14	0.152	1.08
24.05.	68.1170	14.5320	20.0	33.64	6.58	2259	2118	8.016	2.57	1.62	0.02	0.120	2.56
24.05.	68.1170	14.5320	10.0	33.30	6.43	2253	2102	8.051	2.72	1.72	0.06	0.105	0.85
24.05.	68.1170	14.5320	5.0	33.27	6.73	2236	2054	8.122	3.15	1.98	0.08	0.096	1.02
24.05.	68.1170	14.5320	1.0	32.82	6.43	2225	2038	8.148	3.24	2.04	0.02	0.098	1.37
12.06.	68.1170	14.5320	300.0	34.99	7.59	2314	2177	7.955	2.37	1.51	13.18	0.853	6.84
12.06.	68.1170	14.5320	200.0	34.86	7.62	2325	2179	7.983	2.55	1.62	11.77	0.732	5.99
12.06.	68.1170	14.5320	150.0	34.64	6.99	2337	2172	8.044	2.85	1.80	10.20	0.641	4.44
12.06.	68.1170	14.5320	125.0	34.17	5.58	2289	2148	8.017	2.50	1.58	7.58	0.533	4.89
12.06.	68.1170	14.5320	100.0	33.94	5.19	2279	2123	8.068	2.72	1.72	4.33	0.418	3.24
12.06.	68.1170	14.5320	75.0	33.67	6.53	2276	2099	8.102	3.05	1.93	1.19	0.279	2.03
12.06.	68.1170	14.5320	50.0	33.58	7.06	2280	2145	7.991	2.49	1.58	0.66	0.256	1.65
12.06.	68.1170	14.5320	30.0	33.42	7.60	2271	2131	7.998	2.57	1.63	0.03	0.139	1.00
12.06.	68.1170	14.5320	20.0	33.36	8.13	2259	2060	8.136	3.42	2.17	0.02	0.082	1.00
12.06.	68.1170	14.5320	10.0	33.21	8.34	2259	2087	8.071	3.03	1.92	0.05	0.074	0.95
12.06.	68.1170	14.5320	5.0	33.22	8.37	2255	2058	8.130	3.41	2.15	0.04	0.061	2.66
12.06.	68.1170	14.5320	1.0	33.11	8.45	2257	2065	8.120	3.35	2.12	0.05	0.059	0.88
15.07.	68.1170	14.5320	300.0	34.99	7.45	2309	2172	7.958	2.37	1.50	12.01	0.763	6.57
15.07.	68.1170	14.5320	200.0	34.64	7.59	2320	2174	7.988	2.56	1.62	12.31	0.731	5.87
15.07.	68.1170	14.5320	150.0	34.46	7.28	2311	2165	7.996	2.57	1.63	11.50	0.672	5.21
15.07.	68.1170	14.5320	125.0	34.23	6.60	2330	2194	7.983	2.47	1.56	9.43	0.586	3.81
15.07.	68.1170	14.5320	100.0	33.71	5.94	2270	2107	8.076	2.81	1.78	3.35	0.278	2.15
15.07.	68.1170	14.5320	75.0	33.27	7.56	2267	2078	8.119	3.24	2.05	0.55	0.222	1.47
15.07.	68.1170	14.5320	50.0	33.06	8.38	2252	2084	8.063	2.96	1.87	0.39	0.135	1.39
15.07.	68.1170	14.5320	30.0	32.88	9.10	2266	2069	8.120	3.42	2.16	0.18	0.185	1.28
15.07.	68.1170	14.5320	20.0	32.76	9.87	2246	2063	8.080	3.21	2.04	0.25	0.174	1.31
15.07.	68.1170	14.5320	10.0	32.61	10.61	2250	2051	8.109	3.49	2.21	0.12	0.096	1.34
15.07.	68.1170	14.5320	5.0	32.55	11.79	2245	2040	8.103	3.58	2.28	0.11	0.102	1.17
15.07.	68.1170	14.5320	1.0	32.54	11.89	2244	2033	8.114	3.67	2.33	0.15	0.113	1.16
14.08.	68.1170	14.5320	300.0	34.99	7.43	2330	2176	8.001	2.60	1.66	11.82	0.809	6.11
14.08.	68.1170	14.5320	200.0	34.92	7.48	2327	2177	7.994	2.60	1.65	11.87	0.786	5.50
14.08.	68.1170	14.5320	150.0	34.80	7.39	2325	2173	8.004	2.66	1.69	11.40	0.749	5.04
14.08.	68.1170	14.5320	125.0	34.56	6.73	2329	2169	8.038	2.78	1.76	10.90	0.690	4.54
14.08.	68.1170	14.5320	100.0	34.35	6.21	2295	2155	8.002	2.50	1.58	9.02	0.635	3.41
14.08.	68.1170	14.5320	75.0	33.91	6.35	2279	2119	8.062	2.81	1.77	5.40	0.413	2.08
14.08.	68.1170	14.5320	50.0	33.31	7.94	2276	2096	8.091	3.12	1.98	2.99	0.286	1.91

14.08.	68.1170	14.5320	30.0	32.90	10.30	2267	2073	8.095	3.39	2.15	0.47	0.187	1.22
14.08.	68.1170	14.5320	20.0	32.59	12.09	2211	2015	8.083	3.42	2.17	0.04	0.077	0.69
14.08.	68.1170	14.5320	10.0	32.42	14.24	2216	1991	8.113	3.89	2.49	0.08	0.038	0.65
14.08.	68.1170	14.5320	5.0	32.32	16.08	2216	1992	8.084	3.91	2.50	0.10	0.048	0.99
14.08.	68.1170	14.5320	1.0	32.17	16.12	2219	2051	7.961	3.09	1.98	0.11	0.038	0.65
11.09.	68.1170	14.5320	300.0	34.95	7.24	2310	2176	7.953	2.32	1.48	12.48	0.830	6.46
11.09.	68.1170	14.5320	200.0	34.87	7.52	2327	2179	7.990	2.58	1.64	11.81	0.791	6.06
11.09.	68.1170	14.5320	150.0	34.71	7.30	2311	2172	7.975	2.48	1.57	10.11	0.633	5.47
11.09.	68.1170	14.5320	125.0	34.48	6.69	2299	2167	7.973	2.40	1.52	10.30	0.669	5.00
11.09.	68.1170	14.5320	100.0	34.00	6.67	2292	2133	8.047	2.77	1.75	3.18	0.352	3.55
11.09.	68.1170	14.5320	75.0	33.43	9.03	2279	2114	8.034	2.90	1.84	1.37	0.227	2.03
11.09.	68.1170	14.5320	50.0	32.92	12.04	2241	2060	8.038	3.17	2.02	0.06	0.126	1.22
11.09.	68.1170	14.5320	30.0	32.60	12.29	2193	2009	8.055	3.23	2.06	0.11	0.188	0.76
11.09.	68.1170	14.5320	20.0	32.31	12.69	2173	1981	8.073	3.35	2.13	0.12	0.124	0.75
11.09.	68.1170	14.5320	10.0	32.03	12.89	2172	1984	8.064	3.30	2.10	0.04	0.134	0.71
11.09.	68.1170	14.5320	5.0	31.83	13.02	2172	1975	8.087	3.46	2.20	0.26	0.146	0.79
11.09.	68.1170	14.5320	1.0	31.71	13.02	2180	2014	8.013	3.00	1.91	0.11	0.107	0.78
26.10.	68.1170	14.5320	300.0	34.97	7.12	2312	2177	7.960	2.35	1.49	12.58	0.842	6.31
26.10.	68.1170	14.5320	200.0	34.80	7.27	2320	2184	7.963	2.41	1.53	12.25	0.787	5.66
26.10.	68.1170	14.5320	150.0	33.99	7.16	2327	2167	8.039	2.79	1.77	9.28	0.620	3.86
26.10.	68.1170	14.5320	125.0	33.74	10.63	2295	2135	7.990	2.82	1.80	6.70	0.467	2.86
26.10.	68.1170	14.5320	100.0	33.30	11.18	2267	2090	8.034	3.09	1.97	3.35	0.289	1.50
26.10.	68.1170	14.5320	75.0	33.05	11.15	2259	2071	8.066	3.28	2.08	2.43	0.210	1.20
26.10.	68.1170	14.5320	50.0	32.51	10.22	2216	2031	8.084	3.21	2.03	2.32	0.188	1.32
26.10.	68.1170	14.5320	30.0	32.34	10.14	2182	2009	8.064	3.03	1.92	2.42	0.205	1.53
26.10.	68.1170	14.5320	20.0	32.23	10.05	2178	2014	8.049	2.92	1.85	2.44	0.199	1.51
26.10.	68.1170	14.5320	10.0	32.04	9.59	2154	1990	8.062	2.91	1.84	2.28	0.206	1.63
26.10.	68.1170	14.5320	5.0	32.03	9.54	2149	1983	8.065	2.92	1.85	2.31	0.199	1.77
26.10.	68.1170	14.5320	1.0	31.97	9.51	2134	1983	8.030	2.70	1.71	2.34	0.266	1.76
12.11.	68.1170	14.5320	300.0	34.96	7.27	2318	2178	7.969	2.41	1.53	13.04	0.824	6.36
12.11.	68.1170	14.5320	200.0	34.81	7.24	2312	2173	7.973	2.45	1.55	12.58	0.814	5.86
12.11.	68.1170	14.5320	150.0	34.50	6.85	2301	2157	8.000	2.54	1.61	10.85	0.605	4.68
12.11.	68.1170	14.5320	125.0	34.19	7.08	2298	2144	8.025	2.69	1.71	7.93	0.504	3.28
12.11.	68.1170	14.5320	100.0	33.52	10.26	2276	2122	7.988	2.75	1.75	3.92	0.276	1.91
12.11.	68.1170	14.5320	75.0	33.00	10.27	2244	2058	8.075	3.21	2.04	2.81	0.239	1.36
12.11.	68.1170	14.5320	50.0	32.23	9.42	2198	2054	8.000	2.61	1.65	2.49	0.210	1.44
12.11.	68.1170	14.5320	30.0	31.95	8.75	2190	2045	8.020	2.64	1.66	2.50	0.213	1.45
12.11.	68.1170	14.5320	20.0	31.90	8.67	2174	2011	8.072	2.89	1.83	2.49	0.189	1.54
12.11.	68.1170	14.5320	10.0	31.88	8.66	2168	2019	8.036	2.69	1.70	2.38	0.199	1.65
12.11.	68.1170	14.5320	5.0	31.87	8.66	2167	2018	8.038	2.70	1.70	2.57	0.209	1.57
12.11.	68.1170	14.5320	1.0	31.77	8.68	2162	2005	8.059	2.81	1.77	2.55	0.219	1.67

**Table 10.** Fugløya-Bjørnøya; January 2018.

Stn	Date	Lat °N	Lon °E	Depth m	S	T C°	A <sub>T</sub> μmol/kg	C <sub>T</sub> μmol/kg	pH <sub>T</sub>	Ω <sub>Ca</sub>	Ω <sub>Ar</sub>	NO <sub>3</sub> μmol/kg	PO <sub>4</sub> μmol/kg	SiOH <sub>4</sub> μmol/kg
20	22.1	74.248	19.164	54.0	34.64	0.37	2292	2164	8.064	2.32	1.46	8.75	0.596	3.48
20	22.1	74.248	19.164	30.0	34.65	0.37	2294	2162	8.075	2.38	1.49	9.02	0.605	3.54
20	22.1	74.248	19.164	21.0	34.65	0.37	2292	2161	8.072	2.36	1.49	9.06	0.625	3.48
20	22.1	74.248	19.164	11.0	34.65	0.37	2294	2168	8.060	2.31	1.45	9.01	0.596	3.50
20	22.1	74.248	19.164	6.0	34.65	0.37	2299	2168	8.074	2.39	1.50	8.77	0.596	3.53
16	23.1	73.670	19.297	342.0	35.04	3.45	2316	2168	8.047	2.44	1.55	11.94	0.742	5.21
16	23.1	73.670	19.297	100.0	34.70	4.76	2316	2156	8.071	2.77	1.75	10.86	0.674	3.62
16	23.1	73.670	19.297	74.0	34.74	4.79	2315	2155	8.072	2.79	1.76	11.32	0.664	3.83
16	23.1	73.670	19.297	50.0	34.79	4.81	2317	2155	8.075	2.82	1.78	11.14	0.664	3.98
16	23.1	73.670	19.297	31.0	34.82	4.81	2324	2163	8.071	2.82	1.78	10.94	0.664	4.07
16	23.1	73.670	19.297	19.0	35.05	4.83	2319	2157	8.073	2.83	1.79	10.82	0.673	4.03
16	23.1	73.670	19.297	9.0	35.06	4.83	2322	2160	8.072	2.84	1.79	11.13	0.673	4.25
12	23.1	72.747	19.513	391.0	35.03	2.65	2323	2188	8.026	2.26	1.43	12.03	0.781	6.61
12	23.1	72.747	19.513	301.0	35.06	4.13	2317	2167	8.042	2.50	1.58	11.70	0.722	4.62
12	23.1	72.747	19.513	201.0	35.06	4.74	2316	2156	8.061	2.69	1.70	11.28	0.683	4.22
12	23.1	72.747	19.513	150.0	35.09	5.26	2320	2159	8.058	2.75	1.74	12.01	0.712	4.55
12	23.1	72.747	19.513	101.0	35.06	5.34	2316	2153	8.065	2.81	1.78	11.06	0.673	4.21
12	23.1	72.747	19.513	76.0	35.06	5.37	2316	2155	8.058	2.78	1.76	11.27	0.673	4.08
12	23.1	72.747	19.513	50.0	35.05	5.40	2317	2152	8.070	2.86	1.81	11.29	0.673	4.15
12	23.1	72.747	19.513	30.0	35.02	5.65	2315	2154	8.059	2.83	1.79	10.90	0.664	4.29
12	23.1	72.747	19.513	20.0	34.98	6.09	2317	2153	8.059	2.88	1.82	10.73	0.654	4.19
12	23.1	72.747	19.513	9.0	34.98	6.11	2322	2155	8.064	2.92	1.85	10.78	0.654	4.12
8	23.1	71.752	19.729	259.0	35.07	5.70	2321	2159	8.048	2.69	1.71	11.59	0.703	4.25
8	23.1	71.752	19.729	201.0	34.98	6.15	2312	2151	8.043	2.72	1.72	10.67	0.664	3.91
8	23.1	71.752	19.729	150.0	35.00	6.56	2312	2151	8.038	2.75	1.74	10.50	0.674	3.96
8	23.1	71.752	19.729	101.0	34.94	6.42	2321	2154	8.059	2.88	1.83	10.53	0.644	3.82
8	23.1	71.752	19.729	76.0	34.91	6.31	2314	2145	8.064	2.90	1.84	9.95	0.634	3.75
8	23.1	71.752	19.729	51.0	34.92	6.32	2314	2146	8.063	2.90	1.84	9.85	0.625	3.91
8	23.1	71.752	19.729	30.0	34.92	6.33	2311	2147	8.057	2.88	1.82	10.23	0.625	3.90
8	23.1	71.752	19.729	20.0	34.92	6.32	2315	2148	8.061	2.91	1.84	10.23	0.625	3.76
8	23.1	71.752	19.729	10.0	34.92	6.32	2317	2149	8.065	2.94	1.86	10.14	0.625	3.75
2	24.1	70.671	19.971	140.0	34.94	7.09	2314	2147	8.046	2.86	1.81	10.74	0.644	3.76
2	24.1	70.671	19.971	98.0	34.58	6.18	2310	2140	8.074	2.92	1.85	8.70	0.547	3.41
2	24.1	70.671	19.971	75.0	34.36	6.14	2296	2130	8.070	2.87	1.82	7.40	0.488	3.11
2	24.1	70.671	19.971	51.0	34.00	6.04	2286	2116	8.089	2.96	1.87	6.20	0.420	2.62
2	24.1	70.671	19.971	29.0	33.84	5.81	2278	2108	8.095	2.96	1.87	5.94	0.391	2.18
2	24.1	70.671	19.971	19.0	33.83	5.79	2284	2116	8.092	2.95	1.86	5.60	0.391	2.18
2	24.1	70.671	19.971	9.0	33.83	5.79	2281	2113	8.092	2.95	1.86	5.76	0.391	2.28

Table 11. Barents Sea; August-September 2018.

Stn	Date	Lat °N	Lon °E	Depth m	S	T C °	A <sub>T</sub> μmol/kg	C <sub>T</sub> μmol/kg	pH <sub>T</sub>	Ω <sub>Ca</sub>	Ω <sub>Ar</sub>	NO <sub>3</sub> μmol/kg	PO <sub>4</sub> μmol/kg	SiOH <sub>4</sub> μmol/kg
P4	14.8	79.750	34.001	325.1	34.80	-0.20	2300	2196	7.992	1.88	1.19	*	*	*
P4	14.8	79.750	34.001	249.8	34.79	0.92	2302	2170	8.054	2.26	1.43	*	*	*
P4	14.8	79.750	34.001	200.0	34.79	1.16	2303	2167	8.064	2.35	1.48	*	*	*
P4	14.8	79.750	34.001	150.0	34.78	1.33	2302	2164	8.067	2.39	1.51	*	*	*
P4	14.8	79.750	34.001	121.4	34.80	1.68	2304	2167	8.061	2.41	1.52	*	*	*
P4	14.8	79.750	34.001	89.9	34.64	0.74	2293	2168	8.049	2.26	1.42	*	*	*
P4	14.8	79.750	34.001	60.3	34.37	-1.14	2286	2151	8.112	2.39	1.50	*	*	*
P4	14.8	79.750	34.001	40.1	34.24	-0.02	2279	2091	8.230	3.15	1.98	*	*	*
P4	14.8	79.750	34.001	30.1	34.13	2.64	2274	2076	8.208	3.31	2.08	*	*	*
P4	14.8	79.750	34.001	20.1	34.13	2.66	2273	2073	8.214	3.36	2.11	*	*	*
P4	14.8	79.750	34.001	10.1	34.13	2.66	2277	2074	8.222	3.42	2.15	*	*	*
P4	14.8	79.750	34.001	5.6	34.13	2.66	2281	2076	8.228	3.47	2.18	*	*	*
P5	15.8	80.501	34.006	155.6	34.55	-0.24	2290	2171	8.047	2.14	1.35	*	*	*
P5	15.8	80.501	34.006	140.9	34.53	-0.29	2286	2165	8.053	2.17	1.36	*	*	*
P5	15.8	80.501	34.006	120.2	34.52	-0.31	2290	2162	8.073	2.27	1.43	*	*	*
P5	15.8	80.501	34.006	90.2	34.48	-0.44	2290	2162	8.080	2.30	1.44	*	*	*
P5	15.8	80.501	34.006	60.7	34.32	-0.51	2283	2138	8.128	2.52	1.59	*	*	*
P5	15.8	80.501	34.006	50.7	34.27	-0.14	2286	2110	8.202	2.98	1.87	*	*	*
P5	15.8	80.501	34.006	40.5	34.24	0.98	2280	2085	8.228	3.26	2.05	*	*	*
P5	15.8	80.501	34.006	30.6	34.15	2.43	2272	2075	8.212	3.31	2.08	*	*	*
P5	15.8	80.501	34.006	20.7	34.15	2.51	2275	2079	8.207	3.30	2.08	*	*	*
P5	15.8	80.501	34.006	10.5	34.15	2.53	2271	2068	8.223	3.40	2.14	*	*	*
P5	15.8	80.501	34.006	5.5	34.15	2.53	2268	2077	8.198	3.24	2.04	*	*	*
23	30.9	77.004	34.005	146.8	34.94	1.11	2304	2201	7.971	1.96	1.23	11.40	0.879	6.43
23	30.9	77.004	34.005	124.6	34.88	0.53	2301	2210	7.947	1.82	1.14	10.94	0.879	5.88
23	30.9	77.004	34.005	99.8	34.86	0.42	2303	2211	7.951	1.83	1.15	9.50	0.869	5.24
23	30.9	77.004	34.005	74.6	34.66	-0.74	2294	2185	8.028	2.05	1.29	6.96	0.654	1.48
23	30.9	77.004	34.005	50.3	34.36	2.30	2277	2116	8.125	2.78	1.75	0.62	0.127	0.00
23	30.9	77.004	34.005	29.8	34.39	2.30	2277	2119	8.117	2.75	1.73	0.45	0.107	0.00
23	30.9	77.004	34.005	9.7	34.39	2.29	2283	2138	8.087	2.60	1.63	0.63	0.107	0.01
24	30.9	77.502	33.987	74.1	34.56	-1.28	*	2176	*	*	*	4.81	0.517	0.87
24	30.9	77.502	33.987	49.1	34.29	2.04	2298	2151	8.093	2.60	1.64	2.28	0.342	0.43
24	30.9	77.502	33.987	29.2	34.32	2.12	2273	2116	8.120	2.74	1.72	0.35	0.078	0.07
24	30.9	77.502	33.987	10.2	34.32	2.11	2273	2115	8.124	2.77	1.74	0.28	0.088	0.11
24	30.9	77.502	33.987	0.0	34.32	2.12	2283	2116	8.144	2.90	1.82	0.31	0.098	0.08
26	30.9	78.000	34.000	185.6	34.91	1.01	2309	2210	7.962	1.90	1.20	*	*	*
26	30.9	78.000	34.000	149.9	34.91	0.99	2311	2211	7.964	1.92	1.21	10.00	0.781	4.23
26	30.9	78.000	34.000	99.8	34.73	0.05	2288	2168	8.044	2.18	1.37	6.56	0.566	1.56
26	30.9	78.000	34.000	73.6	34.61	-0.54	2288	2168	8.058	2.20	1.38	6.39	0.615	1.58
26	30.9	78.000	34.000	49.7	34.45	0.65	2292	2139	8.129	2.66	1.67	1.70	0.273	0.45
27	30.9	78.750	33.995	149.1	34.73	0.36	2289	2180	8.007	2.03	1.28	10.96	0.752	4.76
27	30.9	78.750	33.995	99.5	34.65	-0.45	2285	2182	8.004	1.96	1.23	9.73	0.693	3.31
27	30.9	78.750	33.995	73.8	34.69	0.83	2287	2177	8.005	2.07	1.30	9.67	0.713	3.30
27	30.9	78.750	33.995	49.4	34.42	-0.41	2283	2153	8.089	2.35	1.47	2.91	0.400	0.71
27	30.9	78.750	33.995	8.5	34.25	1.72	2270	2116	8.123	2.72	1.71	0.24	0.186	0.21

27	30.9	78.750	33.995	0.0	34.25	1.72	2278	2116	8.142	2.84	1.78	0.17	0.127	0.35
28	30.9	79.000	33.998	254.3	34.80	0.76	2294	2186	7.988	1.95	1.23	11.64	0.840	7.22
28	30.9	79.000	33.998	199.2	34.79	0.98	2302	2187	8.008	2.07	1.31	11.64	0.820	6.49
28	30.9	79.000	33.998	99.5	34.59	0.01	2281	2166	8.033	2.11	1.33	7.68	0.644	2.55
28	30.9	79.000	33.998	74.8	34.51	-0.34	2279	2161	8.050	2.17	1.36	0.72	0.186	0.33
28	30.9	79.000	33.998	49.4	34.30	1.51	2278	2137	8.088	2.51	1.58	0.42	0.146	0.26
28	30.9	79.000	33.998	29.3	34.24	1.63	2270	2110	8.135	2.76	1.74	0.32	0.137	0.22
28	30.9	79.000	33.998	10.6	34.24	1.63	2269	2112	8.130	2.75	1.73	0.22	0.137	0.28
28	30.9	79.000	33.998	0.0	34.24	1.63	2276	2133	8.095	2.57	1.61	0.27	0.146	0.29

Table 12. Tromsø-Longyearbyen; March, June, August, November 2018.

Date	Lat °N	Lon °E	S	T C°	A <sub>T</sub> μmol/kg	C <sub>T</sub> μmol/kg	pH <sub>T</sub>	pCO <sub>2</sub> μatm	Ω <sub>Ca</sub>	Ω <sub>Ar</sub>	PO <sub>34</sub> μmol/kg	NO <sub>3</sub> μmol/kg	SiOH <sub>4</sub> μmol/kg
3.3	69.71	19.05	33.505	2.27	2123.5	2261	8.078	355	2.49	1.56	0.6	7.26	4.39
3.3	70.24	20.33	33.964	4.5	2122.3	2275.9	8.076	360	2.73	1.72	0.54	6.98	3.09
3.3	70.96	19.82	34.239	5.09	2129.3	2286.2	8.069	368	2.77	1.75	0.88	8.17	3.42
3.3	71.61	19.23	34.848	6.38	2146.3	2307.4	8.05	391	2.84	1.8	0.73	10.47	4.23
3.3	72.23	18.64	34.99	3.33	2149.2	2311.9	8.101	340	2.84	1.79	0.79	11.51	4.55
3.3	72.81	18.01	35.002	6.04	2150.8	2310	8.048	392	2.81	1.78	0.76	11.51	4.71
3.3	73.32	17.5	34.988	6.56	2152.4	2312.6	8.042	399	2.83	1.79	0.79	11.51	4.71
3.3	74.53	16.19	35.012	5.8	2153	2313.1	8.054	387	2.82	1.78	0.79	11.51	4.71
3.3	75.29	15.36	35.034	5.38	2153.3	2310.6	8.053	387	2.77	1.75	1.07	11.86	4.71
3.3	75.87	14.69	35.045	4.97	2154.5	2326.9	8.095	349	2.99	1.89	0.79	11.51	4.71
3.3	76.36	14.12	35.027	5.7	2152	2312.8	8.057	383	2.83	1.79	0.79	11.51	4.71
3.3	76.93	13.32	35.033	5.33	2154.2	2314.1	8.061	380	2.82	1.78	0.79	11.86	4.55
3.3	77.45	12.78	34.96	3.68	2156.1	2305.6	8.063	374	2.65	1.67	0.76	11.16	4.55
3.3	78	12.88	34.975	4.11	2156.8	2306.3	8.056	382	2.66	1.68	0.76	12.91	4.55
3.3	78.27	15.41	34.232	-0.86	2147.2	2269.2	8.077	351	2.25	1.41	0.79	8.66	3.9
13.6	78.26	15.48	34.12	2.91	2026.9	2271.4	8.305	195	4.03	2.54	0.38	0.14	0.7
13.6	78.06	13.45	34.276	1.63	2086.6	2272.3	8.198	259	3.15	1.98	0.28	1.26	1.11
13.6	77.43	13.64	34.55	3.53	2064.2	2288.9	8.247	230	3.74	2.36	0.22	0	2.44
13.6	76.76	14.28	34.757	3.82	2116.5	2300.6	8.148	299	3.15	1.98	0.5	4.4	3.41
13.6	76.27	14.79	35.042	6.25	NaN	NaN	NaN	NaN	NaN	NaN	0.63	7.6	4.39
13.6	75.79	15.17	35.036	6.03	NaN	NaN	NaN	NaN	NaN	NaN	0.54	5.86	4.23
13.6	75.12	15.81	35.037	6.42	NaN	NaN	NaN	NaN	NaN	NaN	0.63	7.81	3.9
13.6	74.44	16.46	35.001	7.32	2125.7	2318.7	8.107	339	3.31	2.1	0.54	6.56	3.41
13.6	73.34	17.25	35.028	7.11	2101.6	2316.5	8.157	296	3.63	2.3	0.5	4.88	2.28
13.6	72.8	17.66	34.975	7.6	2124.9	2314.6	8.095	349	3.27	2.07	0.54	6.21	2.93
13.6	72.26	18.05	34.985	7.69	2127.3	2314.9	8.089	355	3.23	2.05	0.54	6.21	3.25
13.6	71.47	18.66	34.55	7.8	2110.3	2297.2	8.093	349	3.23	2.05	0.38	3.14	2.44
13.6	70.78	19.13	34.273	8.23	2083.1	2287.1	8.13	316	3.49	2.21	0.19	0.42	1.63
13.6	70.29	19.42	34.082	8.05	2094.7	2269.4	8.07	368	3.06	1.93	0.35	2.3	2.11
13.6	69.71	19.04	32.678	7.93	NaN	NaN	NaN	NaN	NaN	NaN	NaN	NaN	NaN
22.8	69.7	19.05	32.592	9.77	2013.2	2194	8.086	346	3.16	2	0.25	0.98	1.43
22.8	70.19	19.51	33.575	11.03	2059.8	2264	8.098	344	3.53	2.25	0.22	0.63	0.86
22.8	70.83	19.09	34.381	10.58	2083.6	2295.1	8.106	339	3.63	2.31	0.22	0.63	1.07
22.8	71.62	18.5	34.53	11.14	2088	2301.7	8.099	346	3.66	2.33	0.25	1.47	0.81
22.8	72.22	18.09	34.862	10.5	2098.7	2319.3	8.117	332	3.76	2.39	0.28	1.4	1.79
22.8	72.83	17.63	34.855	9.81	2098.4	2338.9	8.165	293	4.06	2.58	0.25	1.4	1.33
22.8	73.36	17.23	34.877	8.25	2084.8	2282.1	8.108	333	3.37	2.14	0.16	0.21	0.86
22.8	74.65	16.19	34.815	9.27	2102.2	2313.8	8.119	329	3.61	2.29	0.32	2.44	1.79
22.8	75.37	15.55	34.864	7.62	2087.9	2313.5	8.174	283	3.8	2.41	0.19	0.56	1.2
22.8	75.88	15.07	34.89	8.74	2102.9	2315.2	8.128	321	3.61	2.29	0.35	3.14	1.95
22.8	76.35	14.66	34.831	8.7	2093.5	2304.9	8.129	319	3.59	2.28	0.28	1.95	1.51
22.8	76.92	14.11	33.48	6.36	2046	2201.3	8.066	361	2.74	1.73	0.13	0.07	1.19
22.8	77.48	13.64	32.961	6.65	2016.7	2197	8.13	306	3.11	1.96	0.13	0.07	1.43

22.8	78	13.09	32.619	6.94	1999.6	2315.8	8.383	162	5.3	3.34	0.13	0	1.5
22.8	78.26	15.44	30.311	8.03	1911	2096	8.168	270	3.22	2.02	0.09	0.14	1.96
13.11	69.72	19.04	32.817	7.94	2068.6	2236.1	8.076	360	2.98	1.88	0	4.61	3.91
13.11	69.92	18.65	32.948	8.31	2065.1	2236.2	8.076	360	3.02	1.91	0.38	3.98	2.28
13.11	70.94	17.74	34.195	8.63	2109.2	2279.1	8.047	393	2.99	1.9	0.5	6.07	2.93
13.11	71.58	17.4	34.255	8.58	2103.4	2300.9	8.108	338	3.41	2.16	0.44	5.58	2.44
13.11	72.22	17.03	34.224	8.58	2115	2302.9	8.086	358	3.27	2.07	0.5	6.42	2.6
13.11	72.83	16.67	34.696	7.32	2136	2313.2	8.075	369	3.09	1.96	0.6	8.44	2.93
13.11	73.32	16.38	34.751	7.5	2131.2	2318.2	8.093	352	3.23	2.05	0.6	8.23	3.09
13.11	74.58	15.58	34.875	7.13	2138.2	2325.2	8.096	349	3.23	2.04	0.66	9.21	3.41
13.11	75.28	15.12	34.859	6.7	2141.3	2321.5	8.089	356	3.13	1.98	0.66	9.42	3.41
13.11	75.78	14.74	34.89	6.65	2142.8	2342.8	8.131	321	3.42	2.17	0.66	9.63	3.41
13.11	76.27	14.39	34.864	6.84	2144.5	2336.7	8.112	337	3.31	2.09	0.66	9.7	3.58
13.11	76.94	13.88	34.427	3.32	2139.1	2297.7	8.1	340	2.79	1.76	0.57	7.33	2.93
13.11	77.48	13.46	34.895	5.81	2142.6	2305.1	8.062	377	2.86	1.81	0.6	8.09	3.09
13.11	78.09	13.33	34.805	4.58	2147.4	2312.9	8.09	352	2.9	1.83	0.63	9.42	3.9
13.11	78.26	15.42	34.281	2.51	2134.5	2281.1	8.086	349	2.61	1.64	0.47	5.86	3.09

**Table 13.** Oslo-Kiel; February, May, August, November 2018.

Date	Lat °N	Lon °E	S	T C°	A <sub>T</sub> μmol/kg	C <sub>T</sub> μmol/kg	pH <sub>T</sub>	pCO <sub>2</sub> μatm	Ω <sub>Ca</sub>	Ω <sub>Ar</sub>	PO <sub>34</sub> μmol/kg	NO <sub>3</sub> μmol/kg	SiOH <sub>4</sub> μmol/kg
18.2	59.81	10.58	26.25	0.82	2012.5	1953.6	7.959	446	1.4	0.9	0.86	13.69	19.8
18.2	59.2	10.63	24.99	2.36	2098.2	2012.5	8.046	383	1.8	1.1	0.64	8.57	14.25
18.2	59	10.64	22.69	2.55	2064.3	1975.7	8.091	346	1.9	1.2	0.6	6.83	14.11
18.2	58.85	10.63	22.66	2.51	2049.7	1967.1	8.072	360	1.8	1.1	0.6	6.83	13.94
18.2	58.66	10.62	23.33	2.74	2078.5	1989.5	8.078	357	1.9	1.2	0.6	7.18	13.61
18.2	58.46	10.64	33.72	6.02	2295.4	2140.8	8.054	387	2.8	1.7	0.95	5.73	4.88
18.2	58.25	10.75	33.52	4.62	2291.8	2154.5	8.035	404	2.5	1.6	0.6	7.19	7.65
18.2	58.05	10.91	32.9	4.9	2261	2124.9	8.038	398	2.5	1.6	0.57	6.5	6.35
18.2	57.85	11.06	26.53	3.47	2124.4	2030.9	8.031	399	2	1.2	0.63	7.3	13.25
23.5	59.82	10.59	19.44	16.56	1572.7	1486	7.98	384	1.8	1.1	0.1	6.63	15.46
23.5	59.2	10.63	12.28	17.4	1138.6	1113	7.826	458	0.8	0.5	0.13	4.97	25.46
23.5	59	10.64	18.4	17.26	1670	1565.2	8.043	354	2.2	1.3	0.1	1.55	11.85
23.5	58.85	10.62	19.98	18.34	1956.8	1832.9	8.022	430	2.7	1.6	0.1	0.49	2.96
23.5	58.65	10.61	21.01	18.51	2046.3	1903.7	8.045	417	3	1.9	0.1	0.14	1.61
23.5	58.41	10.64	22.64	18.59	2102.3	1949.7	8.037	428	3.2	2	0.1	0.14	1.46
23.5	58.25	10.75	27	17.24	2142.7	1966.3	8.045	403	3.4	2.1	0.1	0	1.39
23.5	58.03	10.92	18.9	16.76	2025.7	1898.5	8.065	403	2.8	1.7	0.13	0.35	1.97
23.5	57.85	11.08	18.62	17.8	1974.8	1864.9	8.006	460	2.5	1.5	0.1	0	1.5
5.8	59.82	10.59	23.13	22.65	1865	1658.2	8.142	284	4	2.5	0.13	0.14	1.28
5.8	59.2	10.63	25.47	22.12	1984.3	1790.4	8.061	365	3.7	2.3	0.1	0	1.49
5.8	59	10.63	24.5	21.62	2107.8	1921.4	8.047	409	3.7	2.3	0.16	0	0.93
5.8	58.85	10.62	25.01	21.46	2123.6	1929	8.058	397	3.8	2.4	0.16	0	0.82
5.8	58.65	10.62	27.35	20.38	2182.5	1969.6	8.07	383	4	2.6	0.1	0	0.52
5.8	58.45	10.69	31.24	19.6	2237.7	2011.4	8.047	400	4.1	2.6	0.09	0.14	0.64
5.8	58.25	10.83	31.88	19.32	2251.2	2019.7	8.051	396	4.1	2.7	0.13	0.14	0.49
5.8	58.05	10.99	31.47	18.62	2244.9	2014.7	8.066	381	4.1	2.6	0.09	0.07	0.57
5.8	57.85	11.16	31.13	19.33	2235.3	2006.5	8.058	389	4.1	2.6	0.09	0.07	0.57
1.11	59.8	10.57	25.94	8.73	2010	1878.1	8.091	332	2.5	1.6	0.1	1.55	1.52
1.11	59.2	10.63	30.21	10.99	2182	2021	8.052	385	3	1.9	0.25	2.66	3.92
1.11	58.97	10.64	30.5	11.13	2239.3	2061.2	8.08	366	3.2	2	0.13	1.75	3.59
1.11	58.85	10.64	30.55	11.1	2243.7	2054.8	8.105	343	3.4	2.2	0.22	2.24	3.42
1.11	58.65	10.64	29.86	11.08	2220.8	2045.5	8.086	360	3.2	2	0.22	2.1	3.92
1.11	58.45	10.66	32.24	10.48	2299.6	2101.3	8.106	346	3.5	2.2	0.19	0.77	1.55
1.11	58.25	10.82	32.79	10.44	2300.6	2102.3	8.099	351	3.5	2.2	0.22	0.49	2.28
1.11	58.05	11	30.58	10.24	2267.2	2084.4	8.101	350	3.3	2.1	0.22	0.49	3.26
1.11	57.85	11.13	29.77	10.35	2261.9	2080.9	8.107	347	3.3	2.1	0.25	0.63	4.24

**Table 14.** Cold water coral reefs, Hardangerfjord (Huglhammaren, Straumsneset, Bekkjarvik, Hornaneset, Nakken, Terskel), Møre og Romsdal (Aktivneset), Vesterålen (Hola); April, October 2017 (\*) and May, July 2018.

Date	Site	Station	Lat	Lon	Depth	S	T	A <sub>T</sub>	C <sub>T</sub>	pH <sub>T</sub>	Ω <sub>Ca</sub>	Ω <sub>Ar</sub>
			°N	°E	m	‰	°C	µmol/kg	µmol/kg			
17.05	Bekkjarvik	559	59.998	5.292	243	35.07	7.12	2319	2158	8.023	2.70	1.72
17.05	Bekkjarvik	559	59.998	5.292	141	34.95	7.22	2312	2153	8.024	2.74	1.74
17.05	Bekkjarvik	559	59.998	5.292	99	34.80	7.23	2314	2158	8.020	2.73	1.73
17.05	Bekkjarvik	559	59.998	5.292	53	34.46	7.44	2305	2156	8.008	2.68	1.70
17.05	Bekkjarvik	559	59.998	5.292	13	31.89	6.34	2230	2084	8.059	2.67	1.68
21.05	Bekkjarvik	567	59.999	5.292	250	35.09	7.15	2323	2159	8.029	2.74	1.74
21.05	Bekkjarvik	567	59.999	5.292	142	34.97	7.19	2314	2155	8.024	2.74	1.74
21.05	Bekkjarvik	567	59.999	5.292	101	34.82	7.18	2309	2153	8.022	2.73	1.73
21.05	Bekkjarvik	567	59.999	5.292	51	34.37	7.41	2299	2152	8.004	2.64	1.67
21.05	Bekkjarvik	567	59.999	5.292	11	31.45	9.21	2211	2030	8.108	3.20	2.02
17.05	Straumsneset	558	59.941	5.468	213	35.09	7.33	2316	2163	8.002	2.62	1.66
17.05	Straumsneset	558	59.941	5.468	140	34.98	7.54	2315	2167	7.992	2.61	1.65
17.05	Straumsneset	558	59.941	5.468	100	34.82	7.44	2310	2157	8.008	2.68	1.70
17.05	Straumsneset	558	59.941	5.468	49	34.59	8.32	2305	2170	7.957	2.50	1.58
17.05	Straumsneset	558	59.941	5.468	9	30.86	8.86	2193	2015	8.117	3.17	2.00
21.05	Straumsneset	568	59.941	5.469	270	35.11	7.20	2317	2154	8.026	2.71	1.72
21.05	Straumsneset	568	59.941	5.469	140	34.98	7.18	2313	2156	8.021	2.73	1.73
21.05	Straumsneset	568	59.941	5.469	101	34.78	7.36	2308	2159	8.000	2.63	1.67
21.05	Straumsneset	568	59.941	5.469	51	34.50	8.23	2301	2167	7.955	2.47	1.57
21.05	Straumsneset	568	59.941	5.469	11	31.84	7.67	2211	2054	8.069	2.83	1.78
17.05	Huglhammaren	555	59.815	5.592	214	34.93	7.67	2311	2167	7.979	2.52	1.60
17.05	Huglhammaren	555	59.815	5.592	141	34.90	7.77	2312	2166	7.984	2.58	1.64
17.05	Huglhammaren	555	59.815	5.592	99	34.82	8.01	2308	2172	7.957	2.47	1.57
17.05	Huglhammaren	555	59.815	5.592	49	34.52	8.62	2301	2177	7.923	2.35	1.49
17.05	Huglhammaren	555	59.815	5.592	10	30.48	8.65	2176	2001	8.119	3.12	1.96
21.05	Huglhammaren	571	59.814	5.592	215	34.97	7.41	2319	2169	7.996	2.59	1.64
21.05	Huglhammaren	571	59.814	5.592	141	34.87	7.54	2309	2163	7.987	2.57	1.63
21.05	Huglhammaren	571	59.814	5.592	101	34.79	7.66	2306	2166	7.973	2.51	1.59
21.05	Huglhammaren	571	59.814	5.592	51	34.65	8.12	2311	2171	7.970	2.56	1.62
21.05	Huglhammaren	571	59.814	5.592	10	31.01	7.65	2193	2031	8.096	2.92	1.84
17.05	Hornaneset	557	59.890	5.537	201	35.09	7.29	2316	2153	8.031	2.78	1.76
17.05	Hornaneset	557	59.890	5.537	140	35.02	7.40	2316	2159	8.019	2.74	1.74
17.05	Hornaneset	557	59.890	5.537	100	34.80	7.58	2312	2163	8.000	2.65	1.68
17.05	Hornaneset	557	59.890	5.537	50	34.41	8.38	2302	2171	7.947	2.44	1.55
17.05	Hornaneset	557	59.890	5.537	10	31.51	7.76	2204	2041	8.088	2.92	1.84
21.05	Hornaneset	569	59.891	5.537	302	35.11	7.22	2317	2155	8.024	2.70	1.71
21.05	Hornaneset	569	59.891	5.537	141	34.94	7.21	2320	2161	8.025	2.76	1.75
21.05	Hornaneset	569	59.891	5.537	101	34.75	7.49	2308	2155	8.011	2.70	1.71
21.05	Hornaneset	569	59.891	5.537	53	34.58	8.16	2301	2168	7.955	2.47	1.57
21.05	Hornaneset	569	59.891	5.537	10	31.71	7.44	2214	2061	8.065	2.78	1.75
17.05	Nakken	554	59.830	5.556	209	35.09	7.25	2314	2157	8.016	2.69	1.70
17.05	Nakken	554	59.830	5.556	142	34.92	7.48	2312	2163	7.996	2.61	1.66
17.05	Nakken	554	59.830	5.556	101	34.76	8.00	2311	2175	7.960	2.48	1.58

17.05	Nakken	554	59.830	5.556	50	34.01	8.37	2292	2165	7.942	2.39	1.52
17.05	Nakken	554	59.830	5.556	11	31.08	8.12	2185	2012	8.116	3.08	1.94
21.05	Nakken	570	59.829	5.560	205	35.01	7.21	2315	2158	8.017	2.69	1.70
21.05	Nakken	570	59.829	5.560	141	34.94	7.21	2314	2159	8.018	2.71	1.72
21.05	Nakken	570	59.829	5.560	101	34.85	7.39	2311	2160	8.006	2.67	1.69
21.05	Nakken	570	59.829	5.560	51	34.60	8.08	2301	2169	7.951	2.45	1.55
21.05	Nakken	570	59.829	5.560	11	31.22	7.74	2209	2060	8.056	2.73	1.72
17.05	Terskel	556	59.811	5.586	175	35.01	7.74	2315	2168	7.987	2.59	1.64
17.05	Terskel	556	59.811	5.586	141	34.88	7.75	2312	2167	7.984	2.57	1.63
17.05	Terskel	556	59.811	5.586	101	34.81	7.90	2311	2171	7.971	2.53	1.61
17.05	Terskel	556	59.811	5.586	51	34.29	8.66	2292	2170	7.922	2.33	1.48
17.05	Terskel	556	59.811	5.586	11	31.36	7.57	2205	2040	8.098	2.96	1.86
11.04*	Hola	22	68.931	14.378	234	35.06	7.35	2328	2155	8.050	2.89	1.84
11.04*	Hola	22	68.931	14.378	229	35.06	7.34	2315	2147	8.042	2.83	1.80
11.04*	Hola	22	68.931	14.378	230	35.06	7.34	-	-	-	-	-
17.10*	Hola	22	68.931	14.378	50	33.78	11.38	2275	2093	8.037	3.18	2.03
17.10*	Hola	22	68.931	14.378	100	34.44	10.21	2298	2119	8.036	3.09	1.97
17.10*	Hola	22	68.931	14.378	150	34.67	9.42	2304	2129	8.034	3.00	1.91
17.10*	Hola	22	68.931	14.378	247	34.74	8.15	2305	2151	7.997	2.63	1.67
17.10*	Hola	22	68.931	14.378	11	33.42	11.38	2266	2067	8.081	3.46	2.20
17.10*	Hola	22	68.931	14.378	51	34.21	11.78	2291	2088	8.071	3.50	2.23
17.10*	Hola	22	68.931	14.378	101	34.44	9.86	2297	2121	8.036	3.06	1.94
17.10*	Hola	22	68.931	14.378	150	34.62	9.14	-	-	-	-	-
17.10*	Hola	22	68.931	14.378	233	34.74	8.19	-	-	-	-	-
17.10*	Hola	22	68.931	14.378	11	33.40	11.27	2266	2066	8.085	3.47	2.21
17.10*	Hola	22	68.931	14.378	52	33.96	11.28	2285	2085	8.076	3.44	2.19
17.10*	Hola	22	68.931	14.378	101	34.47	9.84	2296	2121	8.032	3.03	1.93
17.10*	Hola	22	68.931	14.378	150	34.66	9.11	2303	2132	8.031	2.94	1.87
17.10*	Hola	22	68.931	14.378	241	34.76	8.19	2303	2150	7.996	2.63	1.67
17.10*	Hola	22	68.931	14.378	240	34.73	8.21	2305	2152	7.993	2.62	1.66
17.10*	Hola	22	68.931	14.378	240	34.74	8.20	2305	2146	8.010	2.71	1.72
17.10*	Hola	22	68.931	14.378	240	34.74	8.20	2307	2147	8.013	2.72	1.73
12.07	Hola	22	68.931	14.378	240	34.99	7.17	2327	2075	8.222	4.00	2.54
12.07	Hola	22	68.931	14.378	240	34.99	7.17	2324	2114	8.139	3.41	2.16
12.07	Hola	22	68.931	14.378	240	34.99	7.17	2318	2151	8.043	2.81	1.79
15.07	Aktivneset	553	62.619	3.719	332	35.17	7.00	2286	2161	7.934	2.19	1.39
15.07	Aktivneset	553	62.619	3.719	332	35.17	7.00	2291	2160	7.948	2.26	1.44
15.07	Aktivneset	553	62.619	3.719	332	35.17	7.00	2321	2150	8.048	2.80	1.78

## 6.3 Definitions

$$A_T = [HCO_3^-] + 2[CO_3^{2-}] + [B(OH)_4^-] + [OH^-] + [HPO_4^{2-}] + 2[PO_4^{3-}] + [SiO(OH)_3^-] + [NH_3] + [HS^-] - [H^+] - [HSO_4^-] + [HF^-] + [H_3PO_4] - \dots \quad (4)$$

$$C_T = [CO_2^*] + [HCO_3^-] + [CO_3^{2-}] \quad (5)$$

$[H^+] \sim [H^+]_f + [HSO_4^-]$ ,  
 der  $[H^+]_f$  er den frie hydrogenkonsentrasjonen  
 $pH = -\log_{10} ([H^+])$  \quad (6)

$$pCO_2 = [CO_2^*]/K_0 \quad (7)$$



**Norwegian Environment Agency**

**Telephone:** +47 73 58 05 00 | **Fax:** +47 73 58 05 01

**E-mail:** post@miljodir.no

**Web:** [www.miljodirektoratet.no](http://www.miljodirektoratet.no)

**Postal address:** Postboks 5672 Torgarden, N-7485 Trondheim

**Visiting address Trondheim:** Brattørkaia 15, 7010 Trondheim

**Visiting address Oslo:** Grensesvingen 7, 0661 Oslo

The Norwegian Environment Agency is working for a clean and diverse environment. Our primary tasks are to reduce greenhouse gas emissions, manage Norwegian nature, and prevent pollution.

We are a government agency under the Ministry of Climate and Environment and have 700 employees at our two offices in Trondheim and Oslo and at the Norwegian Nature Inspectorate's more than sixty local offices.

We implement and give advice on the development of climate and environmental policy. We are professionally independent. This means that we act independently in the individual cases that we decide and when we communicate knowledge and information or give advice.

Our principal functions include collating and communicating environmental information, exercising regulatory authority, supervising and guiding regional and local government level, giving professional and technical advice, and participating in international environmental activities.